Durham E-Theses

The mount Tawai Peridotite, north Borneo

Hancock, W. G.

How to cite:

Hancock, W. G. (1964) *The mount Tawai Peridotite, north Borneo*, Durham theses, Durham University. Available at Durham E-Theses Online: http://etheses.dur.ac.uk/9224/

Use policy

The full-text may be used and/or reproduced, and given to third parties in any format or medium, without prior permission or charge, for personal research or study, educational, or not-for-profit purposes provided that:

- a full bibliographic reference is made to the original source
- a link is made to the metadata record in Durham E-Theses
- the full-text is not changed in any way

The full-text must not be sold in any format or medium without the formal permission of the copyright holders.

Please consult the full Durham E-Theses policy for further details.

Academic Support Office, Durham University, University Office, Old Elvet, Durham DH1 3HP
e-mail: e-theses.admin@dur.ac.uk Tel: +44 0191 334 6107
http://etheses.dur.ac.uk

THE MOUNT TAWAI PERIDOTITE, NORTH BORNEO.

W. G. HANCOCK, B.Sc.

Thesis submitted for the degree of
Doctor of Philosophy in the University
of Durham.

Saint Cuthberts' Society. June, 1964.

DURHAM UNIVERSITY SCIENCE
13 AUG 1964
LIBRARY

ABSTRACT.

The Mount Tawai peridotite is a batholith, elongate north-south, situated between the Kinabatangan and Labuk rivers in the North Borneo ultrabasic belt. The surrounding country rocks are Upper Cretaceous and Tertiary sediments and volcanics which strike predominantly E.N.E. They are separated from the peridotite by a fault breccia which contains inclusions of metamorphic rocks.

The batholith comprises at least three partially separated tectonic units, the largest of which is the Main Tawai block. The outer parts of the tectonic units exhibit a crude gneissose foliation and peripheral serpentinization.

The batholith is composed mainly of harzburgite with scarce dunite, pyroxenite and gabbro phases. The dunite occurs in lenticular pods which dip steeply westward in the Main Tawai block. Some of the dunite lenses contain thin chromite bands showing evidence of rudimentary gravity stratification. The harzburgite is composed mainly of forsterite and enstatite with only minor endiopside. The alumina content of the enstatite varies from 1.3 to 7.4 per cent and that of the endiopside from 2.9 to 7.2 per cent. The dunite bands contain forsterite and chrome spinel, the composition of the latter varying from $Cr_{65.5}\ Al_{32.2}\ (Mg_{68.1})$ to $Cr_{32.6}\ Al_{66.9}\ (Mg_{63.8})$ on Thayer's (1946) shortened formula.

The gabbroic rocks are irregularly distributed within the batholith occurring mainly as tectonic inclusions.

Both the ultrabasic and basic rocks are considered to have been derived from the same parent magma. The absence of anorthite from

the ultrabasic assemblages is explained by an initial phase of differentiation at very high temperature and pressure which suppressed the precipitation of plagioclase but favoured the introduction of alumina into the pyroxenes. During the initial phase of differentiation only olivine, enstatite, endiopside, and spinel were precipitated, but there must have been frequent but short-lived intervals in which only olivine and spinel were precipitated; these are thought to have accumulated in hollows and channels on the floor of a crystal pile. A systematic increase of alumina in the pyroxenes and spinels of the Main Tawai block has been traced and is attributed to a crystallisation sequence.

A gabbroic phase is thought to have been precipitated on top of the ultrabasic crystal pile following a drop in temperature which resulted in the precipitation of plagioclase and the lowering of the Mg/Fe ratio in the pyroxene and olivine.

A calculation of the average composition of the rocks of the North Borneo belt is in close agreement with the average mantle composition suggested by Ringwood (1959). This evidence together with the high temperature and pressure conditions needed to explain the ultrabasic assemblages has led to the conclusion that the parent magma of the Mount Tawai complex was derived by fusion of upper mantle material.

After or during the final stages of differentiation the gabbroic fraction was injected into the crust creating a pre-heated path up which the hot, already-differentiated peridotite rose as a series of almost crystalline units.

During this stage a gneissose foliation developed roughly parallel to the sides of the intrusive units. Thermal metamorphism

of the country rocks to garnet amphibolite facies accompanied the process. After cooling beneath the surface the intrusive units were serpentinised and emplaced in their present position by faulting, which also disrupted the thermal metamorphic aureole. Late lime bearing solutions, deposited calc-silicate veins and altered some of the gabbro to rodingite.

The final emplacement had profound effects on the drainage system and occurred in late or post Pleistocene.

PREFACE AND ACKNOWLEDGEMENTS.

From February 1959 until August 1961 the author was employed as a geologist by Naylor Benson and Company Ltd. and took part in the geological investigation for chromite of the ultrabasic batholiths in the Labuk area of North Borneo. The investigation was of a first phase nature involving geological mapping on the scale of 1:25,000. From September 1961 onward the specimens collected during the investigation were examined in the Department of Geology, Durham University.

The author wishes to thank Professor K. C. Dunham, F.R.S., for his advice during both the field and the laboratory investigation and for the provision of research facilities in this department.

The permission of Naylor Benson and Company Ltd. to use the material collected between 1958 and 1961 is gratefully acknowledged.

The author is indebted to Dr. D. M. Hirst and Mr. R. A. Lambert for instruction on the methods of wet chemical analyses.

Personal acknowledgement is due to Dr. H. D. Holland, Mr. R. Phillips and Mrs. J. Kaye for help with X-ray investigations. The help provided by Mr. C. Chaplin and Mr. G. Dresser and other members of the Technical staff throughout the laboratory study are especially acknowledged.

The author would like to thank Dr. H. C. Kirk and Dr. F. H. Fitch of the North Borneo Geological Survey for many interesting ideas and advice.

The author gratefully acknowledges the advice and clinopyroxene specimens given by Dr. G. M. Brown and wishes to thank Dr. M. J. O'Hara for his ideas on petrogenesis.

LIST OF ILLUSTRATIONS.

			Page.
Fig.	1.	Simplified Geological sketch map of Borneo.	2.
"	2.	Map showing the distribution of ultrabasics in North Borneo.	4.
"	3.	Geological map of the Labuk area.	7.
"	4.	Topographical sketch map of the Labuk area.	9.
"	5.	Photograph of the Meliau range.	11.
"	6.	Air photograph of an ultrabasic intrusion.	11.
"	7.	Photographs of Mount Tawai.	13.
"	8.	Photograph of Mount Gombaran.	15.
"	9.	Photographs of Melio and Nobusu falls.	17.
"	10.	Photograph of Melio village.	19.
"	11.	Geological map of the Mount Tawai area.	25.
"	12.	Photomicrograph of banded chert.	31.
"	12a.	Photograph of pillow lava.	31.
"	13.	Chemical data of North Borneo spilites and keratophyres.	40.
"	14.	Geological map of part of the Melio valley.	46.
"	15.	Photograph of finely banded amphibolite.	48.
"	16.	Photograph of coarsely " "	48.
"	17.	Photomicrograph of metamorphosed shale.	50.
"	18.	Photomicrograph of massive amphibolite.	54.
"	19.	Photograph of Patud range.	64.
"	20.	Sections showing the contact relations.	66.
"	20a.	Photographs of the peridotite contact.	67.
"	21.	Structural map of the Mount Tawai peridotite.	69.
"	21a.	Sections shown on Fig. 21.	70.

		Page.
Fig.	22a. Mylonitic banding.	77.
"	22. Photographs of the Kuun-Kuun breccia zone.	85.
"	23. Photographs of calcified breccias.	87.
"	24. Photograph of foliation harzburgite.	89.
"	25. Diagram showing relationship between primary igneous banding and foliation.	94.
"	26. Photograph of clinopyroxenite bands.	97.
"	27. Photographs of dunite bands.	99.
"	28. Map of dunite lenses.	101.
"	29. F.M.A. diagram of ultrabasic rocks.	112.
"	30. Diagram of approximate mineral composition of ultrabasic rocks.	113.
"	31. Photomicrograph of mesh textured serpentinite.	120.
"	32. Photomicrograph of trellis structure.	120.
"	33. Photomicrograph of antigorite.	123.
"	34. Photograph of slip fibre.	123.
"	35. Photomicrograph of picrolite.	126.
"	36. Photograph of cross fibre asbestos.	126.
"	37. Photograph of massive harzburgite.	151.
"	37a. Photomicrograph of lamellar structure in olivine.	151.
"	38. Photomicrograph of relatively undeformed harzburgite.	152.
"	39. Photomicrograph of kink band in enstatite.	155.
"	40. Photomicrograph of clinopyroxene in harzburgite.	155.
"	41. Photomicrograph of myrmekitic intergrowth.	157.
"	42. Photomicrograph of Phase 2 deformation.	157.

			Page.
Fig.	43.	Photomicrograph of broken kink band.	159.
"	44.	Photomicrograph of sutured kink band.	159.
"	45.	Photomicrograph of Phase 3 deformation.	161.
"	45a.	Photomicrograph of warped enstatite.	161.
"	46.	Photomicrograph of mylonite.	163.
"	47.	Photomicrograph of mylonite.	163.
"	48.	Photomicrograph of polygonal olivine grains.	167.
"	49.	Photomicrograph of feldspathic peridotite.	171.
"	50.	Photomicrograph of saussurite peridotite.	171.
"	52.	Diagram of orthopyroxenite bands.	176.
"	53.	Photmicrograph of ortho-clino band.	179.
"	54.	Diagram of minor structures in chromite bands.	184.
"	55.	Drawings of chromite bands.	186.
"	56.	Photograph of giant chain chromite.	188.
"	57.	Photograph of chromite bands.	188.
"	58.	Plans and sections of Intrusive dunite.	190.
"	59.	Photographs of chromite bands.	192.
"	60.	Photomicrographs of chain chromite.	194.
"	61.	Photograph of entire thin section of Type 2 ore.	194.
"	62.	Photomicrograph of chromite blotches.	196.
"	63.	Photomicrograph of euhedral chromite.	196.
"	64.	Photomicrograph of chromite bands (Type 2)	198.
"	65.	Photomicrograph of chromite bands (Type 2)	198.
"	66.	Photomicrograph of T230.	200.
"	66a	Photomicrograph of T230.	200.
"	67.	Photomicrograph of olivine gabbro.	204.

		Page
Fig. 68	Photograph of banded gabbro.	204.
" 69.	Photograph pf gabbro pegmatites.	211.
" 70.	Photomicrograph of pyroxene gabbro.	214.
" 71.	Photomicrograph of gabbro pegmatite.	214.
" 71a.	Photomicrograph of albitised gabbro.	217.
" 72.	Olivine determinative curve.	220.
" 73.	Photomicrograph of gas bubbles in olivine.	224.
" 74.	Diagram of alumina variation in orthopyroxenes.	233.
" 75.	Photomicrograph of orthopyroxene lamellae.	236.
" 76.	Variation in cell parameters of orthopyroxene.	243.
" 77.	Tracing of diffraction record of orthopyroxene.	249.
" 78.	Graph of d 10, 3, 1, versus d 060 for orthopyroxenes.	251.
" 79.	Determinative chart for orthopyroxenes.	252.
" 80.	Determinative curve for orthopyroxenes.	254.
" 81.	Determinative curve for orthopyroxenes.	255.
" 82.	Co-existing pyroxenes.	265.
" 83.	Alumina variation in clinopyroxenes.	267.
" 84.	Tracing of deffraction record of clinopyroxene.	273.
" 85.	Unit cell dimensions of selected clinopyroxenes.	279.
" 86.	Ca:Mg:Fe plot of clinopyroxenes.	281.
" 87.	Clinopyroxene Trends.	282.
" 88.	Spinel cell edge variation.	296.
" 89.	Map of orthopyroxene alumina variations.	300.
" 90.	Map of spinel Cr_2O_3 variations.	301.
" 91.	Orthopyroxene-spinel variation.	303.

			Page
Fig.	92.	Part of the tetrahedron (MgFe)O-Al_2O_3-CaO-SiO_2.	314.
"	93.	Photomicrograph of rodingite.	328.
"	94.	Photomicrograph of prehnite fans.	331.
"	95.	Photomicrograph of hydrogarnet vein.	339.
"	96.	Specimen locality map.	356.

LIST OF TABLES.

		Page
Table 1.	Probable stratigraphy of the Labuk area.	21.
" 2.	Basalt analysis.	39.
" 3.	Amphibolite analysis.	57.
" 4.	Peridotite analyses.	115.
" 5.	C.I.P.W. norms of peridotites.	116.
" 6.	Gabbro analyses.	117.
" 7.	X-ray diffraction pattern of lizardite and brucite.	128.
" 8.	X-ray diffraction pattern of bastite pseudomorph.	130.
" 9.	X-ray diffraction pattern of chlorite.	132.
" 10.	X-ray diffraction pattern of clinochrysolite.	134.
" 11.	Dunite analyses.	136.
" 12.	Dunite analyses recalculated to 100 per cent.	137.
" 13.	Optical data for olivines and orthopyroxenes.	222.
" 14.	Comparison of olivines and orthopyroxenes.	226.
" 15.	Orthopyroxene analyses.	228.
" 16.	Recalculated orthopyroxene analyses.	229.
" 17.	Recalculated orthopyroxene analyses.	230.
" 18.	Comparison of minor oxides of orthopyroxenes.	238.
" 19.	Trace element analyses of pyroxenes.	239.
" 20.	Cell dimensions of orthopyroxenes.	242.
" 21.	X-ray diffraction data for orthopyroxenes.	245.
" 22.	Mineral determinations.	257.
" 23.	Clinopyroxene analyses.	261.
" 24.	Recalculated clinopyroxene analyses.	262.
" 25.	Recalculated clinopyroxene analyses.	263.
" 26.	Comparison of minor oxides of clinopyroxenes.	270.

Page

Table 27. Clinopyroxene unit cell dimensions. 275.

" 28. Clinopyroxene unit cell dimensions. 277.

" 29. Chromite analyses. 288.

" 30. Chromite analyses. 290.

" 31. Comparison of chromites. 292.

" 32. Trace element analyses of chromites. 294.

" 33. Chromite unit cell dimensions. 297.

" 34. Average composition of North Borneo peridotite belt. 324.

" 35. X-ray diffraction pattern of hydrogarnet. 335.

" 36. Tremolite analyses. 337.

" 37. X-ray diffraction pattern of goethite. 345.

" 38. Goethite analyses. 347.

CONTENTS.

	Page
Abstract	i
Preface and Acknowledgements	iv
List of Illustrations	v
List of Tables	x
INTRODUCTION	1
The geological setting.	1
Previous work.	5
THE GEOGRAPHY OF THE LABUK AREA	6
Situation	6
Relief	6
Climate	18
Population	18
Travel	18
THE STRATIGRAPHY OF THE LABUK AREA	20
UPPER CRETACEOUS AND EOCENE SEDIMENTS OF THE MOUNT TAWAI AREA.	26
Field Occurrence	26
Petrography	29
Sandstone	29
Mudstone and shale	30
Limestone	30
Chert	32
UPPER CRETACEOUS AND EOCENE VOLCANICS OF THE MOUNT TAWAI AREA.	33
Field Occurrence	33

Page

Petrography 34

Chemistry 37

Petrogenesis 38

THE METAMORPHIC ROCKS OF THE MOUNT TAWAI AREA 45

Distribution and Field Occurrence 45

Petrography 49

Chemistry 56

Petrogenesis 58

THE ULTRABASIC AND BASIC INTRUSIVE ROCKS OF MOUNT TAWAI 62

General Features 62

The structure of the batholith 62

The contact relations 63

The internal faults and the main tectonic units 74

Breccias 84

Foliation 88

Primary Igneous banding 93

The history of emplacement 102

The age of the batholith 105

The major rock types 109

Chemistry 111

Serpentinites 118

Distribution 118

Petrography 118

Mineralogy 125

Chemistry 135

Serpentinisation 140

Page

Harzburgites 150

Distribution and Field Occurrence 150

Petrography 150

Mineralogy 168

Feldspathic peridotite 169

Distribution 169

Petrography 169

Mineralogy 172

Pyroxenites 173

Field Occurrence 173

Petrography 177

Mineralogy 180

Dunite 181

Field Occurrence 181

Petrography 189

Mineralogy 201

Olivine gabbro 201

Field Occurrence 201

Petrography 203

Mineralogy 206

Pyroxene gabbro 208

Field Occurrence 208

Petrography 212

Mineralogy 216

THE MINERALOGY OF THE ULTRABASIC AND BASIC ROCKS 219

Olivine 219

Page

Composition 219

Inclusions in olivine 221

Orthopyroxenes 225

Chemistry 225

X-ray diffraction studies 240

Distribution of iron between co-existing olivines and orthopyroxenes 256

Clinopyroxenes 260

Chemistry 260

X-ray diffraction studies 271

Composition 278

Relations between co-existing ortho and clinopyroxenes. 280

Chrome spinel 286

Chemistry 286

X-ray diffraction studies 293

THE VARIATION OF THE PRIMARY MINERALS 298

Olivine 298

Orthopyroxene 298

Clinopyroxene 299

Chromium spinel 302

Olivine gabbro - pyroxene gabbro 304

THE PETROGENESIS OF THE BASIC AND ULTRABASIC ROCKS 306

The field evidence 306

The nature and differentiation of the parent magma 309

THE HYDROTHERMAL ROCKS 325

Rodingites 325

Field Occurrence 325

Petrography 326

Page

Hydrogarnet rocks 329

Field Occurrence 329

Petrography 329

Mineralogy 330

Tremolite rocks 333

Field Occurrence 333

Petrography 334

Chemistry 336

Silico-carbonate rocks 336

Field Occurrence 336

Petrography 338

Petrogenesis 340

THE WEATHERING DEPOSITS 343

Field Occurrence 343

Mineralogy 344

Chemistry 346

Origin 346

THE HISTORY OF THE MOUNT TAWAI PERIDOTITE 349

Pre-Intrusive phase 349

Intrusive phase 350

Fault emplacement phase 351

COMPARISON OF THE MOUNT TAWAI PERIDOTITE WITH OTHER AREAS 353

APPENDIX 357

REFERENCES 360

INTRODUCTION.

The Mount Tawai peridotite is situated in the country of North Borneo. North Borneo (now referred to as Sabah), Sarawak, and Brunei are the three, formerly British administered, territories that occupy the northern fringe of the island of Borneo. Kalimantan, Indonesian Borneo, occupies the greater part of the island (Fig.1).

The Geological setting.

Borneo is part of the Indonesian archipelago which may be divided into three tectonic units as follows:-

The Sunda shelf
The Sahul shelf
The Banda geosyncline

The Sunda shelf, which is the south-western extension of the Asiatic continental shelf, contains numerous islands, the largest of which is Borneo. The Sahul shelf, the north-western Australian continental shelf, includes the island of New Guinea. The area in between the Sunda and Sahul shelves has been termed by Umbgrove (1938) the Banda geosyncline and consists of a complex series of island arcs, peridotite belts, and deep sea troughs. The geological literature abounds in accounts of this area, notable contributions being made by Vening Meinesz (1940), Hess (1948), and Van Bemmelen (1949). The two shelf areas contain cores of old crystalline rocks and are generally interpreted as the "jaws" of the geosyncline.

The island of Borneo is part of the Sunda area and its general geology has recently been reviewed by Fitch (1960); his sketch map of the island is reproduced in Fig. 1. A core of old crystalline granites and gneiss is exposed in the southern and central parts of the island, and to the north of this core Palaeozoic, Mesozoic, and Tertiary sediments occur. Liechti (1960) considers the Tertiary sediments have been deposited in a geosynclinal trough that has gradually migrated northwards. This geosyncline has developed on the northern edge of the Sunda shelf. As a general rule as the island is traversed northward away from the core the sediments

DURHAM UNIVERSITY SCIENCE 13 AUG 1964 LIBRARY

GEOLOGICAL MAP OF THE LABUK AREA

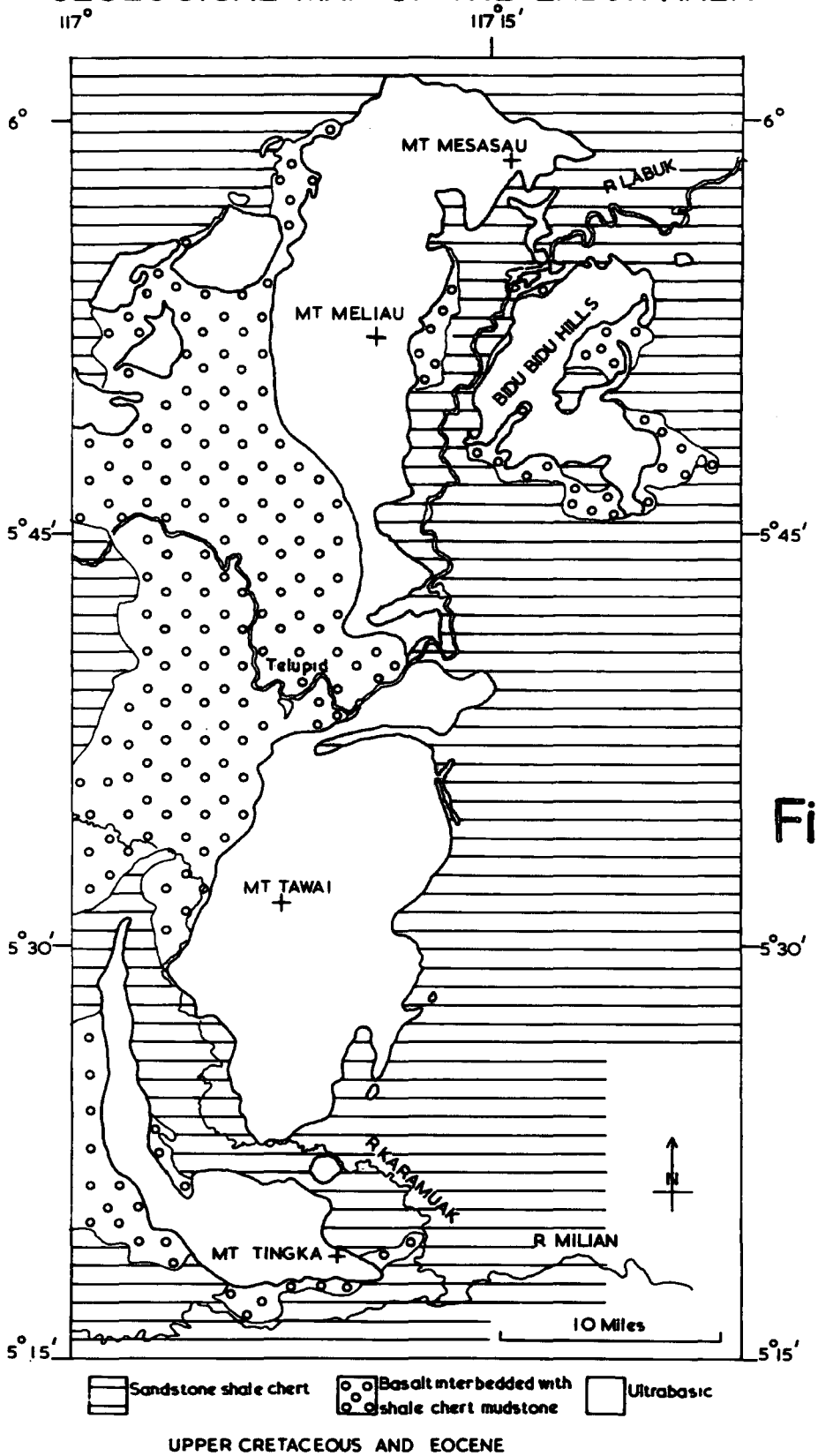

Fig.3.

the strike of the Tertiary folds is approximately east-west and roughly parallel to the elongation of the individual peridotite intrusions and to the general strike of the belt. However in the Kinabatangan-Labuk area the elongation of the intrusions and the general strike of the belt is north-south whilst the local folds are striking east-north-east. In the Ranau area the ultrabasics appear to be grouped around the Kinabalu quartz-monzonite intrusion. The relationship between the peridotite belt and the Tertiary fold belts is therefore of a complex nature and the simple picture shown in other areas of the world where the ultrabasics occur in swarms arranged en-echelon along the axes of contemporary fold-mountain chains is not found in North Borneo.

Previous work.

The only comprehensive work on the geology of North Borneo was compiled by Rheinhard and Wenk and published in 1951. This report was based largely on data obtained during the search for oil by various oil companies. Short references to the Labuk area are made in the report and records of traverses made up the Karamuak and Tankulap rivers given.

Dr. F. H. Fitch of the North Borneo geological survey completed a reconnaissance survey of the Sandakan and Labuk areas in 1958. It is largely due to his strenuous investigation carried out under extremely hazardous conditions that the general geology of the Labuk area is known. Fitch delimited the ultrabasic batholiths and brought them to the attention of mining companies interested in chromite and nickel. Fitch's report is published as Memoir 9 of the Geological Survey Department of the British Territories in Borneo.

Mesasau-Meliau range from which it is separated by the Labuk river. It forms a prominent group of high ridges and occupies an area some 25 miles long by fifteen miles wide between the Labuk and Karamuak rivers.

The Tingka intrusions give rise to an arcuate group of hills to the south and south-east of the Tawai batholith from which it is separated by the Karamuak river.

The ultrabasic mountains are particularly noticeable on the air photographs, for they are clothed with a thin pole-like vegetation, Fig. 6, in marked contrast to the primary jungle found on the eastern plains and in the western hilly district.

The eastern plains are formed mainly of Tertiary sediments and are covered by thick primary jungle. These plains are part of the extensive Lokan peneplane that extends from the eastern margin of the ultrabasic belt to the sea and occupies over a 1000 square miles. The area is extremely flat and hills over 300' are rarely found.

The western hilly region is built mainly of basaltic rocks. This area comprises numerous irregular-shaped hills seldom rising over 800'. Prominent spine-like features rising above the general level which are seen on the air photograph to the west of the Mesasau intrusion may be volcanic necks. The basaltic areas are notable for large numbers of ground leeches that live on the low undergrowth beneath the high forest trees.

The northern part of the area is drained by the Labuk river and its tributaries and the southern part by tributaries of the Kinabatangan. The Labuk river enters the area to the west of Telupid and flows eastward between the Mesasau-Meliau and Tawai batholiths. East of these intrusions it turns sharply northwards and flows between the Meliau-Mesasau and Bidu-Bidu mountains. North of these intrusions

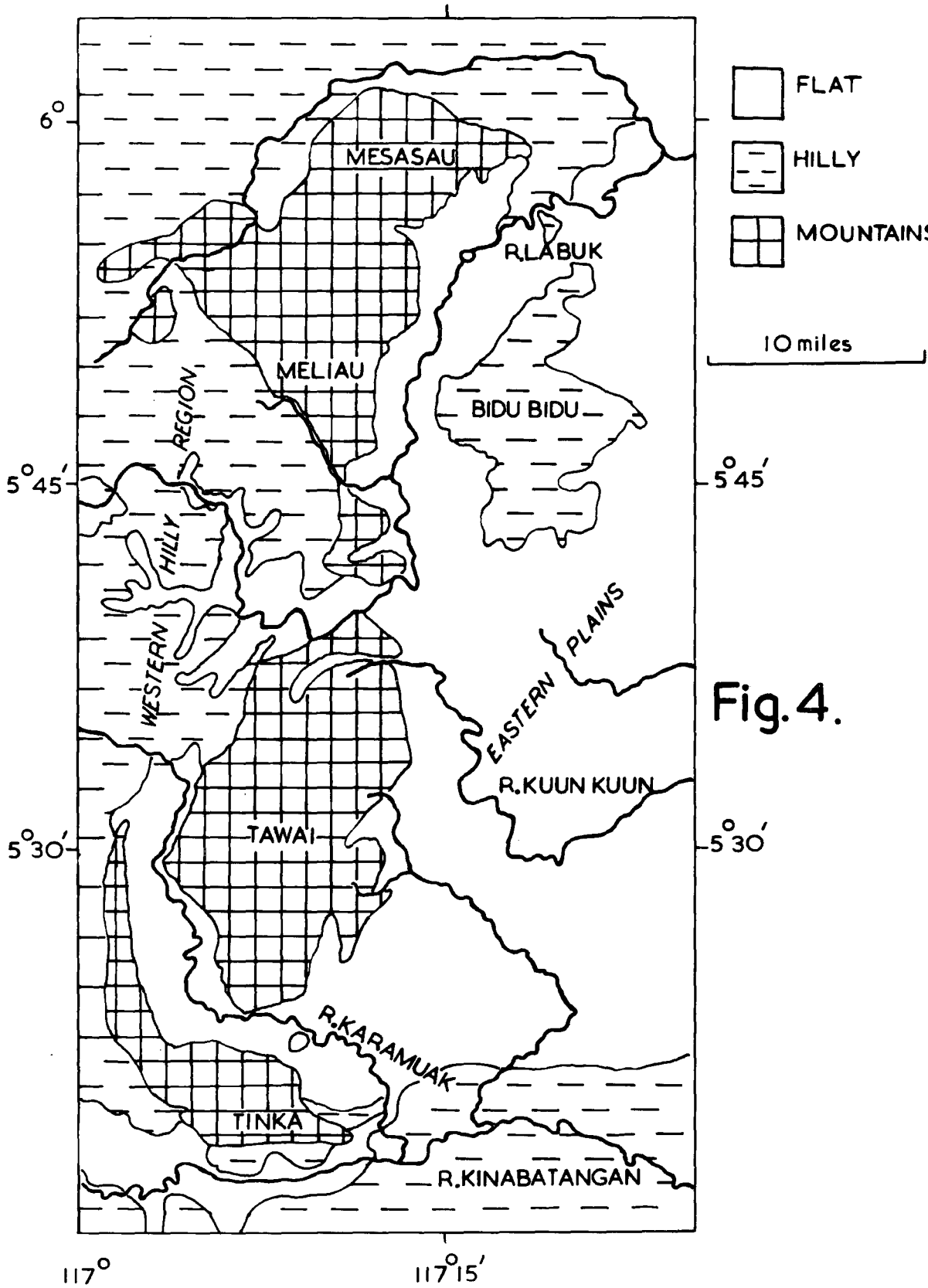

Fig. 4.

TOPOGRAPHICAL SKETCH MAP OF THE LABUK AREA

it turns eastward into the sea through a mass of anastomising ditributaries.

The south of the area is drained by tributaries of the Kinabatangan notably the Karamuak and the Tankulap.

No major river is found draining the Lokan peneplain and Fitch (1958) has suggested that the eastward-draining part of the Labuk once reached Sandakan Bay through this area but has since been captured by another stream cutting back between the Mesasau-Meliau and Bidu-Bidu mountains.

The Labuk mountain belt has an eccentric position with regard to the regional drainage system. Both the Kinabatangan and the Labuk rivers rise well to the east of this mountain belt in the Crocker range and have to cross through the ultrabasic belt on the way to the sea. Once clear of the foothills of the Crocker range these rivers are mainly in a state of old age as is clearly shown by their numerous meanders and 'ox bow lakes', and their deltas of anatomising distributaries. The relief of the ultrabasic on the other hand is of extreme youth, with sharp razor backed ridges and fast flowing ungraded streams.

The Tawai mountains are composed of a series of razor-back ridges separated by fast flowing streams. The ridges contain numerous peaks and cols and many gashes, caused by land slipping, scar the steep slopes. The ridges are clothed by a vegetation of closely grouped pole-like trees with intertwining bamboo at certain horizons. Undergrowth is poorly developed. A thick talus deposit of peridotite boulders is normally found distributed around the base of the hill slopes. Tor-like masses of peridotite form the largest peaks.

The main ridge, the Tawai range, is found in the central part of the area and stretches right across the block from east to west.

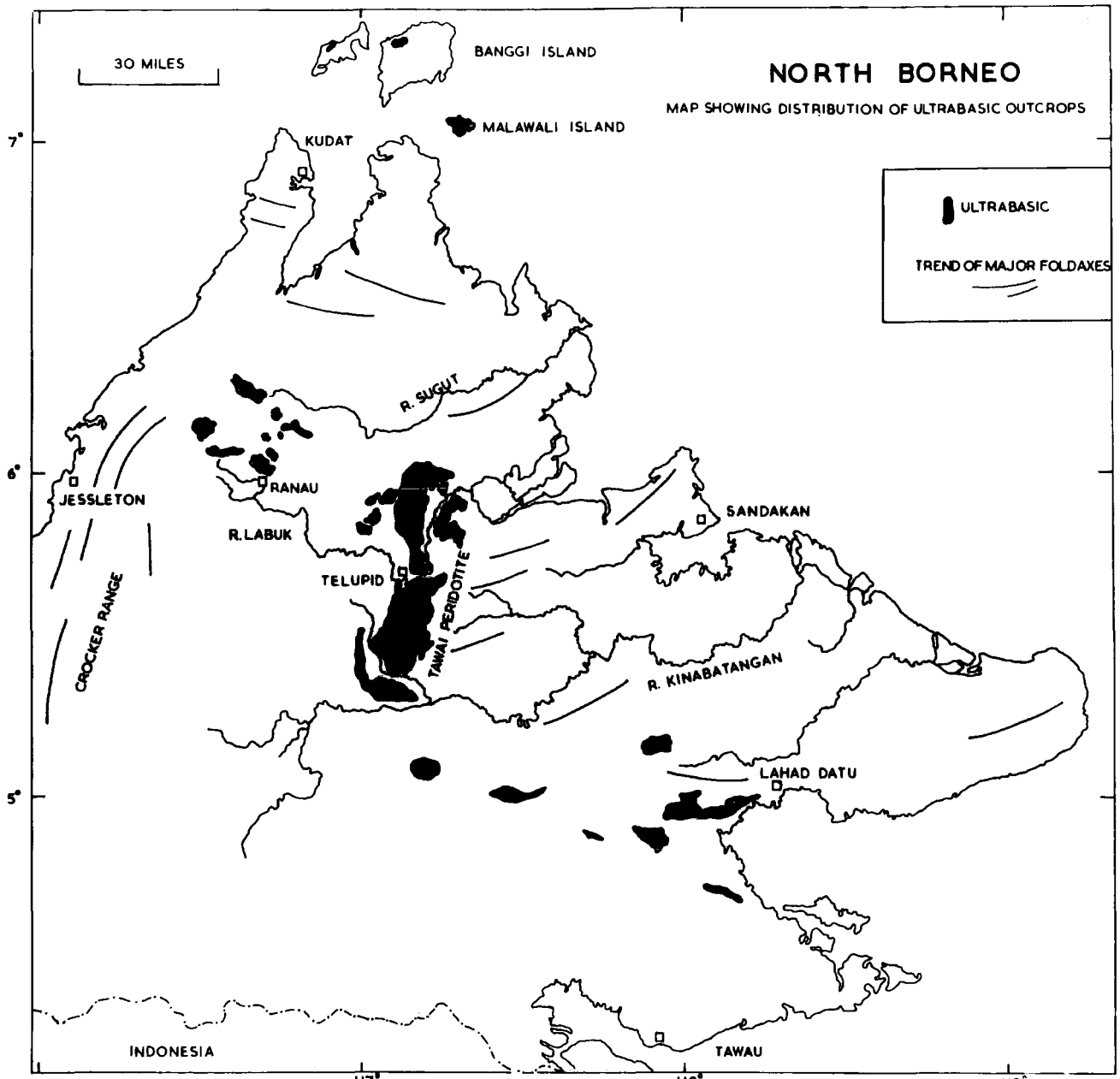
30 MILES
BANGGI ISLAND
NORTH BORNEO
MAP SHOWING DISTRIBUTION OF ULTRABASIC OUTCROPS
MALAWALI ISLAND
KUDAT
ULTRABASIC
TREND OF MAJOR FOLDAXES
7°
6°
5°
R. SUGUT
RANAU
JESSLETON
R. LABUK
SANDAKAN
TELUPID
TAWAI PERIDOTITE
CROCKER RANGE
R. KINABATANGAN
LAHAD DATU
INDONESIA
TAWAU
117°
118°
119°

Fig. 2.

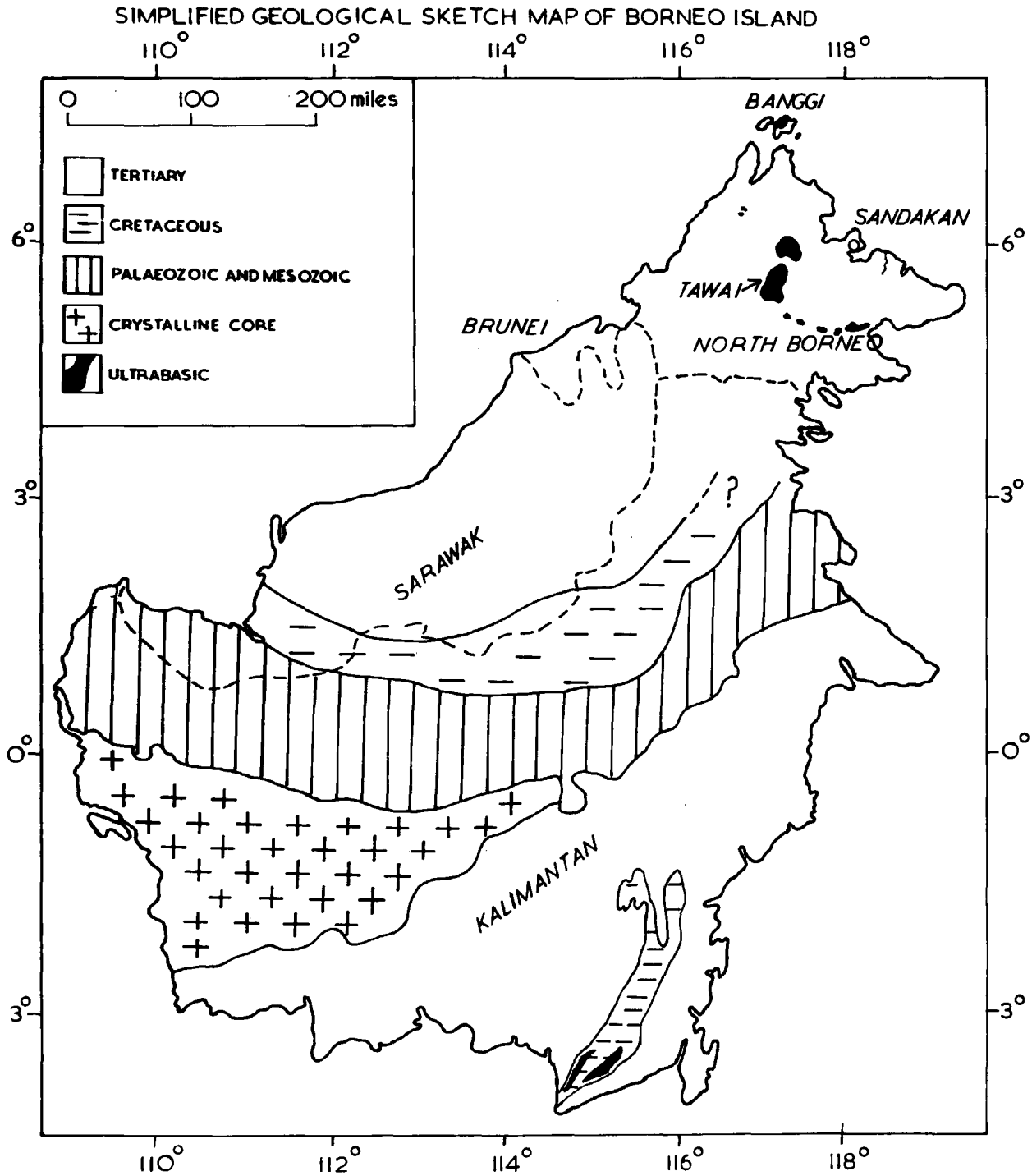
SIMPLIFIED GEOLOGICAL SKETCH MAP OF BORNEO ISLAND
110°
112°
114°
116°
118°
0
100
200 miles
TERTIARY
CRETACEOUS
PALAEOZOIC AND MESOZOIC
CRYSTALLINE CORE
ULTRABASIC
BANGGI
SANDAKAN
TAWAI
BRUNEI
NORTH BORNEO
SARAWAK
?
KALIMANTAN
6°
3°
0°
3°

Fig.1.

Fig. 5. Photograph of Maliau Range from Telupid.

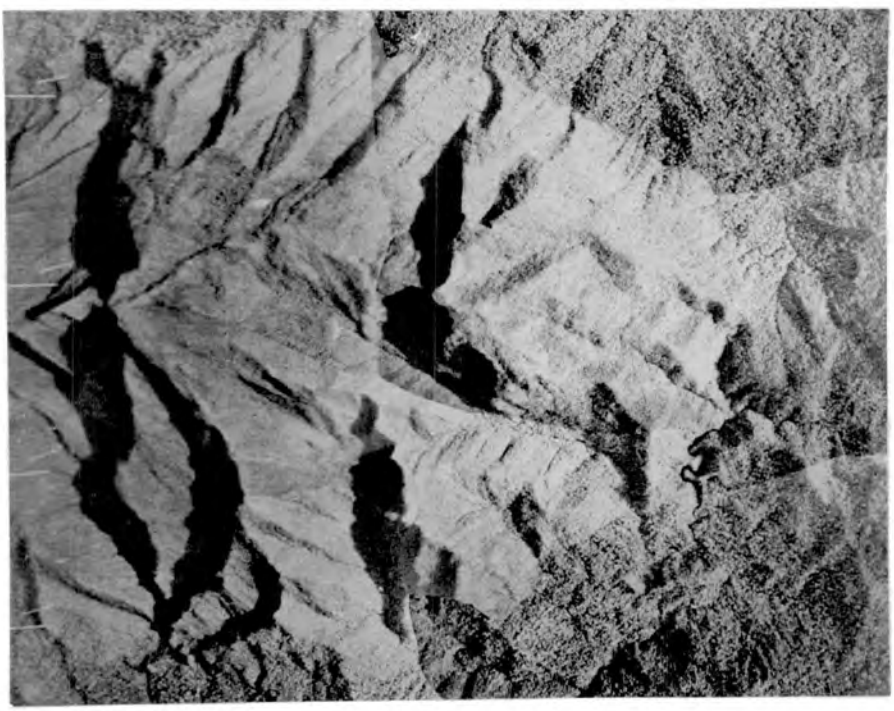

Fig. 6. Air photograph of an ultrabasic intrusion, south of the Kinabatangan river.

It contains a number of prominent peaks, the highest of which is Mount Tawai (4,176') Fig. 7.

To the north the Tawai range gives rise to three main ridges all of which rise to over 3,000 feet.

The most westerly of these is the Patud range which forms the north-western margin of the Tawai batholith. Here it trends N.E.-S.W. but as it approaches the Labuk river it swings round in an arcuate curve and trends E.-W. along the southern bank of the Labuk. This east-west trending range, the Gombaran range, (Fig. 8), is breached by the Meliau river, a tributary of the Labuk.

The Giram range is the middle member of the three north-south prolongations off the Tawai range, and the Sawar range the most easterly. Both trend northward to within a mile of the Gombaran range from which they are separated by a tongue of low swamp country.

A low N.-S. trending range, about 3 miles long, separated from the main batholith, is found to the east of the Sawar range.

To the south the main Tawai range gives rise to five N.-S. trending prolongations. On the western flank two ridges extend southward to the Melio river and on the east three descend to the Tankulap river.

In the headwaters of the Melio and Tankulap streams a prominent plateau is found at an elevation of just over 1000'. It occupies an area of about six square miles and is bounded on the north by the Tawai range. The southern part of the plateau is rimmed by an arcuate range of hills which drop abruptly away to the South Tankulap and Talibu rivers. On the east and west the Tankulap and Melio rivers respectively leave the plateau over spectacular waterfalls. The Melio falls, just over 800' high, are shown in Fig. 9. The

Fig. 7. Photographs of Mount Tawai from the Karamuak river.

plateau surface is extremely swampy and much of the drainage is underground.

To the south of the plateau the Pantagaluang range rises to 3,500'. It is separated from the Tawai plateau by the deeply incised valley of the South Tankulap stream. East of the Pantagaluang mountains a N.-S. trending range, partially separated from the main batholith, is found. This is the Binalik range.

The drainage pattern of the batholith is of a radial nature. Most of the large streams are deeply incised and wind between sinuous gorges flanked on either side by steep-sided cliffs. The northern part of the batholith is drained by the Telupid and Meliau, and Kuun-Kuun rivers and the south by the Melio, Ruku-Ruku, Tankulap and many small tributaries of the Karamuak.

The Meliau river rises from near Mount Tawai and winds through numerous gorges and small waterfalls to the Labuk.

The course of the Kuun-Kuun is peculiar. It rises from the Tawai range close to the source of the Meliau, then flows parallel to the course of this stream, between the Giram and Sawar ranges, but before it reaches the ultrabasic contact it turns sharply eastward roughly parallel to the Labuk from which it is separated by the Gombaran range. It then flows eastward for three miles until it turns sharply south and flows to the Kinabatangan. Clearly this course is extremely irregular and it is suggested that the upper Kuun-Kuun was once a tributary of the Meliau but has since been captured by the lower Kuun-Kuun cutting back along a fault zone between the Giram and Gombaran ranges.

The Tankulap stream is composed of two main branches. The northern branch flows off the Tawai plateau over a series of rock

Fig. 8. Photograph of Gombaran Range from Kualą Meliau.

steps formed by faults. The southern branch on the other hand is deeply incised and is certainly flowing in a major fracture zone.

The general relief picture of the Mount Tawai is therefore one of extreme youth with powerful streams cutting down along weak zones between razor-backed ridges.

Fig. 9. Photographs of Melio Falls (above) and Nobusu Falls (below)

Climate.

The climate of the Labuk area is extremely hot and wet. The average yearly rainfall for Sandakan is 124" with December and January the wettest months. The mean minimum temperatures vary from 71.4 to 74.3°F and the mean maximum temperatures from 83.7 to 90.7°F. The mean relative humidity varies from 64 to 80.

Population.

The Labuk area is very thinly populated. A number of small villages are found along the banks of the main rivers, the largest being Telupid on the Labuk and Melio on the Karamuak (Fig. 10). The river bank villages however are continually shifting due to the cultivation of dry padi by the inhabitants. These villages are inhabited by people of Dusan stock who exist by collecting damar gum and growing padi, tapioca, and maize. Near the mouth of the Labuk larger settled communities are found in which Chinese and Bajau Malays predominate.

Travel.

There are no roads in the Labuk area. A government programme to build a road from Sandakan to the middle Labuk area is in progress. The large rivers provide access to the Labuk area. The Labuk is navigable by launch for a distance of five miles above its mouth. Above this point the river is navigable only by native canoes. These craft fitted with outboard motors are the standard means of transport away from the Labuk and Kinabatangan deltas.

In between the rivers there are only a few jungle paths, the only one in constant use being that which connects the villages of Telupid and Melio.

Fig. 10. Photograph of Melio village.

THE STRATIGRAPHY OF THE LABUK AREA.

Following a reconnaissance survey of the Labuk area Fitch (1958) concluded that the region was underlain by rocks of Upper Cretaceous, Tertiary and Quaternary age. His postulated stratigraphical succession for the Labuk area and the surrounding area is shown in Table 1 . The general geology of the Labuk area is shown in Fig. 3. This map was compiled by Fitch and has been amended in the light of recent work carried out during the investigation of the ultrabasic batholiths. Fitch showed that the oldest rocks of the area comprised a series of cherts, volcanics and sediments of Upper Cretaceous and Eocene age. This group he called the Chert-Spilite formation, which is equivalent to the Danau formation of Rheinhard and Wenk (1951). Fitch considered that some of the rocks shown in Fig. 3 as basalt interbedded with shale, chert and mudstone, were of Upper Cretaceous and Eocene age, notably those in the north-east corner of the map and those situated to the east of the Bidu-Bidu hills. Small ultrabasic bodies were also considered to have been intruded at this time. Fitch postulated that the chert-spilite formation was overlain unconformably by a thick series of red, grey and purple sandstones of middle and upper Eocene age. He divided the sandstones into a lower group, the Kulapsis sandstone, and an upper group, the Crocker sandstones. Oligocene sediments were not located in the area but Aquitanian (Lower Miocene) sandstones, shales and limestones were found in the Kinabatangan valley to the south of the Labuk area. Fitch again postulated an unconformity between the Aquitanian and Crocker sediments and suggested that most of the basaltic rocks of the Labuk were extruded during the Oligocene. The major ultrabasic batholiths he also envisaged as having been emplaced during this time. The Upper

TABLE 1.

Probable stratigraphy of the Sandakan area and parts of the Kinabatangan and Labuk Valleys. (After Fitch 1958).

Age.	Sediments	Igneous Rocks
Quaternary	Coastal alluvium	Volcanic Ash
Pliocene	High level gravel	
Upper Miocene	Sandstone, shale, mudstone Conglomerate and reef limestone	
	Unconformity	
Lower Miocene	Sandstone, shale, limestone	
Oligocene	Unconformity	Large ultrabasic intrusions Basalt extrusions
Eocene	Crocker formation-Sandstone and shale. Kulapsis formation-Sandstone and shale	
	Unconformity	Minor ultrabasic intrusions
Eocene to Upper Cretaceous	Chert-spilite formation Chert, shale, sandstone Limestone	Spilite, basalt, tuff, agglomerate

Miocene is restricted to small isolated basins and consist of limestone, mudstone and sandstone. It does not occur in the Labuk area. The base of the Upper Miocene is marked by a thick conglomerate and the beds are deposited with marked unconformity on folded pre-Upper Miocene strata. This is the only proven unconformity in the Sandakan region and it marks the most important Tertiary orogeny of North Borneo.

During the investigation of the Labuk ultrabasic batholiths two types of country rocks have been recorded:

(1) Volcanic rocks interbedded with chert, mudstone, shale and infrequent sandstone and limestone.

(2) Grey, red and purple sandstones with thin shales.

The first group forms extensive areas on the western flank of the main Labuk ultrabasic batholiths and also small areas to the east of them. The sandstone shale rocks occur down the eastern flank of the batholiths and also build large areas between the Tawai and Tingka intrusions. The distribution of the two groups is shown in Fig. 3.

Fitch considered the large basaltic field west of the ultrabasic batholiths to be mainly Upper Eocene and Oligocene in age and distinct from the volcanic rocks of the Chert-Spilite formation. Numerous traverses were made into the areas dated on palaeontological evidence as Upper Cretaceous and Eocene in age (Chert-Spilite) but no distinction could be made between these volcanics and those suggested as being of Upper Eocene or Oligocene in age. Both are interbedded with similar sedimentary rocks, notably chert and mudstone, and all the volcanic rocks show some evidence of pillow structure. In the

absence of clear palaeontological evidence it must be tentatively concluded that the volcanic rocks range from Upper Cretaceous to Eocene in age.

The sandstone group was dated by Fitch (1958) on palaeontological evidence as being of Eocene age by means of the foraminifera found in the associated shale. Fitch considered there was an unconformity between the chert-spilite formation and the Eocene sandstone group. Fitch (1958 p.51) describes an exposure in the lower Karamuak where sandstone and shale is found overlying serpentinised peridotite. The latter he considers to be a small intrusion of Chert-Spilite age. The exposure, at Kuala Malung, is to the south of the area mapped in the present survey but the locality was visited. In a very poor stream-exposure extremely brecciated serpentinised peridotite veined with calcite can be seen in contact with equally distorted shale and sandstone. The contact is under water and not clear; it is suggested that this is a fault contact. No other field evidence has been found indicating an unconformity between rocks of the chert-spilite type and the Eocene sandstone in the Labuk area.

Grey and red sandstone typical of the Eocene strata are also found interbedded with chert-spilite type rocks. In the Upper Kuun-Kuun valley, Fig. 14, sediments and volcanics of the chert-spilite type pass along the strike into Eocene sandstones. Similar relations have also been noted east of the Bidu-Bidu batholith. The field evidence therefore suggests that in the Labuk area the chert-spilite formation and the sandstone-shale rocks may be different facies of the Upper Cretaceous-Eocene. Obviously the stratigraphy of the Labuk area is far from certain. The two contrasting types of country rock are so closely folded that it is impossible to

determine with certainty their relationships. In the field the country rocks around the batholith have been mapped as either belonging to the chert-spilite association or to the sandstone-shale type and in this way are recorded on the map - Fig. 11.

The age of the Mount Tawai ultrabasic batholith is discussed in a later section after a review of the contact phenomena.

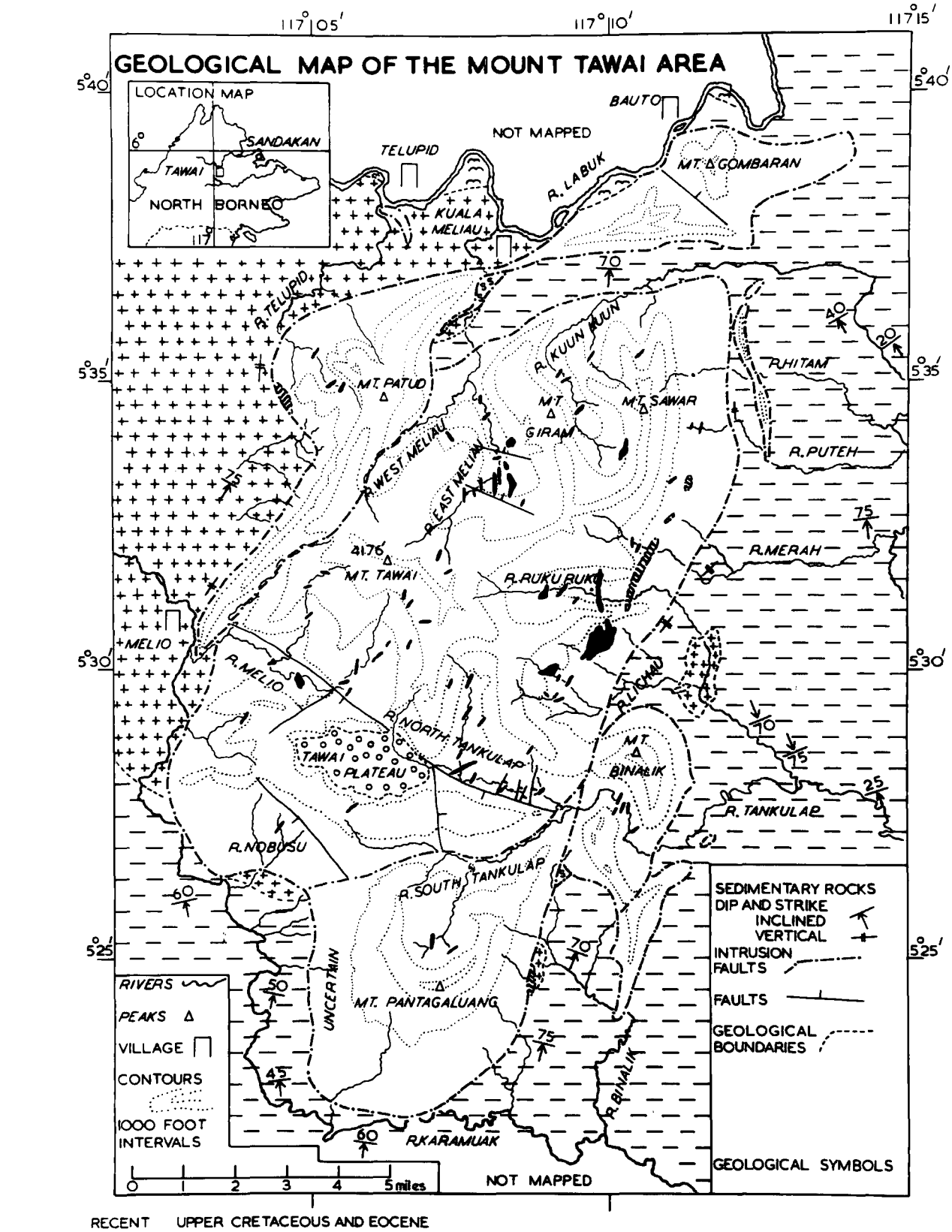
GEOLOGICAL MAP OF THE MOUNT TAWAI AREA
LOCATION MAP
SANDAKAN
TAWAI
NORTH BORNEO
117°05'
117°10'
117°15'
5°40'
5°35'
5°30'
5°25'
BAUTO
NOT MAPPED
TELUPID
KUALA MELIAU
R. LABUK
MT. GOMBARAN
R. TELUPID
R. KUUN KUUN
R. HITAM
MT. PATUD
MT. GIRAM
MT. SAWAR
R. WEST MELIAU
R. EAST MELIAU
R. PUTEH
R. MERAH
4176'
MT. TAWAI
R. RUKU RUKU
MELIO
R. MELIO
R. LIKHAU
TAWAI PLATEAU
R. NORTH TANKULAP
MT. BINALIK
R. TANKULAP
R. NOBUSU
R. SOUTH TANKULAP
UNCERTAIN
MT. PANTAGALUANG
R. BINALIK
R. KARAMUAK
RIVERS
PEAKS
VILLAGE
CONTOURS
1000 FOOT INTERVALS
0 1 2 3 4 5 miles
NOT MAPPED
SEDIMENTARY ROCKS
DIP AND STRIKE
INCLINED
VERTICAL
INTRUSION
FAULTS
FAULTS
GEOLOGICAL BOUNDARIES
GEOLOGICAL SYMBOLS
RECENT
ALLUVIUM
GOETHITE
UPPER CRETACEOUS AND EOCENE
SANDSTONE SHALE
BASALT SPILITE CHERT MUDSTONE
SCHIST
OLIVINE GABBRO
PYROXENE GABBRO
HARZBURGITE
DUNITE

Fig.11.

UPPER CRETACEOUS AND EOCENE SEDIMENTS OF THE MOUNT TAWAI AREA.

Field Occurrence.

The greater part of the area surrounding the Mount Tawai ultrabasic batholith is underlain by the Upper Cretaceous and Eocene sandstone-shale facies. The volcanic facies occurs mainly in the north-western part of the area.

Sediments interbedded with basalt and spilite occur on the western and northern flank of the Patud-Gombaron range and in the valley between that range and the main Tawai ultrabasic block. Small exposures are also found in the Ruku-Ruku and Binalik river sections off the eastern flank of the batholith.

The main area of the volcanic facies occurs between the village of Melian on the Karamuak and the village of Telupid on the Labuk. It extends westward from the ultrabasic contact for at least six miles and is part of the large basalt field that extends down the western flank of the main Labuk ultrabasic belt (Fig. 3). In the present survey it has not been investigated for more than a mile away from the ultrabasic contact. The area is very poorly exposed and outcrops are rare between stream sections. The available outcrops indicate that basaltic rocks build most of the area but thin intercalations of chert, red shale, and mudstone are found which increase in number eastwards. The majority of the exposures examined were close to the ultrabasic contact where the country rocks are considerably disturbed and no regional strike pattern could be determined.

The best exposures of sediments interbedded with volcanics are found in the Meliau river section south of the Patud-Gombaron ultrabasics and north of the main Tawai block. They occur at the extreme western end of the long tongue of country rocks that partially

separates these two intrusions. In this area, shown in Fig. 14, radiolarian cherts, mudstone, thin limestone and sandstones are found interbedded with basalt. The beds are tightly folded and numerous large scale slump features which result in intermingling of the various rock types are seen.

Individual beds can only be traced for short distances along the strike and no correlation between stream sections could be established. Eastwards along the tongue, the volcanic facies gives way to the sandstone-shale facies. In the extreme west of the tongue the regional strike is mainly north-east south-west but as the area is traced eastward it changes to an east-north-east west-south-west strike. A typical section measured in a small west bank tributary of the Meliau is given below.

Brown mudstone	- 23'	Youngest
Porcellaneous limestone	- 2'	
Pale yellow chert	- 13'	
Basalt	- 26'	
Red mudstone	- 40'	
Brown chert	- 16'	
Basalt	- 32'	
Brown limestone	- 11'	
Grey sandstone	- 15'	Oldest

The thick cherts are always closely associated with basalt and mudstone. In the majority of exposures chert is overlain by mudstone and underlain by volcanic rocks. The thicker chert beds contain mudstone partings at irregular intervals. The cherts are frequently broken up into small blocks the interstices being filled by vein calcite

or quartz. In hand specimen the cherts are compact, resinous, and break with a conchoidal fracture. The majority are brownish-red in colour but green, yellow, white and variegated varieties have been found. The thickest chert recorded is found in a small area of the volcanic facies that occurs at the confluence of the Ruku-Ruku and Lichau rivers off the east flank of the main batholith. It is between forty and fifty feet thick, is massive and a deep chocolate brown in colour. Black earthy lenticles of manganese wads are found in the majority of the cherts. Extremely porous cherts are also common. They are yellowish in colour and are frequently mantled with colloform chalcedony. These deposits closely resemble siliceous sinters.

Two types of limestone have been found. A coarse grained recrystallised reddish-brown variety, containing a network of white calcite veins, was found in the above recorded Meliau section. Normally the limestones occur in thin beds, and are extremely fine grained. Yellowish varieties transitional into chert also occur.

The mudstones are usually unbedded dark brown to red in colour and frequently contain earthy wads of manganese ores. Gradational varieties with chert are common.

The sandstone-shale facies occurs down the length of the eastern flank of the batholith and surrounds the southern and south-western margins. A detailed examination of this facies has not been undertaken. Short traverses outwards from the main ultrabasic contact and along the Kuun-Kuun valley were made in order to determine the regional strike. From these observations it was concluded that the regional strike of the country rock to the west of the main batholith is east-north-east west-south-west. This confirms the photogeological interpretation of Fitch (1958). The beds occur in open folds and

do not show the tight folding and slumping seen in the volcanic facies of the Meliau area. The formation consists mainly of poorly bedded grey sandstone. Graded bedding is occasionally seen but current bedding is noticeably absent. Bright red shale interbedded with the sandstone has been recorded close to the main ultrabasic contact on the Ruku-Ruku river and near the mouth of the Binalik river. The shales are coarsely bedded and contain fragmentary plant remains suggesting they were deposited at a considerable distance from the source. Thin beds of chert occasionally occur interbedded with the sandstone. The chert splits easily into slabs and seldom shows veining by quartz or calcite. The sandstone at these localities contains small chips of chert.

Two samples of shale from the Karamuak valley and one from the Meliau-Telupid path were collected by Fitch (1958) and dated by the Shell Company of North Borneo on microfossil content as Upper Cretaceous and Eocene in age. No unconformities have been found in the area and it must be assumed that all of the rocks are of this age.

Petrography.

Sandstones (Specimens S110, S138, S228, S323, S326).

The above listed sandstones were collected at various exposures along the eastern flank of the main batholith. In thin section they are seen to consist of angular, ill-sorted fragments of quartz and feldspar set in a microcrystalline groundmass of quartz, feldspar, chlorite and sericite. Accessory minerals present include zircon, tourmaline, and pyrite. The fragments are always in excess of the groundmass and the rock is best described as a graywacke. A limy cement is occasionally present as in specimen S 132. The feldspar

seldom exceeds five per cent by volume and is mainly oligoclase. It occurs as limpid grains sometimes showing polysynthetic twinning. Extremely turbid orthoclase and grid-twinned microcline also occur but in minor amounts. Fragments of foraminifera and carbonised plant remains occur in the groundmass. The sandstones are sometimes stained red by iron oxide. Rheinhard and Wenk (1951 p.19) describe red sandstones of Eocene age from the Kudat area which shows well-rounded equigranular quartz grains. No examples of this type of sandstone have been found in the Tawai area.

Mudstone and Shale (Specimens S113, S114, S226).

Unfortunately most of the mudstones and shales were in a bad state of preservation on arrival in England and unsuitable for thin section examination. One red mudstone, S113, was sectioned and is seen to consist of a fine aggregate of chlorite, quartz feldspar and calcite. No traces of bedding could be determined in the slide. Red iron oxide pigmentation colours the slide.

Limestone.

Two of the extremely fine grained limestones were examined in thin section. Specimen S110 consists of a fine matte of crypto-crystalline calcite. A few small angular crystals of quartz are present in the groundmass. An X-ray diffraction trace showed the absence of a clay mineral fraction. No trace of microfossils could be found in the specimen, which has the appearance of an inorganic precipitate. Specimen S338 is similar in hand specimen to S110 but the thin section shows it to consist of a mass of small radiating carbonate crystals with wavy extinction. An X-ray diffraction trace indicates the rock contains calcite, quartz, and chlorite.

Fig. 12. Photomicrograph of banded chert. The circular areas are radiolaria. S73 (crossed nicols X20)

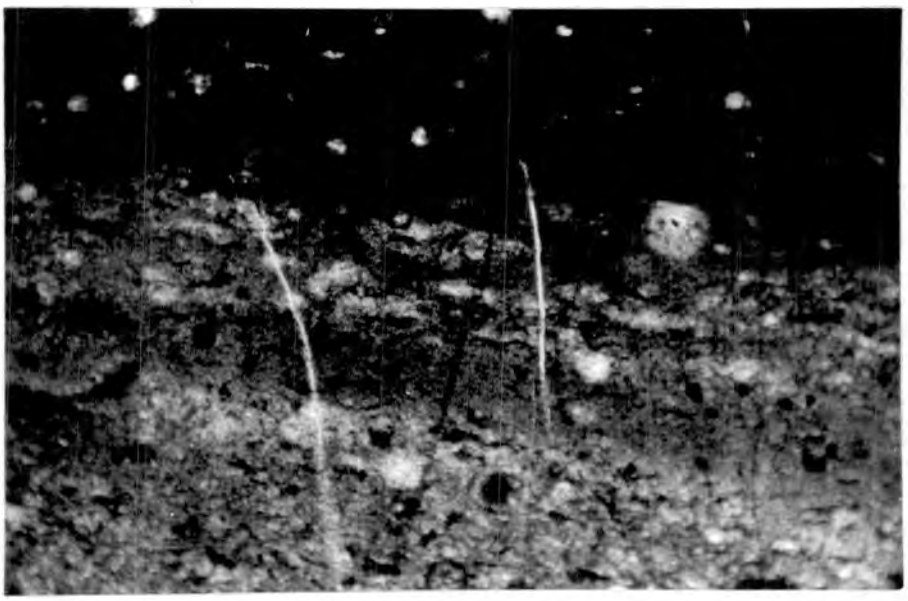

Fig. 12a. Photograph of Ruku-Ruku pillow lavas.

Again no microfossils were found.

Specimen S63 is a coarse reddish-brown limestone found in the recorded Melliau section. The thin section shows a partially recrystallised limestone stained with reddish-brown iron oxide. Veins of coarse grained calcite forms a network within the partially recrystallised carbonate.

Cherts.

In thin section the cherts are seen to consist of a micro-crystalline aggregate of amorphous silica speckled with circular and elliptical areas, .02-.05mm. in diameter, containing radiolaria. Sometimes a concentric radial structure can be determined but more frequently recrystallisation has occurred and the circular areas are filled with specks of quartz. A banded chert, specimen S73, in thin section (Fig. 12) is seen to consist of alternate bands of dark brown and light brown amorphous silicia. Radiolaria are present in both bands. An X-ray fluorescence trace of a dark brown band was made and a strong manganese peak recorded. This would suggest that the dark brown amorphous mineral is the manganese opal neotocite $XMnO\ YSiO_2\ ZH_2O$. The fact that the radiolaria in the dark brown bands are not replaced by manganese opal would suggest a primary syngenetic origin for the neotocite. Numerous veins of quartz cut the banding at an angle. Specimen S125 in hand specimen is a red chert and in thin section consists of numerous radiolaria set in a fine grained matrix of cryptocrystalline silica and calcite. The rock is pigmented with red iron oxide. This specimen is transitional between chert and limestone.

UPPER CRETACEOUS AND EOCENE VOLCANICS OF THE MOUNT TAWAI AREA.

Field Occurrence.

The location of the areas around the Tawai ultrabasic batholith in which rocks of the volcanic facies occur have been outlined in the last section. The largest area, found on the north-west flank of the batholith is very poorly exposed but the available outcrops suggests it is made mainly of basaltic rocks with sedimentary intercalations increasing in the eastern portion. Away from the contact zone with the ultrabasic the basalt is seen in the stream sections as a massive, often closely jointed black rock, usually microporphyritic, and often speckled with amygdales. In the Telupid river section the basalt is seen interbedded with mudstone and chert. Three miles upstream from the mouth of the river in a small west bank tributary an exposure occurs when mudstone overlies basalt. The mudstone dips 55° to the north. An undulating top to the basalt can be made out with abundant amygdales. The sandstone is unmetamorphosed. Poorly developed pillow structure can be made out in the basalt. Amygdaloidal basalt also occurs a few hundred yards upstream from the mouth of the river exposed in a prominent waterfall. Badly weathered tuff breccias occur at the top of the fall. Black glassy basalt (specimen V 170) is found just outside the ultrabasic contact in the first east bank tributary of the Telupid river and the outcrop suggests it forms the selvedge of a dyke crosscutting normal basalt. Extremely coarse-grained basalt (specimen V 69) with sub-ophitic texture occurs at mile 9 on the Telupid-Meliau path and again the field relations indicate it is part of a dyke intrusive into basalt. Over the rest of the area only sporadic outcrops are found. In the

these, relict pillow structure can occasionally be seen and the long axis of the pillows are always markedly inclined. More often the basalt shows closely spaced rectangular joint pattern. The joints are mostly filled with calcite or quartz. The best pillows (specimen V 63) observed are found in the Ruku-Ruku river section on the eastern flank of the batholith (Fig.2a). Their long axes measure about eighteen inches and they show prominent concentric cracks. Glassy selvedges are absent. Ropy- and slaggy-topped lavas are completely absent. Badly preserved beds of tuff and agglomerate are fairly frequent.

Close to the ultrabasic contact the basalt is extremely broken up and veined by calcite and quartz. The quartz veins frequently contain disseminations of pyrite, chalcopyrite and rarely zinc blende. Locally small ore bodies occur notably at Karang, two miles north of the village of Meliau, and at the ultrabasic contact on the Binalik river. These ores and the accompanying silicification and calcification are considered to be associated with the intrusion of ultrabasic batholith.

The overall picture given by the brief examination of the volcanic areas is one of a dense basalt field to the west of the batholith, in which sedimentary intercalations increase as the area is traversed eastwards. The main part of the field is made up of closely spaced flows, almost certainly laid down underwater. The lack of sediment in the western part of the field can be attributed to distance from land.

Petrography.

All the thin sections of basalt examined show some degree of

alteration, but in general the further away from the ultrabasic contact the less the degree of alteration observed. The basaltic rocks also vary in texture and mineralogy. To illustrate these changes a series of specimens is described.

Specimen V 374 is representative of the least altered specimen examined and was collected 5 miles east of the main ultrabasic contact. The basalt shows a megaphyric texture, the groundmass consisting mainly of closely packed microlites of plagioclase with subordinate clinopyroxene. Finely divided ore is disseminated throughout the groundmass. Sparse phenocrysts of ragged, dusty plagioclase laths between 0.5 and 2 mm. in length occur. They show faint polysynthetic twinning, measurements of the maximum extinction angle in the symmetrical zone indicating a composition of An_{51}. Limpid albite replacing the edges of the laths is present only in a few laths. Small, 0.5 mm. in length, sub-euhedral and euhedral phenocrysts of colourless clinopyroxene showing aborescent extinction are prominent. All the clinopyroxenes in the groundmass show alteration to green uralitic amphibole but the majority of the phenocrysts are fresh and clear. These clinopyroxene phenocrysts have a 2V gamma = 46° and nX = 1.692 indicating a normal augite. Some of the minute clinopyroxenes have optic axial angles between approximately 20° and 30°, suggesting pigeonite. Amygdales filled with fibrous zeolites, green chlorite and occasionally quartz are common. The green chlorite is optically negative, has nZ = 1.693 and shows the following pleochroic scheme:-

X - yellowish green

Y - grass green

Z - dark green

X-ray diffraction indicates the zeolite is okenite.

Specimen V 69 is a coarse grained basalt collected just over a mile west of the main ultrabasic contact north of the village of Meliau. The thin section shows a sub-ophitic texture with laths of plagioclase up to 2 mm. in length set in a groundmass of green uralite and rare, partially altered clinopyroxene. The plagioclase laths show albite and pericline twins, are turbid and strongly zoned. Measurement of the maximum extinction angle indicates normal zoning from An_{58} at the core to An_{30} at the edge. Limpid albite occurs in jagged edges around most of the feldspar laths. No fresh olivine or serpentine pseudomorphs are found.

Specimen V 157 was collected 200 feet from the main ultrabasic contact north of the village of Meliau. The thin sections show a microphyric texture; microlites of feldspar and clinopyroxene occur set in a turbid brown glassy groundmass. Small phenocrysts of extremely turbid feldspar occur together with sparse laths of altered clinopyroxene. The feldspar is so altered to granular epidote that it is difficult to obtain an accurate optical determination but nZ is lower than 1.54 indicating an albitic composition. Pale green chlorite, and chlorite showing anomalous blue interference colours are present replacing clinopyroxene. Veins of calcite up to 2 mm. in thickness are present in an irregular network.

Specimen V 70 was collected close to the ultrabasic contact in the Meliau stream section. The basalt at the exposure is interbedded with chert and mudstone. In thin section the rocks shows a megaphyric texture consisting of a groundmass of denticulate albite laths (nZ less than 1.54) 0.01-0.05 mm. in length. The laths are set in a turbid brown groundmass. A glassy orange brown mineral, resembling

spinel, is also prominent in the groundmass. The feldspar laths contain a central rod of titanite. A few extremely cloudy phenocrysts of feldspar up to 4 mm. long occur showing weak albite twinning. Optical measurements indicate the phenocrysts are also albite. Small patches of relict plagioclase can be made out in the core. Veins of calcite are prominent and irregular intergrowths of albite and quartz occur.

Specimen V 163 was collected from the Ruku-Ruku pillow lava and in thin section is seen to have aphyric texture. It consists of minute laths of albite(nZ less than 1.54) set in a turbid brown glass. Clinopyroxene microliths are extremely rare. Numerous veins of calcite and amygdales are present. The latter, 0.02-0.05 mm. in diameter are filled with clear quartz, calcite and green chlorite.

Specimen V 170 is the unusual black vitreous rock probably forming a selvedge to a dyke. The thin section shows phenocrysts of clinopyroxene and feldspar set in a black isotropic tachylitic glass. The latter shows fine flow structure and in places is altered to greyish palagonite. The feldspar occurs as plates and laths up to 2 mm. long, shows albite twinning, well developed prism facies and is strongly zoned from An_{56} at the core to An_{32} at the margin. Clusters of radiating feldspar laths are common. The clinopyroxene occurs as colourless sub-euhedral and euhedral crystals, .05 mm. in diameter, showing only slight alteration to green chlorite. The clinopyroxene has nY = 1.685 and 2V = 48° indicating a diopsidic augite. Numerous amygdales are filled with green chlorites, zeolites and calcite.

Chemistry.

An analysis of basalt from the Karamuak river is quoted by

Fitch (1958 p.78 Table 8 No. NB 1667) and is shown in Table 2, where it is compared with the average spilite of Sundius (1930). The Karamuak basalt is lower in titania and shows a greater magnesia to iron ratio, than the average spilite. The soda values are however comparable. Relatively high titania is a feature of most spilites. Rheinhard and Wenk (1958 p.76) quote spilite analyses from other parts of Borneo two of which potash values comparable with published keratophyre analyses (loc.cit. No.St.189, J 154). Keratophyre has not been noted in the Tawai area. In describing the potash-rich sample the authors do not mention the presence of orthoclase feldspar but only record the presence of albite, pyroxene, amphibole and glass. This may be of significance for the potash could well be present in the glass. Fenner (1931) describes black glassy selvedges rich in potash from pillow lavas. The black glassy specimen, V 170, from the Tawai area may therefore be potash-bearing.

The analyses given by Rheinhard and Wenk and that quoted by Fitch are plotted in Fig. 13. In the FeO-MgO-Na_2O+K_2O triangle it is seen there is a general decrease in MgO with increasing alkalies, the trend being most marked in the keratophyres. This general trend is accompanied by an increase in silica. No general trend however can be found in a plot of the analyses on an Na:Ca:K diagram.

Petrogenesis.

The chert, spilite, mudstone group belongs to a peculiar suite of rocks found in many other parts of the world associated with the early development of geosynclines. This suite of rocks is

Table 2. Basalt analyses.

	NB 1667	Average Spilite
SiO_2	49.94	51.22
TiO_2	0.41	3.32
Al_2O_3	13.68	13.66
Fe_2O_3	2.71	2.84
FeO	6.93	9.20
MnO	0.26	0.25
MgO	8.50	4.55
CaO	7.66	6.89
Na_2O	4.11	4.93
K_2O	0.56	0.75
H_2O^+	2.88	)1.88
H_2O^-	0.57	)
CO_2	tr	.94
P_2O_5	1.91	0.29
Cr_2O_3	nil	
NiO	0.06	
Total	100.18	100.72

N.B. 1667 From near mouth of Malung River. Karamuak. Fitch. (1958 p. 78 Table 8).

Average Spilite, Sundius (1930 p. 9).

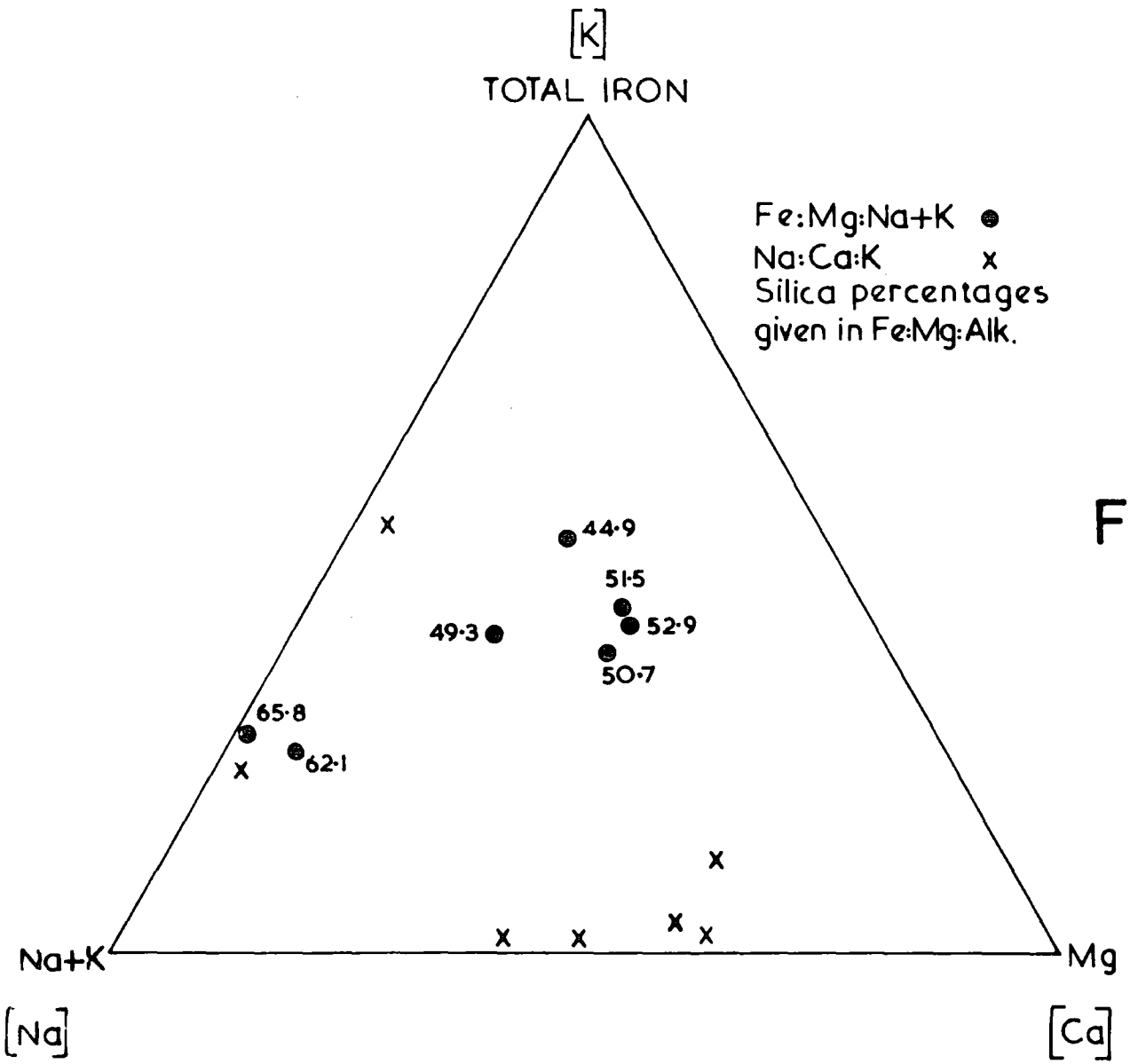

Fig. 13.

Chemical data of North Borneo spilites and keratopyres.

characterised by spilitic lava, usually showing pillow structure, and is invariably associated with radiolarian chert. The origin of both the chert and the spilite are the subject of considerable controversy. The pillow structure seen in the volcanic rocks indicate they were extruded under water. In the past it has been claimed, notably by Steinmann (1905), that the associated radiolaria cherts are indicative of deep water conditions.

In the Mount Tawai area there is a close association between chert and spilite. Thick cherts are absent from the sandstone-shale facies, and only occur interbedded with spilite. Davis (1918) also noted this association in other areas and concluded that the silica of the chert was introduced to the sea floor by siliceous springs accompanying volcanism. Sea water contains only 4 parts per million of silica and although this concentration may be slightly boosted by addition from river water it must remain doubtful that direct precipitation could account for the large amount of chert present and addition of silica from an outside source seems necessary. The presence of porous cherts resembling siliceous sinters found in the Tawai area points very strongly to the past existence of volcanic springs. If this is the case then it seems unnecessary to invoke a deep water origin for the cherts. The part played by the radiolaria is not clear, possibly they aided precipitation of chert from the siliceous solutions by a biochemical process or it may be that the organisms thrive in a silica-rich environment.

The very fine grained limestones associated with the chert resemble inorganic precipitates. Specimen S 338 although now made of calcite, resembles aragonite mud. Such deposits are at present being formed on the Great Bahama Bank at a depth of only twenty feet.

The presence of these deposits would suggest a shallow water origin, but the absence of current bedding argues against it. In general the sediments of the volcanic facies are extremely fine grained but coarse clastic sandstones are also present at infrequent intervals. The overall evidence suggests a depositional environment in which little sediment was being laid down but which was occasionally subject to influx of coarse clastic material. The pillow structure in the basaltic and spilitic rocks indicate they were laid down under water in this environment. The origin of spilites involves one or other of the following hypotheses:-

(1) Alkali metasomatism of basalt.

(2) Autometamorphism of basalt.

(3) Differentiation of basalt under hydrous condition.

(4) Differentiation from a spilitic magma.

The arguments for and against these hypotheses are well known and are ably summarised in Turner and Verhoogen (1960 Chapter 10). The petrographic evidence from the Tawai spilites suggest they have been derived by alteration of tholeiitic basalt. In the unaltered basalt specimens the feldspar is labradorite, pigeonite microliths are present in a glassy groundmass and olivine is absent, all of which indicate tholeiitic basalt. In the spilite and altered basalts albite can clearly be seen replacing calcic plagioclase. The unaltered specimens occur in the western part of the main volcanic area and are not interbedded with sediments. The field evidence suggests a thick pile of flows quickly deposited in an area of non-deposition. In the Telupid and Meliau river sections sediments

are found interbedded with partially albitised basalts and spilite. The field and petrographic evidence therefore argues against hypotheses (3) and (4) and a process involving metasomatism or autometamorphism must be invoked. The latter may be discounted for the normal basalts, although showing pillow structure, are not spilitic. The greywacke sandstone and mudstone which are interbanded with the spilites contain sodic plagioclase and when deposited they were probably impregnated with sea water. It is possible that during the extrusion of the basaltic magma complex reaction between sea water, sediments and magma led to the contamination of the latter with consequent alteration of the plagioclase to albite. Further complications may be envisaged if at the same time siliceous springs were discharging into the area. Eskola et.al. (1937) has shown that at temperatures below 330°C and confining pressures of 220 bars anorthite reacts with sodium carbonate and silica in a closed system to give albite and calcite. In the Tawai basalt labradorite has been altered to albite and therefore is equal volume relations are maintained introduction of sodium and silicon require removal of calcium and aluminium according to the following general equation:-

$$NaCaAl_3Si_5O_{16} + Na^{+} + Si^{4+} = 2\ NaAlSi_3O_8 + Ca^{+1} + Al^{3+}.$$

The abundance of calcite, zeolite and epidote in the altered basalt suggests such an hypothesis. Manganese wads and lenticles are always found close to the spilites suggesting derivation from the basaltic magma during alteration. It is possible that the manganese has been derived from breakdown of the ferromagnesian minerals.

The overall evidence suggests that the spilites have been derived by metasomatism of tholeiitic basalt extruded into a soda

rich environment. The present outcrop of the basaltic rocks in the Labuk, Fig. 3, suggests that they were deposited in a long thin trough, bordered on either side by an environment in which the sandstone-shale facies was deposited.

THE METAMORPHIC ROCKS OF THE MOUNT TAWAI AREA.

Distribution and Field Occurrence.

Metamorphic rocks are found only rarely in the Mount Tawai area. Isolated blocks of schist, quartzite and calc-silicate occur in places in the contact fault zone around the margins of the batholith and occasionally as inclusions within the peridotite. The largest concentration of blocks is found in a narrow belt along the southern contact of the Patud-Gombaran intrusion and is exposed by the Meliau river (Fig. 14). The river Meliau flows through this intrusion in a prominent gorge, at the northern end of which unmetamorphosed basalt is seen faulted against peridotite. However immediately on emerging from the southern end of the gorge blocks of metamorphic rocks are found exposed in the bank of the river. They occur in all attitudes and are confined to a narrow belt less than a thousand feet wide and about two and a half miles long. Some of the blocks are up to two hundred feet in length and are of a composite nature. They are surrounded by strongly brecciated peridotite and local country rock.

A large block of striped amphibolite is found at the southern end of the Meliau gorge and can be traced for up to a hundred feet on either side of the river. It is faulted against the peridotite; and the foliation suggests that it dips at a high angle underneath the peridotite. The foliation is due to layering of alternate hornblende and feldspar-rich bands. Occasional coarse half inch feldspathic bands occur, as in specimen T 35, and four green streaks of calc silicate minerals were found parallel to the foliation.

Further upstream at the section marked C - D on the map, Fig.14,

Fig.14.

GEOLOGICAL SKETCH MAP OF PART OF THE MELIAU VALLEY

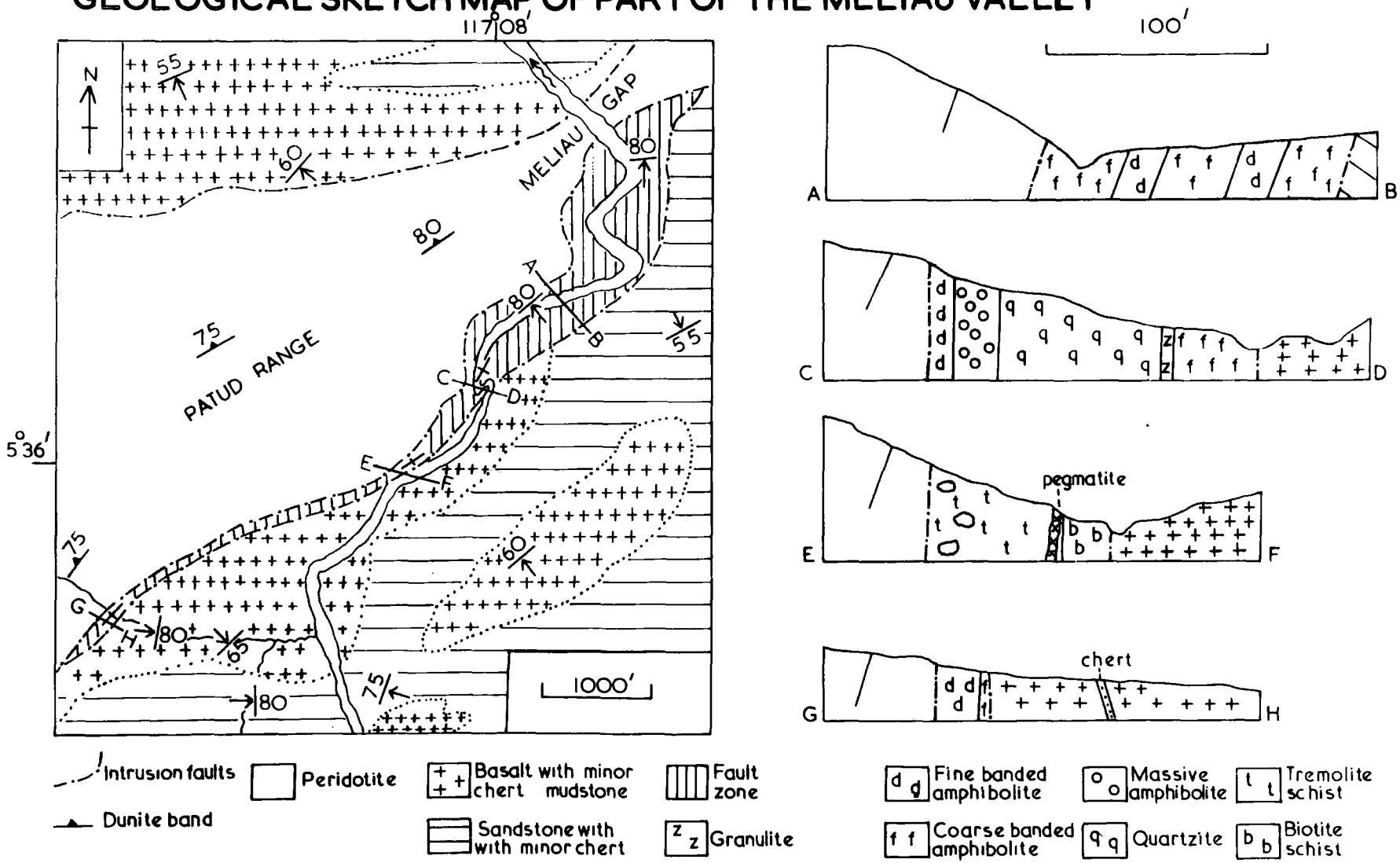

a composite block of quartzite and amphibolite is seen exposed in a sinuous gorge. The following succession was measured and is shown in Fig. 14.

Peridotite

6'	Finely banded amphibolite	- Specimen T59
22'	Massive banded amphibolite	- Specimen T69
86'	Banded quartzite	- Specimen T61
2'	Garnet granulite	- Specimen T60
60'	Coarse banded amphibolite	- Specimen T67

The finely banded amphibolite is faulted against the peridotite. The contacts between the metamorphic rocks are gradational except for that between the massive amphibolite and the banded quartzite which is knife sharp. The foliation in the quartzite and the amphibolite is striking N 12°E and is almost vertical.

At the section marked E - F on the map twenty feet of a black chlorite schist, Specimen T61, is seen faulted against a blue grey corrugated amphibolite, specimen T62. The latter is intermingled in a complex breccia with massive hornblendite, Specimen T66. A thin quartz pegmatite is intrusive into the metamorphic rocks. The chlorite schist shows many minor puckers and contains thin bands of quartz. Peridotite is exposed fifty feet away to the west of the chlorite schist but the actual contact is not exposed.

In a small west bank tributary of the Meliau thirty feet of finely banded amphibolite is found faulted against peridotite at the section marked G - H on the map. The amphibolite shows many minor corrugations and contain patches of chalco-pyrite. The block appears to be dipping 85° to the east.

Fig. 15. Photograph of finely banded amphibolite T59.

Fig. 16. Photograph of coarsely banded amphibolite T35.

Between the above mentioned exposures sporadic blocks of amphibolite, mainly of the finely banded type, are found. No common direction could be deduced for the foliation within the separate blocks.

In the headwaters of the Upper Binalik river numerous small blocks of amphibolite and quartzite, seldom exceeding six feet by eight feet, are found in the contact fault breccia. The amphibolites are mainly of the finely banded type but one coarse massive specimen, T408, was found. The quartzites have a sugary appearance, as in Specimen T347, and do not show the fine banding seen in the Meliau specimens.

Occasional fragments of amphibolite and quartzite are found within the peridotite. They seldom exceed a few feet in diameter and do not show any significant distribution pattern.

Petrography.

Striped amphibolites are the commonest of the metamorphic rocks found. The following assemblages have been determined.

Hornblende-andesine-diopside-epidote	-	Specimen T59
Hornblende-andesine-diopside-quartz	-	" T35
Hornblende-epidote	-	" T69
Hornblende-labradorite	-	" T408

The first type is the most common and consists of extremely fine bands of alternating feldspar- and hornblende-rich layers. Prominent greenish yellow bands, 4 - 6 mm. wide, occur at irregular intervals (Fig. 15). The feldspathic and hornblendic bands merge into each other but the yellowish bands are sharply defined. The

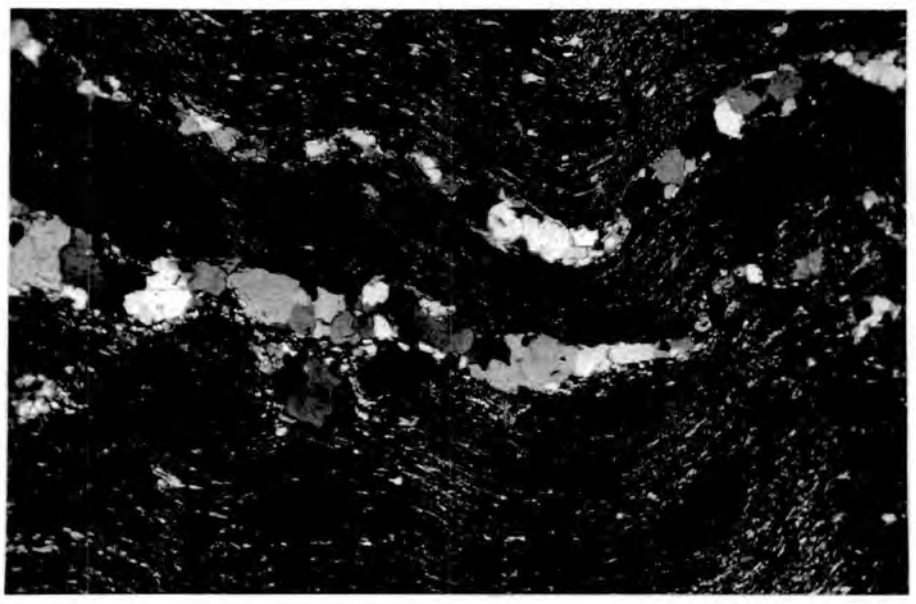

Fig. 17. Photomicrograph, and hand specimen, of metamorphosed shale. The original quartz bands of the sediment are clearly seen in the thin section.

leucocratic bands consist mainly of andesine with minor hornblende. The feldspar shows little dimensional orientation. The dark bands consist of elongate green pleochroic hornblende (nZ = 1.66), 0.1 - 2mm. long, yellowish epidote and minor plagioclase. The yellowish bands are composed mainly of interlocking strongly birefringent epidote 0.1 to .4mm. in diameter. Laths of clinozoisite, showing anomalous interference colours, and green diopside are also present. Elongate sphenes are prominent in the epidote-rich bands.

The second assemblage is found in the more coarsely banded amphibolites (Fig. 16) which are characterised by half inch thick bands of strongly saussuritised andesine and pale green clinopyroxene. The clinopyroxene occurs in irregular elongate-shaped crystals up to 10mm. in length, containing numerous rounded inclusions of saussuritised plagioclase in a prominent sieve texture. Irregular elongate crystals of strongly altered plagioclase up to 8mm. in length occur in these bands. The rest of the rock consists of alternating bands of feldspathic and hornblendic layers, the parallel alignment of the hornblende outlining the foliation. The hornblende of specimen T35 has nZ = 1.680 and shows the following pleochroic scheme.

Z - Dark green

Y - Grass green

X - Pale yellowish green.

Rounded and elongate patches of brownish chlorite suggestive of replaced garnet are present but the latter mineral has not been observed in the amphibolites. Numerous rounded and anhedral crystals of zircon and apatite occur often in tracings parallel to the foliation. Ilmenite-magnetite streaks sometimes parallel the

foliation.

Specimen T69 is a massive banded amphibolite consisting of dark green pleochroic hornblende laths up to .5mm. in length, with nZ = 1.673, and irregular layers of elongate epidote. The hornblende crystals show a crude preferred orientation parallel to the foliation. Opaque minerals are almost absent from this rock.

Specimen T408 is a massive banded amphibolite consisting of over sixty per cent green pleochroic hornblende; with nZ = 1.691. The rock is extremely fresh and the plagioclase present, labradorite, is only slightly altered. The hornblende shows many euhedral faces and a rough preferred orientation parallel to the foliation. Rounded apatite and oval sphene form prominent trains of crystals parallel to the foliation.

Quartzites are represented by specimens T61 and T347. T61 in hand specimen is a finely banded purplish grey quartzite that breaks easily into flags. The thin section shows it is a mica quartzite, the groundmass consisting of interlocking strong strained quartz with extremely crenulate grain boundaries. Strongly saussuritised plagioclase laths are present in the groundmass. Trains of muscovite and brown pleochroic biotite (.01 - .05 in length) outline the foliation. The accessory minerals present are rounded and anhedral zircon, apatite and titanite.

Specimen T347 is an unbanded feldspathic quartzite. The thin section shows coarse rounded, oval, and irregular crystals of oligoclase in a fine grained matrix of quartz and feldspar. The groundmass contains numerous flakes of unorientated faintly green pleochroic amphibole. The feldspar crystals show faint polysynthetic twinning and normal zoning. The groundmass consists mainly of quartz grains

.01 - .1mm. in diameter, which are interlocking but do not show the highly crenulate margins seen in T61. Small anhedral grains of apatite are present in the groundmass and as inclusions in the feldspars.

The garnet granulite, specimen T60, in hand specimen, is a hard grey glassy-looking rock with microfolded trains of ferromagnesian minerals and small pinkish garnets. Irregular bright green patches up to 4 inches long also occur within the granulite. The thin section shows a groundmass consisting of intensely strained quartz with intimately interfering outlines. Bands consisting of 'streaky' quartz alternate with less deformed bands and impart a foliation to the rock. Small laths of extremely altered feldspar are present in the groundmass. Trains of green pleochroic hornblende, nZ = 1.675, and pink garnet are arranged in a foliation oblique to that of the quartz. Anhedral zircon and apatite also occur accompanying this latter foliation. The garnet occurs in pale pink anhedral crystals, .1 to .5mm. in diameter showing extremely corroded margins. It has N = 1.777 and a_o = 11.53 which according to the charts of Srirmadas (1957) indicates a composition intermediate between pyrope and almandine.

The green patches contain anhedral laths of clinopyroxene 0.1 - 1mm. in length, and pale yellow epidote together with extremely ragged garnet. Small elongate sphenes are also found in these patches. Veins of calcite cut both the quartz and hornblendic foliations. The clinopyroxene has cell dimensions a sin β =9.413 and b_o=8.952 which according to the chart of Brown (1960) indicates a composition of $Ca_{45}Mg_{32}Fe_{23}$.

Specimen T64 is a black chloritic schist with a finely corrugated

Fig. 18. Photomicrograph of massive amphibolite T66.
(crossed nicols X20)

structure. The thin section, Fig. 17, shows numerous microfolds. The rock consists mainly of small laths of brown pleochroic biotite and pale green chlorite with their long directions aligned parallel to the foliation. Large laths of chlorite can be seen growing through and against the foliation. The chlorite has $n_Z = 1.665$ and slightly oblique extinction and is probably a ripidolite. Black granular amorphous material probably graphite outlines the foliation. Thin bands, .2 - .5mm. wide, of interlocking quartz are present. These are parallel to the foliation and are also thrown into microfolds.

The light blue amphibole schist, specimen T62 also has a markedly corrugated appearance in hand specimen. The thin section shows the schist to consist of a felt of fine, light brown non-pleochroic needles of amphibole orientated with c parallel to lineation of the rock. The amphibole has $n_Z = 1.639$ and extinction angle $Z \wedge 15^\circ$. The light blue colour of the rock in hand specimen is suggestive of a soda amphibole and a partial analysis was therefore made, with the following result:-

MgO	-	23.6
CaO	-	11.2
Al_2O_3	-	2.0
Total Fe	-	7.7
Na_2O	-	0.4
K_2O	-	tr.

The result indicates the mineral is a tremolitic amphibole. Pods of chlorite and streaks and trains of ore minerals outline the foliation. The chlorite pods consist of a fine unorientated felt containing stringers of tremolite. Minute octahedra of chromite

may be recognised amongst the ore minerals indicating that this schist has been derived from the ultrabasic rocks.

The massive amphibolite, specimen T66, which is found intermingled with the tremolitic schist is made of randomly orientated stout laths, up to 2cm. long, of dark green hornblende with a little interstitial feldspathic material (Fig. 18). A thin section shows most of the laths to be composed of a deep green pleochroic hornblende but a few show hornblende replacing a pale green pleochroic mineral, possibly pyroxene. The laths show numerous minor corrugations and determination of their optical properties is difficult. The leucocratic patches between the laths are composed of oligoclase, showing polysynthetic twinning and normal zoning, and quartz. Numerous small needles of hornblende are present in the feldspar together with small patches of olive coloured mica. Small crystals of chalcopyrite occur in the hornblende laths.

Chemistry.

The finely banded amphibolite T59 has been analysed and the result and norm are given in Table 3. In the same table it is compared with average alkali basalt, average tholeiitic basalt, and average spilite.

The amphibolite analysis is not directly comparable with any of these types. The main difference lies in the high lime content of the amphibolite which is a reflection of the high percentage of epidote present in the rock. The soda content is also higher than that of the average basalts but comparable with that of the average spilite.

Table 3. Analysis of Amphibolite.

	T59		Tholeiite		Alkali Basalt		Spilite
SiO_2	50.1		51.33		46.14		51.22
Al_2O_3	13.9		14.21		14.75		13.66
Fe_2O_3	2.3		2.91		3.18		2.84
FeO	8.7		9.09		8.80		9.20
MgO	4.6		6.40		9.46		4.55
CaO	12.6		10.52		10.82		6.89
Na_2O	4.5		2.25		2.65		4.93
K_2O	0.5		0.83		0.96		.75
H_2O^+	0.7						) 1.88
H_2O^-	0.1						)
TiO_2	1.1		2.05		2.65		3.32
P_2O_5	.2		.23		.39		
	99.3	(a)	100.00	(b)	100.00	(c)	100.00
or	3.34						
ab	25.15						
ne	7.10						
an	15.85						
di wo	18.91)						
di en	9.00)	37.55					
di fs	9.64)						
ol fo	1.75)						
ol fa	2.04)	3.79					
mt	3.25						
il	2.13						
ap	.34						

a - Average tholeiite - Nockolds (1954) includes .22 MnO.

b - Average alkali basalt Nockolds (1954) includes .18 MnO.

c - Average spilite Sundius (1930) includes 125 MnO al .94 CO_2.

T59 Analyst W.G. Hancock. Location 5° 36' 22" N 117° 07' 52" E. R. Meliau.

Petrogenesis.

The metamorphic rocks include undoubted examples of paraschists and paraquartzites. The chlorite biotite schist is clearly a metamorphosed shale. Original quartz bands can still be seen in the thin section. The mica quartzite and the feldspathic quartzite almost certainly represent metamorphosed flaggy sandstone and greywacke respectively. The garnet granulite with calc-silicate patches is suggestive of a metamorphosed impure sandstone with calcareous intercalations.

The origin of the amphibolites is more controversial. Engel and Engel (1951) suggest that nearly identical hornblende amphibolites, in which andesine is a major constituent, may evolve from metamorphism of tuffs and marls, gabbro masses, and basalt flows.

The chemical evidence of the analysed amphibolite is not conclusive but the high lime content suggests a sedimentary rather than igneous origin. The amphibolites in the Meliau metamorphic area are interbanded with undoubted paraschists and paraquartzites, and they contain green streaks of calc-silicate minerals that may be interpreted as metamorphosed impure limestones. This evidence together with the trains of detrital minerals in the amphibolites suggests a sedimentary origin. The high percentage of epidote in the amphibolites suggests derivation from calcareous shales. Harker (1956) indicates that epidote is a characteristic product of such assemblages.

Smith (1958) describes a finely banded calcic hornfels at the contact of the Bay of Islands ultrabasic intrusion. The country rocks are sandstone and shale and Smith suggests that a considerable lime metasomatism took place from the peridotite to the sediment to

account for the lime-bearing minerals present. Turner and Verhoogen (1951) quote other examples of metamorphism of non-calcareous sediments to calc-silicate rocks at peridotite contacts. The extremely low lime content of the peridotite however argues against a metasomatic origin for the lime.

Not all of the amphibolites are epidote bearing. Specimen T408 in addition to hornblende contains labradorite and may possibly be of igneous origin although trains of detrital minerals seen in the thin section argue against this. The massive amphibolite, T66, may also be of igneous origin. The tremolite schist with which it is intermingled is probably derived from the peridotite but this implies introduction of lime. A small pegmatite intruded into the contact zone may have supplied this.

The overall evidence suggests that the bulk of the metamorphic rocks represent a series of shale, feldspathic sandstones, impure sandstones, and impure limestones that have been metamorphosed. The fine banding seen in the metamorphic rocks is considered to be controlled by the original sedimentary bedding. The possibility that one or two of the amphibolites were of igneous origin cannot be ignored. The metamorphosed assemblages represent grades varying from green-schist to amphibolite facies.

The metamorphic rocks found in the contact zones around the batholith may be interpreted as follows:-

1. Faulted up inclusions of a crystalline basement rock.
2. Faulted up remnants of a thermal aureole formed by the intrusion of the ultrabasic rocks in depth.

Strong thermal metamorphism is rarely associated with peridotite

intrusions. It is only recently that Mackenzie (1960), Smith and Macgregor (1960) and Green (1964) have demonstrated high temperature peridotite intrusions. The metamorphic aureole associated with the Mount Albert peridotite (Quebec), described by Smith and Macgregor, ranges from green-schist, through epidote amphibolite to garnetiferous hornblende pyroxene granulite. It is significant that these assemblages are almost identical to those found in the Mount Tawai metamorphic rocks. The local Eocene sediments and volcanics of the Mount Tawai area contain many rock types that if metamorphosed would give a series of paraschists similar to those found in the contact zone. Representatives of metachert and metaspilite have not been found in the present survey but Fitch (1958) has found the former at a similar contact on Malawali Island and Kirk (personal communication) has located glaucophane bearing metabasalt in the Labuk area. It is therefore possible that the base of the Eocene was metamorphosed by the peridotite. Unfortunately similar rock types as those found in the Eocene occur in nearly every formation as far back as the Triassic in the Borneo succession and therefore no definite conclusions as to the age of the postulated metamorphism can be reached. The alternative hypothesis that the metamorphic rocks represent fault inclusions of the crystalline basement cannot be ruled out. It is however noteworthy that granite gneiss, so typical of basement rocks, is not found in the fault zones. Gneiss does occur in the recognised basement rocks exposed in central Borneo.

The suggestion is then that the metamorphic rocks are representative of the original thermal aureole of the peridotite. The highest metamorphic grade recorded in the assemblages is best

placed in the almandine amphibolite facies which according to Turner and Verhoogen (1960) indicates a temperature range of perhaps 550° to 750°C. This temperature is greater than that of the stability range of serpentine and if accepted would indicate that serpentinisation occurred afterthe postulated metamorphism. The temperature range of the amphibolite facies is however well below that of any possible ultrabasic magma and suggests that the peridotite at the time when metamorphism took place was a hot but largely crystallised intrusive body.

THE ULTRABASIC AND BASIC INTRUSIVE ROCKS OF MOUNT TAWAI.

General Features.

The ultrabasic and basic plutonic rocks form an area of rugged mountainous relief approximately twenty five miles long and ten miles wide. The basic plutonic rocks comprise only a minor fraction of the batholith. The batholith is built mainly of enstatite perdiotite. Subordinate amounts of dunite and pyroxenite occur in interesting field situations that tend to offset the monotony of the harzburgite outcrops. A well developed stream system drains the batholith and provides excellent exposure in the valley bottoms. The knife-backed interfluves between the streams only support a thin vegetation and a great deal of the rock material exposed on the valley sides is of a slipped nature. Many valley sides are built completely of loose blocks of peridotite with trees growing up between them. Large landslides are frequent and the more recent ones have stripped clear large areas of trees and rocks leaving the bare hillside exposed. The ridges contain many exposures often in tor-like masses of peridotite. It is only on the Tawai plateau that normal geological mapping is not possible.

The Structure of the Batholith.

Most of the large peridotite bodies of the world have been affected by numerous zones of internal rupture and shearing. The Mount Tawai peridotite is no exception to this general situation and the widespread and often chaotic disturbed zones within and around the margins of the mass often tend to obscure the major structure. Any theory with regard to the general structure of the Mount Tawai peridotite must explain the north-south elongation of the mass, the steep south face of Mount Tawai, the Tawai plateau, and the

great curve on the Patud-Gombaran range.

The contact relations.

The peridotite batholith is surrounded on all sides by rocks of Upper-Cretaceous and Eocene age. The sedimentary rocks on the east, south, and south-western margins of the peridotite have a regional east-west strike which is markedly discordant to the roughly north-south elongation of the batholith. In this respect the Mount Tawai peridotite is markedly different from the so-dalled 'Alpine type peridotites', of Thayer (1960) where the direction of elongation is usually subparallel to the trend of the surrounding rocks. On the north-western margins of the batholith rocks interbedded with mudstone and chert occur but their regional characteristics could not be determined.

A faulted relationship between the peridotite and the surrounding country rocks has been revealed by close examination of the contact zones around the margins of the batholith. As the ultrabasic contact is approached dips in the country rock steepen sharply. Silicification, calcification and general alteration of the country rock increase. There is however no evidence of <u>in situ</u> thermal metamorphism of the country rock. All the contact zones observed show that both the peridotite and the country rock have been strongly disturbed and that they are often separated by a wide fault breccia. The latter consists of intermingled and strongly pulverised country rock and serpentinite. Towards the ultrabasic side of the contact the fault breccia grades into sheared serpentinite which in turn grades into massive peridotite or serpentinite. The sheared serpentinite is traversed by closely spaced parallel planes of slip.

Fig. 19. Photograph of Patud Range from Bauto. The swing of the Patud Range is clearly seen. River Labuk in the foreground.

The best exposures of the fault breccias are found in the stream sections, particularly those on the eastern side of the batholith. Along the line of the contact between stream sections the peridotite rises in steep cliffs containing abundant slickensided surfaces and inclusions of unmetamorphosed country rock. Clearly the peridotite has been emplaced by faulting. No evidence has been found of Tertiary sediments unconformably overlying the peridotite.

The contact faults are remarkable in thzt they do not extend out into the country rocks and as far as is known they do not form part of a regional fault pattern. It would seem unlikely that such a large body of peridotite could be intruded up a fault plane. The wide nature of the Labuk ultrabasic batholith belt (Fig. 3), and the many varied surface outcrop shapes also argue against this. The faults around the margins of the Tawai batholith must be considered as intrusion faults. Small fractures in the country rock en-echelon to the contact are numerous but of a small discontinuous nature.

The northern and north-western margin of the batholith is clearly defined by an arcuate intrusion fault that runs from the mouth of the river Melio northwards to the Labuk river where it swings eastward along the southern bank of the Labuk (Fig. 19). The country rock flanking the peridotite in this area is mainly basalt interbedded with chert and mudstone. Near the intrusion fault the basalt becomes markedly streaky and veined by calcite and quartz. When the Telupid river crosses the intrusion fault 140' of brecciated basalt is seen a few feet away from sheared serpentinite (Figs. 20, 20a). The latter is striking N 40° E and dipping 75° to the northwest. The sheared serpentinite is strongly silicified and intruded by veins of calc-silicate minerals. A similar contact zone is

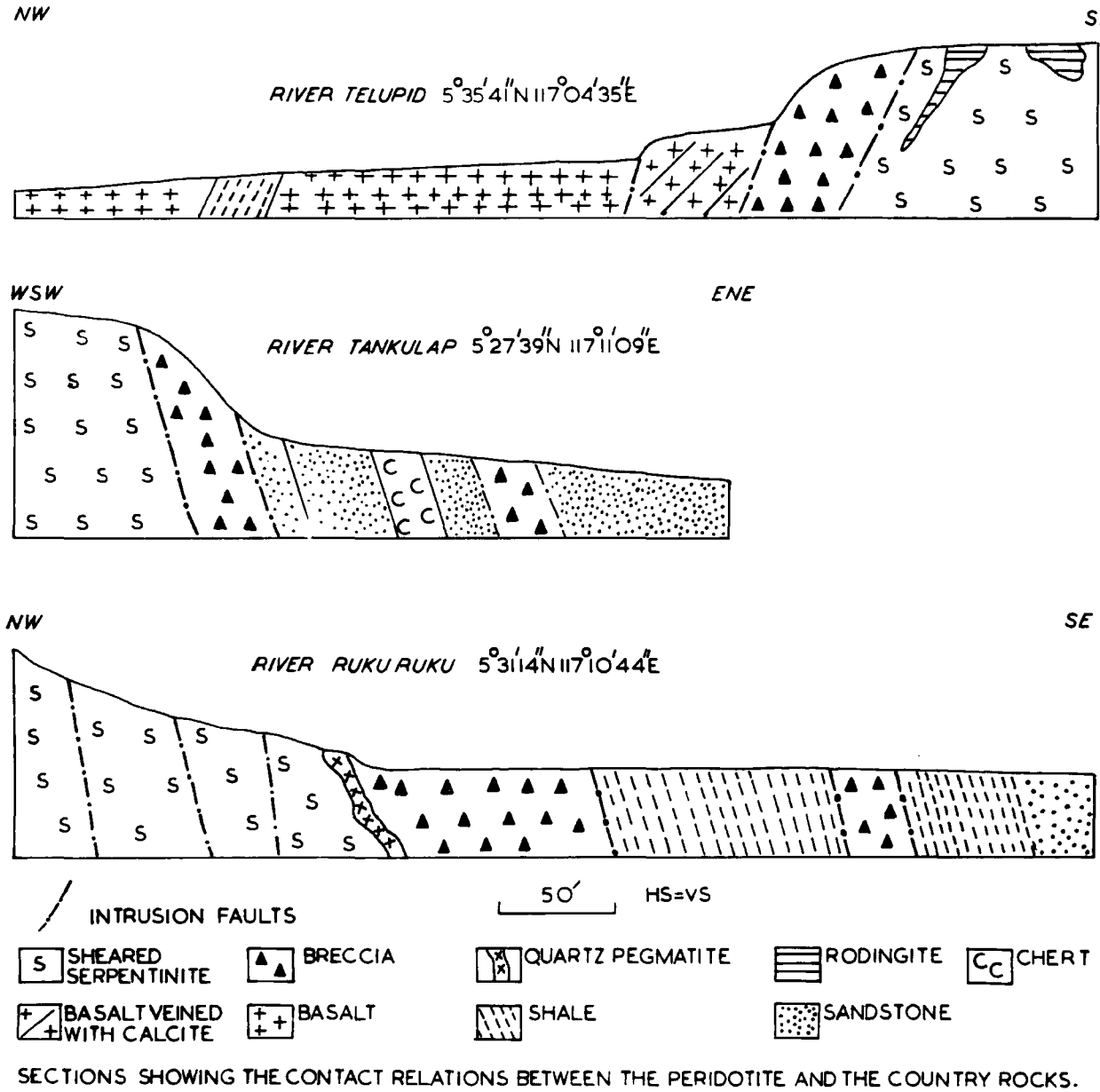

SECTIONS SHOWING THE CONTACT RELATIONS BETWEEN THE PERIDOTITE AND THE COUNTRY ROCKS.

Fig. 20.

Fig. 20a. Photographs of the peridotite contact.
Above, Telupid river.
Below, Tankulap river.

exposed on the Melio river where the basalt is strongly brecciated and impregnated with pyrite. At this locality the country rock is found extending into the peridotite as a thin wedge. One mile to the north of this exposure 30 feet of fault breccia is seen separating upturned red shale from sheared serpentinite. The contact is dipping between 75° and 85° west. Due west of Mount Patud the contact bulges westward before turning sharply eastward to the southern bank of the Labuk river. It is possible that the intrusion contact is offset in this region by a normal fault but it is difficult to prove owing to poor exposure. The intrusion fault is further exposed on the northern flank of the Gombaran range where the Labuk river flows in the contact zone. One mile to the east of the village of Kuala Meliau fractured basalt is observed against slickensided serpentinite. The contact is vertical and striking N 75° E. Between this exposure and the village of Bauto the southern bank of the Labuk is formed by steep cliffs of slickensided peridotite. These cliffs rise to 2,000' above the level of the river to form the Gombaran range.

On the southern side of the Gombaran range a long tongue of sedimentary and volcanic rocks six miles long and one and a half miles wide occurs, which separates the Gombaran range from the main batholith. This tongue is flanked on the north and south by intrusion faults. Along the southern edge of the Gombaran range upturned greywacke sandstone and recrystallised white chert are found at the base of a near vertical wall of slickensided peridotite. At the extreme western end of the tongue of sedimentary and volcanic rocks numerous blocks of metamorphic rocks are found in the contact zone which are discussed in detail elsewhere. On the southern

Fig. 21.

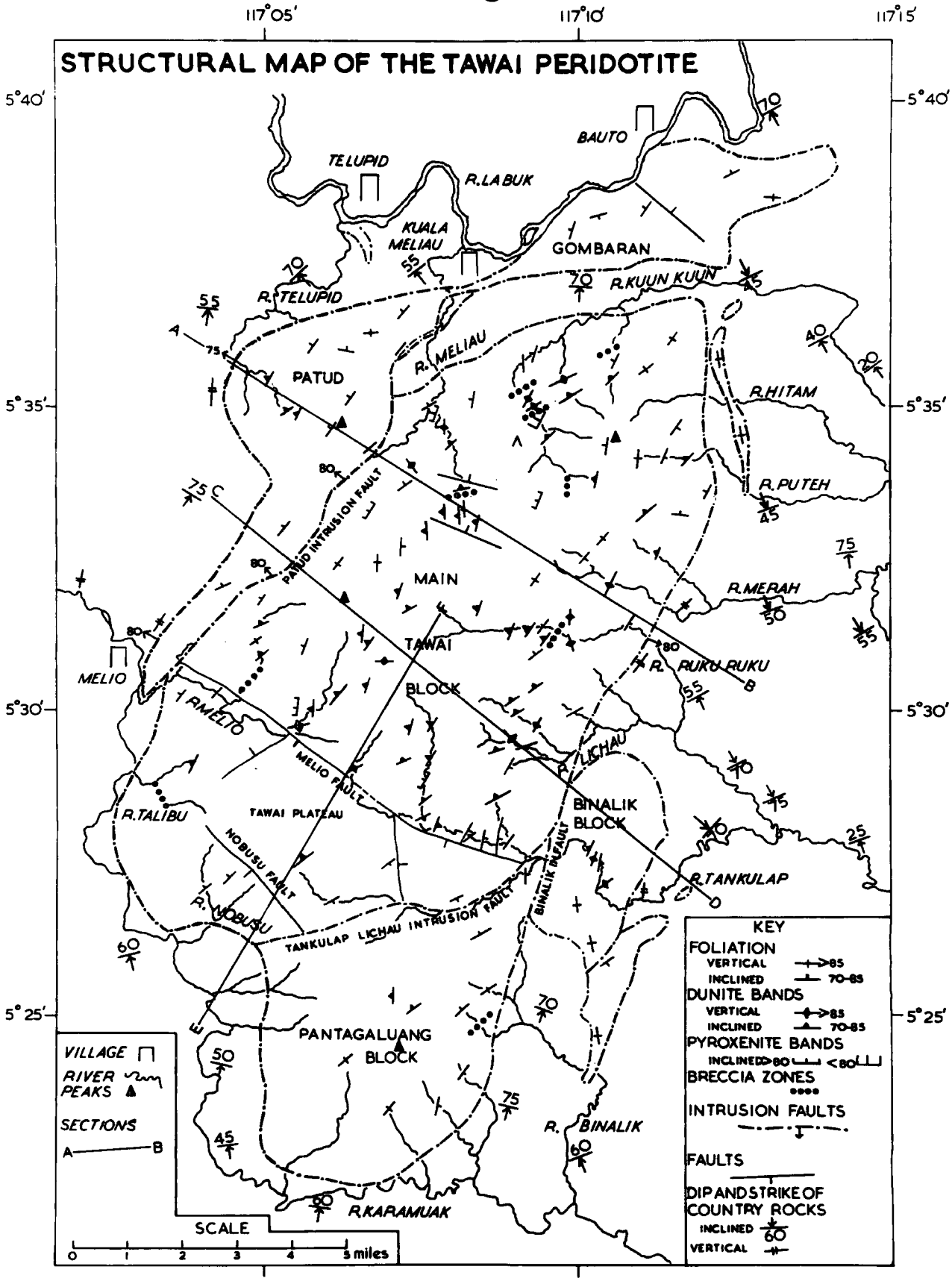
STRUCTURAL MAP OF THE TAWAI PERIDOTITE
117°05'
117°10'
117°15'
5°40'
5°35'
5°30'
5°25'
TELUPID
R. LABUK
BAUTO
KUALA MELIAU
GOMBARAN
R. KUUN KUUN
R. TELUPID
R. MELIAU
PATUD
R. HITAM
R. PUTEH
PATUD INTRUSION FAULT
MAIN
TAWAI
BLOCK
R. MERAH
R. RUKU RUKU
MELIO
R. MELIO
MELIO FAULT
R. LICHAU
BINALIK
BLOCK
R. TALIBU
TAWAI PLATEAU
NOBUSU FAULT
R. NOBUSU
BINALIK FAULT
R. TANKULAP
TANKULAP LICHAU INTRUSION FAULT
PANTAGALUANG
BLOCK
R. BINALIK
R. KARAMUAK
VILLAGE
RIVER
PEAKS
SECTIONS
A—B
SCALE
0 1 2 3 4 5 miles
KEY
FOLIATION
VERTICAL
INCLINED 70-85
DUNITE BANDS
VERTICAL
INCLINED 70-85
PYROXENITE BANDS
INCLINED >80 <80
BRECCIA ZONES
INTRUSION FAULTS
FAULTS
DIP AND STRIKE OF COUNTRY ROCKS
INCLINED 60
VERTICAL

Fig.21a.

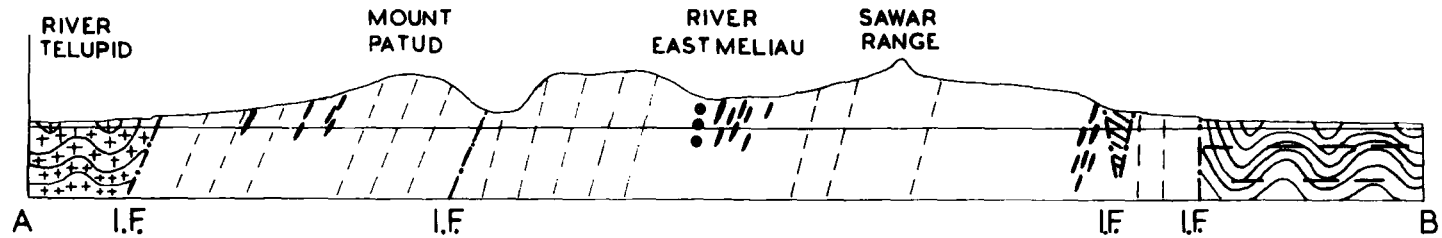

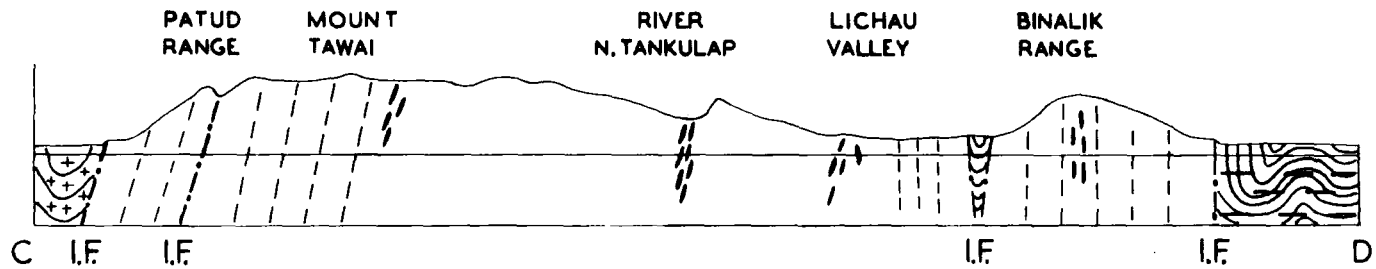

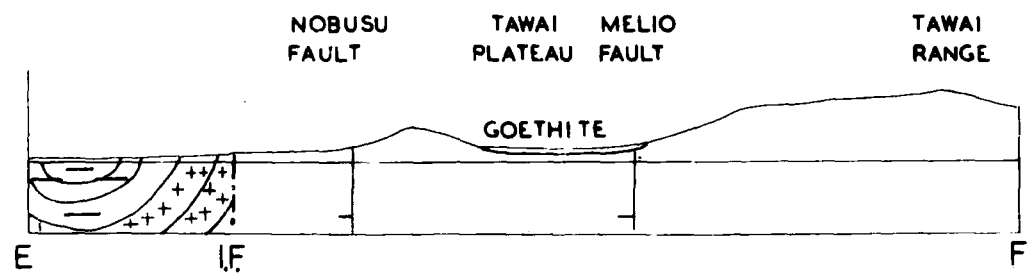

SECTIONS SHOWN ON FIG. **21.**

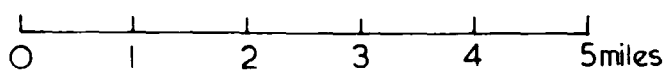

Horizontal scale = Vertical Scale. Symbols as in Figs. **11, 21.**

side of the tongue exposures are rare. Sheared serpentinite striking almost eastward and dipping steeply to the north is exposed in the contact zone by the main Kuun-Kuun river. East of the Kuun-Kuun exposure outcrops are rare and the contact has been mapped by the occurrence of peridotite field debris found in the swamp. The eastern flank of the main batholith between its northernmost point and the Lichau river is formed by a ten mile long intrusion fault trending between N 02° W and N 30° E. The country rocks on the eastern side of the batholith are mainly greywacke sandstone and shale and only minor outcrops of volcanic rocks occur. Five miles away from the contact they are striking almost east-west but as the peridotite is approached the dips steepen (from 25° to vertical) and the strike rotates to a north-east south-west direction. The contact zone on the eastern side of the batholith is well exposed in the Hitam, Merah, Ruku-Ruku and Lichau rivers. At the main contact on the Hitam river brecciated greywacke sandstone and brown manganiferous chert are seen in contact with sheared serpentinite. The latter is dipping steeply eastward (80 - 85°) and striking N 03° E. A similar contact is found just over a mile to the south of this exposure where the greywacke is broken up and veined by calcite. To the east of the main contact exposed in the Hitam river a five miles long elongate (quarter mile wide) lense of sheared serpentinite is located with its long axis roughly parallel to the elongation of the batholith. The contact zone around the sheared serpentinite lens contains vertical fractured greywacke sandstone. The best exposure of the contact zone is found on the Ruku-Ruku river where vertical red shale is seen separated from sheared serpentinite by a fault breccia two hundred feet wide

(Fig. 20), which contains angular fragments of serpentinite set in a soft red gouge. The fault breccia grades westward into sheared serpentinite. Close to the contact a quartz pegmatite is seen intrusive into it and bright green needles and plates of tremolite border the vein. The sheared serpentinite in the contact zone is dipping steeply eastward (75°- 85°) and striking N 07° E.

South of the Ruku-Ruku Lichau river system the straight N.E.-S.W. trending line of the main ultrabasic contact is interrupted by an irregular bulge of peridotite known as the Binalik ultrabasic block. At either end of the bulge thin wedges of brecciated sediments are found separating the main batholith from the Binalik block. The southern wedge is composed of a red shale gouge that contains numerous inclusions of metamorphic rocks similar to those found in the Meliau area.

Contact exposures around the Binalik bulge are rare. Vertical undurated greywacke sandstone and dark brown chert are observed at the base of a cliff of sheared serpentinite where the Tankulap river crosses the contact (Fig. 20). At the southernmost point of the long north-south trending prolongation of the Binalik block brecciated sandstone and shale are found enclosing a wedge of sheared serpentinite.

The main eastern contact intrusion fault passes between the Binalik block and the main batholith but in doing so splits into two main branches, one of which continues southwards as the Binalik intrusion fault. This fault forms the main eastern contact south of the Binalik bulge to the Karamuak river. The path of the intrusion fault is marked mainly by sheared serpentinite but in the southernmost tributary of the Binalik river a two hundred foot wide

breccia zone consisting of angular fragments of gabbro and serpentinite set in a fine red gouge is exposed. Numerous inclusions of unmetamorphosed red shale occur in the contact serpentinite.

Between the mouth of the Melio river and the Nobusu river the peridotite contact follows an irregular arcuate course striking N 10° E in the north and almost east-west in the vicinity of the Nobusu. The sheared peridotite at the contact on the Nobusu river is striking N 85° E and dipping steeply to the south. It appears to merge with the shear zone associated with a large internal intrusion fault. South of the Nobusu contact the sheared serpentinite is striking almost north-south in the contact zone and dipping steeply to the west.

All the observed contacts around the margins of the batholith dip very steeply and the contact phenomena show that the peridotite has been emplaced by fault intrusion. A wide zone of sheared serpentinite is always found on the peridotite side of all the main contacts. This zone may extend inwards for up to two miles and the small ultrabasic lenses off the east flank of the main batholith are made up completely of sheared peridotite. Inclusions of peridotite mylonites, which are exceptionally hard are common in the contact serpentinite zone. They are well exposed a few hundred feet inside the main contact on the Tankulap river where blocks of striped mylonite up to three feet in diameter are seen in the sheared serpentinite. The mylonitic banding of each block as a different orientation; and the blocks have obviously been rotated.

It is noticeable that the contact fault breccias are more strongly developed on the eastern side of the batholith. The

lithology of the country rock into which the batholith has been emplaced plays a dominant part in determining the width of the fault breccia zone. At greywacke sandstone contacts there is only a slight development of fault breccia whilst at shale contacts a wide zone of powdery gouge and angular fragments is found. Comparable shale contacts on the east and west flanks show however that the largest fault breccias are developed on the eastern contact.

The peridotite contact as defined on the map is therefore a complex series of intrusion faults. It is only when the internal fractures within the peridotite mass are examined that the different units of the batholith become apparent.

The internal faults and the main tectonic units.

Numerous fractures and shear zones have been recognised within the peridotite batholith, and they confirm the general picture obtained from the examination of the contact relations that the batholith has been emplaced by intrusion faulting.

Two main types of fracture have been recorded. The first type is characterised by continuous zones of sheared serpentinite or ultrabasic mylonite and the second by clean, slickensided, vertical fractures.

Continuous zones of sheared serpentinite are a major feature within the batholith and are fundamental to the understanding of its complex history. These shear zones extend for distances of up to eight miles along the strike; they follow strong physical features especially deeply incised river valleys and in two clear cases have been followed over high cols. The dip of the shears indicates that these zones are steeply dipping or vertical features. The sheared

serpentinite seen in these zones closely resembles that seen at the margins of the batholith; it flows round large oval and sub-rounded blocks of peridotite and frequently contains rotated fragments of glassy mylonite. In one notable locality the sheared serpentinite is replaced by a continuous zone of disturbed, glassy, unserpentinised mylonite. The shear zones extend to the margins of the batholith where they merge with the disturbed contact serpentinite, but do not extend out into the country rocks. These shear zones are interpreted as intrusion faults and when they are considered together with the mapped contact of the batholith it is seen that they divide the latter up into a number of tectonic units (Fig. 21). The main intrusion faults within the batholith are as follows and are shown in Fig.21 .

The Patud intrusion fault

The Tankulap-Lichau intrusion fault

The Binalik intrusion fault

The Patud disturbance is eight miles long and is a major structure. It trends north-east from the mouth of the Melio stream, strikes up the first north bank tributary of that stream over a marked col on the western spur of Mount Tawai and down into the main west bank tributary of the Meliau river which it follows for a distance of three miles before trending northwards to the main ultrabasic contact below the south-eastern flank of Mount Patud. The sheared serpentinite that marks the path of the intrusion fault is striking between N 30° E and N 45° E and is vertical or steeply dipping to the west (75° - 85°). The fault is best seen in the west bank tributary of the Meliau river where sheared serpentinite wrapped

around boulders or peridotite up tothree feet in diameter is seen continuously exposed for over three miles. Irregular flame-like growths of antigorite and tremolite are abundant. At its south extremity the fault is separated by a thin wedge of volcanic and sedimentary rocks from the contact fault that delimits the Tawai block. At its northern extremity the intrusion fault merges with the contact zone that delimits the southern side of the Gombaran range.

The Tankulap-Lichau intrusion fault is a major structure; it is seven and a half miles long and stretches from the Nobusu river on the western side of the batholith to the Lichau river on the eastern margin. From the Nobusu river the fault strikes almost due east to the headwaters of the south Tankulap stream. From this locality the fault continues along the northern bank of the South Tankulap stream to its confluence with the North Tankulap. The cliff on the northside of the South Tankulap river is extremely steep and overhanging in places. Along the base of the cliff a spectacular sixty foot wide zone of hard grey, glassy, banded mylonite is found (Fig. 22a). The mylonite bands trend roughly north-east south-west parallel to the strike of the fault and are vertical, but they are considerably fractured and cut by thin veins of serpentinite. This is the only locality where true peridotite mylonites have been observed more or less intact, for they are normally found as tectonic inclusions in the sheared serpentinite. At the confluence of the North and South Tankulap streams the fault assumes a more northerly strike and continues over a prominent col to the Lichau river. The mylonite zone is gradually replaced by sheared serpentinite along the strike. At its northernmost

Fig. 22a. Photograph of mylonitic banding in theSouth Tankulap river.

extremity the intrusion fault merges with the fault contact that defines the eastern boundary of the batholith. Along the strike of the intrusion fault the sheared serpentinite is vertical or steeply dipping to the south-east (75°- 85°). At its westernmost extremity the position is less clear but it appears to merge with the contact fault that is striking approximately east-west in that area. It is however markedly discordant to the contact intrusion fault that defines the western margin of the Pantagaluang block which is striking roughly north-south.

Another strong zone of disturbance, the Binalik intrusion fault, runs southwards from the confluence of North and South Tankulap streams through a marked col to the headwaters of the Binalik river. The sheared serpentinite is striking between N 05° E and N 15° E and is vertical or steeply dipping to the east. At its northernmost extremity this intrusion fault joins the Lichau-Tankulap fault, and at its southernmost end it merges with the fault contact zone that defines the eastern side of the Pantagaluang block. To the east of the Binalik fault another continuous zone of sheared serpentinite is located striking N.E.-S.W. from the main ultrabasic contact on the Tankulap river to the headwaters of the Binalik river.

The internal intrusion fault zones divide the batholith up into a number of tectonic units which are shown on the map (Fig.21). They are as follows:-

1. The Patud-Gombaran intrusion.
2. The Main Tawai tectonic block.
3. The Binalik tectonic block.
4. The Pantagaluang block.

These tectonic units have been affected by normal vertical faulting at right angles to their elongation. The main vertical faults are easily recognised in the field for they give rise to prominent waterfalls and large scarp features; whereas the intrusion faults follow streams and give rise to deeply entrenched valleys, the vertical faults cut across rivers. Slickensides are abundant on the fault facies but intense brecciation and sheared serpentinites are absent. It is difficult to judge the degree of movement on the faults but many of the waterfalls are between 200' and 700' high.

The first of the above listed tectonic units is a fifteen mile long arcuate intrusion. This type of arcuate intrusion is particularly common in the Labuk area and further examples are seen in the Tingka and Bidu-Bidu ultrabasic areas (Fig. 3). It forms the north-western and northern part of the batholith and is expressed topographically in the Patud-Gombaran range. Its northern and western margins are defined by the long contact intrusion fault that trends northwards from the mouth of the Melio river to the river Labuk when it swings eastward along the northern flank of the Gombaran range. The eastern and southern margins of the partial ring intrusion are bounded by the Patud intrusion fault, and the long east-west trending contact fault along the southern edge of the Gombaran range. Both bounding fault contacts are extremely steep but there is some evidence to suggest that the eastern and southern boundary is the hanging wall. The Patud intrusion fault is vertical or steeply westward dipping along the strike and this certainly suggests a hanging wall. Moreover the steep cliff on the southern side of the Gombaran range is vertical and overhanging in parts, again suggestive that the bounding fault is plunging steeply to the

north. One of the very large amphibolite blocks in the Meliau contact zone appears to be plunging very steeply northwards under the Patud range.

This arcuate intrusion is truncated at its eastern extremity by a normal vertical fault striking north-south. At its southern extremity a thin wedge of brecciated basalt separates it from the Main Tawai block. Further vertical faults at right angles to the fault intrusion contacts occur in the Gombaran range and are shown on the map.

The main Tawai tectonic block is the largest single unit and occupies the central portion of the batholith. It is an elongate block fifteen miles long and eight miles across at its widest point. It extends from the line of the Nobusu and South Tankulap streams in the south to the Kuun-Kuun river in the north. It is bounded on the north-west by the Patud intrusion fault which separates it from the Patud Gombaran partial ring intrusion. Its northern margin is a contact intrusion fault that runs from just west of the Meliau stream eastwards to the main Kuun-Kuun stream. At its western extremity this fault appears to terminate against the Patud disturbance. North of the fault a long tongue of strongly folded and brecciated country rocks separates the Main Tawai block from the Gombaran range. The eastern boundary is formed by a long swinging contact intrusion fault that strikes north-north-east south-south-west from the Kuun-Kuun river to the Lichau river where it joins the Lichau-Tankulap disturbance. The latter intrusion fault forms the southern boundary of the block. The south-western margin is formed by a contact intrusion fault which appears to be continuous with the Tankulap-Lichau disturbance zone.

The Main Tawai block has been considerably affected by vertical faulting. It contains two parallel vertical faults of extreme importance in the structural interpretation of the area. They are the Melio and Nobusu faults.

The Melio fault is the most impressive of all the internal structures. It trends west-north-west from near the southern extremity of the Patud intrusion fault and strikes parallel to the Melio river for a distance of three miles. Prominent slickensided surfaces are exposed in the south-flowing tributaries of the Melio stream. To the north the main Tawai ridge rises to just over four thousand feet and must be interpreted as a fault scarp. In the headwaters of the Melio a large 700' high waterfall occurs where the main stream crossed the fault (Fig. 9). At the waterfall the main Melio fault is joined by a vertical fault trending N.E.-S.W.. This fault forms the western margin of the Tawai plateau. Small fractures such as this one branching at right angles off the main vertical faults are common. From the Melio waterfall the fault continues on the same strike to the North Tankulap stream. Between the Melio and the North Tankulap stream the path of the fault is largely hidden by the goethite cap of the Tawai plateau. Eastward from the Tawai plateau the fault continues on the southern bank of the North Tankulap stream and eventually terminates against the Tankulap-Lichau intrusion fault. At its western extremity the Melio fault terminates against the Patud intrusion fault. Small north-east south-west fractures branch off the main Melio fault at right angles and give a marked stepped appearance to the North Tankulap stream section. The features associated with the main Melio fault indicates the area to the

north-east of it has been uplifted.

The Nobusu fault can be traced in the field for four and a half miles. It trends N.W.-S.E. from the Tankulap-Lichau intrusion fault on the south-west margin of the Tawai plateau. Its path is marked by prominent waterfalls on the Nobusu river which indicates the fault is upthrowing to the north-east (Fig. 9).

Similar N.W.-S.E. trending faults are found in the main Tawai area and in the Patud-Gombaran range and doubtless have a similar origin. The Tawai plateau undoubtedly holds the key to the tectonic setting of the batholith. The Tawai plateau lies between the Melio and Nobusu faults. It is bounded on the north-west and south-east by right-angled faults branching off the Melio fault. It is suggested that as the Main Tawai block was being emplaced the upward movement was uneven so that fractures therefore developed at right angles to the intrusive contacts thus breaking the block up into a number of segments. Each segment would then move differentially. In this way the area to the north-east of the Melio fault moved upwards more quickly than the area to the south resulting in the large N.W.-S.E. trending fracture. In a similar fashion the area north of the Nobusus fault moved more quickly than the area to the south. This pattern of faulting resulted in the main Tawai area to the north of the Melio fault being uplifted to a greater extent than the Tawai plateau area. The region to the south-west of the Nobusu fault has similarly been uplifted to a lesser extent than the Tawai plateau. It is thought probable that the cross fault on the Melio fault developed simultaneously and thus formed the north-western and south-eastern margin of the plateau. Rapid stream flowing of the huge scarp face of the main north-west

south-east Tawai ridge would soon build up swampy conditions in the area of the Tawai plateau. In this way ideal conditions for the formation of a bog iron ore deposit were formed. It is considered that the goethite cap on the Tawai plateau has formed at the present level. It cannot be considered that the goethite formed on an area of low relief and has since been uplifted. The goethite is not truncated by the Melio fault, indeed in places it is lying on it.

The Binalik block is situated to the west of the Main Tawai block from which it is separated by the Tankulap-Lichau and Binalik intrusion faults. It is divided into two distinct units by another intrusion fault that runs from the main ultrabasic contact on the Tankulap river to the headwaters of the Binalik river. The western part is roughly oblong being two miles wide and four miles long, and is bounded on the east and west by the above mentioned intrusion faults. Its northern and southern contacts are made of sheared serpentinite and must be taken as contact intrusion faults. The eastern part is a six miles long elongate intrusion that extends from the Tankulap river to the lower reaches of the Binalik river. It forms a prominent north-south trending ridge off the east flank of the main batholith and is composed almost entirely of sheared serpentinite and closely resembles similar north-south trending elongate intrusives off the north-eastern contact.

The Pantagaluang block forms a distinct topographical unit to the south of the Tankulap intrusion fault which separates it from the main Tawai block. It is bounded on the east by the Binalik disturbance and on the west by a contact intrusion fault.

Breccias.

Irregular zones of brecciated and pulverised peridotite occur throughout the ultrabasic batholith and often tend to blur the major structural features. The disturbed zones vary in shape from flat lying sheet breccias to pipe-like ones that resemble the dykes. They usually consist of sheared serpentinite in a highly irregular manner. Rounded and sub-angular fragments of peridotite are enclosed in the sheared serpentinite, and the breccias are frequently cemented by calcite. Unsheared calc-silicate minerals abound in the breccias. Usually the margins of the breccia zones are gradational with the undeformed peridotite but sometimes the contacts are sharp and they appear dyke-like in form.

The internal breccias are a local phenomenona and can usually only be traced for a short distance. In general they are irregularly distributed throughout the mass but there can be doubt that the breccias were developed during the final emplacement for they are post-serpentinization in age.

A morphological classification of the breccia zones is not practical and the more important ones are discussed below and shown on the map (Fig. 21).

In the east Meliau tributary a zone of brecciation is exposed two miles upstream from the mouth of the river. The disturbed zone is forty feet wide and contains two low angled shear planes dipping 23° to the north-east. Along the strike the breccia zone can be traced for three hundred feet along a small east bank tributary. The breccia contains a thirty foot serpentinised dunite band that is considerably distorted and cut by thin veins

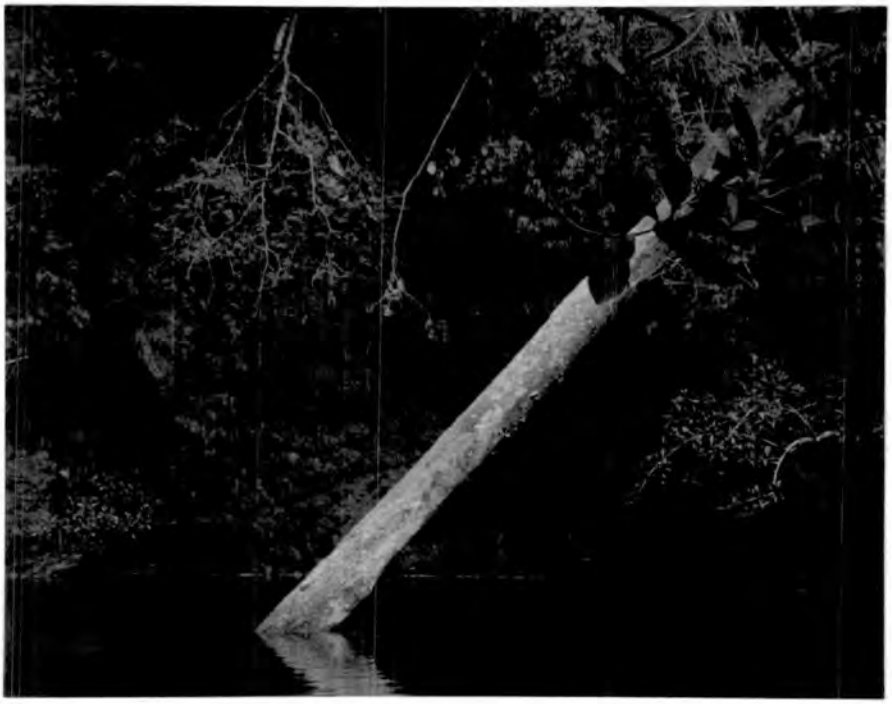

Fig. 22. Photographs of Kuun-Kuun breccia zone.

of chrysolite asbestos, striking N 80° E. Twenty feet upstream from the northern contact of the breccia a small quartz pegmatite occurs but it does not intrude the disturbed zone. Both contacts of the breccia are gradational with massive serpentinised harzburgite.

A prominent zone of brecciated and disturbed peridotite and dunite three hundred ft. wide is located two miles upstream from the ultrabasic contact on the Kuun-Kuun river (Fig. 22). The zone strikes N 80° E roughly subparallel to the sheared serpentinite observed at the downstream contact. The disturbed zone consists mainly of sheared serpentinite. Two serpentinised dunite lenses are completely enclosed in the disturbed zone and have been considerably sheared. Thin chromite bands are displaced and warped. The serpentinised dunites are veined by irregular networks of chrysolite asbestos. The zone can be traced for seven hundred feet to the east of the river but does not cross the Sawar ridge. It can however be traced intermittently for two miles on the east of the Sawar ridge and has considerably affected the dunite lenses of the north-east corner of the main Tawai block. It is not a continuous disturbance zone and it does not contain ultramylonite inclusions; it is therefore not considered to be a major feature.

Two and a half miles upstream from this disturbed belt on the main Kuun-Kuun river an elongate breccia 400 ft. long is found. The disturbed zone is strongly calcified and sheared serpentinite fragments are seen set in a matrix of calcite (Fig. 23). The breccia occupies a fissure 30ft. deep and 50ft. wide. The fissure strikes almost due north and is vertical. The contacts of this fissure breccia are sharp against serpentinised harzburgite.

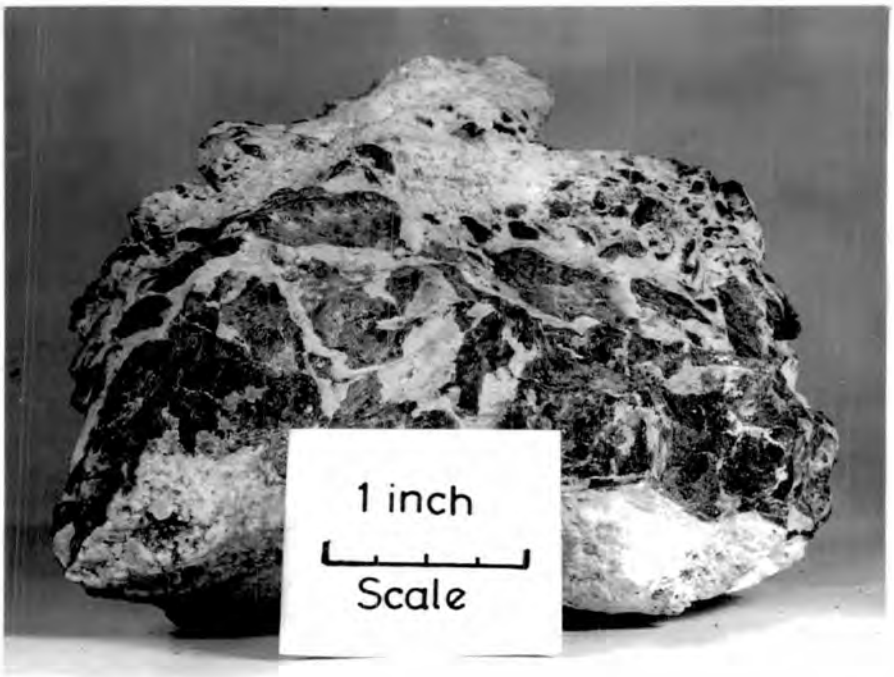

Fig. 23. Photographs of breccia hand specimens. T127.

Prominent veins of calcite extend out from the breccia into the wall rock.

In the headwaters of the Ruku-Ruku river a breccia dyke 30ft. wide striking N 40° E and dipping 70° N.W. is found. The dyke consists almost entirely of sheared serpentinite. The breccia dyke has sharp contacts with the peridotite and can be clearly seen in both banks of the stream. The dyke cannot be traced laterally owing to poor exposure. A similar breccia dyke is found in the Upper Melio stream about a mile upstream from the main waterfall. The dyke is seventy feet wide and strikes N 82° E and is vertical. It can be traced for over 300 ft. along the strike.

Sheet bfeccias are particularly common. An impressive sheet breccia is found in the Talibu stream section. The base of the sheet is exposed in the stream section and is almost flat. Above the base of the sheet brecciated and pulverised peridotite occur to a height of 80 ft.. Both the top and the base of the sheet grade into massive serpentinised harzburgite. The breccia sheet contains abundant calc-silicate minerals and is strongly silicified in places. The sheet however is narrow and cannot be traced in a small tributary of the Talibu half a mile to the north. Fitch (1958) observed this feature during a reconnaissance survey of the Karamuak and considered it to be a low angled thrust. However the gradational nature of the contacts and the lack of mylonite inclusions (so characteristic of intrusion faults in the area) show quite clearly this is a sheet breccia, very similar to those described by Green (1960) from Papua.

Foliation.

Many of the harzburgite outcrops show a crude gneissos foliation

Fig. 24. Photograph of foliation in harzburgite.

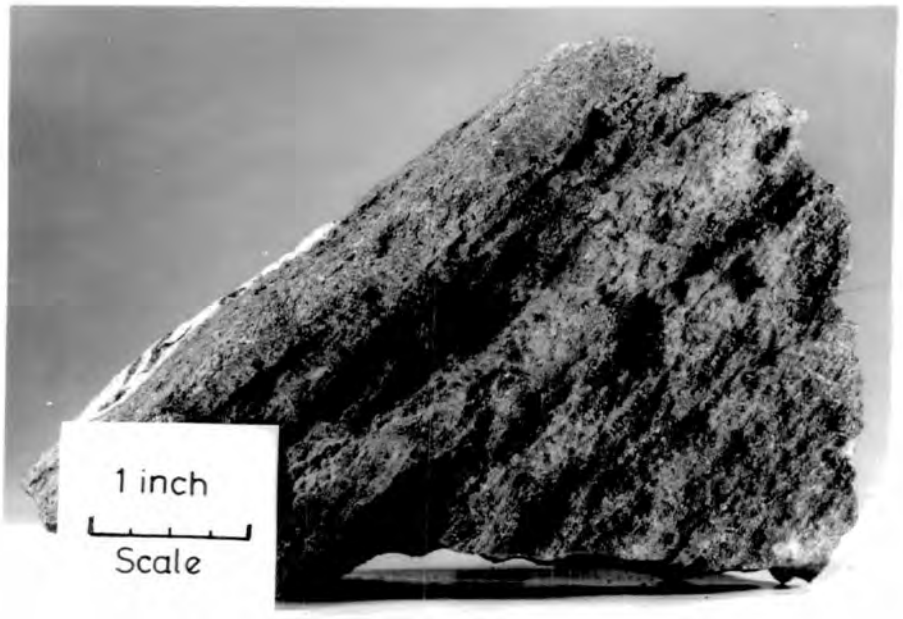

produced by subparallel alignment of the orthopyroxene laths. This foliation is only seen in heavily weathered outcrops (Fig. 24) and is difficult to see in the stream sections. Thin sections of these crudely foliated rocks, described in detail later, show strong evidence of cataclastic deformation. The crude foliation is however difficult to detect in thin section. It is seen that the olivine has suffered mainly by granulation and the orthopyroxene by warping. Weathering of the deformed rocks causes the more persistent pyroxene laths to stand out from the more easily eroded olivine. The ultrabasic rocks forming the central part of the Main Tawai block are weakly foliated and cataclastic structures are absent or poorly developed. However as the main Tawai block is traversed from the central portion to its margins, foliation increases and the thin sections show that the degree of deformation increases. The peridotite mylonites seen along part of the Tankulap-Lichau fault and as inclusions in the sheared serpentinite are considered to be the most advanced form of the cataclastic deformation.

The gneissose foliation is difficult to map with accuracy because it can only be seen in heavily weathered outcrops. Moreover in the contact zones it is considerably broken up and intense serpentinization often obscures it. This makes a regional picture of the foliation difficult to obtain but the more reliable measurements are recorded on the structural map (Fig. 21) and are discussed below. The foliation is best seen on the flanks of the Patud range and on the sides of the Binalik and Sawar ridges. The best exposures occur about one hundred feet below the ridge crests.

Foliation is well developed in the Patud-Gombaran intrusion. South of Mount Patud the foliation exposed just below the main ridge

is striking between N 05° E and N 30° E and plunging steeply westward. North of the Mount Patud the strike of the foliation changes to a more easterly direction and in the Gombaran range is striking between N 25° E and N 85° E. The dip in the Gombaran range however is very irregular. The strike of the foliation in the Patud-Gombaran range roughly follows the trend of the main ridge and of the intrusion. On the southern side of the Gombaran range ultrabasic mylonites occur as isolated blocks in the central fault breccia.

In the main Tawai block the foliation is best observed on the marginal ridges. On the western flank foliation is seen on the sides of the interfluv separating the two main tributaries of the Meliau. It is striking between due north and N 30° E although it is markedly disturbed near the Patud-intrusion fault. South of the Tawai ridge similar strike directions for the foliation are found on the ridges above the south flowing tributaries of the Melio river. In general the foliation on the western flank of the main Tawai block dips very steeply westward. In the northwestern part of the block good exposures of the foliation are found in the banks of the Kuun-Kuun river close to the main contact. There the foliation strikes between due north and N 15° E and is markedly discordant to the direction of the contact. Further upstream many irregular directions are seen in the breccia zone and have not been recorded.

On the eastern flank of the main Tawai block between the Hitam and Lichau rivers the foliation strikes between N 03° E and N 50° E with most values around N 20° E. South of the Lichau river the foliation swings around to a more easterly direction and strikes between N 30° E and N 60° E. This is particularly noticeable

immediately to the north of the Tankulap-Lichau intrusion fault. No general dip direction for the foliation on the eastern flank could be determined. Close to the main contact the ultrabasic rocks become increasingly disturbed and serpentinised and the foliation is largely obscured. Isolated blocks of ultrabasic mylonite are found in the contact breccias exposed by the Hitam, Puteh, and Merah rivers. In the elongate ultrabasic body, situated off the north-east corner of the main Tawai block the foliation strikes N 355° E.

In the Binalik block good exposures of the foliation occur on the main ridge south of the Tankulap river. The foliation is vertical or very steeply inclined, striking N 355° E. In the eastern arm of the Binalik block the foliation strikes between N 355° E and N 30° E and dips steeply eastward.

In the Pantagaluang block foliation readings have only been recorded on the eastern side where the strike is between N 05° E and N 40° E. No general dip direction could be ascertained.

The main points with regard to the foliation are as follows:-

1. The foliation is caused by subparallel alignment of the pyroxenes.
2. The degree of foliation decreases inwards from the margins of the tectonic units. Near the margins true ultrabasic mylonites are found.
3. The foliation is broken up around the margins of the tectonic units.
4. The foliation is roughly parallel to the elongation of the tectonic units.
5. The foliation is pre-serpentinization.

The gneissose foliation and the peridotite mylonites are interpreted as cataclastic features associated with intrusion in the near crystalline state. Although the foliation is roughly subparallel to the elongation of the tectonic units, in the contact zones it is considerably disturbed. It would therefore appear that at some time in the history of the tectonic units the foliation has developed roughly parallel to their present elongation during intrusion of a nearly crystalline melt but at some later date it has become disturbed during renewed upward movement following serpentinization.

Primary Igneous banding.

Continuous units of distinctive ultrabasic and basic rock types characteristic of the stratiform igneous complexes of Rhum and Stillwater are not found in the Mount Tawai peridotite.

A banded structure, distinct from the foliation, characterises about five per cent of the observed outcrops. The bands consist mainly of dunite but less commonly pyroxenite and feldspathic peridotite types are found. In general the bands are arranged in closely spaced subparallel clusters and are always seen in a vertical or steeply dipping attitude when viewed away from local or minor disturbances.

The overall shape of the bands is lenticular (Fig.28) for when traced along the strike they pinch out and interfinger with the peridotite. Many of the larger lenses also pinch out when traced upwards on to the mountain slopes. The smallest are lenses a few inches wide and from one to two feet in length whilst the largest may be up to 600ft. wide and extend for over a mile along

Fig.25.

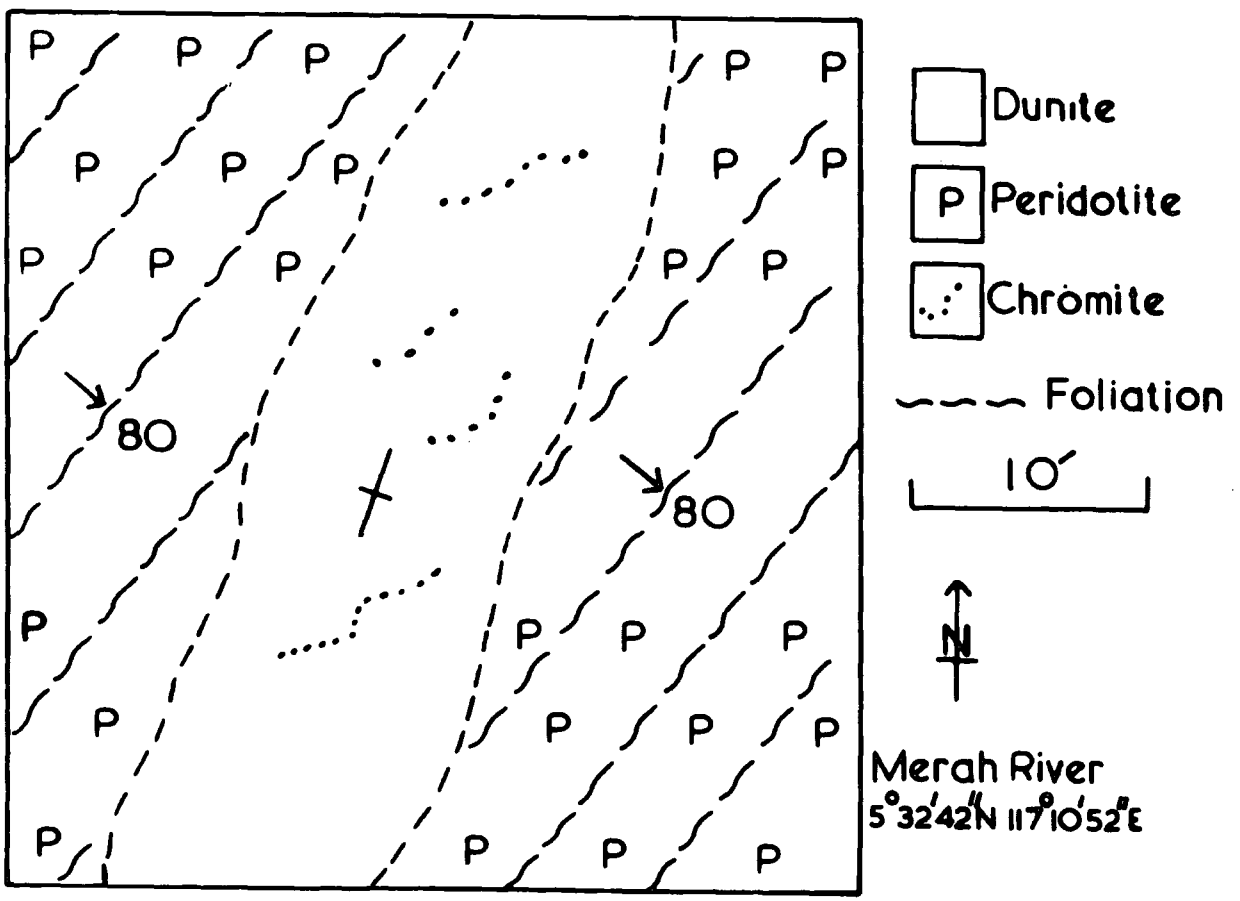

Relationship between dunite lense and foliation,

the strike. The larger ones are usually of a composite nature consisting of a series of lenticular bodies. The pyroxenites and feldspathic peridotite bands never exceed six inches in width and seldom extend for more than 20ft. along the strike.

The bands show both sharp and gradational contacts with the peridotite. At the gradational contacts only rarely can grain size variations of the constituent minerals be seen. The dunite bands are particularly distinctive being outlined by trails of chromite crystals. Bands of chromite within the dunite lenses, though common are but poorly developed.

Mineral banding is found in foliated and non-foliated peridotite. In the latter case the strike of the foliation is often subparallel to that of the mineral banding and both are steeply dipping features. However, examples do occur where there is a slight or even major discordance of strike between the two features. This is best seen where the foliation in the peridotite is markedly discordant to the strike of a chromiferous dunite lens. This situation is rare but in the Merah stream section a clear case is seen (Fig. 25). The lens is striking N 10° E and is vertical whilst the foliation is striking N 47° E and dipping 80° S.E.. The chromite within the dunite lens is streaked out and aligned subparallel to the foliation within the harzburgite.

It is clear that the foliation is a vertical or steeply dipping structure that has been imposed upon the primary mineral banding. The latter has obviously been produced during an earlier phase in the history of the batholith prior to its intrusion in the near crystalline state.

The main areas of primary banding are described below. Detailed

descriptions of the field characteristics associated with these bands are given in a later section.

In the main Tawai block two belts of mineral banding may be defined and they are subparallel to the elongation of the tectonic unit. Within these belts dunite lenses occur whose elongation is usually subparallel to the direction of the belt although marked discordances are sometimes found. Thin pyroxenite lenses also occur within the belt. The belts are as follows:-

(a) Western belt - this belt comprises a group of dunite lenses and occasional thin pyroxenites. It trends from the Kuun-Kuun Valley in north south-westward to the Meliau valley and over the main Tawai ridge to the Melio headwaters.

(b) Eastern belt - this belt comprises mainly dunite lenses and trends southwards from the Hitam Valley on the east flank of the Sawar ridge to the Ruku-Ruku river and then swings north-east south-west to the North Tankulap stream.

The western belt is best seen in the Meliau valley. At the confluence of the West and East Meliau streams a zone of thin pyroxenites 10ft. wide interbanded with peridotite is seen in the eastern bank of the river. The bands are striking N 05° E and dipping steeply westward (75° - 85°). A thin dunite lens 30ft. upstream has a similar strike. Two miles upstream from the main Meliau confluence a series of thin dunite lenses are located in the eastern tributary interbanded and interfingering with harzburgite. The thickest lens is 30ft. and only contains thin irregular bands of 'shot gun' chromite. The northern part of the main Tawai

Fig. 26. Photograph of clinopyroxenite bands in the Kuun-Kuun section.

intrusion is exposed by the north flowing tributaries of the Kuun-Kuun stream in which extremely brecciated chromite lenses are found. The sheared lenses strike between N 40° E and N 55° E and are vertical or dip steeply northwards. The lenses are completely enclosed in local breccia zones. On the southern edge of the breccia zone (Fig. 21) in the main north flowing tributary of the Kuun-Kuun a 10ft. wide zone of banded pyroxenites (Fig. 26) is located striking N 30° E and dipping 35° to the north-west. The dip is the lowest recorded in the area and is attributed to the disturbance caused by the nearby shatter zone. In the uppermost headwaters of this tributary dunite bands occur in an irregular oval-shaped area. The lenses contain thin chromite bands which strike N 10° E and dip steeply westward.

At the southern extremity of the western dunite belt mineral banding is found above the main falls on the Melio river. Chromiferous dunite lenses varying from a few inches (Fig. 27) to over 600ft. are found interbanded with the peridotite and strike between N 02° W and N 25° E and dip steeply westward between 70° - 85°. Near the brow of the fall a six inch pyroxenite band is found striking N 03° E and dipping steeply westward.

Further somewhat irregular lenses are found in the first and second north bank tribuataries of the Melio. On the main Tawai ridge dunite lenses are not exposed but blocks of dunite are found in the slipped material below the ridge summit.

The western group of dunite lenses in general dip steeply westward.

The eastern belt of dunite contains thicker lenses than the western one; and the dunite is more strongly mineralised. By far

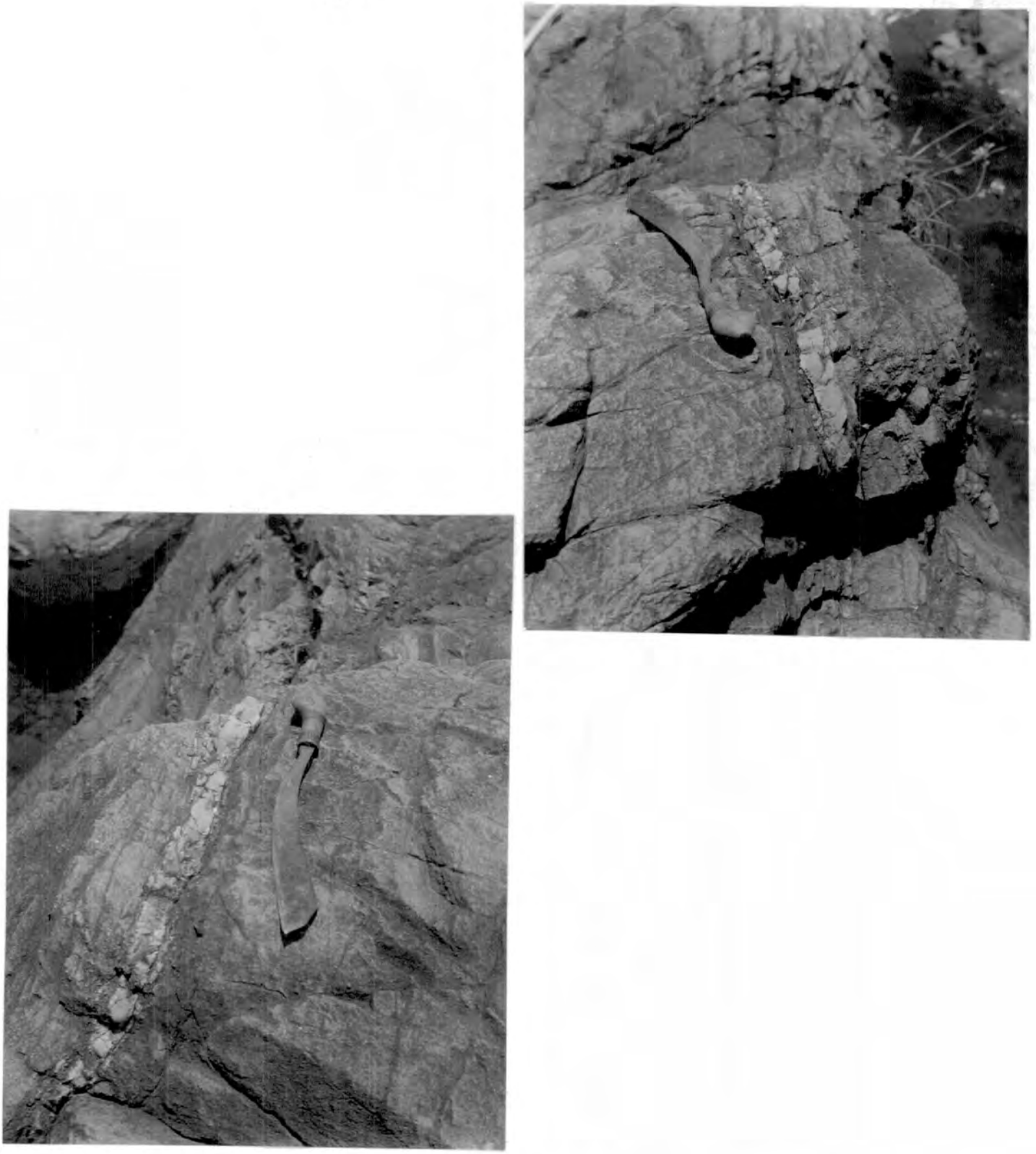

Fig. 27. Photographs of dunite bands in the Melio section.

the greatest concentration of dunite is found between the Ruku-Ruku and North Tankulap rivers. In the former dunite bands striking between N 05° E and N 25° E are located, one of which is over a mile long. However it appears to be of a composite nature being made up of a series of small lenses. In the many tributaries of the Lichau river numerous dunite lenses occur, the majority striking between N 30° E and N 50° E. Local variations of strike are noticeable in this area. Many of these lenses contain small banded chromite ore bodies. The Lichau lenses and those found in the Ruku-Ruku have an extremely steep inclination. One dunite lens is the Lichau river (Fig. 28) contains chromite bands dipping 75° - 85° S.E. and the rudimentary gravity banding of the chrome ore suggests the lens is upside down. In the south flowing part of the North Tankulap stream numerous dunite lenses are found in non-foliated peridotite. The lenses vary from a few inches in width to over 300ft. and nearly all contain thin bands of chromite. The lenses strike between N 05° E and N 50° E and are vertical or steeply dipping toward the north-west. Near the Melio fault dips as low as 45° have been recorded. South of the Melio fault dunite is rarely found but may be hidden under the goethite of the Tawai plateau. In the northern part of the eastern dunite belt only thin lenses are found in the Merah, Puteh, and Hitam valleys.

The overall picture given by the mineral banding within the main Tawai block is of an intrusion dipping steeply westward. The vertical nature of many of the dunite lenses of the eastern belt suggests that a slight decrease in dip occurs from east to west in the intrusion. It is also possible from the evidence of the inverted chromite band in the Lichau exposure that some lenses in the

Fig. 28.

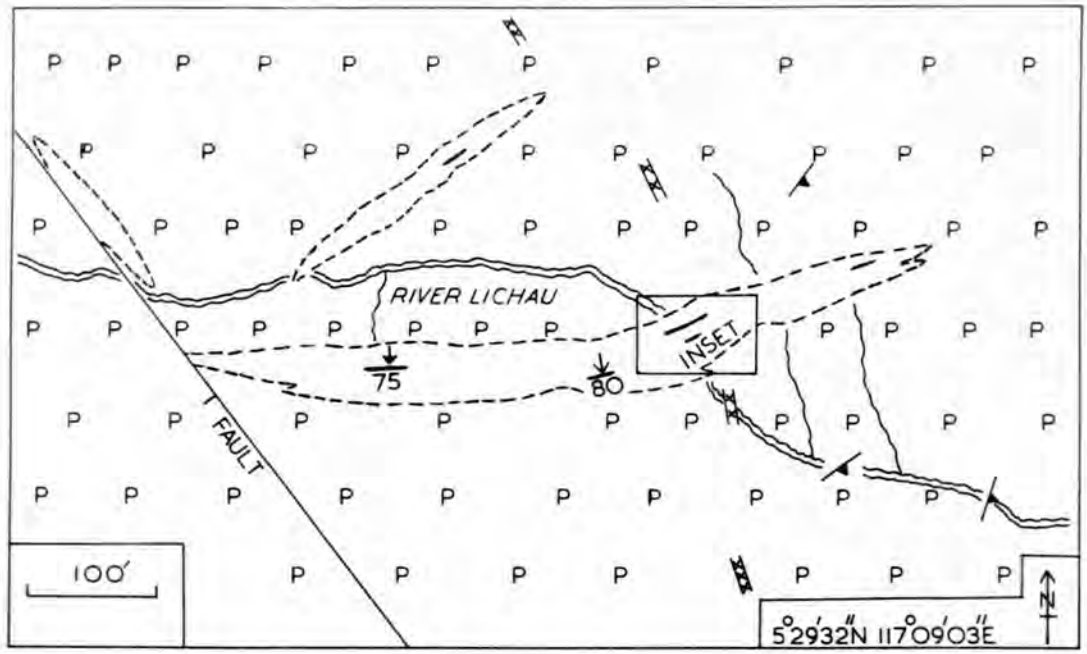

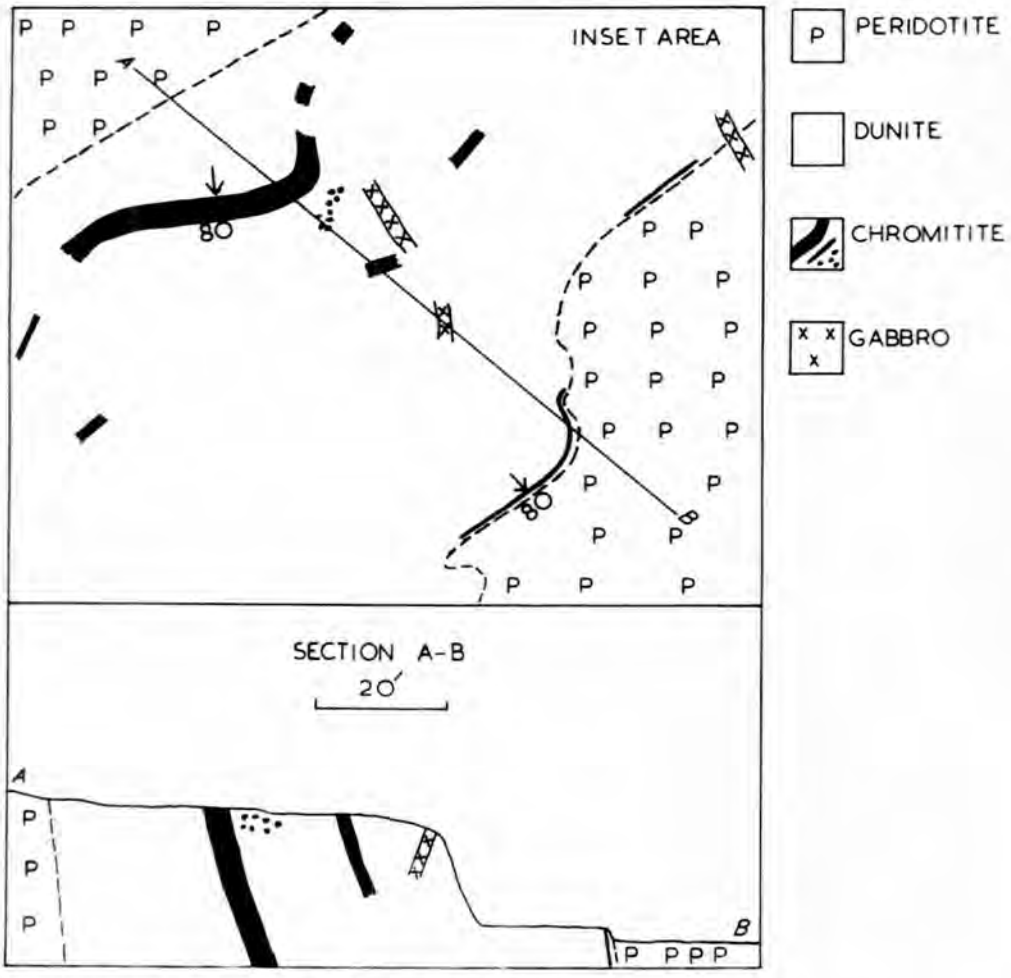

DUNITE LENSES IN THE RIVER LICHAU

13 AUG 1964
LIBRARY

eastern belt may have been overturned during intrusion.

In the Binalik block thin lenses of chromiferous dunite striking between N 10° E and N 50° E are exposed in the main Tankulap river section. Dips on either side of vertical have been recorded. The mineral banding indicates that the main Binalik block is a very steep or vertical intrusion.

Mineral banding is unfortunately poorly exposed in the Patud-Gombaran partial ring intrusion and the Pantagaluang block. In the former unit thin dunite lenses are found in the Telupid section striking between N 10° E and N 50° E and dipping 70 - 80° N.W.. These lenses tend to confirm the hypothesis that the Patud-Gombaran intrusion dips steeply to the north-west and that its eastern and southern fault contact forms a hanging wall. Mineral banding could not be located in the Gombaran range.

In the Pantagaluang block two dunite lenses striking between due north and N 40° E and dipping steeply W. are found in the headwaters of the South Tankulap stream. Thin bands of feldspathic peridotite do however occur and away from the Tankulap-Lichau fault zone strike between N 30° E and N 40°. They dip very steeply and no general direction could be determined. Mineral banding is too poorly developed in the Pantagaluang block and the structure cannot be elucidated.

The History of Emplacement.

At this point it is necessary to draw together the history of emplacement of the Mount Tawai batholith. Detailed discussion involving the points where petrogenesis and structural evolution

clash are left to a later chapter.

The major anomaly in the evidence so far presented is that although the foliation is roughly parallel to the present contacts of the main tectonic units it is broken up in the contact zones. Moreover blocks of unserpentinised mylonite, which are considered to be the most extreme expression of the foliation, are found in the contact sheared serpentinites. It could be postulated that the foliation developed at a pre-intrusive period during the history of the batholith but this seems unlikely in view of the facts that the foliation is a cataclastic effect and that the batholith has obviously been emplaced by solid intrusion. It seems more likely that the foliation developed at an early stage in the emplacement of the mass and during the later stages became broken up around the margins. This could be explained by postulating an initial crystalline intrusion that halted below the sedimentary cover and then at a later date was finally emplaced by renewed movement along practically the same margins. If a long period of erosion separated the two phases of upward movement then this would explain the scarcity of roof pendants on top of the ultrabasics.

It is suggested that marginal serpentinization occurred shortly after the initial intrusion. It is possible that during the initial intrusion the temperature of the ultrabasic mass was above the stability point of serpentine; and that between the initial intrusion and the second emplacement the mass cooled below 400^{o}C allowing serpentinization to take place. During the second intrusion the marginal serpentinites would greatly reduce the friction at the contacts as envisaged by Hess (1955), by acting as lubricants and accelerating the final stage of emplacement. The intense shearing

of the marginal serpentinites would then have largely distorted the original cataclastic contacts. The mylonite blocks are interpreted as having resisted serpentinization owing to their compact nature; they were carried up and rotated during the final emplacement. It is only along a part of the Tankulap-Lichau intrusion fault that they have been observed relatively intact. Bowen and Tuttle (1949) suggest that strong mylonitised rocks will resist serpentinization because of their compact nature.

The postulated history of emplacement may therefore be summarised into three distinct stages.

Stage I.

Solid intrusion at depth of a large slice or series of slices derived from a large ultrabasic body. It is not possible to be certain whether the original intrusion was of a single large peridotite slice that broke up into a series of smaller units during the initial emplacement, or if the tectonic units represent different parts of an original large ultrabasic body. The latter hypothesis is favoured for there are slight differences in mineralogy between the main blocks and tectonic inclusions of gabbro are also found. During the first stage the tectonic units were affected by cataclastic deformation and developed a crude gneissose foliation roughly parallel to the sides of the units. In places true ultrabasic mylonites were produced.

Stage II.

After the initial intrusion at depth serpentinization occurred.

Stage III.

The tectonic units were emplaced in their present position by renewed uplift along the same intrusive margins but greatly aided by the lubricating effect of the marginal serpentinites. During this second uplift some of the tectonic units became partially separated from the main mass and it is almost certain that they rose to different levels and at different speeds. The Patud-Gombaran ring intrusion appears to be later than the main Tawai block whilst the Binalik block is probably contemporaneous with it. The Pantagaluang block has not been separated from the main Tawai block and it may be postulated that the non-serpentinised mylonite zone is responsible for this, in that marginal serpentinites could not be formed along the contact zone. The large Melio fault may well have been caused by the northern part of the main Tawai block moving upward faster along serpentinised contacts than the southern part which would have been impeded by the non-lubricated mylonite zone. All of the vertical fractures probably developed during the final emplacement.

The thin elongate lenses of sheared serpentinite located off the flanks of the batholith were probably intruded at this time along marginal fractures.

The age of the batholith.

The fault emplacement.

The batholith has clearly been emplaced by intrusion faulting

into rocks of Upper Cretaceous and Eocene age. The major unconformity in the North Borneo Tertiary sedimentary sequence is between the lower and upper Miocene. (Rheinhard and Wenk 1951 p.14). The major orogeny in North Borneo undoubtedly occurred in the Miocene period and the E.-W. striking folds seen in the Eocene sediments on the east of the Mount Tawai batholith were developed during that period. The basal conglomerate of the Upper Miocene is found to the south of the Tawai area and does not contain pebbles of ultrabasic rocks. Indeed it is built almost entirely of white sandstone pebbles. Throughout the Upper Tertiary sedimentary sequence there are no conglomerates containing large quantities of ultrabasic material and moreover the sediments do not contain detrital chromite. It is only at the present day that large conglomerates and talus deposits of ultrabasic material are being formed.

The Lokan peneplane out of which the Labuk ultrabasic batholiths rise so abruptly were proabably developed in the Pleistocene (Fitch 1958). At the present time there is no major river crossing the Lokan peneplane yet it is apparent that a large stream once drained it. It has been suggested (Fitch 1958) that a large stream once drained this area coming into the sea in Sandakan Bay through the Segaliud valley but has since been captured by another stream cutting back along the line of the present Labuk river between the Meliau and Bidu-Bidu batholiths. In this thesis it is strongly suggested that the origin of this major adjustment to the drainage pattern was caused by the fault emplacement of the ultrabasic batholiths in late or post-Pleistocene times and that a tributary of the present Tongod river cut back rapidly into the contact zone between the Meliau and Bidu-Bidu batholiths (Fig. 4) to capture the river

that once drained the Lokan peneplane. Many other instances of river capture are obvious within and around the ultrabasic batholiths.

The sedimentary record and the geomorphological evidence point strongly to a late- or post-Pleistocene date for the fault emplacement. However it is noticeable that large roof pendants of unmetamorphosed sediments are lacking from the batholiths. Although several streams cut down through the goethite cap on the Tawai plateau no exposures of Tertiary sedimentary rocks have been found on it. A similar plateau in the Bidu-Bidu hills is not capped by sedimentary rocks. It must therefore be assumed that at the time of emplacement only a thin layer of sediments were present above the roof of the batholith. After emplacement the thin cover would have been quickly removed by the powerful streams draining the area today. The main Labuk area was considered by Fitch (1958) to be a land area from the Oligocene onwards. Oligocene rocks are absent from the area and Miocene rocks are restricted to comparatively small basins. A long period of erosion from the Oligocene onwards is therefore probable.

A late- or post-Pleistocene age for the fault emplacement is therefore postulated. The Mount Tawai peridotite does not conform with the normal pattern of Alpine type peridotites with regard to orogeny. Alpine type peridotites are usually associated with the earlier orogenic movements. The main Tertiary orogeny in North Borneo occurred in the middle Miocene and the Mount Tawai peridotite is therefore later than the main earth building movements. In this respect it is similar to the Twin Sisters dunite described by Ragan (1963).

The age of the initial intrusion at depth cannot be ascertained

with accuracy. The metamorphic rocks found in the contact zone of the batholith have been tentatively interpreted as remnants of an original thermal metamorphic aureole. These rocks are representative of metamorphosed sediments and volcanics of the chert-spilite type. The base of the chert-spilite formation is not known in North Borneo but similar rocks which have been described from Indonesian Borneo are of Permo-Carboniferous, Triassic, and Jurassic age. The chert-spilite formation is by no means confined to the Tertiary and to quote Rheinhard and Wenk (1951 p.97): "the conditions necessary tonproduce such a rock association have been repeatedly fulfilled".

In the absence of age determinations on the thermal metamorphic rocks it is not possible to state the age of the original intrusion, which must be tentatively assigned to a pre- or early-Tertiary epoch.

The major rock types.

The Mount Tawai igneous complex is built almost entirely of ultrabasic rocks. Minor areas of basic rocks belonging to the gabbroic suite occur but they never form continuous horizons capable of being mapped. The vast majority of the ultrabasic rocks are composed, in varying proportions, of olivine, orthopyroxene, clinopyroxene and spinel. Feldspar bearing varieties are comparatively rare. All the ultrabasic rocks have undergone a certain degree of alteration by serpentinization but only relatively few may be classed as true serpentinites. The ultrabasic rocks have also been affected to varying degrees of cataclastic deformation resulting in granulation and in extreme cases mylonitisation. The majority of the ultrabasic rocks are extremely coarse grained (grains from 5mm. to 10mm. in diameter being common) and accurate modal analysis by point counting is difficult. Approximate modes have been obtained by placing a grid on the peridotite outcrops and estimating the areas occupied by the distinctive pyroxene laths. Orthopyroxene is readily distinguishable from the emerald green clinopyroxene. Further studies have been made on polished specimens but only in the relatively unserpentinised non-deformed rocks can semi-quantitive results be obtained. The results of these studies are shown in Fig. 30 in which the terminology of Johannson (1938) has been used to make possible comparison with other areas.

Over ninety per cent of the Mount Tawai complex is built of harzburgite, in which olivine always makes up more than seventy five per cent of the rock; the rest of which is composed mainly of orthopyroxene with minor amounts of clinopyroxene and spinel.

About five per cent of the Mount Tawai ultrabasic area is built of dunite, composed almost entirely of olivine with minor amounts of chrome spinel. Rarely this latter mineral forms small ore bodies within the dunite. The contacts between dunite and harzburgite are very distinctive owing to the former weathering to an uneven brown colour speckled with black chromite and the latter to an uneven knobbled appearance. The contacts vary from knife sharp to gradational. The graduation from harzburgite to dunite takes place in less than a foot.

Thin bands of pyroxenites consisting of varying proportions of orthopyroxene and clinopyroxene with minor olivine are rarely found.

Gradational rock types between the ultrabasic and gabbroic rock types are rare. Thin bands of feldspathic peridotite occur in the Pantagaluang block but are not widely developed. Peridotite containing dead white patches of an interstitial mineral are also found in the Pantagaluang block and the Patud-Gombaran partial ring intrusion. Thin section examination has shown these interstitial patches to consist mainly of zoisite and calcite and very occasionally relict plagioclase has been observed. The 'saussurite' pockets, however, never make up more than five per cent of the rock, and are unevenly distributed in the above mentioned areas.

Small areas of gabbro have also been located in the area. They consist of two main varieties depending upon the relative abundance of olivine. The olivine gabbro is only found in the Patud-Gombaran intrusion whilst the pyroxene gabbro is more widespread forming small lenticular areas mainly on the eastern flank of the main Tawai block. True troctolites, plagioclase olivine rocks, have not been found in the Mount Tawai area. Both gabbro

types have been considerably affected by secondary alteration.

In its simple mineralogy the Mount Tawai ultrabasic complex is comparable with the Alpine type peridotites described by Thayer (1960). Large areas of diopside peridotite typical of the layered ultramafic complexes of Alaska (Ruickmick and Noble 1959) do not occur in the Mount Tawai area. Rheinhard and Wenk (1951 p.68) suggest that in North Borneo lherzolites are more common than harzburgites but no evidence has been found in the Labuk area to substantiate this.

Chemistry.

Two peridotites and three dunites have been analysed and are shown in Tables 4 and 11. A peridotite from the Porog valley in the Bidu-Bidu Hills has been analysed by the Geological Survey of North Borneo and is shown in Table 4. The peridotites are extremely coarse grained and chemical analyses are of little comparative value. The peridotite and dunite analyses show high magneium contents characteristic of the Alpine Type peridotites and small but variable amounts of lime and alumina. The C.I.P.W. norms (Table 5) show the presence of anorthite which is absent in the rocks analysed and suggests that the pyroxenes are aluminous. The degree of serpentinization of the ultrabasic rocks is reflected in the weight per cent of water present.

Only one gabbro analysis is available; this was supplied by the Geological Survey Department of North Borneo. It is shown in Table 6, together with four gabbro analyses from the Blantian river ultrabasics, quoted in Rheinhard and Wenk (1951 p.69). The Blantian river ultrabasics occur to the south of the Tawai area,

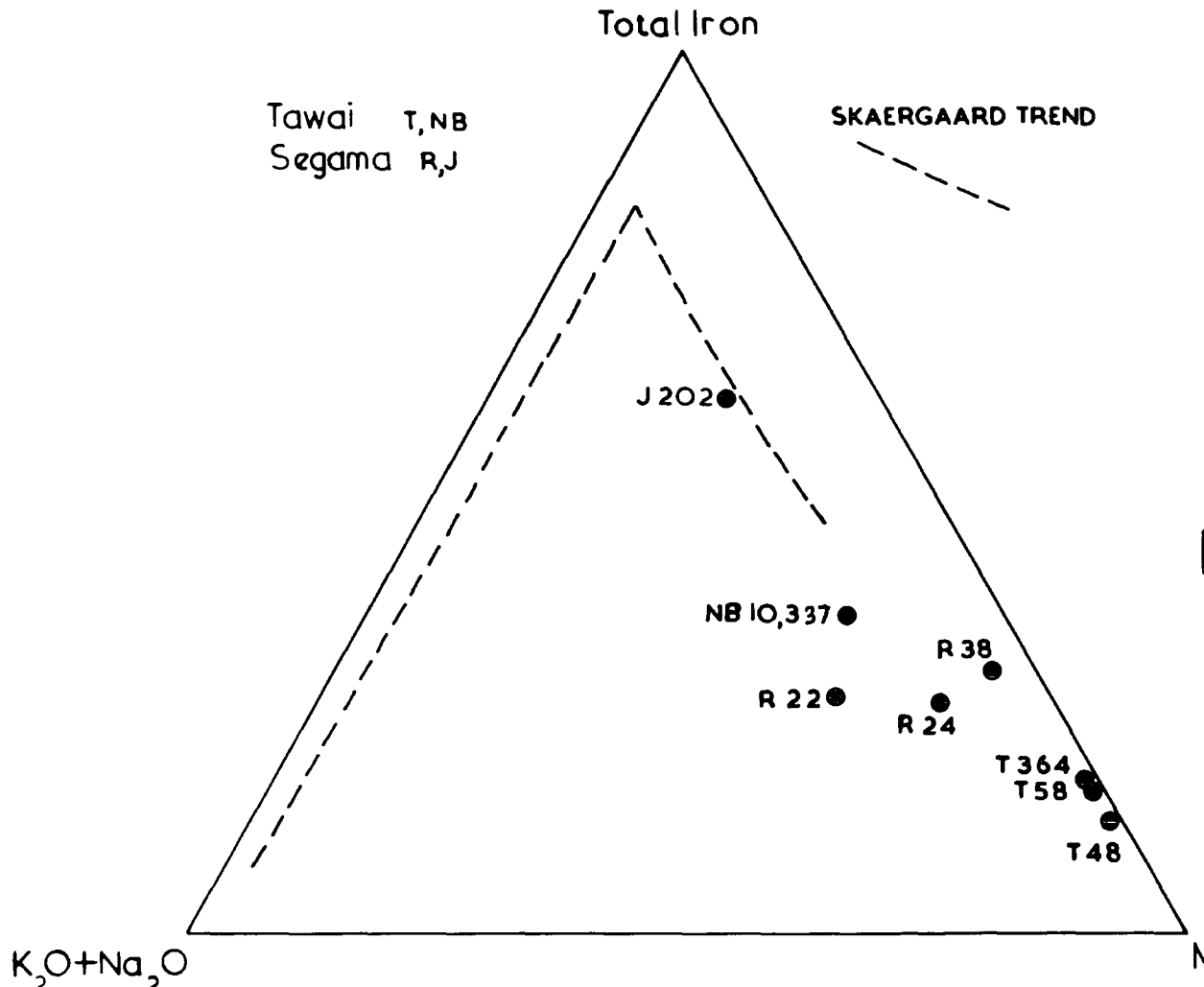

Fig. 29.

FMA diagram of Mount Tawai and other North Borneo ultrabasic and basic rock analyses.

Fig. 30.

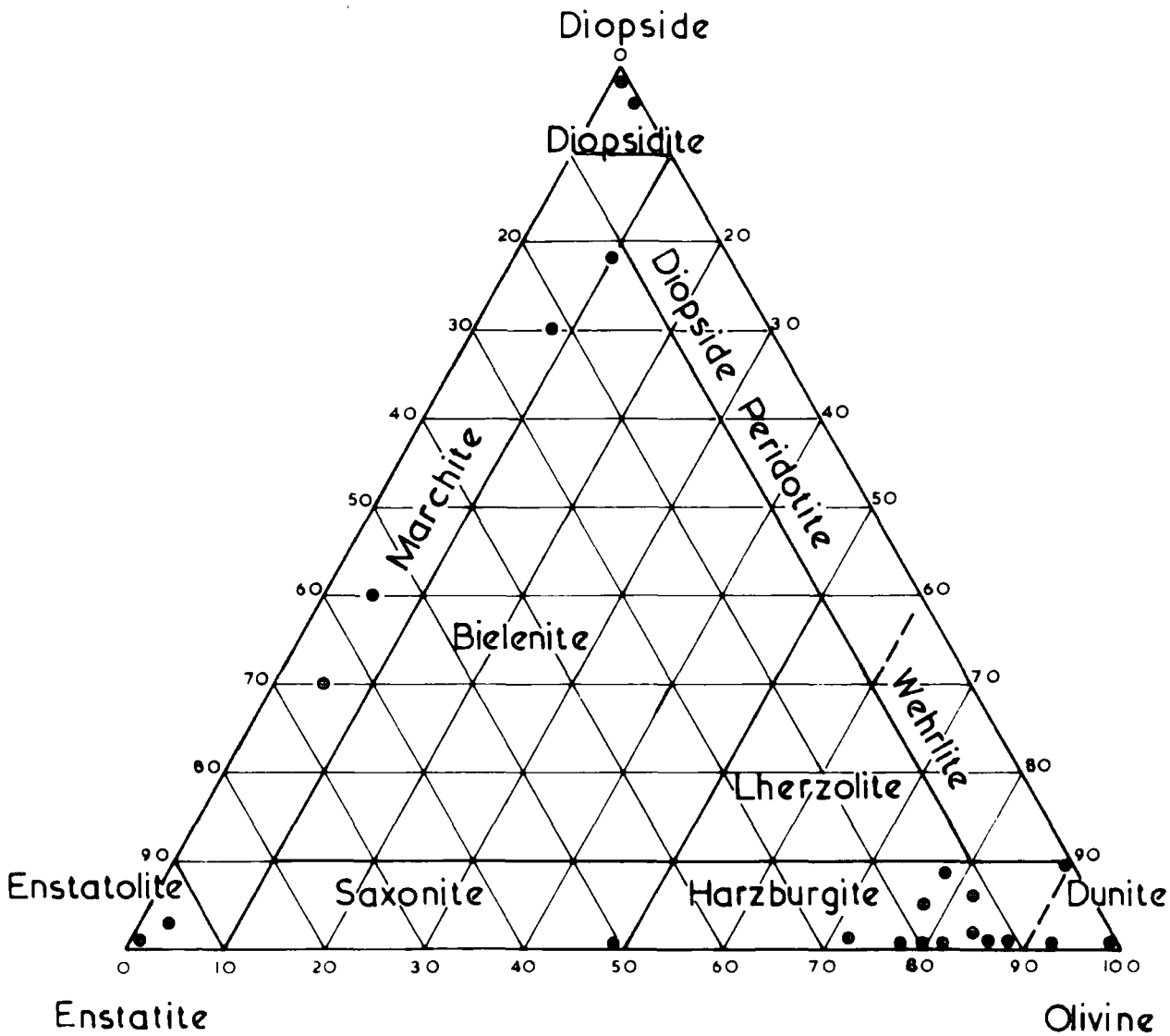

. The approximate mineral content of the Mount Tawai ultrabasic rocks.

but are part of the main Borneo peridotite belt. The gabbros described by Rheinhard and Wenk from this locality are similar to those found in the Tawai area except for the presence of rare troctolite (R38 Table 6).

The rocks analyses have been recalculated on a water free basis and in Fig. 39 are plotted on an $FeO-MgO-Na_2O+K_2O$ triangular diagram. This diagram shows that in passing from peridotite to olivine gabbro to pyroxene gabbro there is enrichment in iron and alkalies. This trend is also reflected in the mineral determinations of olivine, pyroxene and plagioclase. It fits below that of the Skaergaard trend of Wager and Deer (1939) and could be interpreted as what might be expected in the "Hidden Layered series", of that intrusion.

Trace element data for the ultrabasic rocks is given in Tables 4, 11. Turekian and Wedepohl (1961) quote the following average values for the elements examined in ultrabasic rocks:-

Ni	2000
Cr	1600
Mn	1620
Cu	10
Zn	50

Nickel, chromium, and copper are higher than the average values whilst zinc and manganese are in general agreement. Sulphides have not been found in the analysed rocks and the copper and zinc must be present to be in the silicate and spinel minerals. Sandel and Goldich (1943) consider copper does enter silicate structures.

Table 4. Peridotite Analyses.

	No.T364	No.T58	NB.10,381
SiO_2	39.8	41.7	37.2
Al_2O_3	1.9	2.9	.63
Fe_2O_3	4.4	4.2	3.90
FeO	4.3	4.1	3.40
MgO	39.6	38.6	37.90
CaO	1.5	1.9	.90
Na_2O	.1	.0	.08
K_2O	tr	0.0	tr
TiO_2	.1	.1	.01
NiO	.3	.4	.34
MnO	.2	.1	.1
Cr_2O_3	.5	.6	.42
H_2O^+	7.2	5.9	13.50
H_2O^-	.7	.4	1.12
CO_2			.72
Total	100.6	100.9	100.24
Analyst.	W.G. Hancock.	W.G. Hancock.	N.B. Survey.

T.364 - North Tankulap River. 5° 29' 58" N, 117°, 07' 40" E.

T.58 - Meliau River. 5° 36' 52" N, 117° 07' 57" E.

N.B., 10381 - Porog River Bidu-Bidu Hills.

N.B. 10,381. Analyses and norm supplied by Geological Survey Department, British Territories in Borneo.

Trace elements ppm.

	T364	T58
Ni	2510	2790
Cr	3090	4160
Mn	1625	715
Cu	85	75
Zn	85	65

Table 5. C.I.P.W. Norms.

		T364	T58	N.B. 10,381.*
Quartz				
Orthoclase				
Albite		1		.7
Anorthite		4.7	7.8	1.4
Leucite				
Nepheline				
Corundum				
	$CaSiO_3$	1.2	.7	1.3
Diopside	$MgSiO_3$	1.0	.6	1.1
	$FeSiO_3$	-	.1	-
Hypersthene	$MgSiO_3$	17.3	25.5	19.3
	$FeSiO_3$	.8	1.1	.7
Olivine	Mg_2SiO_4	56.6	49.2	52.1
	Fe_2SiO_4	2.9	2.4	2.1
Magnetite		6.6	6.0	5.7
Ilmenite		.1	.2	
Haematite				
Chromite		.5	.6	.6
Water		7.9	6.3	15.34
Total		100.6	100.5	100.34

* Geological Survey Department, British Territories in Borneo.

Table 6. Gabbro Analyses.

	R.38.	R.22.	R.24.	J.202.	N.B.10,337
SiO_2	41.46	46.17	46.33	45.31	50.30
TiO_2	0.14	.13	0.32	3.16	0.30
Al_2O_3	16.29	27.16	22.60	16.53	18.50
Fe_2O_3	4.74	1.64	1.03	8.33	1.06
FeO	3.37	0.88	3.18	6.26	5.10
MnO	0.12	0.01	0.06	0.11	0.11
MgO	16.97	4.55	10.16	5.44	8.20
CaO	9.35	15.24	12.84	8.96	11.30
Na_2O	1.19	1.92	1.40	2.97	2.75
K_2O	-	0.03	.52	0.48	0.12
H_2O^-	0.49	0.16	.13	0.16	0.64
H_2O^+	6.33	2.43	1.37	2.71	1.64
P_2O_5	0.05	0.23	tr	tr	.03
CO_2	-	-	-	-	.06
Cr_2O_3	0.06	-	-	-	-
Less O=S	.07				.03
Total	100.64	100.55	99.94	100.42	100.19
Type	Troctolite	Olivine Gabbro	Olivine Gabbro	Pyroxene Gabbro	Pyroxene Gabbro
Locality	Blantian River	Blantian River	Blantian River	Subahan River	Melrau River

R - 38)
R - 22) Rheinhard and Wenk (1951) Page 69.
R - 24)
J - 202)

N.B. 10,337. North Borneo Survey.

Serpentinites and Serpentinization.

Distribution.

The majority of the ultrabasic rocks show some degree of alteration by serpentinization. Intense serpentinization however is most prominent around the margins of the mass, along the intrusion fault zones and in the breccias. In the central parts of the Tawai and Binalik blocks serpentinization is slight. It is also noticeable that serpentinization decreases upwards along fault planes.

Petrography.

The textures of the serpentinites are controlled by the original rock type and the degree of post-serpentinization shearing. The latter when present completely obliterates textures indicative of the original rock type. The marginal sheared serpentinites in thin section are seen to be composed of a mass of small flakes of serpentine showing strong undulose extinction. The schistose nature of the rock is accentuated by wavy bands of a turbid brown amorphous substance and streaks of magnetite and chromite granules. Apart from the highly sheared serpentinites it is possible to recognise four main textures as follows:-

Mesh texture.

Bastite texture.

Thorn texture.

Asbestiform texture.

Mesh texture.- The totally serpentinised dunites have a characteristic dull black matte appearance. The thin sections show they consist

of serpentine collars and flakes arranged in irregular, closely spaced, trellis structures around nearly isotropic cores (Fig. 31). The meshes always show shearing effects and the regular mesh textured serpentinites described by Tertsch (1922) and Francis (1956) never occur. The serpentine collars are of a composite nature and appear to be interwoven with another mineral showing anomalous interference colours. This mineral, which is biaxial positive, also occurs in minute flakes and scales in the serpentinites and is difficult to identify but its optical characteristics are suggestive of brucite. A fibrous bipartite structure to the collars can sometimes be determined; the fibres showing positive elongation, arcuate extinction and higher birefringence than the cores. The cores of the meshes are usually made up of a near isotropic matte of serpentine but occasionally they contain a mineral showing good basal cleavage and negative elongation. A more ordered mesh structure described by Tertsch (1922) as Maschenstruktur consists of bipartite fibres of length slow serpentine (gamma serpentine) surrounding cores of length fast serpentine (alpha serpentine). The above described serpentinites are probably a sheared variety of this Maschenstruktur. The opposite arrangement described by Tertsch (1922) as Fensterstruktur and consisting of length fast fibres arranged around length slow cores has not been found in the Mount Tawai serpentinites, but it is recorded by Francis (1956) from Glen Urquhart.

A more open macroscopic trellis structure (Fig. 32) sometimes found in the serpentinised dunites and in thin section is seen to consist of flakes and collars of serpentine arranged around olivine pseudomorphs the centres of which contain a reddish brown mineral,

Fig. 31. Photomicrograph of mesh textured serpentinite with thin asbestos vein. T23. (crossed nicols X200)

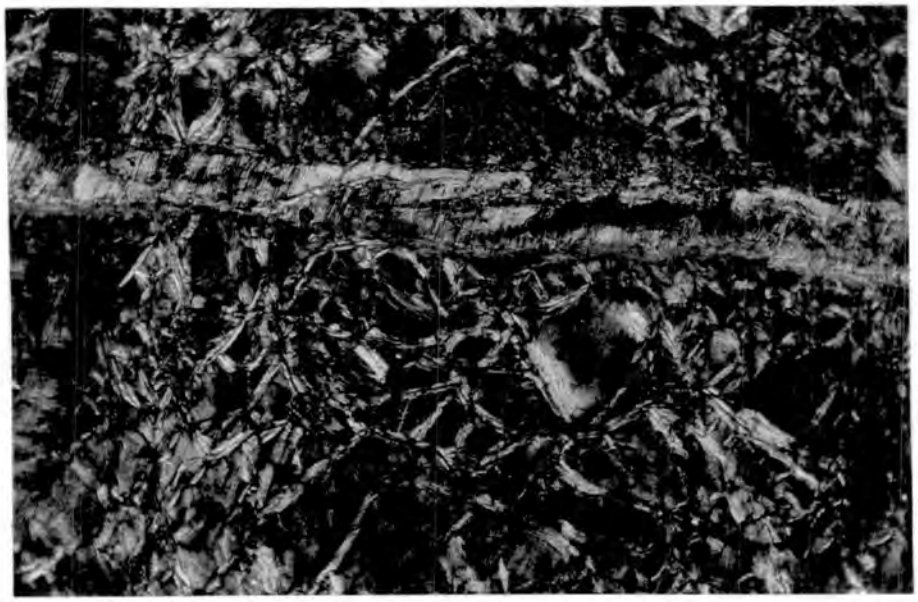

Fig. 32. Photomicrograph of trellis structure in serpentinite T184. (crossed nicols X25).

probably bowlingite, set in a near isotropic groundmass. Magnetite granules and streaks are always present in the serpentinites, while thin veins of clinochrysolite and small needles of tremolite are not uncommon. A chlorite showing ultrablue interference colours may be present in small flakes or in prominent cross cutting veins. Unaltered crystals of chromite are frequently the only relict mineral of the original dunite. Most of the thin sections examined are low in carbonate content.

Bastite texture - The serpentinised peridotites show distinct brassy coloured pseudomorphs of bastite after orthopyroxene set in a dark green groundmass. In thin section the groundmass is seen to consist of a very similar material to the mesh-textured serpentinites. The orthopyroxene appears to show four modes of alteration. In many of the strongly serpentinised peridotites it is seen replaced by a platy serpentine mineralshowing basal cleavage whilst at other times both the olivine and the orthopyroxene are replaced by continuous networks of serpentine veinlets and collars. Frequently however the serpentine collars swing around partially altered orthopyroxene crystals and impart a distinctive knitted texture to the rock. In the partially serpentinised peridotites however talc is the most common alteration product and it is seen as prominent rims around the margins of the orthopyroxene and as irregular patches and veins within their margins. A fourth mode of alteration is seen in the strongly sheared peridotites where a random thorn-like aggregate of serpentine minerals replaces both mesh-textured serpentine and primary orthopyroxene. The exsolution lamellae of clinopyroxene contained within the orthopyroxene are altered to

tremolite amphibole. The clinopyroxene crystals are also altered to tremolitic amphibole but they also show replacement by chlorite.

Thorn texture - An extremely fine grained massive rock is frequently found in irregular flame-like masses wrapped around peridotite boulders in the shear zones. The rock varies from pale green to whitish green in colour and resembles jade. Thin sections show this rock to consist of a strongly sheared aggregate of orthopyroxene and tremolite being replaced by an aggregate of serpentine flakes arranged in a prominent thorn-like texture (Fig. 33). The serpentine mineral has wavy extinction, anomalous blue interference colours and is optically negative with n_Y near 1.565. X-ray diffraction has shown this mineral to be antigorite and it resembles the variety described by Selfredge (1936) as bowenite. Large flakes of antigorite as described by Hess et al (1952) and Francis (1956) do not occur. Small deformed plates of orthopyroxene being replaced by antigorite are seen in the thin sections; which is also replacing mesh-textured serpentine and tremolite.

Asbestiform texture - Small veins filled with serpentine asbestiform minerals only occur in totally serpentinised dunites found in the internal breccia zones. They are particularly well seen in the disturbed dunite lenses in the lower part of the Kuun-Kuun ultrabasic section. The veins may be divided into two types; coarse picrolite veins and cross fibre flexible asbestos veins. The former are the most common and consist of white and pale green veins of poorly fibrous material. Both cross fibre and slip fibre picrolite occur, the former being the most common. Both however may occur in the same vein. The slip fibre varieties (Fig. 34) show a faint banding

Fig. 33. Photomicrograph of antigorite T210 (crossed nicols X50)

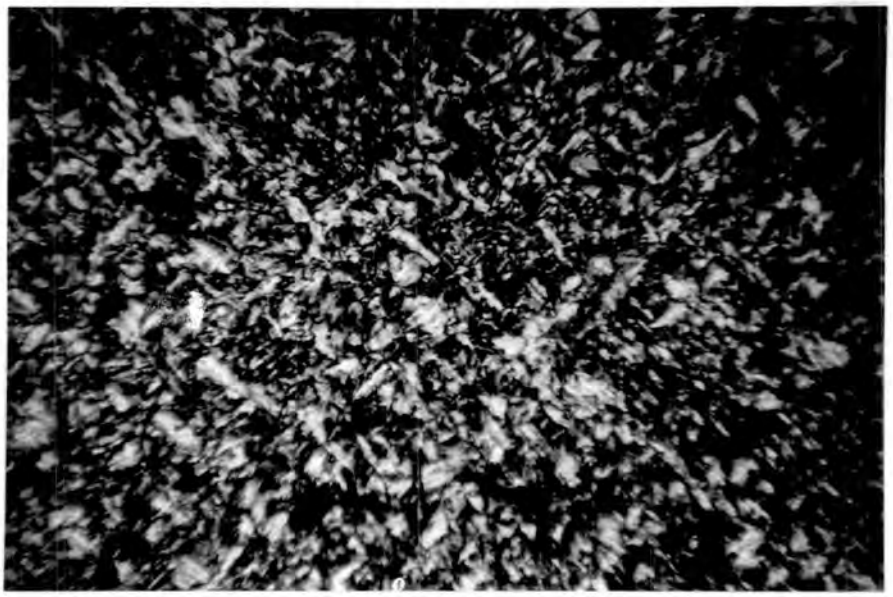

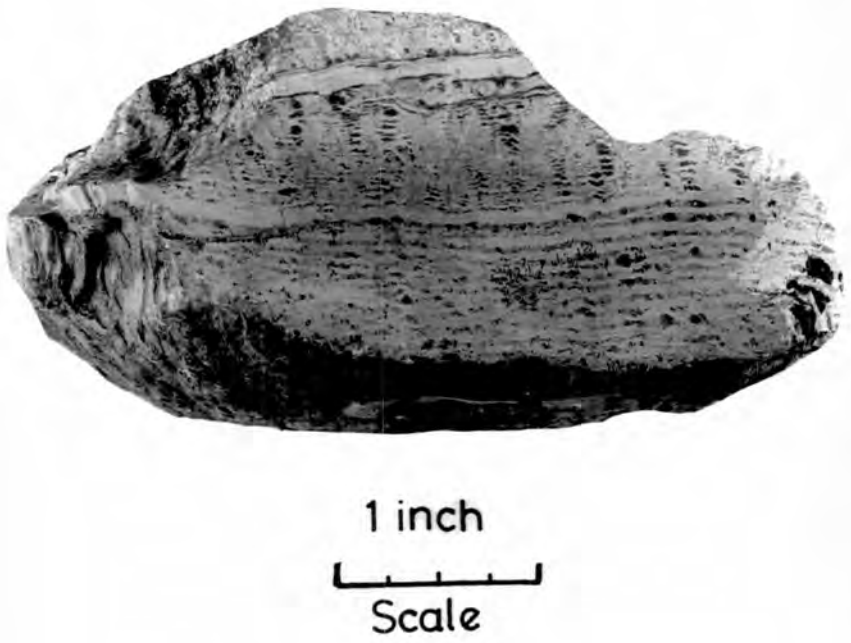

Fig. 34. Photograph of slip fibre. T209.

subparallel to the wall rock but near it grades into compact picrolite. The banded slip fibre veins are frequently wavy following irregularities in the wall rock. Thin sections of these rocks show intricately folded bands of serpentine (Fig. 35) separated by a brown amorphous looking mineral. Under high power this mineral is seen to be fairly fibrous. The compact wall rock mineral is composed almost entirely of this mineral. The cloudy nature of this compact picrolite may be due to iron staining. The contacts of the picrolite veins with the wall rock are sharp. These picrolitic rocks are quite often magnetic due to small concentrations of granular magnetite. The cross fibre picrolite is extremely brittle. The fibre varies in length from less than one quarter of an inch to over two inches.

The cross fibre flexible asbestos veinlets are rare. They are seldom well developed and no deposits of economic size were located. The veins vary from pencil line thickness to half an inch in width and are seldom more than fifteen feet long. They usually occur in subparallel groups; the individual veinlets split and intersect along the strike. Small offshoots are common and the veins terminate by pinching out into the serpentinite. Prominent cross cutting veins are absent. The asbestos veinlets are also orientated parallel to the walls of the sheared dunite lens and the larger ones appear to be filling longitudinal tension joints. The main occurrences of flexible asbestos veinlets are found in the East Meliau, lower Kuun-Kuun, and Ruku-Ruku breccia zones. All the known occurrences in the Labuk area occur in strongly disturbed, totally serpentinised dunite.

The fibre is apple green in colour and separates fairly easily.

It never however reaches the length and silky nature of the Thetford asbestos. Only cross fibre varieties have been observed; although the fibre is seldom exactly normal to the wall rock. Deviations up to 20^{o} have been recorded. Partings within the bands are common and are never exactly in the middle of the veins. In the majority of the veins the parting contains granular magnetite. Thin sections of the smaller veins however show non-fibrousserpentine in the parting, and what appears to be 'ghosts' of wall rock interrupting the fibre. Most of the veins are partially bordered by picrolite on one or both of the margins. Frequently the silky asbestos passes laterally into picrolite. A prominent banded specimen (Fig. 36) consists of alternate bands of slip fibre picrolite and cross fibre asbestos. Many cross fibre picrolite bands contain subordinate amounts of flexible asbestos.

Mineralogy.

The minerals of the serpentinites are particularly difficult to distinguish although recent advances in their identification by X-ray diffraction (Whittaker and Zussman 1956) has considerably simplified the task. Various workers including Warren and Hering (1941) and Whittaker (1953) have shown that serpentine has a layered type of structure similar to kaolinite. The serpentine structure consists of a pseudo-hexagonal network of SiO_4 tetrahedra which is linked to a brucite layer by means of the apical oxygens. However the linking of the pseudo-hexagonal tetrahedra sheets and the brucite layers involve appreciable mis-matching. Various polymorphs of serpentine are produced by the intricate ways in which the two components strive to reduce the degree of mis-matching. The main

Fig. 35. Photomicrograph of slip fibre picrolite T209.

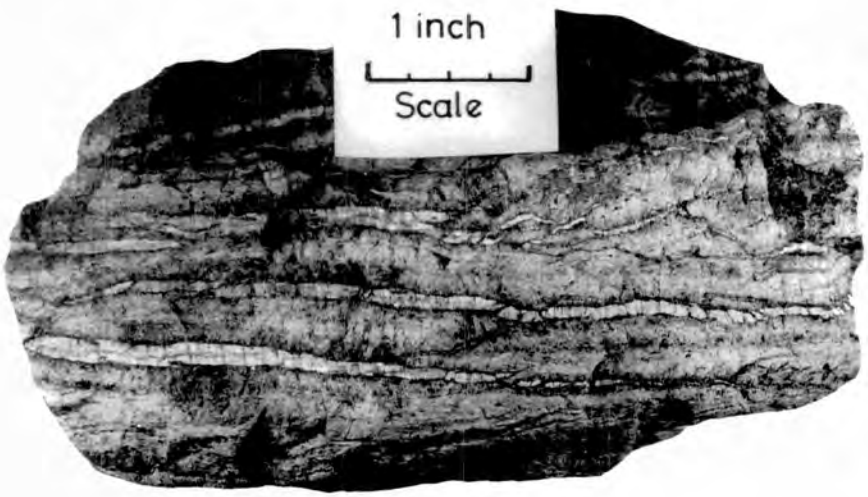

Fig. 36. Photograph of cross fibre asbestos T411.

polymorphs are chrysolite, antigorite and lizardite. Lizardite and antigorite have one layer per unit cell and chrysolite two. The latter has a tube-like structure whilst lizardite and antigorite are generally platy although fibrous antigorites have been reported (Deer, Howie and Zussman 1963 vol. 3). Antigorite is distinguished from lizardite and chrysolite by its large aÅ unit cell dimension. All three have characteristic X-ray diffraction patterns and the serpentine minerals of the Mount Tawai serpentinites have been distinguished by using them together with the data of Whittaker and Zussman (1956). The serpentine minerals were examined on the Phillips High Angle diffractometer using a scan speed of 1° per minute, chart speed 800mm. per hour and rate meter X 8. The specimens were examined as full mounts and scans were made from $6^{\circ}2\theta$ to $65^{\circ}2\theta$ using Cu filtered radiation and pulse height discrimination.

Other secondary minerals besides those of the serpentine group are found in the serpentinites and these have been identified by X-ray diffraction and optical techniques.

The main minerals found in the Mount Tawai serpentinites are lizardite, chlorite, brucite, magnetite, antigorite and clinochrysotile.

Lizardite - X-ray diffraction patterns of the mesh textured serpentinites indicate that lizardite is the chief mineral present. Other lines suggestive of clinochrysolite and brucite are also present. Lizardite gives a characteristic X-ray diffraction pattern (Table 7) which is distinguished from that of antigorite by a moderately strong pair of lines at d = 1.536 Å and d = 1.503 Å. (The lizardite pair).

Table 7. Mineral Identification. Lizardite and brucite.

Lizardite			T23 Serpentinite		Brucite		
hkL	I	dÅ	dÅ	I/I_2	dÅ	I/I_2	hkL
002	10	7.36	7.37	100			
			4.76	22	4.77	90	001
020	7	4.62	4.60	17			
022	2	3.89	3.90	6			
004	10	3.64	3.67	45			
					2.725	6	100
130	4	2.65	2.652	5			
202	8	2.495	2.494	22			
			2.444	18*			
			2.367	27	2.365	100	101
203	2	2.299	2.295	3			
204	6	2.148	2.149	3			
206	4	1.794	1.794	10	1.794	56	102
310	4	1.737					
028	1	1.695	1.694	2			
			1.574	9	1.573	36	110
060	7	1.534	1.535	18			
208	6	1.503	1.500	8			
			1.494	4	1.494	18	111

Whittacker and Zussman 1956. p. 117 Table II no. 14. Clinochrysotile* reflexion. A.S.T.M. 7-239.

The serpentine examined (T23 Table 7) contained both alpha and gamma serpentine and it therefore appears that the distinction between these two is either one of optical orientation or that gamma serpentine is a mixture of interwoven brucite and lizardite thus accounting for its higher birefringence.

X-ray diffraction patterns of bastite pseudomorphs from non-deformed serpentinites indicate they are formed of lizardite rather than antigorite (Table 8). This finding is in agreement with similar identifications of bastite pseudomorphs made by Whittaker and Zussman (1956). The bastite pseudomorphs often appear plate-like in thin section.

Platy lizardite has been reported from Kennack Cove, Cornwall, by Deer, Howie and Zussman (1963 vol. 3, Table 29 No. 7) and it is noticeable that this mineral has a higher aluminium content than other lizardites.

Lizardite is the major serpentine mineral found in the ultra-basic rocks at Hangha, Sierra Leone (Dunham and Phillips, et al 1958), and in the mesh textured serpentine breccias described by Green (1961) from Papua.

Chlorite - Small amounts of chlofite are constantly present in the serpentinites. This chlorite is usually found in small plates in the mesh and bastite textured serpentinites and is difficult to separate. Occasionally large plates up to 2cm. wide are found in veins intrusive into the serpentinites. In thin section the chlorite shows ultrabasic birrefringence colours with slightly inclined extinction. The mineral is biaxial positive with Nx = 1.585 and its X-ray diffraction pattern is very similar to that

Table 8. Mineral Identification. Bastite Pseudomorph.

Specimen T342		Lizardite.*		
dÅ	I/I_2	dÅ	I	hkL.
7.35	100	7.36	10	002
4.60	16	4.62	7	020
		3.89	2	022
3.67	42	3.64	10	004
		2.65	4	130
2.495	20	2.495	8	202
		2.299	2	203
2.146	3	2.148	6	204
		1.830	2	008
1.795	2	1.794	4	206
		1.737	4	310
		1.695	1	028
1.537	16	1.534	7	060
1.505	8	1.503	6	208

Platy serpentine
pseudomorph.

*Whittaker and Zussman 1956.

of sheridanite (Table 9). When the chlorite is found as the dominant interstitial gangue mineral in the chromite ore bodies it imparts a violet tinge to the ore. Usually however the chlorite is dark green in hand specimen which suggests the violet coloured variety is chromiferous.

The relation of the chlorite to lizardite suggests there are two generations of the former. The small plates in the mesh textured serpentinites are interwoven with serpentine and appear contemporaneous with it. Prominent veins of coarse chlorite definitely intrude the serpentinites in certain localities and are of a later origin.

Brucite - Minute fibres, often matted together into irregular areas or interwoven with the serpentine collars are suggestive of brucite. These fibres are biaxial positive, show anomalous interference colours and a higher birefringence than the serpentine cores. The X-ray diffraction pattern of brucite (Table 7) is very similar to that of the serpentine minerals but on the trace of the mesh textured serpentinite (T23 Table 7) peaks at d = 4.77 Å, d = 2.365 Å, d = 1.573 Å and d = 1.494 Å are suggestive of the 001, 101, 110 and 111, reflections respectively of brucite. Moreover the lizardite peak at d = 1.794 Å (206) is broad suggesting admixture of another peak possible the brucite 102 reflections. The other peaks cannot be explained by chlorite for neither the 14 Å or 7 Å reflections were recorded on the chart. Antigorite could possibly account for the peak at 4.76 Å (810) reflections but the antigorite pair at d = 1.563 Å and d = 1.541 Å is absent from the trace. The overall pattern of the peaks that cannot be satisfied

Table 9. Mineral Identification of Sheridanite.

Specimen H44.	I/I_2	Sheridanite	I/I_2	hkL
14.2	16	14.1	60	001
7.079	49	7.114	70	002
4.745	65	4.750	50	003
4.599	4	4.578	40	020
3.546	100	3.558	50	004
2.836	20	2.852	20	005
2.580	2	2.655	5	$130,20\bar{1}$
		2.686	40	$131,20\bar{2}$
2.542	3	2.543	100	132,201
2.442	3	2.442	50	$132,20\bar{3}$
2.380	1	2.381	20	$13\bar{3},202$
2.259	1	2.260	10	133,204
2.024	3	2.075	5	134,205
2.005	3	2.006	20	$13\bar{5},204$
1.888	1	1.887	10	135,206
		3 peaks omitted		
1.565	1	1.570	10	137,208
1.540	1	1.538	60	331,060

by lizardite or clinochrysolite reflections strongly suggests the presence of brucite. It may be noted that Dunham and Phillips (op. cit.) produced evidence suggesting that brucite occurs in appreciable quantity in serpentinite at Hangha.

Magnetite - Granular magnetite is a common accessory in the serpentinites. Usually it is concentrated in the centres of the olivine pseudomorphs and along the edges of the serpentine collars though occasionally it is concentrated into irregular areas up to one foot by six inches in dimension. X-ray fluorescence analysis of the magnetite shows that it is nickeliferous with NiO varying from 0.1 to 0.8 per cent. This magnetite appears to be similar to that described from Mwahanza Hill, Tanganyika by Fawley (1959).

Antigorite - The massive fine grained jade-like mineral found in the sheared serpentinites has been identified as antigorite. Antigorite gives a much clearer X-ray diffraction pattern than lizardite or clinochrysotile. It is distinguished from lizardite by a medium strong line at d = 1.563 Å which forms a pair with a medium strong line at d = 1.541 Å. This antigorite pair is distinctive from the corresponding "Lizardite pair", at d = 1.536 Å and 1.503 Å. This method of distinguishing between lizardite and antigorite given by Whittaker and Zussman (1956 p. 124) is the most reliable. The X-ray diffraction of the thorn-like mineral thus confirms the view of Selfridge (1936) that bowenite is a form of antigorite.

Clinochrysotile - The asbestiform mineral found as small veinlets in serpentinised dunite has been identified as clinochrysotile admixed with lizardite (T411 Table 10). The mineral has characteris-

Table 10. X-ray diffraction identification of clinochrysotile - Lizardite mixtures.

	Chrysotile [x]		Lizardite [x]		Specimen T411		Specimen T150		Specimen T209	
hkL	dÅ	I	dÅ	I	dÅ	I/I_2	dÅ	I/I_2	dÅ	I/I_2
002	7.36	10	7.36	10	7.37	100	7.31	100	7.32	100
020	4.58	6	4.62	7	4.60	21	4.53	32	4.55	29
022			3.89	2						
004	3.66	10	3.64	10	3.66	68	3.65	95	3.68	90
130	2.66	4	2.65	4	2.66	8	2.66	5	2.64	8
201	2.594	4			2.593	11	2.593	8		
202	2.549	6			2.543	20				
202			2.495	8	2.504	18	2.494	43	2.495	50
202	2.456	8			2.458	35	2.442	28		
040			2.299	2			2.332	2	2.332	14
203	2.282	2								
$20\bar{4}$	2.215	2								
204			2.148	6			2.151	5	2.149	8
204	2.096	6			2.099	13				
008	1.829	2	1.830	2						
206			1.794	4					1.794	6
206	1.748	6			1.746	12				
310	1.737	4								
028	1.695	1								
060	1.536	8	1.534	7	1.537	21	1.535	29	1.540	30
208			1.503	6	1.506	7	1.506	8	1.504	15

[x] Whittacker and Zussman (1956).

Mainly clinochrysotile. Lizardite plus clinochrysotile. Mainly lizardite.

tic peaks at d = 2.45 Å (202), d = 2.09 Å (204), d = 1.74 Å (206 Å) and d = 1.53 Å (060). The presence of the lizardite reflection 202 and the "lizardite pair", indicate admixture of this mineral. The clinochrysotile shows positive elongation and is biaxial negative with a low 2V.

Two specimens of picrolite were also examined and shown to consist of varying mixtures of clinochrysotile and lizardite (Table 10).

Specimen T150 is a coarse cross-fibre picrolite and shows relatively strong lizardite reflections admixed with clinochrysotile reflections. Specimen T209, which is the compact form of picrolite, shows mainly lizardite reflections with only minor clinochrysotile reflections.

Chemistry.

In order to study the changes occurring during serpentinization three dunites showing varying degrees of alteration were analysed (Table 11). Serpentinised non-mineralised dunites were chosen for this study because of their simple mineralogy; and because analysis of serpentinised peridotites would be more difficult to compare on account of the coarse grain size of the original minerals.

A comparison of the analyses given in Table 11 suggests that serpentinization involves considerable hydration, a loss of megnesia, total iron, and silica, and a slight increase in nickel oxide. The process also involves an in crease of the Fe_2O_3/FeO ratio. Whether the decreases in the major oxides are real or simply due to the addition of water is examined in the next section.

The optical and X-ray diffraction identifications of the

Table 11. Serpentinised Dunite Analyses and Norms.

	T48	T217	T23
SiO_2	40.1	36.4	35.9
Al_2O_3	.4	.5	.3
Fe_2O_3	2.3	3.0	5.6
FeO	5.5	4.2	1.1
MgO	49.8	46.2	39.8
CaO	nd	.7	.7
Na_2O	nd	nd	.1
K_2O	nd	nd	nd
TiO_2	nd	nd	nd
NiO	.2	.4	.5
MnO	.1	.1	.1
Cr_2O_3	.4	.6	.5
H_2O^+	1.9	7.2	14.1
H_2O^-	.2	.5	1.9
Total	100.9	99.8	100.6

Weight per cent.

		T48	T217	T23
Chromite	Cr_2O_3 FeO	.7	.9	.9
Chlorite	$5MgOAl_2O_3 3SiO_2 4H_2O$	1.7	2.8	1.7
Tremolite	$2CaO 5MgO 8SiO_2 H_2O$		5.3	5.3
Haematite	Fe_2O_3			2.6
Magnetite	$FeOFe_2O_3$	3.2	4.4	4.4
Brucite	$MgOH_2O$	1.2	8.4	8.3
Serpentine	$3MgO 2SiO_2 2H_2O$ ‡	12.1	23.6	74.1
Olivine	$(MgFe)_2SiO_4$	82.0	53.0	-
Water unaccounted for			1.0	1.5
Water H_2O^-		*	.5	1.9
		100.9	99.8	100.7

*H_2O^- used in brucite calculation.

‡Olivine composition 92 mol. per cent Fo.

Trace elements p.p.m.			
Ni	1300	2770	3560
Cr	3080	4172	3570
Mn	810	715	1120
Cu	70	75	20
Zn	75	75	85

Location - (T48 5° 33' 34" N 117° 08' 07" E.
(T217 5° 29' 24" N 117° 07' 41" E.
(T23 5° 35' 29" N 117° 08' 45" E.

n.d - not detected.

Analyst W.G. Hancock.

Table 12. Serpentinised Dunite Analyses - Recalculated on water free basis.

	T48	T217	T23
SiO_2	40.7	40.2	43.6
Al_2O_3	.4	.5	.4
Total iron*	7.6	7.0	6.2
MgO	50.6	51.1	48.5
NiO	.2	.4	.6
MnO	.1	.1	.1
Cr_2O_3	.4	.7	.6
Total	100	100	100

*Total iron as FeO.

minerals present in the serpentinised rocks are largely confirmed by the analysis. The X-ray diffraction data strongly suggests the presence of brucite although it is difficult to see in thin sections. If all the water present is assumed to be in the lizardite then calculations show that in specimen T217 as much as 6.6% magnesia cannot be accounted for. The small amounts of chlorite and tremolite present are insufficient to account for this anomaly. If a similar assumption is made for the totally serpentinised rock then there is insufficient silica to satisfy the serpentine formula. These anomalies may be removed however if brucite is included in the calculations. Bowen and Tuttle (1949) show that brucite and chrysolite are formed by the serpentinization of magnesian and olivine and it is interesting to note that in their experiments brucite crystallised as large easily identified plates.

A reasonable estimate of the 'serpentine norm', can only be achieved by including brucite together with the other known minerals in the calculations. The 'norms' have been calculated in the following way from the molecular proportions and are presented in Table .

(1)	Allot Cr_2O_3:FeO	Chromite 1:1
(2)	Allot Fe_2O_3:FeO	Magnetite 1:1
(3)	Residual Fe_2O_3 to haematite	Residual FeO see step 6.
(4)	Allot Al_2O_3 to chlorite.	This determines the silica, water, and magnesia allotments in chlorite $5MgO\ Al_2O_3\ 3SiO_2\ 4H_2O$.

(5)	Allot CaO to tremolite	This determines the silica, water, and magnesia allotments in tremolite. $2CaO\ 5MgO\ 8SiO_2\ H_2O$.
(6)	Allot residual FeO from step 2 to olivine.	This determines the magnesia and silica allotments for the olivine if the composition is known.
(7)	Allot residual SiO_2 to serpentine.	This determines magnesia and water allotments for serpentine. $3MgO\ 2SiO_2\ 2H_2O$.
(8)	Remaining MgO to brucite.	This determines the water allotment for brucite.

The composition of the olivine was estimated from X-ray diffraction as 92 mol. per cent. Fo for specimens T48 and T217 and was assumed to be the same for the total serpentinite T23. Using the above scheme a fair balance can then be achieved. In analysis T48 not quite enough water was available to satisfy the residual magnesia for brucite whilst in T217 and T23 1 per cent and 1.5 per cent water respectively remained unaccounted for. This remaining water may be partly reconciled by a hydrous iron oxide although the majority of the unexplained water could be due to analytical error.

Serpentinization.

The serpentinization problem has been studied by many workers including Benson (1918), Hess (1933 and 1955) Du Rietz (1935) and Bowen and Tuttle (1949). The major experimental work has been carried out by Bowen and Tuttle (1949) and their study of the system $MgO - SiO_2 - H_2O$ has done much to clarify the problem. Their experimental work has shown that when a mass of forsterite crystals in water is cooled from 1000°C serpentine and brucite begin to form from the olivine around 400°C. The study also showed that if carbon dioxide was present in the hydrous phase, to remove excess magnesia, serpentine will form from olivine at temperatures up to 500°C. Bowen and Tuttle found no evidence to suggest that serpentine can form from olivine above 500°C.

However general equations show that if magnesia and silica are not removed from the system a large increase in volume occurs i.e.

$$2\,Mg_2SiO_4 + 3H_2O = Mg_3Si_2O_5(OH)_4 + Mg(OH)_2$$

88cc — 120 cc — 24 cc

Forsterite — serpentine — brucite

$$2Mg_2SiO_4 + 2H_2O + Co_2 = Mg_3Si_2O_5(OH)_4 + MgCo_3$$

88 cc — 120 cc — 28 cc

Forsterite — serpentine — Magnesite

If the excess of magnesia and silica are removed in solution their equal volume conditions may be maintained.

$$5Mg_2SiO_4 + 4H_2O \quad 2Mg_3Si_2O_5(OH)_4 + 4MgO + SiO_2$$

219 cc — 220 cc — Removed

Olivine — serpentine

The effect of iron in the olivine is to lower the temperature of serpentinization. According to the evidence of Bowen and Tuttle (1949) an olivine containing ten mol per cent fayalite is serpentinised at 340°C (water vapour pressure = 15,000 lb/in ^{2}). Hess (1933) suggested an alternative hypothesis and invoked a serpentine magma containing olivine and residual aqueous silicic acid solutions. Bowen and Tuttle (1948) however have shown that no liquid phase in the system MgO - SiO_2 - H_2O at temperatures up to 1000°C and pressures of 15, 000 lb/in ^{2} and the possibility of a serpentine magma appears remote. However it must be noted that chrysotile was the only serpentine polymorph formed in their experiments and the results are not strictly comparable with the natural assemblages observed in serpentinites where lizardite is the dominant alteration product.

The three serpentinised dunite analyses have been examined in the light of Bowen and Tuttle's (1949) findings. The three analyses have been recalculated to a hundred per cent on a water-free basis (Table 12). The small amounts of soda and lime were also removed. The results of the three recalculated analyses show that the content of all the major oxides appears approximately constant. Of the minor oxides nickel shows a sharp increase. Total iron also remains constant. These results suggest that if equal volume relations have been maintained during serpentinization the weight per cent of oxides has been almost equal to the weight per cent of water introduced. Moreover the major oxides would have been removed in the proportions in which they were present in the original olivine. This indeed seems unlikely. The petrographic evidence suggests that the chief serpentinization products of forsterite are lizardite, brucite, and magnetite. The X-ray diffraction data tend to confirm the presence

of brucite and it is impossible to recalculate the analysis in terms of the mineral composition if brucite is not included. This is also the case in the analysis and recalculation of the Hangha dunite given by Dunham and Phillips (1958). It is interesting to note that in the 'normative' calculations the same weight per cent of brucite is derived from the partially serpentinised dunite T217 and the total serpentinite T23. This may well suggest that brucite reaches a maximum value during serpentinization after which only serpentine is formed.

The recalculated analyses strongly favour a constant composition and an increase in volume. The field evidence shows that many of the highly serpentinised areas are strongly sheared and brecciated but it is difficult to correlate this with expansion due to an increase in volume. Totally serpentinised rocks that have not been strongly sheared have been located out of the disturbed zones. Moreover numerous examples from many parts of the world of non-cataclastic serpentinites are known. The alternative hypothesis that equal volume relations are maintained during serpentinization is not confirmed by the recalculated analysis. Moreover this process would involve considerable amounts of water to remove the excess magnesia and silica in addition to that needed for the serpentine. It would also be expected that widespread deposits of silica and magnesia would be found around the peripheral margins of the ultrabasic batholith. Silicification of the ultrabasics and the country rocks is fairly common but may be attributed to factors other than serpentinization. Deposits of magnesite are unknown in the Labuk area but small veins do occur in the Silam-Beeston ultra-basics described by Fitch (1956).

The source of the water necessary for serpentinization is important. Hypothesis on the source of the water may be divided into three main groups:-

1. The water is of magmatic origin, the process of serpentinization being autometasomatic. This view was held by Benson (1918) and has been supported by Francis (1956).
2. The water has been introduced by neighbouring granite intrusives.
3. Perhaps the most widely held theory at the moment is that invoking the derivation of the water from enclosing sedimentary rocks. This is the view held by Turner and Verhoogen (1960) for the majority of serpentinites.

The second hypothesis has no foundation in the Labuk area but it must not be disregarded for regions where younger acid intrusions are in close proximity to serpentinites. Cases of this phenomena have been described by Keep (1929) and du Rietz (1935).

The Tertiary sediments surrounding the Mount Tawai area are mostly greywacke sandstones with thin shales and mudstone. Basaltic and spilitic volcanic rocks also occur in the contact areas. These rocks are an ideal source of water but in no locality has dehydration phenomena been noted close to the contact. If the water necessary for serpentinization has been obtained from the surrounding rocks then it must be postulated that it was obtained below the present surface.

The case for an autometasomatic origin seems more positive. A small but significant rise in the nickel oxide content with increasing serpentinization has been recorded which might indicate

that the water originated via the peridotite. Additional evidence is also suggested by the presence of talc rims around altered orthopyroxene crystals. Bowen and Tuttle (1949) indicate that autometasomatism of peridotite involves alteration of enstatite to talc at high temperatures and replacement of olivine by serpentine and brucite below 400°C. Pseudomorphs composed totally of talc after orthopyroxene are however rare. The chemical evidence suggests that a reaction involving maintenance of constant composition with an increase in volume has taken place during serpentinization, although little field or petrographic evidence can be found to confirm that an increase in volume has occurred. It is possible that serpentinization involves the movement of water from the lower levels of the ultrabasic body to the upper parts; the decrease in volume suffered by the former area being compensated by an increase in the latter.

It has been suggested earlier that the final stages of emplacement have been accomplished by faulting greatly facilitated by a lubricant of serpentinites around the margin and along the major faults. Peripheral serpentinization has been observed elsewhere notably by Benson (1918) in New Zealand and Taliaferro (1943) in California. The metamorphic rocks brought up in the fault contact zone of Mount Tawai have been tentatively interpreted as the remnants of an original thermal aureole associated with some stage in the initial emplacement of the mass. During this stage temperatures would have been above 400°C and therefore above the stability point of serpentine. The evidence suggests that serpentinization occurred after cooling and was followed by the final fault emplacement.

Petrology of antigorite and clinochrysotile.

The formation of antigorite and clinochrysotile is closely related to the main serpentinization problem. Both minerals have been observed replacing mesh-textured lizardite.

In the Mount Tawai area antigorite is confined to the highly deformed shear zones. In thin section it has been observed replacing mesh textured lizardite and orthopyroxene. It would thus appear that stress is an important factor in antigorite formation.

Various theories have been advanced to account for the formation of antigorite. At Glen Urquhart, Francis (1956) observed antigorite forming directly from olivine and orthopyroxene but is usually seen replacing mesh-textured serpentine. In this locality antigorite is most common in areas showing shearing effects but it is also found in undeformed rocks. In discussing antigorite from Venezuela, Hess et al (1952) concluded that antigorite forms mainly by serpentinization of orthopyroxene. Whittaker and Zussman (1956) have shown however that most bastite pseudomorphs after orthopyroxene are lizardite. The X-ray diffraction chart of a bastite pseudomorph (Table 8) from the Mount Tawai area confirms this. In the sheared serpentinites however antigorite has been observed replacing orthopyroxene. Antigorite from the Queensland Alpine type serpentinites has been described by Wilkinson (1953) who suggested that the mineral was formed by thermal metamorphism of chrysotile by neighbouring granites. Hess et al (1952) however has shown that at low temperatures chrysotile changes only slowly to antigorite. A grade of metamorphism above the chlorite-biotite-greenschist facies and below the albite-epidote amphibolite facies is suggested for the formation

of antigorite.

It is most noticeable in the Mount Tawai area that bowenite antigorite is always seen replacing sheared serpentinites and has never been observed in disturbed dunite serpentinites. Moreover in the shear zones antigorite only occurs associated with tremolite and other calc silicate minerals. Francis (1956) noted the association of actinolite and antigorite at Glen Urquhart and Bilgrami (1961) has described antigorite replacing vesuvianite at an ultrabasic contact with limestone at Zhob Valley, Pakistan. Antigorite analyses usually show a high Si and Al content than olivine and the chemical environment may be of importance in its formation. That a source of alumina is not the sole requirement is shown by the fact that many orthopyroxenes are replaced by platy lizardite. The Mount Tawai antigorite occurrences suggest that chemical environment allied with strong shearing stress are important in the formation of this mineral.

The origin of the clinochrysotile asbestos veins is even more problematical. It is clear from published clinochrysotile analyses that this mineral is very similar to lizardite in composition, there being no need to invoke addition of extra material. Many theories on the formation of clinochrysotile veins in plutonic ultrabasic rocks have been advanced in the past. These theories fall into two main groups.

1. The veins are filling fractures within the serpentinite, the clinochrysotile having been either deposited in the veins from circulating solutions, as suggested by Taber (1917) or that the silky fibre has grown from, and at the expense of, the wall rock as advocated by Graham (1917).

Riorden (1955) suggests a combination of these two methods.

2. The veins have grown in narrow fissures pushing aside the wall rock. This theory is supported mainly by Cooke (1937).

3. The veins have formed by rearrangement of minerals existing in the original rock. Hall (1930) invokes this theory.

In the Mount Tawai deposits cracks, in disturbed serpentinite after dunite, partially filled with picrolite and clinochrysotile favour the first of the above hypothesis. It is noticeable that in the partially filled cracks that the fibre is very irregular. However it is difficult to reconcile the narrow veins that intersect and split along the strike with a fissure filling hypothesis. Thin sections of these veins show the walls to have sharp contacts but occasionally inclusions or a central parting of lizardite are noticeable suggesting replacement. However in no case has a chromite grain been found as an inclusion. There is no evidence to suggest that the veins have pushed apart the wall rocks. The larger veins appear to be filling fissures but whether the chrysotile has been deposited in the fissures or whether it has grown from, and at the expense of, the wall rock is uncertain. The smaller veins may be replacement veins but it is difficult to prove. The problem is far from clear and the ultimate solution may well lie with the mineralogist. If replacment has occurred the formation of clinochrysotile invokes an origin from the serpentine polymorph lizardite. Lizardite has not been prepared synthetically and little is known about its detailed structure. Deer, Howie and Zussman (1963 vol.3) suggest that in the lizardite structure strain resulting

from mis-matching may prevent its growth. Clinochrysotile on the other hand forms good crystals which the electron microscope has shown to be tubular. This tubular structure may be a better readjustment to mis-matching than the arrangement in lizardite thus allowing free growth. The change from lizardite to clinochrysotile involves change from a single layered platy serpentine to a tubular two layer one. Even in a replacement hypothesis is not invoked the structural differences between the two point to a contrasting medium of growth. Clearly more information about the change from lizardite to clinochrysotile is required.

The constant association of picrolite with clinochrysotile in the Mount Tawai area suggests that the former may be an intermediate phase between lizardite and clinochrysotile. The compact picrolite is in fact mainly lizardite whilst the brittle variety is a mixture of clinochrysotile and lizardite. The picrolites show abundant evidence of having undergone strong shearing for the slip fibre has a remarkably crenulate appearance in thin section (Fig. 35). It is not known whether the 'picrolite' lizardite has a tubular structure. It is possible that picrolite forms during a period of stress and that clinochrysotile forms from it afterwards in a period of quiescence thus allowing its free growth. Riorden (1955) has suggested that clinochrysotile may crystallise from picrolite during a cooling stage involved in the formation of the silky asbestos, the picrolite being formed in the colloidal state at an earlier stage by leaching of the vein wall rocks.

The ideal environment, in the Mount Tawai area, for the formation of clinochrysotile asbestos appears to be in cracked and disturbed serpentinised dunites. Only thin veins are found in widely

scattered localities and it must be concluded that conditions suitable for large scale growth of clinochrysotile have never been achieved. Cooke (1937) and Riorden (1955) both suggest that temperature is an important factor, the close proximity of acid intrusives being responsible for heating the mineralised solutions. However at Hangha, Sierra Leone, Dunham and Phillips et al (1958) have described partially serpentinised dunite intruded by quartz pegmatites and cut by numerous faults yet clinochrysotile veins are not found. In Cyprus, Wilson (1958) describes commercial deposits of clinochrysotile in sheared serpentinite and acid intrusives are absent.

It must be concluded that the clinochrysotile asbestos problem is far from solved although it appears that this mineral is only formed in large quantities in total serpentinites and that its formation post-dates the main serpentinization.

Harzburgite.

Distribution and Field Occurrence.

Enstatite peridotite and its serpentinised equivalent build over ninety per cent of the Mount Tawai ultrabasic complex. It is also the major rock type of the Meliau and Bidu-Bidu batholiths located to the north of the Tawai complex.

Around the margins of the Mount Tawai batholith the peridotite is strongly broken up and altered but in the headwaters of all the major streams undeformed and only partially serpentinised harzburgite is found (Fig. 37). In the stream sections fresh harzburgite outcrops with evenly scattered olive green orthopyroxene laths (1 to 20mm. in length) together with sparse emerald green clinopyroxene and pin head disseminations of chromite are seen set in a mosaic of dark green olivine. On the ridge sides the undeformed peridotite weathers to a reddish brown colour studded with crystals of greenish brown orthopyroxene. All of the major peaks of the area are built of harzburgite often showing only slightlyweathering effects. The contact between weathered and fresh rock is knife edge sharp. Many of the non-foliated harzburgite outcrops exhibit well developed oblique jointing patterns. Two parallel joints slanting at 45° are usually cut obliquely by a second set of parallel slanting joints.

Petrography.

The harzburgites are composed mainly of olivine and orthopyroxene together with minor amounts of clinopyroxene (0 - 5 per cent) and spinel (0 - 1 per cent). Olivine is always the dominant constituent comprising seventy five per cent or more of the rock.

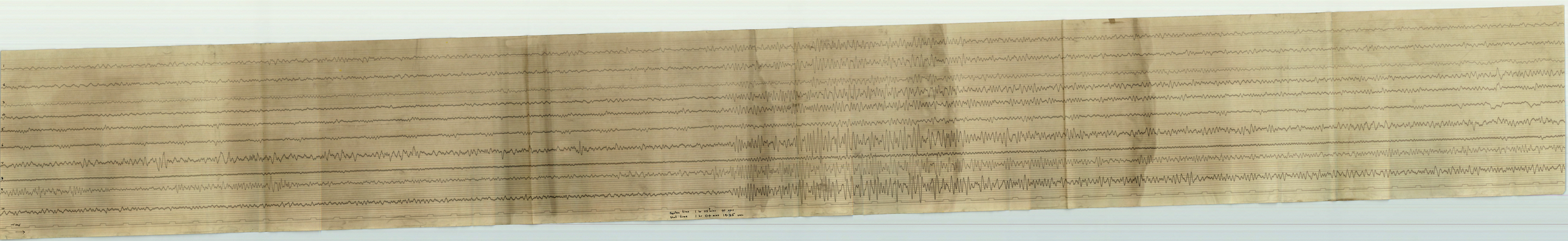
1
2
3
4
5
6
7
8
9
10
TIME
System time 1 hr 08 mins 01 secs
Start time 1 hr 06 mins 14.35 secs

Fig. 37. Photograph of massive harzburgite.

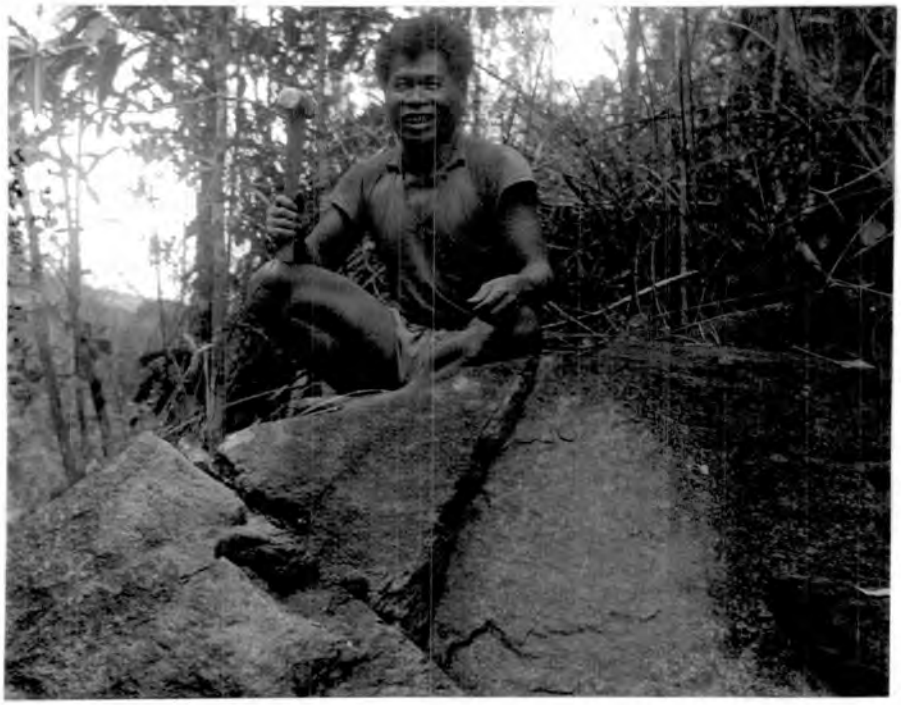

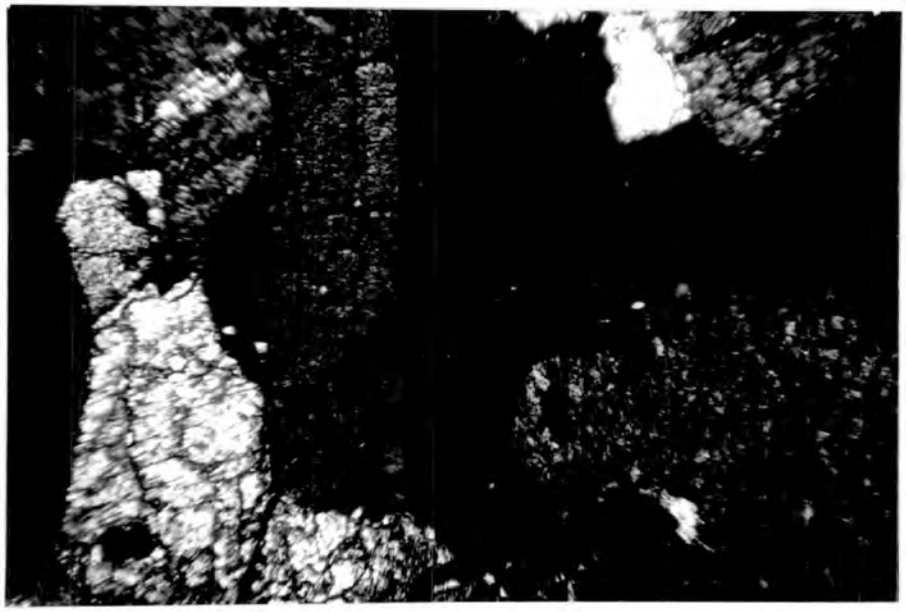

Fig. 37a. Photomicrograph of lamellar structure in olivine T207. (crossed nicols X20).

The orthopyroxene content varies from five per cent to twenty five per cent but over the greater part of the Tawai complex, and in the Meliau and Bidu-Bidu batholith, the orthopyroxene content remains constant at around twenty per cent. The variations occur where, by decrease of orthopyroxene and increase of olivine, the harzburgite grades into dunite. Varieties intermediate between pyroxenite and harzburgite are confined, with one exception, to thin millimetre thick zones on the edge of the pyroxenites.

Deformation phenomena associated with intrusion in the near crystalline state were found in all of the harzburgite thin sections examined. The degree of deformation varies from mild granulation around crystal boundaries to extreme mylonitization. The degree of deformation decreases as the blocks are traversed inwards from the contacts. Four main phases of deformation have been distinguished:-

Phase I (Fig. 38) - Thin sections of the harzburgites from the upper reaches of the North Tankulap and Melio streams show only minor granulation effects. These thin sections show a hypidiomorphic texture in which the olivine occurs as coarse anhedral crystal (2 - 8mm. in diameter) with intimately interfering boundaries. Under crossed nicols the majority of the olivines are seen to contain broad (.1 to .5mm. wide) sub-parallel sections each varying slightly in optical orientation (Fig.37a). These sections resemble twin planes but under ordinary light no physical break can be seen. The section boundaries are straight and sub-parallel to 100. Sometimes they extend right across the olivine crystal but frequently they extend only half way. Three to five sections are common in a single crystal. No preferred orientation of the bands between separate crystals was found in the slightly deformed harzburgites.

Fig. 38. Photomicrographs of relatively undeformed harzburgite, Phase 1. T373. (crossed nicols X20). Notice the interlocking texture of the enstatite (centre), and the olivine.

The orthopyroxene occurs as anhedral laths (.2 to 8mm. in length) containing fine exsolution lamellae of clinopyroxene parallel to 100. These exsolution lamellae (Fig. 38) extinguish in different positions from the host orthopyroxene, are about .002mm. thick and form closely spaced parallel series. Occasionally they are grouped together in the centre of the orthopyroxene and pinch out towards the edges. The lamellae extinguish from 38° to 42° on either side of the c axis of the host orthopyroxene and are best seen when the latter is in the extinction position. In sections cut oblique to 100 the lamellae appear as broad bands. Irregular blebs of exsolved clinopyroxene in optical continuity with the exsolution lamellae also occur in the orthopyroxene. There is no evidence to suggest that the orthopyroxenes are inverted pigeonites. The boundaries of the orthopyroxenes are moulded into the olivine with no reaction rim in between. Rounded and elongate olivine crystals are found enclosed within the orthopyroxene but no clear case of resorbtion of the forsterite has been observed. The orthopyroxene crystals show a marked tendency to form clusters comprising three to five crystals. A minority of the orthopyroxene occurs as small plates interstitial to the olivine.

Many of the orthopyroxene laths are divided into sharply defined divisions of different optical orientation (Fig. 39). The division boundaries, known as kink bands, are sub-parallel to 001 and normal to 010. Two or three sections in one crystal are common. The 100 exsolution lamellae show that the different sectors differ in orientation from between two and five degrees. This structure is best seen in groups of orthopyroxene laths.

The clinopyroxene occurs as small isolated anhedral crystals

Fig. 39. Photomicrograph of kink band structure and clinopyroxene exsolution lamellae in orthopyroxene. T208 (crossed nicols X20).

Fig. 40. Photomicrograph of endiopside in harzburgite. T373. (crossed nicols X110).

(Fig. 40) (.5 to 2mm. in length) interstitial to the olivine and as large plates (2 - 5mm. in length). The large crystals show a marked tendency to form bunches. The clinopyroxenes show a partially developed diallage cleavage accentuated by minute rods of iron ore. Broad exsolution lamellae (.05 - .1mm. in width) of orthopyroxene parallel to 100 are developed in the larger plates which also contain inclusions of olivine and chrome spinel. In the partially serpentinised peridotites clinopyroxene is always the least altered primary silicate mineral.

Chrome spinel is present in small, discrete, anhedral and euhedral crystals occurring mainly between the olivine crystals. Myrmekitic intergrowths of olivine and spinel (Fig. 41) occasionally occur. The mineral varies in colour from light olive brown to deep brown or black. All of the silicate mineral grain boundaries are interlocking in this primary texture and only occasionally can slightly granulated crystals be found.

Phase 2 (Fig. 42) - This next phase of deformation is characterised by the development of a true hypidiomorphic granular texture. The rock is still coarse grained but granulated grain boundaries replace the interlocking texture of the first phase. The most marked effects are seen in the olivine which becomes broken and ragged around the grain boundaries. Small unstrained crystals (.1 to .5mm. in diameter) often showing polygonal outlines occur between large unstrained olivines suggesting recrystallisation has occurred. The lamellae boundaries show sutured outlines and deviation of up to 8° from 100 are common. Undulose extinction is very marked in the larger olivines.

Fig. 41. Photmicrograph of myrmekitic intergrowth of olivine and spinel. T313 (crossed nicols X250).

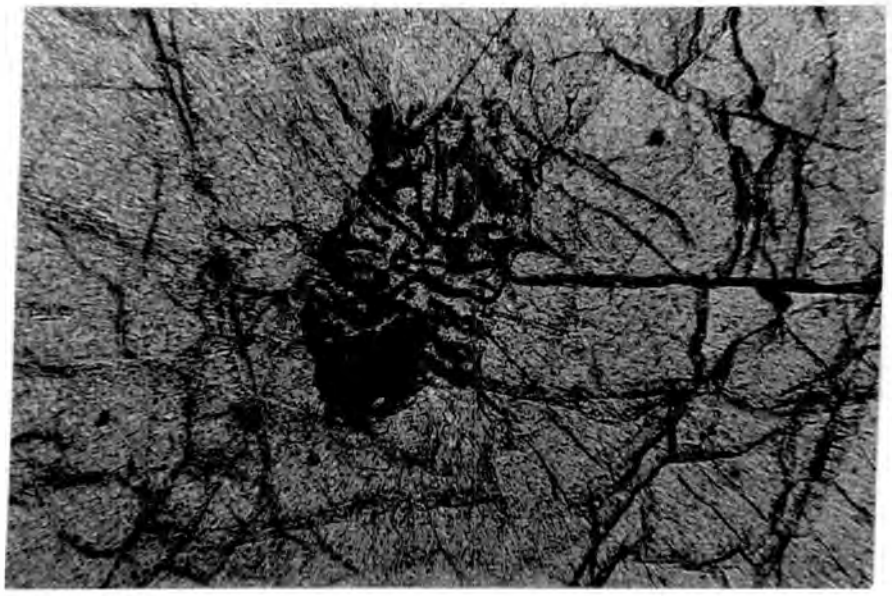

Fig. 42. Photomicrograph of Phase 2 deformation of harzburgite. T175 (crossed nicols X20).

Small deformed olivines embay the large orthopyroxene laths giving their outlines a ragged appearance. The exsolution lamellae within the orthopyroxene laths are usually straight but some show slight banding indicative of warping about the b crystallographic axis. Some of the section boundaries within the orthopyroxene laths show distinct fractures at right angles to their length (Fig. 43) whilst others take on a more sutured outline (Fig. 44). The clinopyroxene exsolution lamellae increase in birefringence and thickness towards the section boundaries.

The small orthopyroxene plates are deformed together with the olivine at this stage.

The clinopyroxene shows ragged edges and a series of strain lamellae at an angle of 15° from the 100 exsolution producing a pseudo herringbone structure. (personal communication, Dr. G. M. Brown).

Phase 3 (Fig. 45) - Strong cataclastic textures are shown in this stage and hand specimens have a crude gneissose foliation (Fig. 24). Thin sections show the orthopyroxene laths are strongly distorted and often markedly warped (Fig. 45a), as is clearly shown by the bent 100 exsolution lamellae (Fig. 45). Mugge (1898) has attributed this warping to post-crystalline deformation by translation gliding on (100) parallel to (001). The orthopyroxenes also show strong undulose extinction and are often completely torn in half, or veined by mosaics of minute crystals of similar composition. The kink bands are strongly sutured and rupture of the laths takes place along these boundaries. The crude gneissose foliation is produced by rough alignment of the orthopyroxene crystals. These crystals

Fig. 43. Photomicrograph of broken kink band in orthopyroxene. T176. (crossed nicols X50).

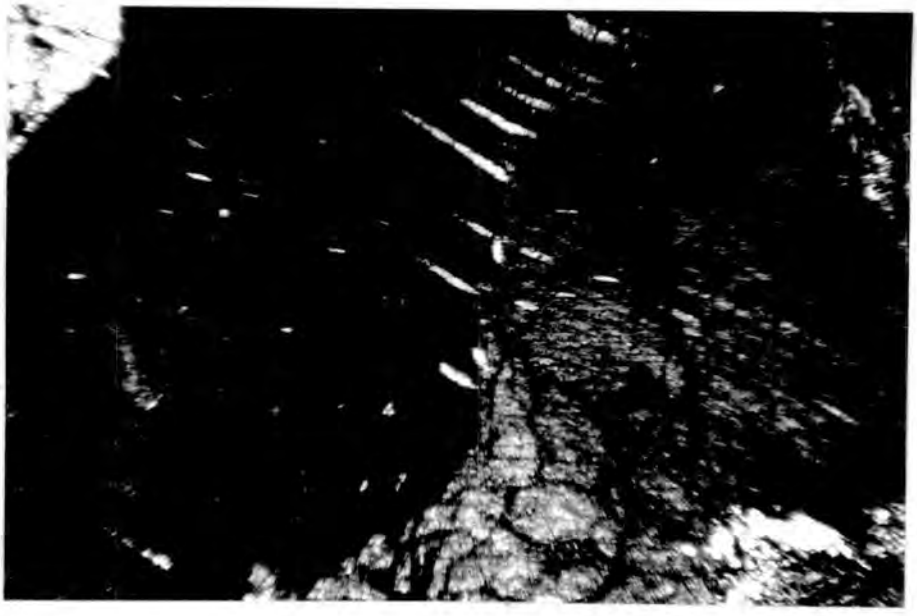

Fig. 44. Photomicrograph of sutured kink band in orthopyroxene T179. (crossed nicols X100).

however show little preferred orientation. There is a tendency for the 100 exsolution in the larger grains to be aligned to the foliation but in general their arrangement is haphazard. In thin section the macroscopic foliation is difficult to recognise.

The groundmass between the distorted orthopyroxene laths is filled with granulated olivine crystals (.01 to 2mm. in diameter). Stringers of broken chromite crystals accentuate the foliation.

The clinopyroxene at this stage deforms by granulation and not by warping.

This phase of deformation is frequently strongly serpentinised and gives rise to the prominent knitted bastite serpentine texture.

Phase 4 (Fig. 46) - The ultimate phase of deformation is only found in the deformed rock along part of the Tankulap-Lichau fault and as inclusions in the sheared serpentinite zones and is best described as a mylonite. These mylonites are almost completely unserpentinised. In hand specimen the rock is very hard and has a marked streaky appearance. Their sections show oval and elongate porphyroclasts of olivine and orthopyroxene set in a minutely granulitic groundmass of the above two minerals, clinopyroxene and spinel. The groundmass has a finely banded structure caused by alternating layers of very small crystals with layers of somewhat larger ones. The contacts of the bands are sometimes sharp and at other times indefinite. The grain size of the first bands is approximately .01 - .02mm. in diameter and the largest .07 - 1mm.. The mineral grains in the groundmass show no preferred orientation but the banding is accentuated by streaks of an almost isotropic chloritic material and granulated chromite and magnetite crystals.

Fig. 45. Photomicrograph of Phase 3 deformation of harzburgite T242. (crossed nicols X20).

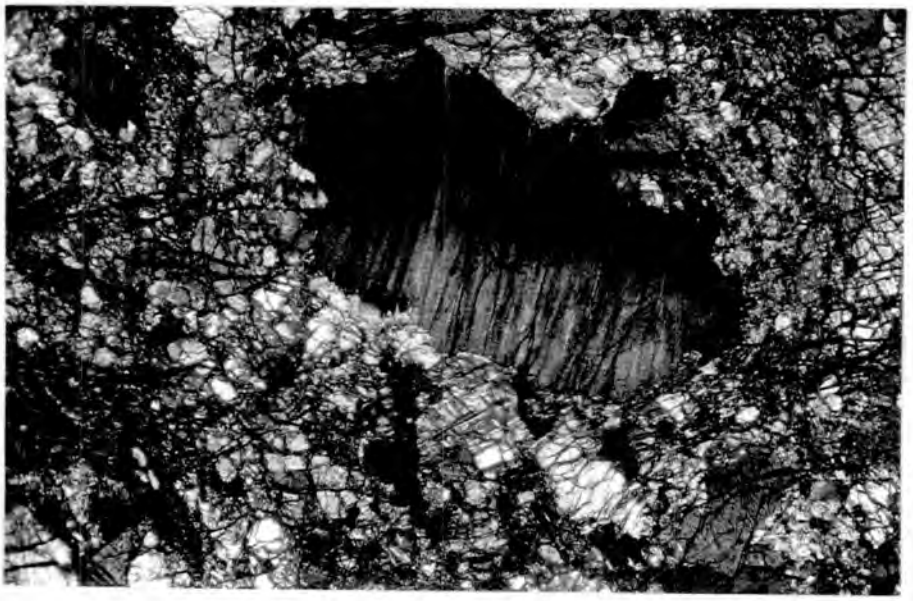

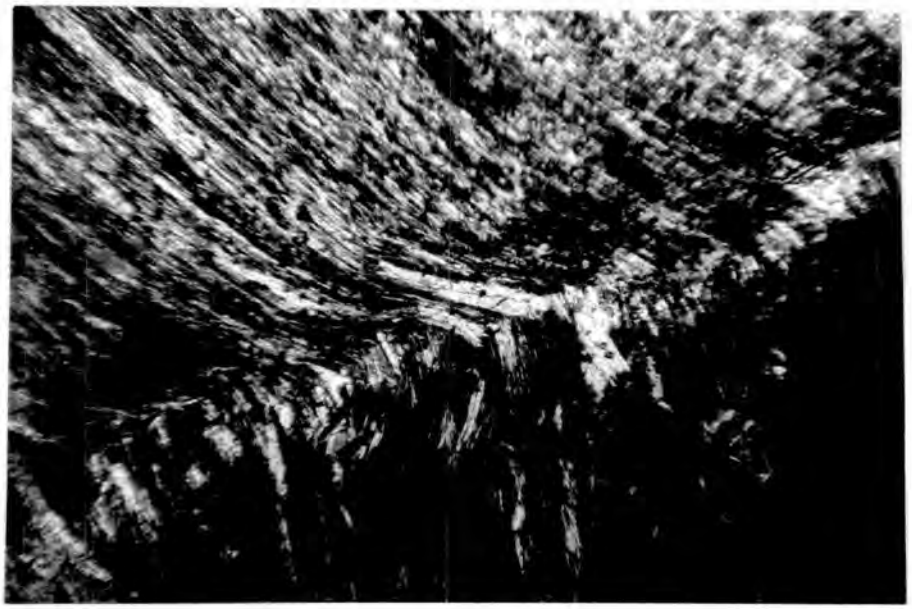

Fig. 45a. Photomicrograph of warped orthopyroxene T178. (crossed nicols X50).

The porphyroclasts vary in shape from elongate (1mm. long 2 wide) to oval (.5mm. to 1.5 long dimension) and consist of highly strained orthopyroxene and olivine crystals. The long dimension of the porphyroclasts is sub-parallel to the fine banding of the groundmass. Some of the porphyroclasts show irregular embayments harbouring clusters of small crystals. The olivine porphyroclasts contain numerous closely spaced undulatory extinction bands (sub-parallel to 100). These bands show no preferred orientation with regard to the fine banding sometimes being normal to it and at other times sub-parallel.

The orthopyroxene porphyroclasts are highly strained but do not contain kink bands.

The fine banding flows round the porphyroclasts but both are cut by fine veins of serpentine which are the only signs of serpentinization in the rock.

Deformed peridotites showing a recognisable orientation pattern are rare. One specimen was found as an inclusion in the sheared serpentinite contact on the Puteh river. The rock shows a marked preferred orientation in thin section, although no marked lineation can be seen in the hand specimen and consists of elongate (1mm. - 2mm. long, .1 - .2mm. wide) olivine and pyroxene crystals set in a granulated matrix of similar composition (Fig. 47). The olivines show undulose extinction and are flattened on 010 showing marked elongation of 001. They contain abundant lamellae arranged normal to the long axis of the crystal. The orthopyroxenes show elongation of 010 and do not contain exsolution lamellae of clinopyroxene. Larger oval porphyroclasts of orthopyroxene and spinel (1mm. in diameter) are found, the former containing thin exsolution lamellae

Fig. 46. Photomicrograph of ultrabasic mylonite, Phase 4 deformation. T276 (crossed nicols X20).

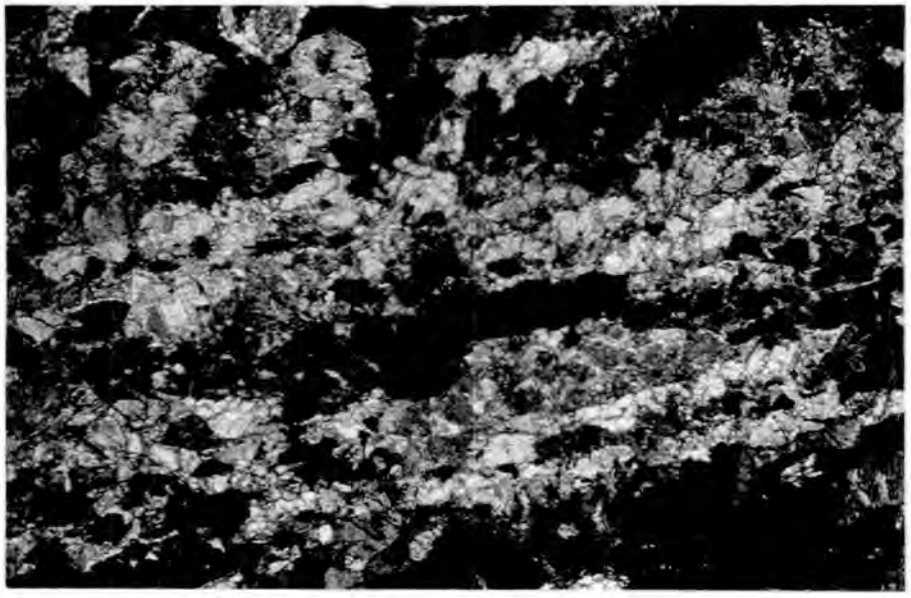

Fig. 47. Photomicrograph of ultrabasic mylonite showing orientated olivine. T1386 (crossed nicols X25).

of clinopyroxene. The rock is almost completely unserpentinised.

The rarity of fabrics showing dimensional orientation is a feature of the deformed ultrabasic rocks of Mount Tawai and they resemble the mylonites described by Turner (1942) from Milford Sound, New Zealand, but are unlike those examined by Tilley (1947) in which there is preferred orientation of olivine and orthopyroxene. That this is not the case in the majority of the Mount Tawai ultrabasics is seen by the haphazard orientation of the lamellar structure in the olivines and exsolution lamellae in the orthopyroxenes which may be, if present, at right angles or normal to the foliation or in any intermediate position in any one thin section. The overall impression given by the granulation effects seen in the Mount Tawai ultrabasics is of mechanical deformation and comminution in which the individual fragments do not conform to a recognisable orientation pattern.

Olivines containing lamellae sub-parallel to (100) have been described from many different environments including Alpine Type peridotites, phenocrysts in basalt and olivine nodules. Turner (1942) considers they originate by translation gliding and from recent experiments Griggs, Turner and Heard (1960 p.54) conclude "development and strengthening of the undulatory bands to relative external rotation of subgrains in response to localised translation gliding upon some systems or systems yet unknown".

Brothers (1960) on the other hand considers they originate as a result of gravity deformation by a load of overlying crystallates in a magma chamber.

With higher grades of deformation the lamellar structure in the olivines from Mount Tawai becomes increasingly deformed and is

accompanied by an increase in undulatory extinction. The fact that lamellar structure is present in the relatively undeformed assemblages of Mount Tawai and in non-tectonites of other areas (e.g. Brothers (1960) describes lamellar structure in olivine from euhedral phenocrysts in some New Zealand lavas) suggests that either it is a type of strain structure to which olivine is particularly susceptible even with small stress effects or that it is connected with the primary crystallisation of the mineral.

Preferred dimensional orientation of the olivine is seldom seen in the Mount Tawai ultrabasics. The one specimen found and mentioned above is similar to those found in a banded peridotite from Rhum by Turner (1942) and which Fairbairn (1949 p.146) believes is formed by semi-solid flow when crystallisation is far advanced.

The kink bands found in the orthopyroxene crystals are in many ways similar to the lamellar structure in the olivines for with increasing deformation they become more and more irregular until the crystals actually rupture and are torn apart along the sector boundaries. In the mylonites kink band structure is completely absent. Turner, Heard and Griggs (1960) have produced this structure artificially by deformation of pyroxenite at 5000 bars/cm^2 and between 500°C and 800°C and attribute it to translation gliding during rotation about 010. However this structure is present in relatively undeformed orthopyroxenes showing only slight warping effects of the 100 exsolution lamellae (Fig. 38) and, although there can be no doubt that it is accentuated during deformation by warping, it may well originate from crystallisation at high pressure. The fact that it is commonly found in bunches of orthopyroxene crystals suggests that it may be caused by intergranular strain during

growth. A kink band structure has also been noted by the writer in the peridotite nodules from Kidlaw in Scotland.

The small unstrained olivine grains sometimes found between, (Fig. 48) and embaying large strained ones suggest that limited recrystallisation may have occurred during or shortly after cataclastic deformation. Hess (1947) noted small cross cutting veinlets of olivine in the dunite mylonites of St. Paul's Rocks suggesting regeneration of olivine subsequent to mylonitization and Rothstein (1957) indicates that parts of the Dawros peridotite recrystallised whilst still hot into a metamorphic mosaic of olivine and pyroxene. The temperature of recrystallisation of deformed olivine is not known. Griggs, Paterson and Heard (1960) have shown that cold-worked metal is strongly modified by annealing recrystallisation at temperatures about half way between absolute zero and their melting points. If the above principle is applied to forsterite (melting point 1800°C for Fo_{90}) then annealing recrystallisation is possible at 900°C although it is by no means certain that minerals behave in the same way as cold worked metals. Griggs, Turner and Heard also show that with decreasing strain rate the temperature for recrystallisation decreases. The petrographic evidence from the Mount Tawai peridotite shows that serpentinization is subsequent to the postulated recrystallisation textures, indicating a lower limit for the regeneration of olivine as 400°C. It is therefore tentatively postulated that if recrystallisation has occurred it has done so between 900° and 400°C. The textures suggestive of recrystallisation are however only occasionally found.

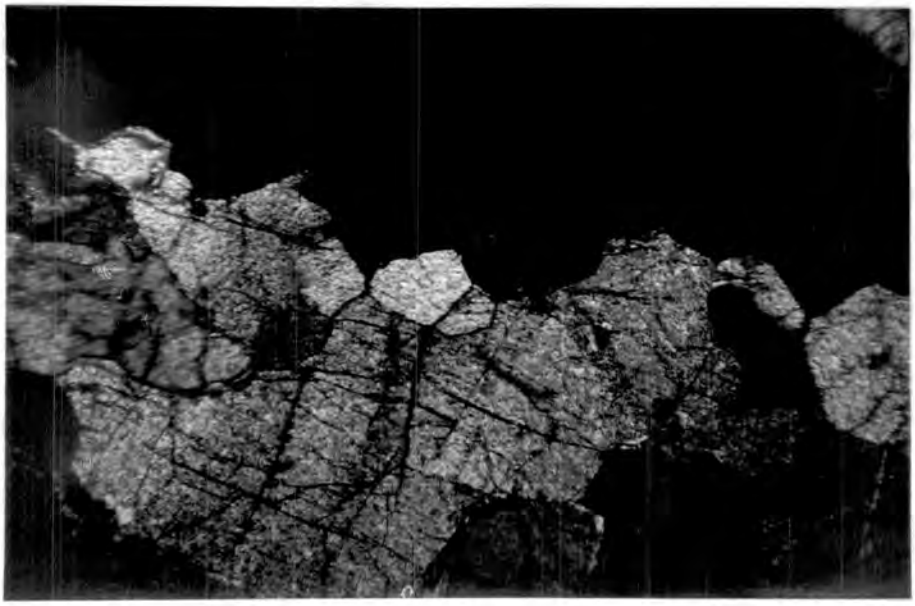

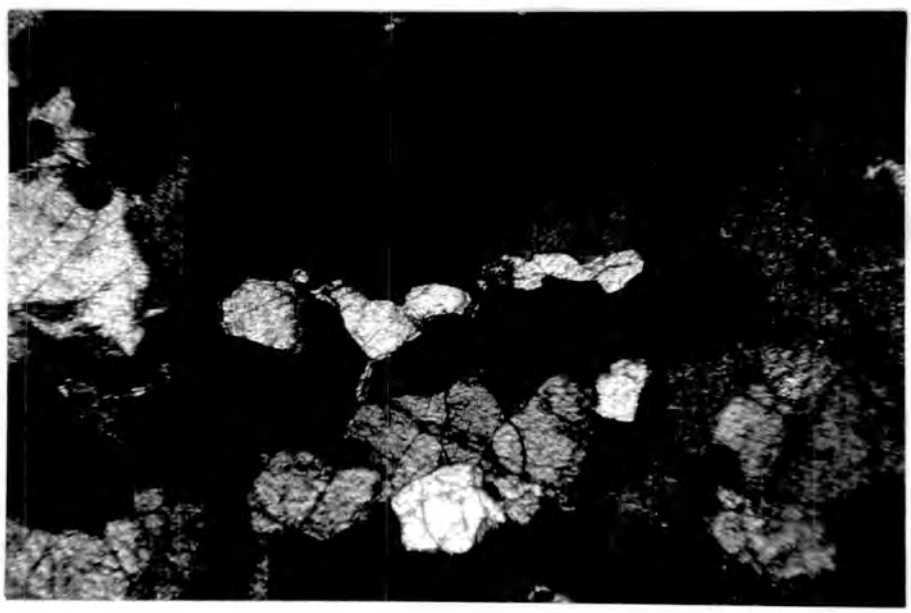

Fig. 48. Photomicrographs of small unstrained olivine grains between large strained crystals. T175 (crossed nicols X200).

Mineralogy.

Olivine - Optical and X-ray diffraction measurements, Tables 13, 22, indicate the olivine is forsterite with a composition varying from $Fo_{90}\ Fa_{10}$ to $Fo_{93}\ Fa_{7}$. The mineral is biaxial positive with nY varying from 1.662 to 1.666 ($\pm$.005).

Orthopyroxene - X-ray diffraction and optical measurement (Tables 13, 22) show the orthopyroxene to be enstatite approaching bronzite in composition and varying from $En_{88}\ Fs_{12}$ to $En_{90}\ Fs_{10}$. A chemical analysis is given in Table 15. (No. 383). The enstatite is biaxial positive and nZ varies from 1.672 to 1.680 ($\pm$.005). Some varieties are very faintly pleochroic.

Clinopyroxene - X-ray diffraction measurements indicate the mineral to be endiopside (Table 28). A chemical analysis is presented in Table 23. The mineral is sometimes faintly pleochroic with nY a very pale green.

Spinel - The spinel has not been examined directly but is similar to the chromite found in the dunites. Its extremely variable colour from light olive brown to dark brown or black indicates a variable Cr_2O_3 content.

Feldspathic peridotite.

Distribution.

Feldspathic peridotite is rarely found in the Mount Tawai ultrabasic rocks. It occurs in thin impersistent bands and as interstital patches largely replaced by saussurite in the Pantagaluang block. However it is not widespread enough to merit mapping this unit as feldspathic peridotite. Nevertheless, its presence in the Pantagaluang block is of importance for north of the Tankulap-Lichau fault and east of the Bonalik disturbance feldspar is absent in the main Tawai block. The thin feldspathic bands are best seen in the South Tankulap river away from the fault disturbance zone. In the rest of the area they occur in sporadic exposure showing no distribution pattern that can be related to height above sea level or distance from contact. They seldom extend for more than a few feet along the strike and vary from pencil line thickness to four inches in width. They show gradational contacts with the peridotite and occasionally grade in into thin gabbroic bands.

Petrography.

The feldspathic peridotite bands show a variety of texture varying from strongly cataclastic to hypidiomorphic granular. They all have a marked banded appearance due to platy alignment of the feldspar. The bands consist of olivine, plagioclase, orthopyroxene, and a brown pleochroic amphibole. Green translucent spinel may also be present. Specimen 271 gave the following mode:-

Per Cent.

Feldspar	Olivine	Orthopyroxene	Amphibole	Ore
18	73	4	3	2

One extremely granulated band (specimen 273) grades into a rock containing more than 50 per cent of plagioclase and about 10 per cent pleochroic amphibole which is a gabbro. The gabbroic band is half an inch thick. At the gradational contacts there is no change in grain size feldspar merely increases in amount at the expense of olivine and orthopyroxene.

Specimen 271 (Fig.49) has a relatively undeformed texture and plagioclase feldspar occurs as discrete laths (1 - 2m. in length) with a rough platy alignment; the albite twin planes being aligned to the banding. Periclinal and complex twins are also present.

The olivine occurs in interlocking, partially serpentinised grains (.1 - 4mm. in diameter) and shows no reaction relation with the plagioclase. Lamellar structure is absent and only the occasional crystal shows undulose extinction. The majority of olivine crystals are anhedral but occasionally tabular form parallel to the banding is seen.

Orthopyroxene is only found in sparsely distributed laths (.5 - 2mm. long) which contain 100 exsolution lamellae of clinopyroxene. The laths are arranged with their long axis (010 in direction of crystallographic c) arranged sub-parallel to the banding.

A brown pleochroic amphibole is found as discrete laths (.5 - 1mm. long) and as replacement edges on the orthopyroxene. In the more feldspathic bands orthopyroxene is absent and the amphibole

Fig. 49. Photomicrograph of feldspathic peridotite. T270 (crossed nicols X50).

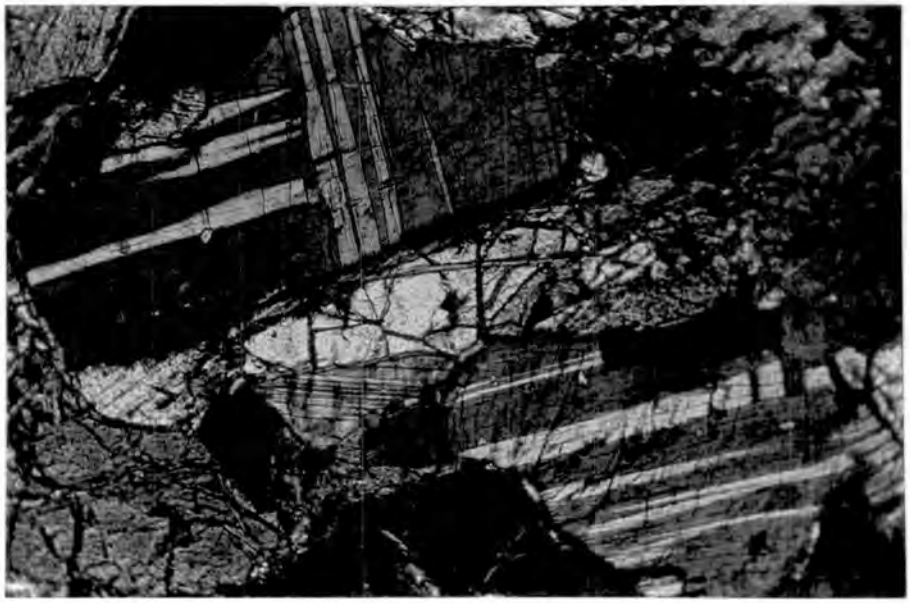

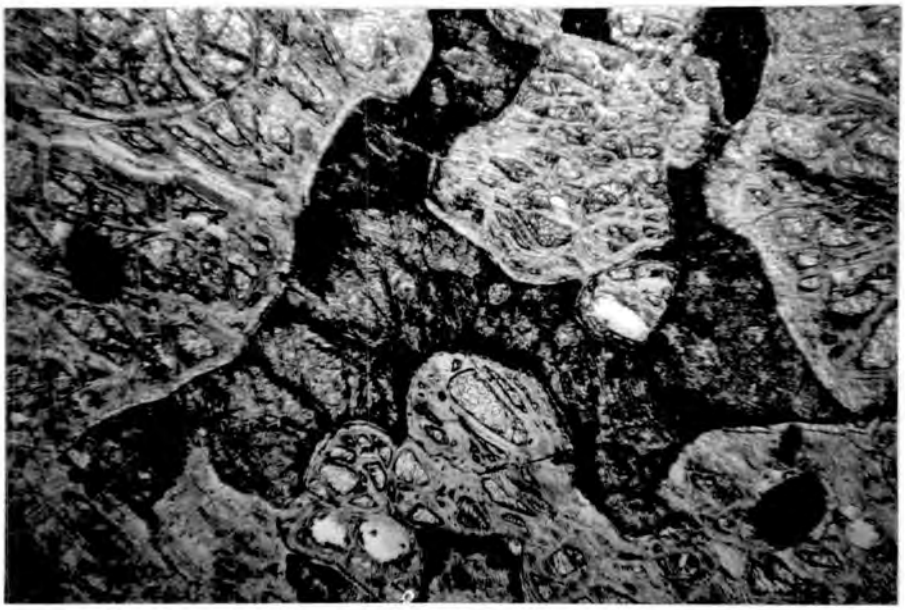

Fig. 50. Photomicrograph of saussurite peridotite. T171 (crossed nicols X75).

content increases to around ten per cent. Clinopyroxene is absent in the feldspathic band.

A spinel that is black in hand specimen and light translucent green in ordinary light is often found in the feldspathic bands. It forms crystals up to 5mm. in diameter and is always surrounded by a halo of coarse grained plagioclase. Episcopic examination shows the presence of fine exsolution lamellae of ilmenite.

The saussurite peridotites (Fig. 50) only differ from the harzburgites in that they contain irregular patches of an interstitial turbid looking substance. Occasionally relicts of plagioclase feldspar may be distinguished. In most cases the turbid brown substance is made up of a granular aggregate of calcite and epidote. Hydragarnet has never been observed replacing the plagioclase.

Mineralogy.

Plagioclase - Maximum extinction angle measurements indicate that the plagioclase is bytownite-anorthite varying from $An_{84}Ab_{16}$ to An_{90} to Ab_{10}. Only weak normal zoning is present.

Olivine - The olivine (Table 22) is optically positive and X-ray diffraction indicates a composition of $Fo_{90}Fa_{10}$.

Orthopyroxene - The orthopyroxene (Table 22) is enstatite as shown by X-ray diffraction.

Amphibole - The amphibole mineral is optically positive with a large 2V. It has the following pleochroic scheme:-

X - Colourless

Y - Faint brown

Z - Light brown

The optical properties suggest the mineral is pargasitic hornblende.

The spinel could not be concentrated in sufficient quantities for analysis. The unit cell edge is 8 - 15Å which suggests a high alumina chromite approaching hercynite in composition.

Pyroxenites.

Field Occurrence.

Pyroxenites constitute only a minor fraction of the ultrabasic complex. They may be divided into two groups on the basis of their mode of occurrence.

Pyroxenite interbanded with peridotite.

Irregular shaped bodies of pegmatitic pyroxenite.

Thin impersistent bands of pyroxenite occur interbanded and interfingering with the peridotite. The bands seldom exceed a few inches in width and quickly die out along the strike. Pyroxenites are exceedingly rare and usually occur as single bands although in two exposures they form prominent groups. The pyroxenite bands are relatively more common in the western part of the main Tawai block, and they nearly always occur in a steeply dipping attitude, and strike sub-parallel to the dunite lenses and bands. The pyroxenites never form continuous mappable horizons.

On the basis of their mineralogy the pyroxenite bands may be divided into the following groups.

Clinopyroxenites.

Orthopyroxenites.

Clino-orthopyroxenites.

Clinopyroxenites.

These bands are exceedingly rare. A prominent group, however, is found in the middle course of the north flowing part of the Kuun-Kuun river, where ten feet of coarse grained banded pyroxenites dipping 35°N.W. are seen (Fig.26). The exposure contains thin ½" to 4") whitish green clinopyroxenite bands interbanded with orthopyroxene rich peridotite. The peridotite is strongly serpentinised and contains mostly bastite pseudomorphs after enstatite. Measurements made on the surface exposure indicate an orthopyroxene content of sixfy per cent; the rock therefore falls in the saxonite division. The clinopyroxene bands are less heavily serpentinised and consist of coarse (2 - 4mm.) crystals of endiopside with minor orthopyroxene and olivine. Thin gradational zones are found on all sides of the bands. The bands thin and pinch out along the strike sometimes forming lenses.

Over the rest of the Mount Tawai area clinopyroxenites are rare. Thin bands occur below the main falls on the Melio river and in the upper reaches of the South Tankulap stream.

Orthopyroxenites.

Thin impersistent bands of orthopyroxenite are relatively common. Good exposures are found in the Melliau and Tankulap streams. In the main east bank tributary of the Meliau river (150 yards above confluence with W. Meliau) steeply dipping bands (pencil line thickness to 15mm.) are found interbanded with thin dunite (2 - 3mm. wide) bands in a zone one foot wide. One contact of each pyroxenite band is sharp against dunite but the other is gradational, orthopyroxene gradually fading out and olivine

increasing. The transition zone though is restricted to a few millimetres. The dunite band is sometimes missing and two pyroxenite bands occur divided by a thin layer containing olivine and orthopyroxene (Fig. 52).

In the upper reaches of the North Tankulap stream massive 6 inch bands of orthopyroxenite are found interbanded with the peridotite (specimen T208). The contacts are sharp and no gradational facies have been observed. Thin orthopyroxenites bands are also found in the Melio stream, above the main falls, and on the flanks of the Patud and Sawar ridges.

Ortho-clinopyroxenites.

Thin bands consisting of mixed pyroxenites occur only in the north-western part of the main Tawai block. At the main bifurcation of the Meliau stream a ten foot zone of strongly banded peridotite is found. The bands are dipping steeply north-west and vary from pencil line thickness to four inches in width (specimen T22). The contacts of the bands are sharp against the peridotite. Along the strike the bands quickly die out.

Single bands of mixed pyroxenes are also located on the northern flank of the Tawai ridge and on the western flank of the Sawar range.

Pyroxenite pegmatites.

Irregular shaped bodies of clinopyroxenite containing giant crystals up to seven inches in length, (specimen T352) are found scattered irregularly throughout the peridotite. The clinopyroxenite masses vary from sixty feet to ten feet in length and twenty

Fig.52.

ORTHOPYROXENITE BANDS
Specimen T42

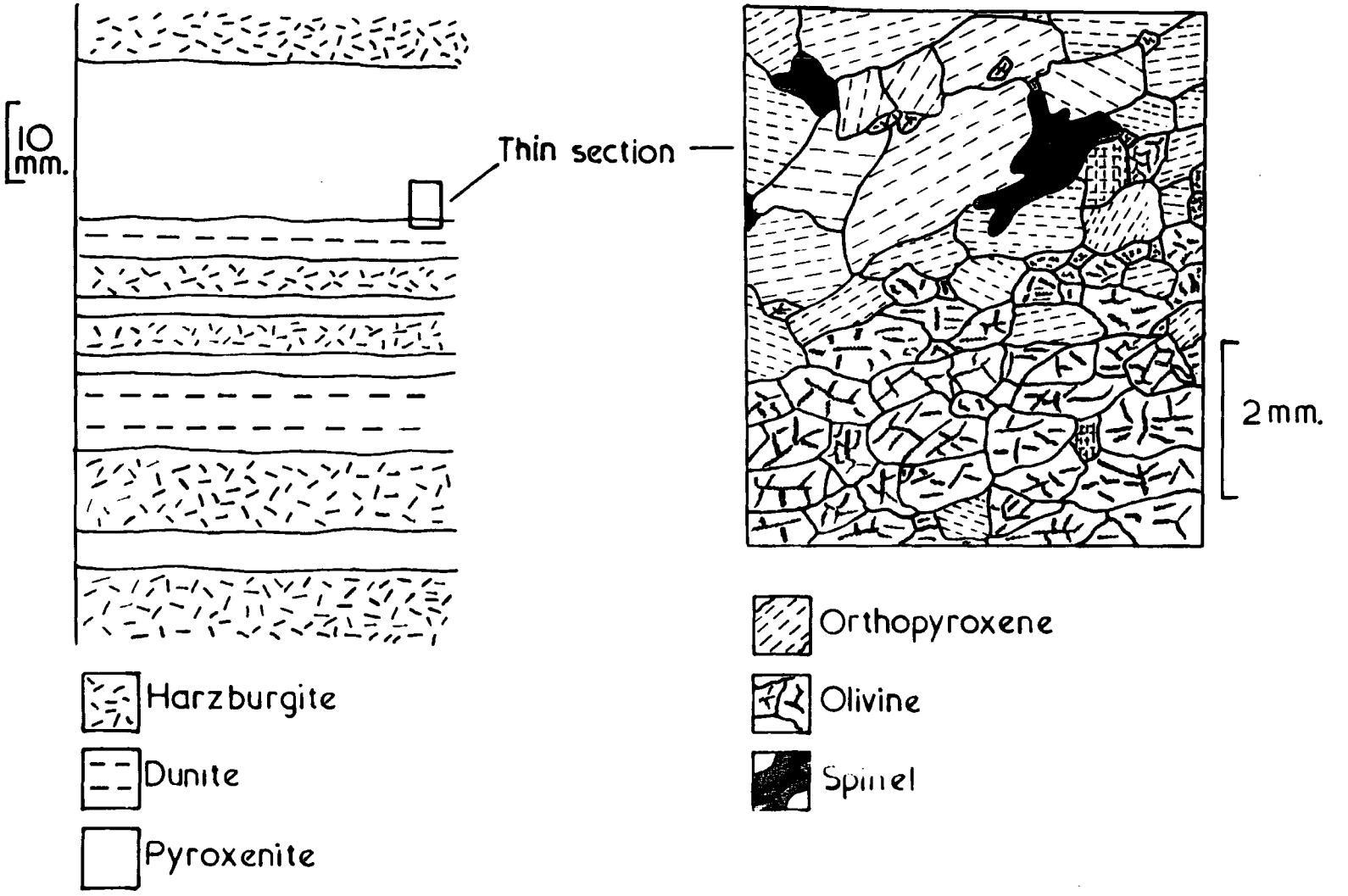

feet to two feet in width. The margins of the mass are sharp being frequently wavy and scalloped against the peridotite and dunite. Excellent exposures are found in the Hitam river about half a mile upstream from the main ultrabasic contact and in the second north bank tributary of the Melio.

Petrography.

The thin bands of clinopyroxenite are composed of diopside (70 - 80%) orthopyroxene (5 - 10%) and olivine (5 - 10%). The rock texture seen in the Kuun-Kuun bands is hypidiomorphic granular, with crystals varying from .5 to 6mm. in length. The clinopyroxene occurs as pale green crystals and show prominent 100 exsolution lamellae of orthopyroxene. The clinopyroxenes are altered to tremolite and in length fast chlorite. The orthopyroxene occurs in irregular anhedral grains (.5 to 2mm. in length) in between and keyed into the clinopyroxene. Thin exsolution lamellae of clinopyroxene occur in the orthopyroxene. Olivine and green brown spinel occur in small anhedral grains. On the edges of the clinopyroxenite bands a zone (5mm. wide) of a gradational facies is seen consisting of orthopyroxene, (30 per cent) clinopyroxene (30 per cent) and olivine (40 per cent). All of the minerals present show strong strain effects.

The orthopyroxenite bands are made up of massive crystals of enstatite with minor amounts of olivine (0.5 per cent), clinopyroxene (0.5 per cent) and spinel (0.2 per cent). The texture of the orthopyroxenites varies from hypidiomorphic to hypidiomorphic granular.

The thin sections of the orthopyroxene -dunite bands from the

Meliau river show a medium grade of deformation. The thin dunite bands (2 - 3mm. thick) are mostly strongly granulated and serpentinised but one shows some rounded and oval olivine crystals (.5 - 2mm. in diameter) forming an interlocking texture (Fig.52). The long axis of the oval olivine crystals (010) are sub-parallel and strain lamellae are poorly developed. Immediately above the dunite band a 15mm. thick orthopyroxenite band is seen containing large enstatite laths (4m - 6mm. in length) which show a crude preferred orientation of 010 (crystallographic c). These laths are ragged and show sutured kink bands, bent exsolution lamellae and a green spinel occurs enclosed and between the grain boundaries. Below the dunite band a mixed assemblage of orthopyroxene (25 per cent) clinopyroxene (15 per cent), and olivine (70 per cent) is seen. Although other bands may be seen in the hand specimen they are difficult to distinguish in the thin section on account of the deformation. Nevertheless the three bands that can be determined (Fig.52) represent harzburgite, dunite and pyroxenite and more probably represent minor fluctuation during crystallisation rather than bands streaked out during emplacement. They have obviously however been affected by later deformation.

The ortho-clinopyroxenite bands (Fig.53) consist of coarse crystals of orthopyroxene (66 - 55%) clinopyroxene (30 - 40%), olivine (0 $\leq$ 5%) and spinel (1 - 2%). The texture of these bands is hypidiomorphic granular; the individual crystals showing no preferred orientation. The orthopyroxene occurs as anhedral and sub-euhedral crystals (.5 to 4m. in length) showing fine 100 exsolution lamellar of clinopyroxene. Blebs of clinopyroxene occur with the orthopyroxene and are in optical continuity with the

Fig. 53. Photomicrograph of ortho-clino pyroxenite band. T22 (crossed nicols X50).

exsolution lamellae.

The clinopyroxene is seen as anhedral sub-euhedral crystals (1 - 5mm. in length). The mineral shows an imperfectly developed diallage cleavage and a strong series of broad 100 exsolution lamellae of orthopyroxene. The majority of the crystal boundaries are slightly crushed but occasionally the pyroxenes are seen interlocking. A brown pleochroic amphibole sometimes occurs along and between crystal boundaries.

The olivine occurs in partially serpentinised anhedral crystals (.2 to .5mm. in diameter) clustered around greenish brown spinel. The greenish brown spinel occurs as anhedral crystals (.5 to 4mm. in diameter). Euhedral spinel does not occur and thin arm-like projections off the main crystals can be seen moulded between the pyroxene boundaries.

The coarse grained clinopyroxenites consist almost entirely of giant sub-euhedral and euhedral crystals of diopsidic augite. The crystals show a strongly developed diallage cleavage. Exsolution lamellae of orthopyroxene are rare; but blebs and irregular areas of exsolved orthopyroxene are common. The boundaries between the crystals are sharp often keyed into each other. Chrome spinel seldom occurs in these clinopyroxenite pegmatites. The clinopyroxenites are strongly altered in some localities to tremolite, a green chlorite and zoisite. Irregular veins of talc and carbonate are also present. A turbid brown amorphous material clouds many of the crystals.

Mineralogy.

The minerals found in the pyroxenites have similar composition

to those found in the enclosing harzburgites and dunites.

Clinopyroxene - The clinopyroxene from the clinopyroxenite bands is endiopside (Table 28). Specimen T81 has the following optical properties: nY=1.680 - 1.684, ZΛC 41° - 44°. X-ray diffraction measurements show b_o to be strongly depressed outside the enstatite diopside join on the determinative chart.(Brown 1960). The cell parameters are similar to those observed fromT22 which is an aluminous en-diopside. The clinopyroxene from the pyroxenite pegmatites are diopside and diopside augite (Analysis 352, Table 23).

Orthopyroxene - The orthopyroxenes from the clino-orthopyroxenites band (T22) and the orthopyroxenite band (T42) are aluminous enstatite (Table 15). These orthopyroxenes are faintly pleochroic and nZ varies from 1.675 to 1.680. The orthopyroxene from the orthopyroxenite bands in the upper reaches of the North Tankulap (T208) are normal enstatite with low alumina.

Spinel - The spinel in the aluminous pyroxenites is olive green and X-ray diffraction measurements (Table 22, No. T22, T42), show the mineral to be chrome spinel. Dark brown spinel is found in the non-aluminous orthopyroxenites.

Dunite.

Field Occurrence.

Dunite forms less than five per cent of the ultrabasic rocks of Mount Tawai. The division between dunite and harzburgite has

been taken when the orthopyroxene content of the rock exceeds five per cent. This is a purely arbitrary value and other workers have taken up to ten per cent for the dividing line. In practice the harzburgite and dunite outcrops are sufficiently distinctive to map directly in the field. All the dunites contain a little orthopyroxene but on the other hand large areas of harzburgite with an orthopyroxene content of less than ten per cent are rare. Dunite weathers to a smooth buff coloured rock containing a few grains of black chromite crystals. In the fresh stream sections it varies from light to dark green in colour and is easily distinguished from the pseudo-porphyritic harzburgite. The serpentinised dunites are also easily recognised on account of their dull black appearance and lack of bastite pseudomorphs.

Dunite never forms a continuous horizon which can be mapped but occurs in belts of steeply dipping, impersistent bands, lenses and irregular shaped bodies. The location of these belts have been described in an earlier section.

Two types of interbanded dunite have been distinguished on a basis of their contact relations with the peridotite and on the occurrence of the contained chrome spinel.

Type one interbanded dunite lenses invariably have one contact gradational where the orthopyroxenes gradually fades out from the peridotite leaving dunite; whilst the other contact is relatively sharp against the peridotite. A thin chromite band is usually found just within the sharp contact. Steeply dipping chromite bands are seen within the dunite lenses varying from $\frac{1}{4}$" to 6" in width. These chromite bands occur singularly and in closely spaced sub-parallel groups. The chromite bands thicken and thin and change

direction in marked rotary movements along the strike (Fig.28). Minor folds and puckers also occur (Fig. 54). Rudimentary gravity banding (Fig. 55) and structures resembling wedge bedding (Fig. 54) are seen in the chromite bands. Irregular shaped clots of ore sometimes arranged in discontinuous circular areas (Fig. 54) occur between the bands. In all of the above mentioned structures brecciation of the dunite and ore is slight. The chromite bands are usually concentrated near to the gradational contact with the peridotite. The size of the individual dunite lens does not appear to be related to the amount of ore contained within it. A group of lenses found in the river Lichau is shown in Fig. 28.

The type one interbanded lenses are only found on the eastern flank of the main Tawai block in the belt of dunites that run from the North Tankulap to the Hitam river.

The type two interbanded dunite lenses have two gradational contacts with the peridotite. In the field they are less clearly defined and are much smaller than the type one lenses. The type two lenses are characterised by irregular bunches and globules of chromite. The bunches vary from $1/_{10}$" to $\frac{1}{2}$" in diameter. The bunches are sometimes arranged in irregular bands but more commonly occur in a haphazard manner. When the bunches are concentrated they are best described as grape shot ore. Occasionally the chromite crystals are arranged in a giant chain structure (Fig. 56). Here globules of olivine are seen set in chromite chains. This type of interbanded dunite always contains one to five per cent of chrome diopside which is seen as bright green crystals often enclosed by chrome spinel. Regular bands of chromite seldom occur in the type two lenses. A thin lens in the headwaters of the Kuun-Kuun

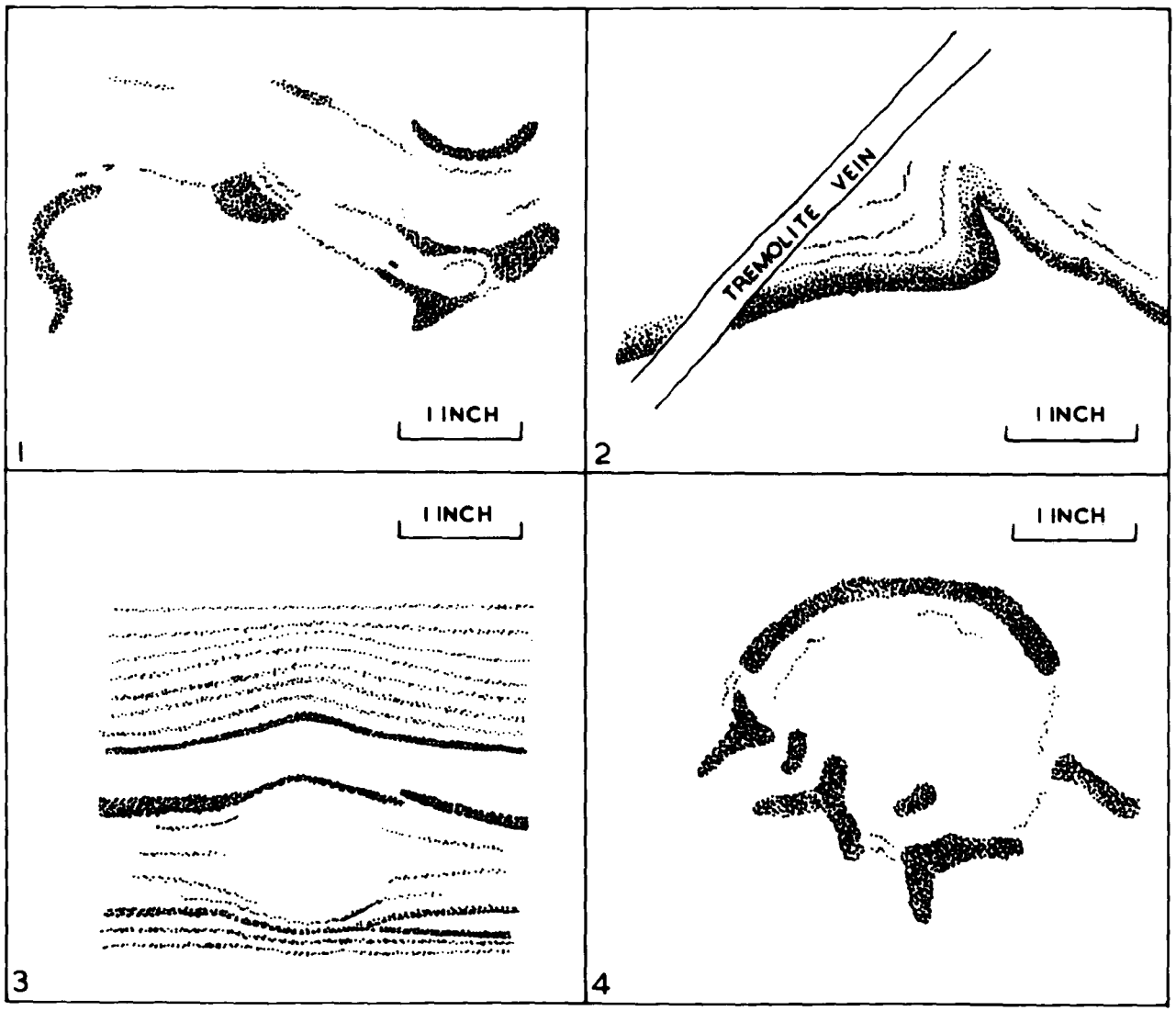

Fig.54.

.MINOR STRUCTURES IN DUNITE LENSES.

does however show banding. Thin bands of chromite and pyroxene alternate rapidly with dunite over a distance of six inches (Fig. 57).

The type two interbanded lenses occur in the western belt of dunite in the main Tawai block. Type two dunite lenses also occur in the Binalik block exposed in the lower Tankulap and in the Patud-Gombaran intrusion.

Intrusive dunite.

A number of exposures suggesting that dunite has been intruded into harzburgite are found within the dunite belt in the eastern flank of the main Tawai block. These suggested intrusive dunites may be divided into two types:-

Small pod and pipe like intrusives.

Large irregular masses.

Examples of the first group (Fig. 58) are found in the North Tankulap stream two miles upriver from the confluence with the South Tanuklap. Two dunite pods about 100ft. long and 30ft. wide are seen in the stream section. The lenses are elongate, sharply defined and markedly cut across thin pyroxenite bands. Both contain small irregular inclusions of harzburgite. Only one of these pods is mineralised and is seen to contain irregular disseminations and blotches of powdery chromite. Another similar but smaller pod is found in the Ruku-Ruku stream section (Fig. 58), two miles upstream from the main ultrabasic contacts, and it contains a prominent elongate bunch of powdery chromite. The chromite bunch is elongate parallel to the main direction of the dunite lens. A small irregular

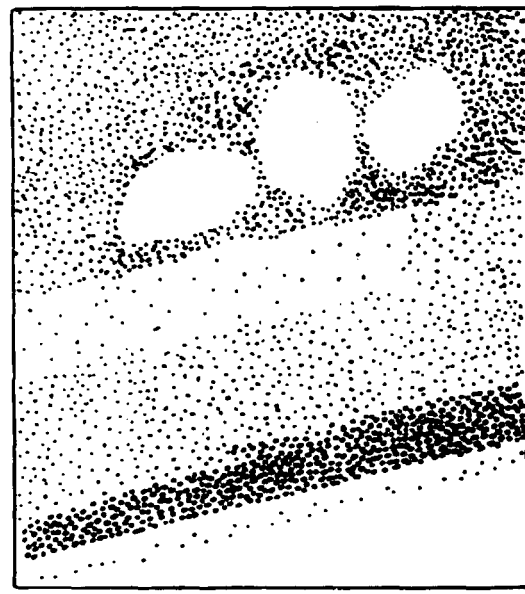

Specimen T 268 a

1"

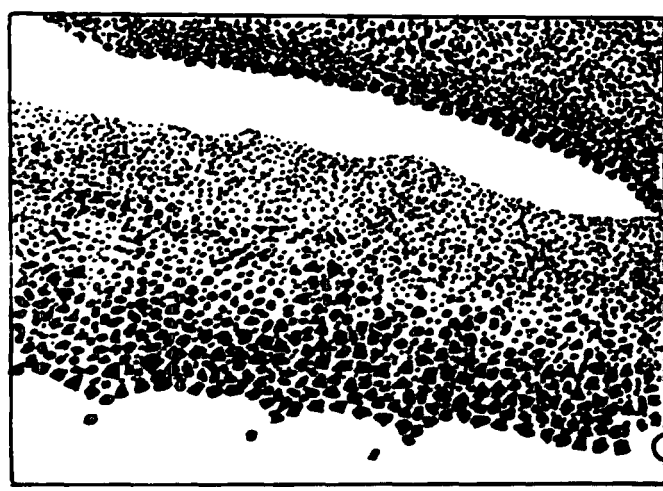

Specimen T 268 b

1"

Chromite bands from the Lichau dunite lense

Fig. 55.

rounded intrusive dunite (Fig. 58) appears in the Hitam river section one and a half miles upstream from the main contact. The lens is intruded by a stringer of gabbro. The Hitam dunite appears to be pipe-like in form and it contains irregular blotches of powdery ore. Further examples are found in the side of the ridge dividing the Ruku-Ruku river from the Lichau. They are largely obscured by slipped material, but they appear to be pipe-like in form and may be traced for two hundred feet up the hill slope.

All the pod and pipe like dunites are characterised by powdery bunches of chromite which always appear concentrated in one part of the intrusive (Fig. 58). Their contacts with the surrounding peridotite are sharp but no contact metamorphism has been recorded.

A large irregular shaped mass of dunite is located in the watershed between the two northernmost arms of the Lichau river. It forms a prominent rounded hill and is a marked unusual feature. The hill is made almost completely of totally serpentinised dunite and thin sections show that bastite pseudomorphs after orthopyroxene are absent. Numerous arms of serpentinite extend out from the mass into serpentinised harzburgite. On account of the heavy serpentinisation it is difficult to elucidate the contact relations but the mass appears from its outcrop to be vertical. It is the largest area of dunite seen in the Tawai area being just over a mile in length. Unfortunately the dunite serpentinite is unmineralised and not a chromite band could be found in it. One of the arms projecting out into the serpentinised harzburgite has a four foot breccia zone on either contact. Irregular inclusions of harzburgite (4' by 2') were located within the mass. It is tentatively suggested that this dunite serpentinite is an intrusive feature.

Fig. 56. Photograph of giant chain structure of chromite in dunite lens. T230.

Fig. 57. Photograph of Kuun-Kuun chromite bands. Type 2 ore. T89.

Intrusive dunites have been described in similar situations from Cyprus (Wilson 1958), Alaska (Ruickmick and Noble 1960) and Greece.

Petrography.

The type one interbanded dunites consist of olivine, and its serpentinisation products, and chromite. The degree of deformation varies from slight granulation of the grain boundaries to extreme granulation depending upon the position of the lens within the batholith.

The undeformed non-mineralised dunites of this type consist of coarse grained olivine with intimately interfering outlines. Slight brecciation of some crystal boundaries is present. Many of the olivine crystals exceed 10mm. in diameter and the majority of the crystals lie in the range 5 - 8mm.. Chrome spinel occurs in minor amounts between the olivine grain boundaries when it shows sub-euhedral and euhedral form. Spinel enclosed within the olivine is often rounded.

The disseminated chromite bands found in the type one dunites are unfortunately strongly serpentinised. Polished specimen examination shows the spinel bands to have one contact fairly sharp and the other gradational. At the sharp contact a single crystal thick layer of small spinels is often found (Fig. 59). Only slight grain size variation can be detected within the thinnest bands. They usually consist of between $^{1}/8$"and $\frac{1}{4}$" layer of closely spaced euhedral crystals which grade up into a disseminated layer $\frac{1}{4}$" to $\frac{1}{2}$" thick. · Sometimes the bands pass up into mineralised serpentinised dunite showing a macroscopic chain structure (Fig. 55). Thin

Fig.58.

EXAMPLES OF INTRUSIVE DUNITE

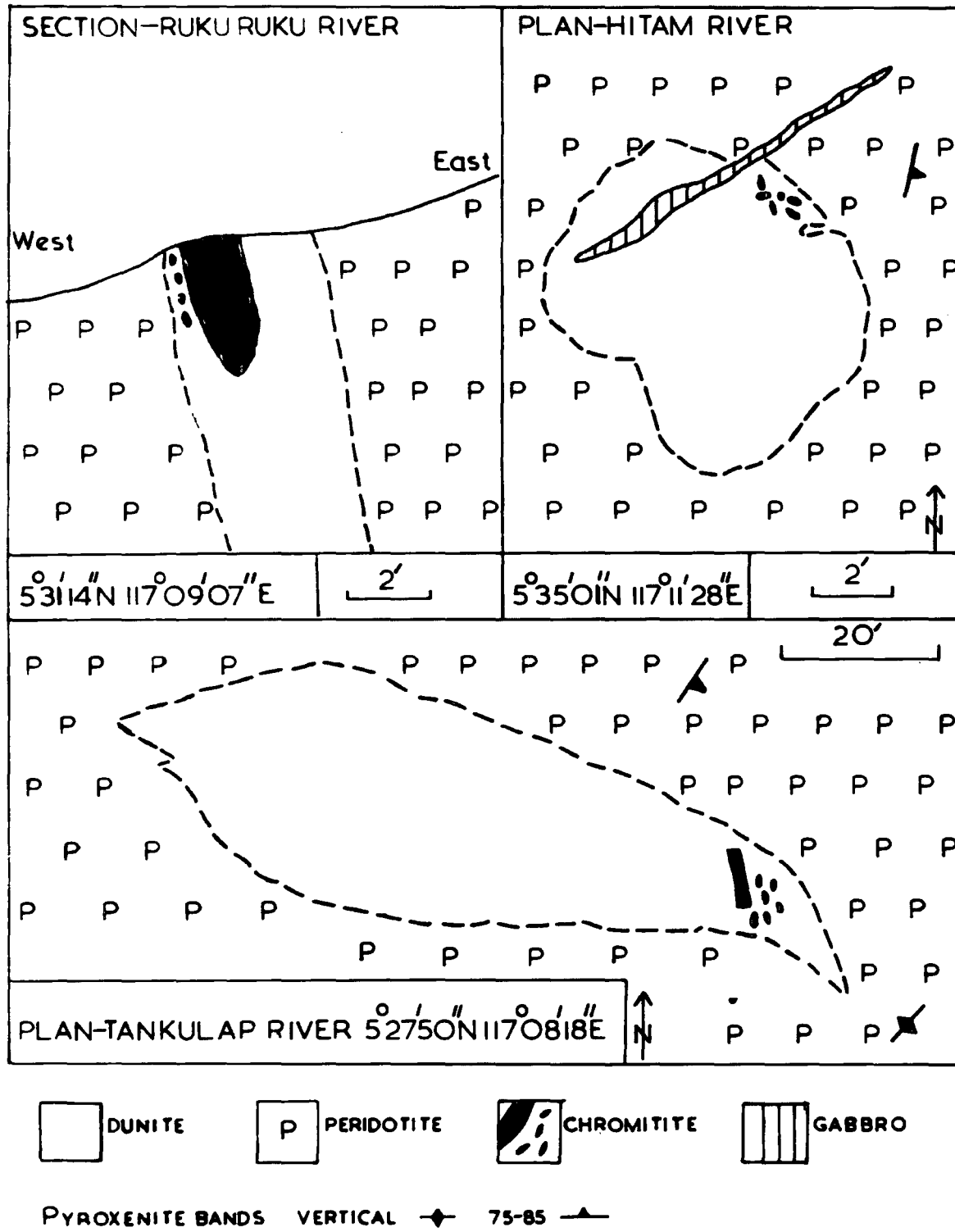

sections show the bands to consist of rounded and euhedral crystals of chrome spinel, .2 to 1mm. in diameter, arranged around serpentine pseudomorphs in a micro chain structure (Fig. 60). This chain structure is a variety of the synneusis texture of Bastin (1950) and is characteristic of chrome spinel olivine accumulates. A four inch thick chromite band (Fig. 55) from the Lichau group of lenses, specimen 268, shows two sharp contacts but there is a marked grain size variation within the band, from between 2 and 4mm. at the base to 1 to .3mm. at the top. The base of the band is markedly cuspate and very similar to specimens described from the Stillwater complex by Jackson (1961).

The chrome spinel clots (Fig. 54) consist of coarse grained (1.0-4mm. in diameter) tightly packed sub-euhedral crystals. These clots again closely resemble specimens described from the Stillwater by Jackson (1961).

The type two interbanded dunites consist of olivine, chrome spinel and chrome diopside and their alteration products. In the non-mineralised type two dunites olivine is dominant, chrome spinel (1 - 2%) and chrome diopside (1 - 3%) occurring in subordinant amounts. The olivine occurs in large anhedral grains (5 - 15mm. in diameter) with intimately interfering boundaries, and cannot be distinguished from the olivine of the type one lenses. The chrome spinel is markedly different. It varies from orange brown to olive brown in colour and is seldom euhedral. Within the type two dunite lenses chrome spinel occurs as irregular blotches, poorly developed bands, and occasionally in a giant chain structure. The well developed chrome spinel bands of the type one lenses is never seen.

The type two dunites are characterised by irregular splotches

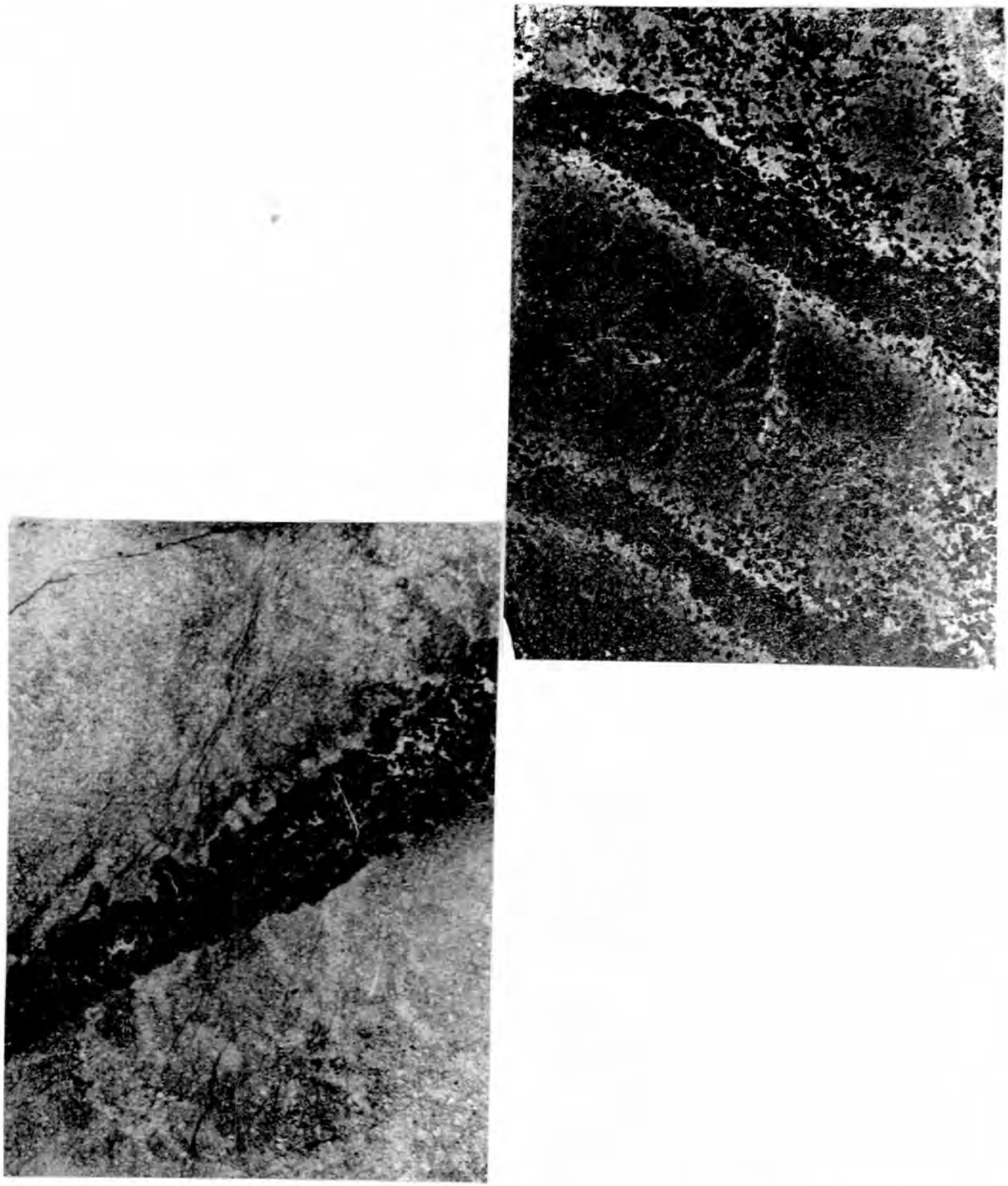

Fig. 59. Photographs of Lichau chromite bands. Above T268d - Notice small spinel crystals at base of upper band. Below T268e - Notice sharp base of chromite band. (Natural size).

and spots of chromite which when concentrated give rise to the shot gun ore texture. The blotches are sometimes arranged in crude bands (Fig. 61).

In thin section the blotches are seen to be made up of single crystals and aggregates of crystals. The spinels (1 - 4mm. in diameter) are seldom euhedral and are usually rounded or oval and have thin arm-like projections extending out from the main crystals between olivine and clinopyroxene grain boundaries (Fig. 62). The crystals show a tendency to form bunches in the vicinity of clinopyroxene crystals and the spinel in these cases may be euhedral (Fig. 63). Many of the spinels completely enclose olivine and clinopyroxene. The spinel is often markedly interstitial to the olivine and clinopyroxene forming irregular elongate crystals around the grain boundaries. In many of the thin sections it is apparent that the spinel has continued to grow in the grain boundaries after the crystallisation of the olivine and clinopyroxene. Episcopic examination of the spinel reveals no sign of zoning in the spinels which would indicate that during their growth temperature conditions remained constant.

Chrome spinel bands, as compared with crude bands of chrome spinel blotches, are rare in the type two lenses. In one of the upper Kuun-Kuun lenses however, thin (5mm. thick) bands of chrome spinel, specimen 89, are seen alternating with slightly thicker bands of dunite over a distance of six inches. Thin section examination of spinel bands shows them to consist of 64% chromite, 21% clinopyroxene, 3% orthopyroxene, and 12% olivine. The spinel is markedly interstitial to the pyroxenes and olivine (Fig. 64). In the thicker bands the spinel has completely enveloped the gangue

Fig. 60. Photomicrograph of chain chromite arranged around cores of serpentine pseudomorphs after olivine. T268a (crossed nicols X100) Type 1 ore.

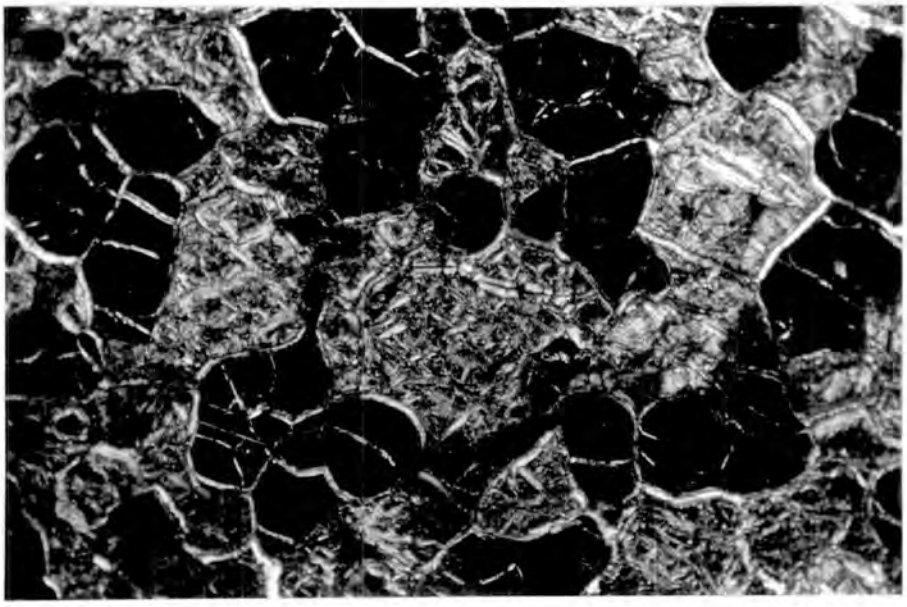

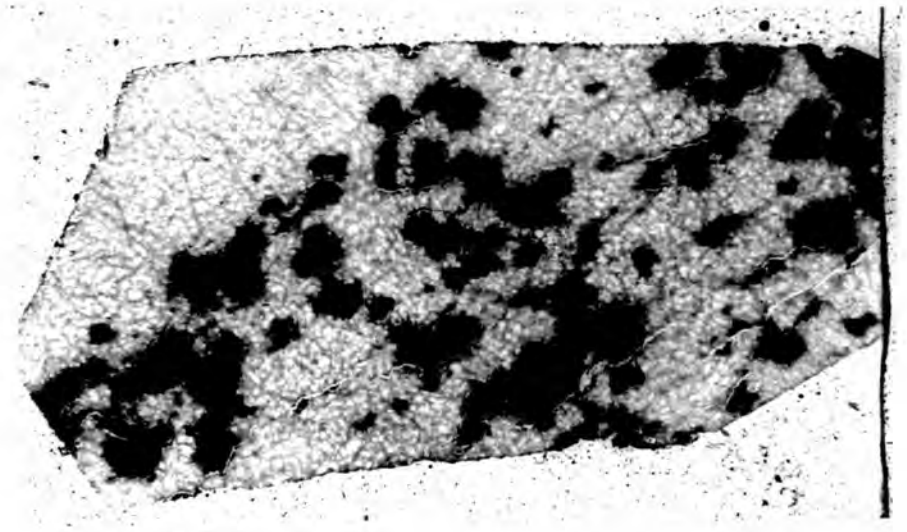

Fig. 61. Photograph of entire thin section of chromite blotches in dunite. Type 2 ore. T85a (ordinary light X3).

minerals and isolated inclusions of olivine clinopyroxene and orthopyroxene are seen set in the chromite. The pyroxene within the bands shows a crude preferred orientation with the long axis of the clinopyroxene and the orthopyroxene crystal lying sub-parallel to the sides of the bands. The clinopyroxene varies from .3 to 3mm. in length and does contain exsolution lamellae of orthopyroxenes. The orthopyroxene is seen in subordinate amounts and as smaller crystals (.3 to 1mm. in length). The orthopyroxene contains 100 exsolution lamellae of clinopyroxene. The pyroxenes show a crude parallel orientation. Hand specimen examination of the chrome spinel bands suggest one contact gradational and the other sharp with the alternating dunite bands. The thin sections show that the sharp contact consists of elongate interstitial spinel situated along the contact between the dunite and the spinel pyroxenite band (Fig. 65). A sharp contact is produced because of the large grain size (10 - 15mm. in diameter) of the olivine in the underlying dunite. At the gradational contact the olivines are much smaller in diameter and there are subsequently more grain boundaries filled with interstitial spinel.

The olivine of the thin dunite bands in the sequence is extremely coarse grained (4 - 15mm. in diameter) and encloses small amounts of subeuhedral and euhedral spinel. Thin elongate interstitial chromite occurs between a few of the grain boundaries.

The pyroxenes are often strongly altered to tremolite and the olivine to lizardite within the spinel bands. Thin veins (.02mm. in width) of carbonate cut the spinel bands at right angles but do not extend out into the dunite on either side. Minor swirls are prominant in the Kuun-Kuun band (Fig. 57).

Fig. 62. Photomicrograph of type 2 ore. T85a. Notice irregular prolongations, and interstitial nature of ore. (crossed nicols X30).

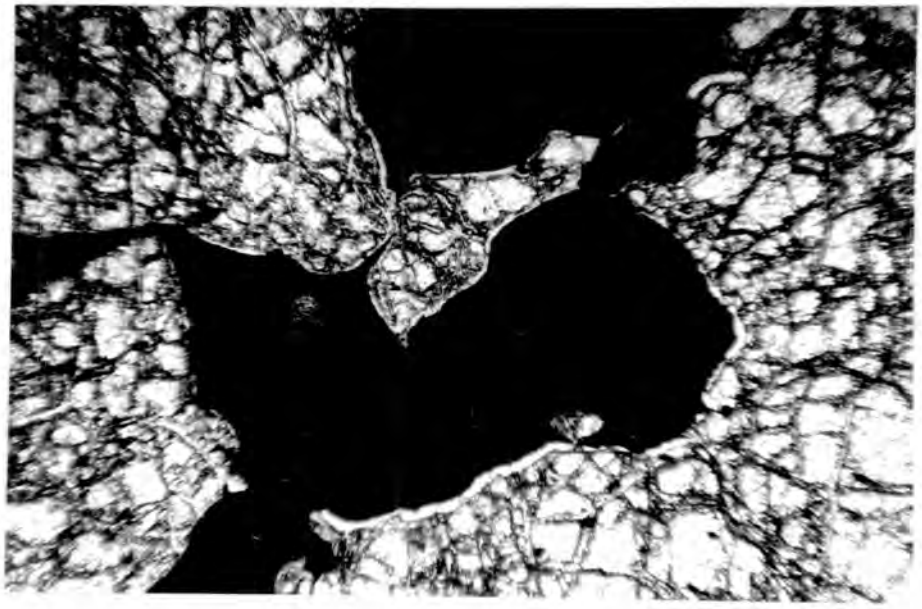

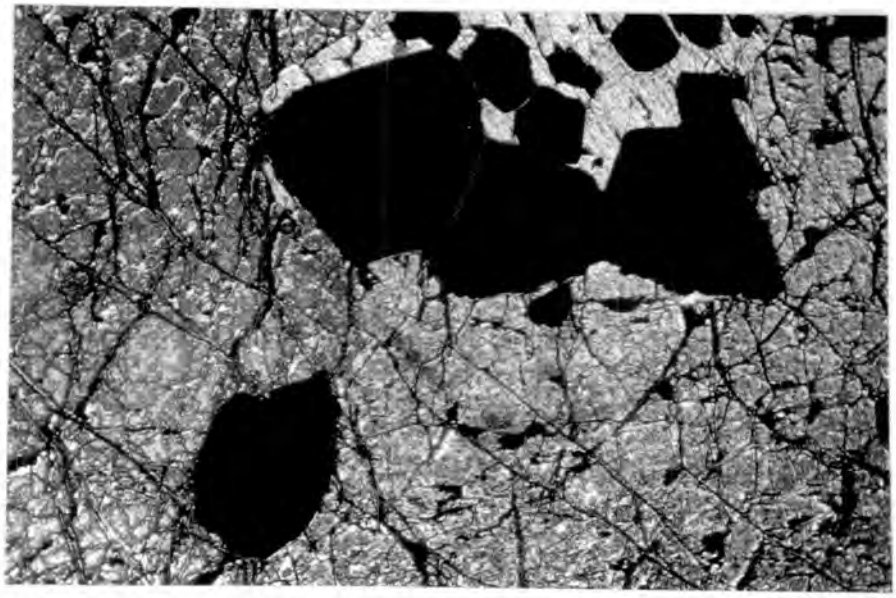

Fig. 63. Photomicrograph of euhedral chromite (Type 2 ore) grouped around clinopyroxene crystals. T100b (crossed nicols X20).

In the Binalik group of type two dunite lenses the shot-gun type of texture predominates. The lens situated at the extreme eastern extremity of the lower Tankulap belt show chromite ore in a giant chain structure (Fig. 56).

The thin section, specimen 230 (Fig. 66), reveals the most complex relationships. The rock is seen to be made up of cores of oval and rounded olivines, up to 5mm. in diameter. The olivines are surrounded by interstitial pyroxene, both enstatite and endiopside, in which perfectly euhedral bunches of chrome spinel crystals are set. Some of the interstitial pyroxene plates measure 10mm. by 8mm.. The spinel crystals are always set in orthopyroxene. When the spinel is set in clinopyroxene it is invariably mantled by orthopyroxene. Both pyroxenes carry complementary 100 exsolution lamellae. Irregular blebs of orthopyroxene which appear to be exsolved from the clino-pyroxene also occur. Some of these blebs have a nucleus of euhedral spinel. Many of the channels between the olivine crystals are narrow and filled with orthopyroxene. Although the latter shows cuspate margins with the olivine there is no suggestion of a reaction rim and there is no evidence to indicate the orthopyroxene has formed by reaction. The relations shown by this slide are complex but the following points are clear.

(a) The olivine crystallised first.

(b) The pyroxenes crystallised in the interstitial gaps.

The role of the spinel is not clear. In places it appears surrounded by orthopyroxene in a manner suggesting the latter crystallised around it whilst occasionally it is seen in a position suggesting it has been exsolved from the clinopyroxene. The delicate

Fig. 64. Photomicrograph of Kuun-Kuun chromite bands showing spinel (black) interstitial to pyroxene. T89 (crossed nicols X50).

Fig. 65. Photomicrograph of the sharp base of Kuun-Kuun chromite bands. T89 (crossed nicols X55).

textures seen in the rock could not possibly have survived severe streaking out and stretching. Clearly the dunite lens containing this rock is a product of magmatic crystallisation and owes its origin to factors other than streaking out of a semi-crystalline mush of crystals. Chrome spinel crystals set in orthopyroxene plates are a feature of the Bushveld chromite deposits and are figured by Cameron and Emerson (1959).

The dunite intrusives are characterised by sac-like ore bodies of chrome spinel (Fig. 58). The olivine of the intrusive dunites invariably shows slight granulation of the grain boundaries and in some cases mortar texture. Inm most of the dunite intrusives the olivine is still extremely coarse grained (3 - 8mm.). The dunite also contains up to three per cent of orthopyroxene scattered evenly throughout the exposures. The chrome spinel occurs in coarse crystals (2 - 4m.) and more often in irregular sac-like bodies. The ore from the larger bunches is extremely powdery and shows many slickensided surfaces in hand specimen. Thin section and episcopic examination shows strong brecciation of the ore (Fig. 67); much greater than is shown by the enclosing dunite. Episcopic examination of the sac-like ore bodies in the Ruku-Ruku and North Tankulap streams shows the presence of small flakes of pyrite in the ore.

The petrographic evidence suggests the dunite dykes have been intruded as a crystalline mush. Although the olivine in most cases is slightly brecciated it never shows strong streaking out or complete granulation. The ore on the other hand is frequently broken and concentrated into irregular low grade ore bodies.

Fig. 66. Photomicrograph of orthopyroxene haloes around euhedral spinel. Notice the exsolution lamellar of enstatite in the endiopside. Opx white and light grey. Cpx - grey. Spinel black. T230 (crossed nicols X10).

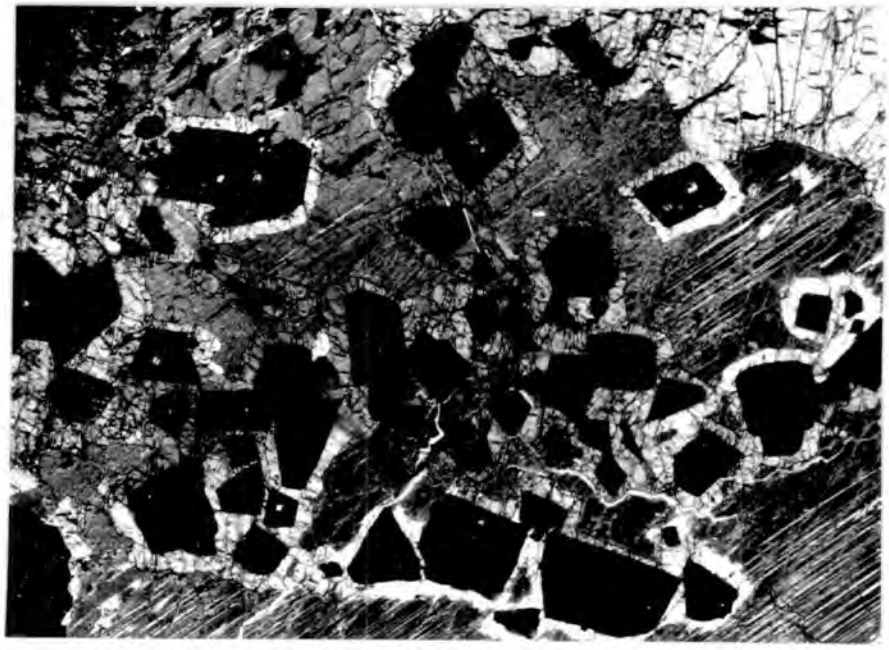

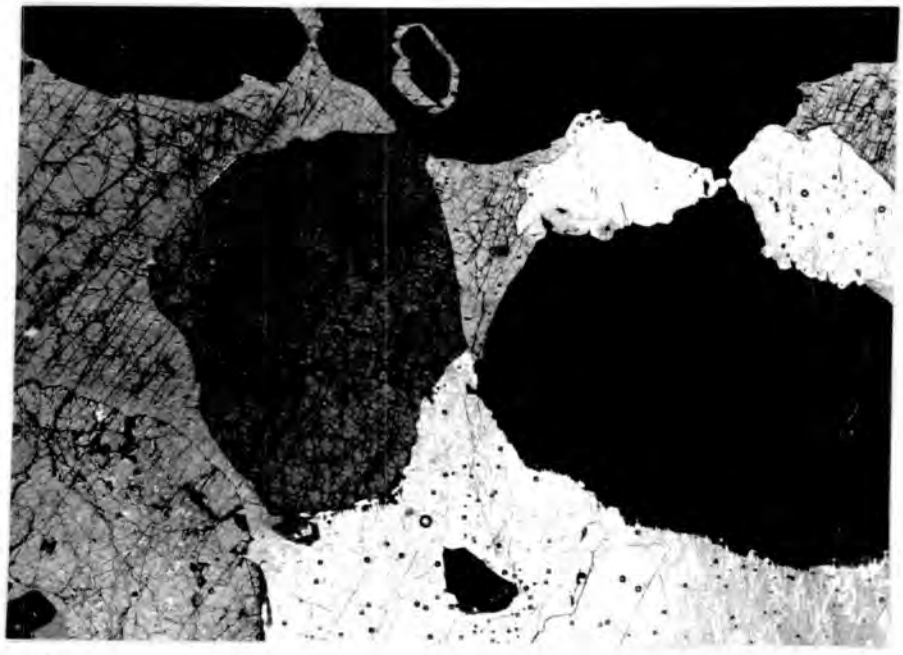

Fig. 66a. Photomicrograph showing olivine (the two oval crystals in centre and centre right of picture) surrounded by enstatite (white) and endiopside (grey). Notice the spinel mantled by opx. set in cpx. top centre.

DURHAM UNIVERSITY
13 AUG 1964
LIBRARY

Mineralogy.

Olivine - X-ray diffraction and refractive indices determinations (Tables 13, 22) indicate the olivine of both the interbanded types of dunite and of the dunite intrusives is forsterite varying from $Fo_{90}Fa_{10}$ to $Fo_{93}Fa_{7}$.

Clinopyroxene - The clinopyroxene from the spinel bands, specimen 89 (Table 29) has been identified by X-ray diffraction as endiopside, and is similar to that found in the pyroxene plates, specimen T230.

Orthopyroxene - Orthopyroxene from specimens T230 and T89 (Table 22) are aluminous enstatite.

Chrome spinel - The chrome spinel shows a marked variation in Cr_2O_3 and Al_2O_3 content (Tables 30, 22). The type one interbanded dunites contain chrome spinel with Cr_2O_3 varying from 48% to 56% and the type two from 43% to 25%.

Olivine Gabbro.

Field Occurrence.

Olivine gabbro is restricted to the western flank of the batholith. In the southernmost tributary of the Telupid river a lenticular area of gabbro elongate N.W.-S.E. is found. The lens is just over four thousand feet long and fifteen hundred feet in width and is situated on the western edge of the batholith. The gabbro forms a narrow ridge seven hundred feet high and is only well exposed in the stream section. The eastern contact of the lens is exposed in the river and a knife-sharp boundary between olivine

gabbro and peridotite is found. The gabbro shows no evidence of a chilled margin or metamorphic effects. The contact peridotite is strongly serpentinised and contrasts strongly with the leucocratic gabbro. Thin sections of the peridotite show that it has not been metamorphosed. The contact is dipping steeply 78° S.W.. The strike of the contact is N 43° W. The western contact of the gabbro lens is poorly exposed. The gabbro near the western contact is strongly brecciated and cut by numerous small fractures trending N.W.-S.E.. Inclusions of unmetamorphosed basalt occur in the breccia zone. Nearby exposures show steeply dipping brecciated basalt interbedded with red shale.

The gabbro exposed in the stream section is a massive greenish black and white mottled rock. The rock is normally massive but a few exposures show banded structures. Thin impersistent feldspathic rich bands ($\frac{1}{4}$" to 3" thick) alternate with normal gabbro in which the greenish brown pyroxenes show a rough foliation parallel to the strike of the bands. Thin melanocratic bands also alternate with leucocratic bands. In most cases the bands merge at their contacts and no definite base or top can be distinguished. The banded exposures are often ribbed, the leucocratic bands standing out against the melanocratic. The latter are usually pitted due to the presence of olivine. Olivine-rich bands have not been observed.

The bands strike between N 10° E and N 20° E and dip steeply westward. They are markedly discordant to the contacts of the lens. The bands do not persist far along the strike where they thin out and merge into massive gabbro. The pyroxene olivine bands sometimes join with other melanocratic bands enclosing leucocratic lenses.

The western contact of the lens shows quite clearly that the

gabbro has been emplaced together with the main peridotite batholith by faulting. The sharp eastern contact strongly suggests that the gabbro is a differentiation phase of the peridotite.

Olivine gabbro also occurs in small exposures in the first north bank tributary of the Melio and in the headwaters of that stream. The exposures show thin lenses of olivine gabbro that have been considerably fractured and altered. The feldspar of the massive gabbro has been bleached white.

Petrography (Fig. 67).

The olivine gabbro of the Telupid lens is a coarse grained hypidiomorphic granular rock consisting of varying proportions of plagioclase, clinopyroxene, orthopyroxene and olivine and their alteration products. Many of the grain boundaries are slightly brecciated but the majority of the crystals are mutually interfering. Modal compositions are difficult to estimate because of the coarse grain size. Approximate modes are as follows:-

Per cent.

Specimen	Olivine	Clinopyroxene	Orthopyroxene	Plagioclase	Ore
168	9	27	5	58	1
384	16	29	2	51	2

The plagioclase occurs in anhedral laths (1 - 4mm.) and shows a strong development of Albite twin lamellae; combined Carlsbad-Albite twins and pericline twins are also found. The lamellae are frequently pinched out and irregular in shape and width but are not strongly bent. Many of the plagioclase crystals are strongly

Fig. 67. Photomicrograph of olivine gabbro. T384 (crossed nicols X20). Notice the chlorite halo around the olivine.

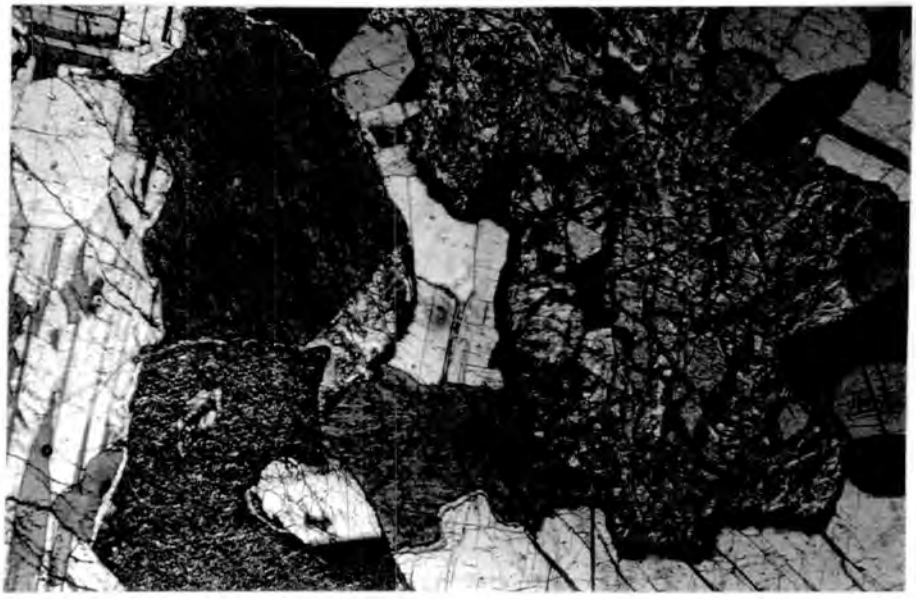

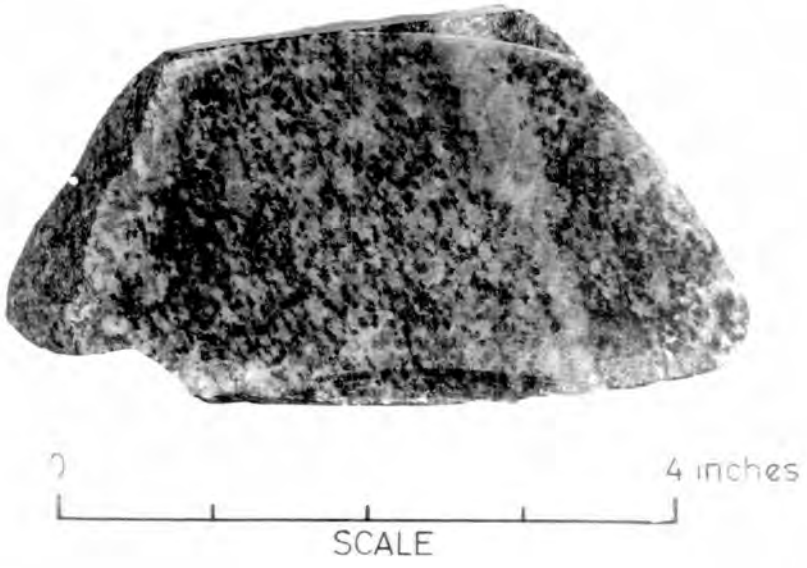

Fig. 68. Photograph of gneissose banding in pyroxene gabbro. T331.

altered to granular epidote and a colourless amphibole. A true ophitic texture between the clinopyroxene and the plagioclase is seldom observed in the olivine gabbros.

The clinopyroxene occurs as anhedral plates (2 - 5mm.) showing a strong diallage cleavage and blebs of exsolved orthopyroxene. Anhedral plagioclase occurs within the clinopyroxenes. Some of the larger clinopyroxenes show weak peripheral zoning. Twinning on 100 is infrequently observed. The majority of the clinopyroxenes are altered to fibrous tremolitic amphibole.

Olivine is never a major constituent of the gabbros. Olivine is seen in anhedral, often rounded and oval crystals interstitial to the plagioclase. The olivine lie in the range 0.1 to 2mm. in diameter but occasionally irregular crystals up to 4mm. are found. The olivines are invariably traversed by a network of irregular serpentine veins outlined with magnetite. The large crystals show a fault lamellar structure. Occasionally the larger crystals are surrounded by a corona, .1 to .2mm. thick, of a low relief fibrous mineral (Fig. 67). The fibres are elongate at right angles to the boundary of the olivine. X-ray diffraction suggests this mineral is a chlorite. Many of the smaller olivine crystals are rimmed by pale pink pleochroic orthopyroxene.

The orthopyroxene occurs as anhedral crystals (.1 to 2mm.) and is always subordinate to the clinopyroxene and seldom make up more than 5% of the rock. The orthopyroxene contains resorbed olivine and never shows exsolution lamellae of clinopyroxene. The orthopyroxene is often strongly altered to an uralitic amphibole.

The plagioclase in the feldspathic bands are usually coarser grained than in the associated massive gabbro. The plagioclase

crystals within the feldspathic bands show no preferred orientation.

Marked variations in grain size are observed between the leucocratic bands that alternate with melanocratic bands. Approximate modes of two contrasted bands (specimen T167) are given below.

Per cent.

Specimen	Olivine	Clinopyroxene	Orthopyroxene	Plagioclase	Ore
167					
Leucocratic band.	2	23	-	76	-
Melanocratic band.	17	37	2	43	1

In the melanocratic bands clinopyroxene varies from 1 to 5mm. and the larger laths show a crude preferred orientation of 100 parallel to the strike of the band. In the leucocratic bands the clinopyroxene is greatly reduced in size and measures.1 to 1mm.. There is however little change in the size of the plagioclase in the contrasted bands. The plagioclase shows no preferred orientation.

Mineralogy.

Olivine - X-ray diffraction and refractive index measurements indicate the olivine to be chrysotile varying from Fo_{86} Fa_{14} to Fo_{84} Fa_{16} (Tables 13, 22). The mineral is biaxial negative, nY varies from 1.675 to 1.684, and is unzoned.

Plagioclase - Measurement of the maximum extinction angles of albite twins out normal to 010 (Method of Michel Levy) in the plagioclase indicates an anorthite contact varying from An_{68} to An_{80} (38° to 45°). The plagioclase is therefore bytownite near

to labradorite in composition. Only weak normal zoning is observed in the plagioclases. It is best seen in small plagioclase crystals enclosed in olivine.

Clinopyroxene - Clinopyroxene from two specimens of olivine gabbro (T384, T168) from the Telupid lens have been analysed (Table 23). Both minerals lie close to the diopside-augite corner of the descriptive chart of Hess (1954). Measurements of the cell dimensions of the larger clinopyroxene crystals occurring in the melanocratic bands suggest they are more magnesian rich than the diopside and diopsidic augite of the normal gabbro. The large clinopyroxene (Table28, Nos. T167, T166, T218) vary from $Ca_{43.5}\ Mg_{51.5}\ Fe_{5}$ to $Ca_{45}\ Mg_{48.5}\ Fe_{6.5}$.

Orthopyroxene - The unit cell dimensions of two orthopyroxenes from the Telupid olivine gabbro have been measured and correlated with the determinative chart of Hess (1952). The results (Table 13, Nos. 168, 384) indicate the mineral to be bronzite close to hypersthene in composition and to vary from $En_{80}\ Fs_{20}$ to $En_{84}\ Fs_{16}$. These values are in close agreement with composition estimates made from correlation of nZ with the charts of Hess (1960). The bronzite is faintly pleochroic in pink and green and is opticallly negative.

Cryptic banding has not been located in the Telupid lens. Specimen T168 was taken close to eastern contact and specimen T389 near to the western contact.

Pyroxene gabbro.

Field Occurrence.

Pyroxene gabbro occurs mainly on the east flank of the Mount Tawai block and in the Ðantagaluang block. In the field it has been found as lenticular bodies, intrusive dykes and veins, and as irregular inclusions.

Large areas of pyroxene gabbro do not occur. The largest body is located on the eastern flank of the Sawar range just over a mile inside the ultrabasic contact and is exposed in, and between, the Merah and Ruku-Ruku streams. The gabbro forms an elongate body, about one and a half miles long, trending north-east south-west, and is completely surrounded by peridotite. At the northern-most exposure the gabbro is eight hundred and twelve feet wide and at the southernmost tip exposed in the Ruku-Ruku stream it is one hundred and sixty feet. The lens is well exposed in the Merah and Ruku-Ruku streams and can be traced across the watershed in between by sporadic outcrops of pyroxene gabbro many of which are of a slipped nature. North of the Merah river isolated outcrops of pyroxene gabbro are found for distances of up to two miles along the continuation of the strike of the main lens. Field debris between these outcrops and the main lens is absent and they have been mapped as separate bodies. To the south the lens cannot be traced over the watershed between the Ruku-Ruku and the northernmost tributary of the Lichau river.

At the northernmost exposure in the Merah stream just over eight hundred feet of gabbro are exposed in a series of waterfalls. The eastern contact at the base of the falls is obscured by large

gabbro blocks but the uppermost western contact is exposed and is seen to be of a faulted nature. The peridotite at the contact is strongly brecciated and in places extremely fissile. Inclusions of slickensided peridotite litter the gabbro outcrops. The contact is vertical and strikes N 34° E.

The gabbro is massive and unjointed. It is extremely variable in grain size changing from fine to pegmatic phases over short distances. Some of the pegmatic phases show a crude gneissose foliation of the black pyroxene crystals. Many of the feldspars are a dull purple. Ophitic texture can be seen in some of the hand specimens but in general the outcrops have a markedly cataclastic appearance. The crude gneissose band is vertical and strikes markedly discordant to the main contact.

At the Ruku-Ruku exposure one hundred and sixty feet of gabbro are exposed in the river bed. Both contacts are exposed and show intensely brecciated peridotite against the gabbro. The contacts are vertical and striking almost due north. The gabbro is of medium to coarse grain and only small pegmatitic phases are seen. Coarse gneissose banding in the gabbro is striking N 46° E and is markedly discordant to the contact.

On the eastern flank of the Pantagaluang range a strongly banded gabbro lens is found exposed in the headwaters of the Binalik river. The gabbro is half a mile in length, and six hundred feet in width at its widest point. The lens occurs on the eastern side of the main fault contact of the peridotite. A two hundred foot wide zone of fault breccia consisting of angular fragments of peridotite and gabbro set in a red gouge separates the main ultrabasic body from the gabbro lens. The western contact of the gabbros is less clearly

exposed. Disturbed basalt that has been strongly veined by quartz and pyrite occurs near the gabbro. Red shale exposed in the River Binalik is dipping steeply north-east, discordant to the strike of the gabbro contact, and is unmetamorphosed. The western contact must be regarded as a fault contact.

The gabbro shows a strong gneissose banding striking (Fig. 68) between N 57° E and N 61° E; markedly discordant to the contacts. The gneissose banding is caused by sub-parallel alignment of pyroxene crystals.

Many small dykes and veins of coarse grained pegmatic pyroxene gabbro are found in the stream sections draining the eastern flank of the main Tawai block. They vary from half an inch to six feet in width. The larger dykes thin and thicken along the strike. An excellent example is seen in a beach on the River Tankulap two hundred yards west of the main stream bifurcation (Fig. 69). The smaller veins frequently occur filling joints within the peridotite. These small veins show knife-sharp contacts with the peridotite (Fig. 69) but the larger veins have pushed the ultrabasic rocks aside; and narrow zones of tremolite and wavy peridotite flank the intrusion. The gabbro veins are seen cutting dunite and pyroxenite in the southernmost tributaries of the Lichau river. The majority of the gabbro pegmatite veins are striking in a northerly direction within the main Tawai block and appear to be following joints, but many of the smaller ones show a haphazard distribution.

Many small irregular inclusions of pyroxene gabbro occur in the peridotite. These inclusions vary from a few feet to blocks two hundred feet wide. The largest inclusion occurs in the South Tankulap stream two and a half miles downstream from the North

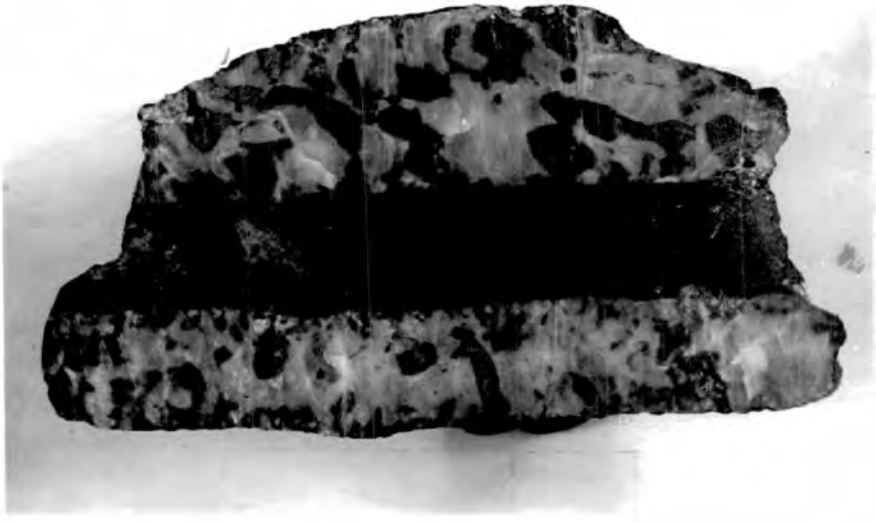

Fig. 69. Photographs of gabbro pegmatites. Above, North Tankulap beach section. Notice tremolite zone around the pegmatite. Below, Hand specimen from Lichau section. Gabbro pegmatite is filling joints in harzburgite. T256.

Tankulap confluence. The inclusion is roughly oval in shape and is strongly altered and deformed.

The large lens on the eastern flank of the Sawar range must be considered as a tectonic inclusion. The prominent line of gabbros that extends from the Ruku-Ruku river northwards to the Puteh river probably marks the line of a fault.

Petrography.

The pyroxene gabbros are composed of varying proportions of plagioclase, clinopyroxene, orthopyroxene and ore. The rocks are seldom fresh and they show alteration by uralitisation, saussuritisation, and sometimes albitisation. The pyroxene gabbros usually show hypidiomorphic granular textures but occasionally ophitic texture between the plagioclase and the pyroxenes is seen. All the thin sections of pyroxene gabbros examined show deformation characteristics.

Accurate modal analysis of the pyroxene gabbros is difficult on account of the coarse grain size and the degree of alteration. Approximate representative modes are as follows:-

Per cent.

Specimen	Plagioclase	Orthopyroxene	Clinopyroxene	Ore
T136	52	13	30	3
T121	45	26	24	5
T331	49	48	2	1
T154	60	31	9	1

According to the nomenclature of Hatch, Wells, and Wells (1952)

these rocks are hypersthene gabbro (T136), Augite Norite (T121), Gabbro (T331) and Norite (T154). In the majority of the thin sections examined clinopyroxene is dominant over orthopyroxene, and hypersthene gabbro and gabbro are by far the most common types.

The large lens of gabbro on the east flank of the Sawar range varies between hypersthene gabbro and augite norite, whilst the Pantagaluang lens shows gabbro and hypersthene gabbro phases. The changes between the gabbro types are not related to the contacts and have a haphazard distribution occurring over short distances. The pegmatic veins and dykes are dominantly hypersthene gabbros that grade occasionally into norite.

The plagioclase of the pyroxene gabbros varies considerably in size from 7mm. to .2mm.. In most of the specimens examined it is anhedral but occasionally prism facies are seen. A marked ophitic texture between the feldspar and clinopyroxene and orthopyroxene is seen in these cases. Albite and combined Carlsbad Albite twins and periclinal twinning has also been observed. Many of the larger plagioclase crystals are strongly bent and they show a spectacular development of twin lamellae (Fig. 70). In these crystals the twin lamellae are concentrated and broad in the areas showing the strongest strain and they pinch out and taper in the least deformed parts of the crystal. The lamellae themselves are commonly bent and they frequently terminate at cracks with the plagioclase crystals.

All the plagioclase feldspars have been affected to some degree by saussuritisation and in hand specimen the more severely affected appear a dull purple colour. X-ray diffraction of one of these specimens showed the alteration product to be iron free epidote. A brown turbid amorphous mineral frequently clouds the more altered

Fig. 70. Photomicrograph of feldspars in pyroxene gabbro. T331. (crossed nicols X50). Notice the pinched out lamellae.

Fig. 71. Photomicrograph of gabbro pegmatite showing granular texture. T256 (crossed nicols X25).

feldspars. The gabbro on the east flank of the Pantagaluang range has been severely altered and the plagioclase crystals afe strongly clouded and replaced by granular saussurite (iron free epidote). Nests of prehnite and zeolites are present in the altered feldspars. This gabbro also shows strong albitisation. Limpid untwinned albite rims many of the crystals. Clear anhedral quartz is found around some of the albitised plagioclase. The strongly altered feldspars also show conspicuous zoning. The plagioclase never shows preferred orientation and platy alignment of the lath is absent in the strongly gneissose specimens.

The clinopyroxene occurs as anhedral laths from .5 to 8mm. in length. Occasionally it is seen markedly interstitial to euhedral plagioclase but normally it is found as broad stumpy laths. In the Pantagaluang gabbro these laths show a crude preferred orientation with their long axis parallel to rough gneissose foliation of the lens. This gneissose banding is easily distinguishable in the stream section but difficult to detect in hand specimen. Thin (100) exsolution lamellae of orthopyroxene occur in some of the pyroxene gabbros.

In the pyroxene gabbros the orthopyroxene occurs in discrete lath (.5 to 4m.) and interstitial to the plagioclase. The orthopyroxene has thin exsolution lamellae (100) of clinopyroxene. In many of the strongly deformed gabbros it is interesting to note that kink band structures and undulose extinction are absent or poorly developed.

Both pyroxenes show varying degrees of alteration. In the least altered specimen tremolite is seen replacing the edges of the

clinopyroxene and attacking the 100 exsolution lamellae in the orthopyroxene. In the more advanced stages the pyroxene are often completely converted to colourless tremolite and actinolitic amphibole and a green pleochroic felt. Granular magnetite is often found in the felt. The strongest uralitisation effects are seen in the Pantagaluang gabbro.

The pegmatitic pyroxene gabbros contain giant crystals of orthopyroxene, clinopyroxene and plagioclase. Crystals up to 20mm. long are frequent. Often the gabbro dykes are strongly deformed and the plagioclase is seen as a mosaic of small fractured crystals (Fig. 71); the pyroxenes in these rocks are ragged and arranged in a crude gneissose foliation. The pyroxene crystals are usually very strongly altered to colourless amphiboles and green pleochroic chlorite.

Ilmenite is a constant accessory of the pyroxene gabbros and is most strongly developed when orthopyroxene exceeds or equals the amount of clinopyroxene. Ilmenite occurs as skeletal crystals and irregular areas.

Mineralogy.

Plagioclase - Optical measurements indicate that there are only small compositional differences between the relatively fresh plagioclase of the various types of pyroxene gabbro. The plagioclase is invariably labradorite ranging from $An_{68}\ Ab_{32}$ to $An_{57}\ Ab_{43}$. These relatively small changes cannot be related to compositional type or the position of the parent rock within the gabbro lens or dyke. The strong saussuritised gabbros of the Pantagaluang lens however show marked zoning and the following changes have been recorded.

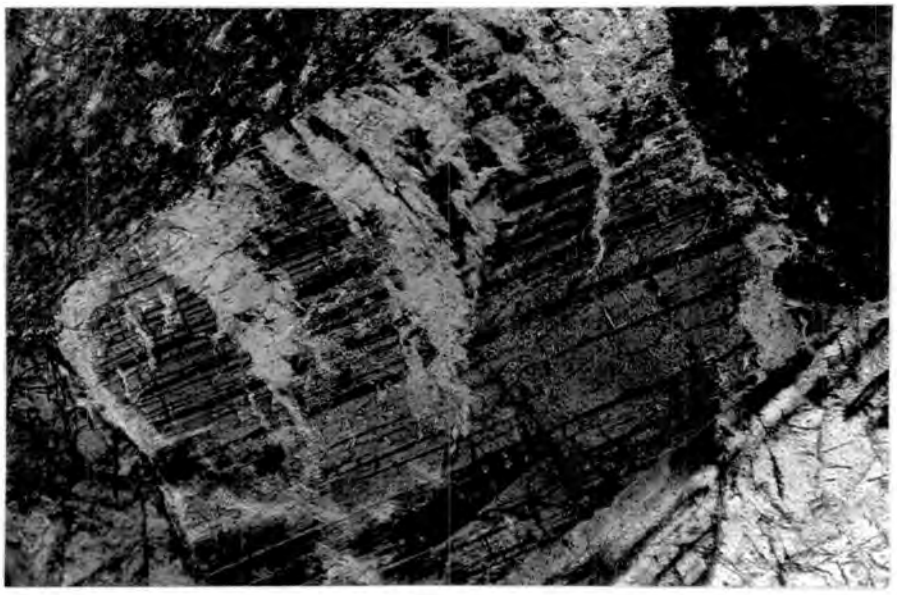

Fig. 71a. Photomicrograph of albitised gabbro. T269.
Above - general picture (crossed nicols X20).
Below - albite attacking plagioclase (crossed nicols X60).

(1) $An_{63}\ Ab_{37}$ in the core - $An_{48}\ Ab_{52}$ margin.

(2) $An_{53}\ Ab_{47}$ in the core - $An_{44}\ Ab_{56}$ margin.

(3) $An_{57}\ Ab_{33}$ in the core - $An_{46}\ Ab_{54}$ margin.

Many plagioclases in the Pantagaluang gabbro have labradorite cores surrounded and attacked by albite (Fig. 71a).

Clinopyroxene - Unit cell dimensions measurements (Table 28) indicate the composition of the clinopyroxene to vary from $Ca_{44}\ Mg_{45}\ Fe_{11}$ (specimen 136) to $Ca_{43}\ Mg_{42.5}\ Fe_{14.5}$ (specimen 143). The mineral is a diopside augite. The mineral is non-pleochroic and has a 2V varying from 50° to 55°.

Orthopyroxene - Unit cell dimension determination and optical measurements (nZ 1.694 - 1.698) indicate the orthopyroxene is bronzite En_{77} - En_{75} (Tables 13, 22). The mineral is pleochroic (specimen 121 - X faint pink, Y pale brown, Z faint green) and has 2V varying between 70 - 75°.

THE MINERALOGY OF THE ULTRABASIC AND BASIC ROCKS.

The Mount Tawai complex belongs to a group of ultrabasic intrusives loosely referred to by Thayer (1960) as "Alpine type peridotites". These complexes consist mainly of harzburgite with minor gabbro arranged in no definite pattern; and in these respects they contrast markedly with the classical stratiform complexes of Skaergaard, Stillwater, and the Bushveld, which are considered to be differentiates of basaltic magma. A major controversy exists as to whether or not the Alpine type peridotites are also derived from basaltic magma and in view of this numerous comparisons are made between the mineralogy of Mount Tawai, other Alpine type peridotites, the stratiform complexes, and peridotite nodules in basalt. A connection between the latter and the Alpine type peridotites has been suggested by Ross et al (1954).

Olivine.

Composition.

The composition of the olivine has been estimated by the X-ray diffraction method of Yoder and Sahama (1957). In this method the d spacing of the olivine 130 reflection is correlated with chemical composition (Fig. 72), and an accuracy of 3 to 4 mol. per cent is claimed. An alternative method using d_{062} has been published by Jackson (1960) in which an accuracy of $\pm$0.4 mol. per cent is claimed. The intensity of the 130 reflection is however superior to that of d_{062} and moreover is free from interference from orthopyroxene, clinopyroxene, spinel and serpentine reflections so that separation of olivine is not necessary. The strong intensity of the 130

Fig.72.

Olivine determinative curve.

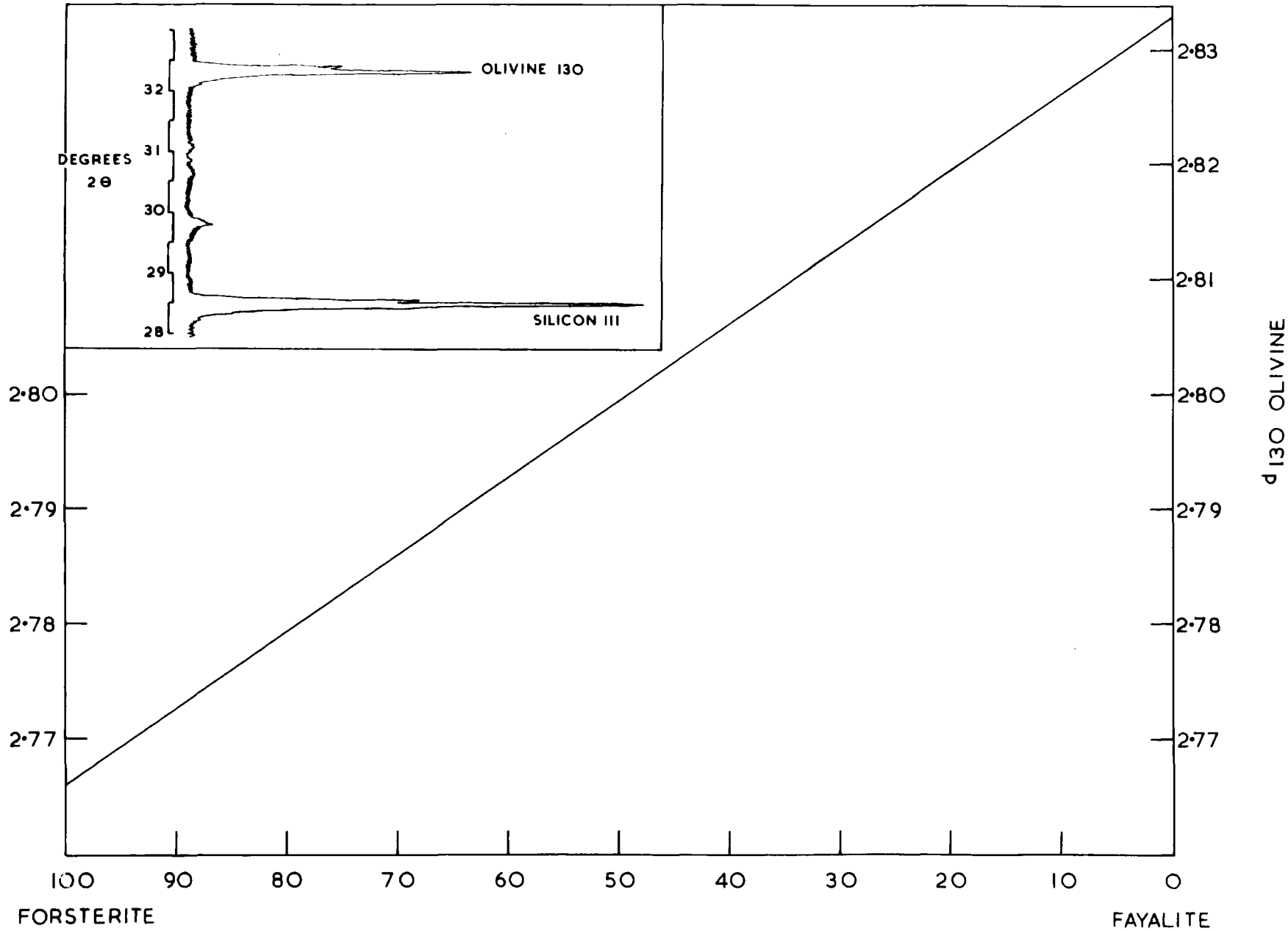

reflection enables whole rock specimens with as little as twenty per cent olivine to be examined which is particularly useful in the case of serpentinised peridotites.

The specimens were examined as smear mounts using the Phillips High Angle diffractometer. About 0.1 grams of finely powdered rock sample admixed with .02 gram of silicon were used in the preparation of the smear mounts. Scans were made from $28^{\circ}2\theta$ to $33^{\circ}2\theta$ using Cu radiation, rate meter X8, time-constant +4 and 1°, 1°, 1°, slits. A scan speed of $1/8^{\circ}$ per minute and chart speed of 200mm. per hour were used. Pulse height discrimination was used to increase peak to background ratios. The observed 2θ position of d_{130} was corrected using the silicon internal standard d_{111} reflection at 2θ 28.445. The method was first tested using olivines of known composition and found to be accurate.

The results are shown in Table 22. In the ultrabasic rocks the olivine is forsterite and varies from $Fo_{90}\ Fa_{10}$ to $Fo_{93}\ Fa_{7}$. No systematic variation could be detected between the olivines of the various ultrabasic rock types or between olivines from the different tectonic units. The olivine from the olivine gabbro is chrysolite and varies from $Fo_{86}\ Fa_{14}$ to $Fo_{84}\ Fa_{16}$. Peaks indicative of zoning were not obtained from the olivine sample examined.

A number of measurements of $n\gamma$ refractive indices have been made and estimates of the composition from the determinative curves of Poldervaart (1950) are in general agreement with those obtained by the X-ray diffraction method (Table 13).

Inclusions in olivine.

Two types of inclusions have been noted in the olivines:-

Table 13. Optical Data for Olivines and Orthopyroxenes.

		Olivine			Orthopyroxene		
No.	Rock Type	n Y	Mol%Fo[*]	X-ray	n Z	Mol%En[t]	X-ray
22	P	1.670	91	91	1.680	88	90.1[-]
42	P	1.670	91	92	1.680	88	89.5[-]
136	P.G.				1.696	75	77
143	P.G.				1.698	73	75
168	O.G.	1.684	85	84	1.690	79	81
198	H	1.665	94	93.2	1.678	89	90.0
208	P	1.667	93	91.8	1.676	91	90.6[-]
383	H	1.667	93	91.7	1.678	89	89.7[-]
384	O.G.	1.680	87	86.1	1.685	83	84

P - Pyroxenite.
H - Harzburgite.
PG - Pyroxene gabbro.
OG - Olivine gabbro.

[*]Based on Poldervaart (1950)

[t]Based on Hess (1960)

[-]Chemical result

Spinel inclusions

Gas inclusions

Thin rods and dedritic growths of spinel are occasionally found in the olivine (Fig. 41). They are light brown in colour and appear to be sub-parallel to 100 of the olivine host. Similar structures have been described by Wilkinson (1953) who noticed them in the Alpine type serpentinites of Queensland and describes them as myrmekitic intergrowths and cites them as evidence for an ultrabasic magma. They have also been recorded in olivine from peridotite nodules in basalt by Wiltshire et al (1963). The growths are probably due to the exsolution on cooling of very small amounts of chromite.

Minute gas inclusions occurring as thin trains of bubbles (Fig. 73) have been located in two specimens of fresh olivine studied under high power on the Panphot microscope. When crushed the inclusions explode and release a gas that forms bubbles in the immersion liquid. Dr. Sawkins has identified the gas as carbon-dioxide by absorbing it in a solution of potassium hydroxide and calcium chloride. Similar inclusions have been identified by Dr. Sawkins in the olivines from peridotite nodules in basalt from Carlton Hill.

The forsterite content of the Mount Tawai olivines is compared with olivines from other magnesium rich environments in Table 14. The olivines from the Tawai ultrabasic rocks are similar to those from the majority of Alpine type peridotites and from peridotite nodules in basalt, but are more magnesium rich than the earliest formed olivines from the majority of the stratiform complexes.

Fig. 73. Photomicrograph of gas bubbles in olivine. Length of picture 2 mm.

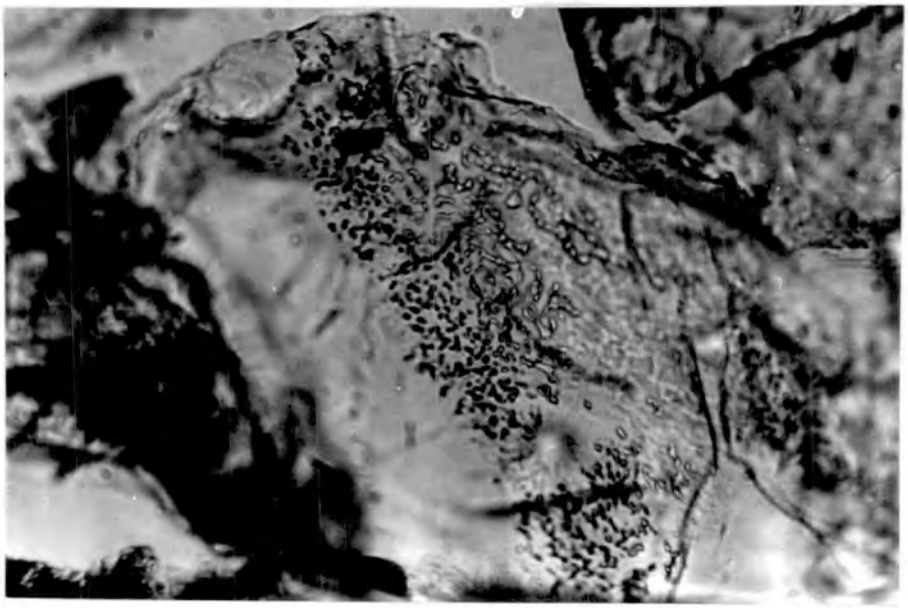

The earliest formed olivines from the differentiated alkaline basaltic intrusives are more iron rich than the other groups shown in Table 14. The olivines from the lowest zones of the Great Dyke are comparable with those from Alpine type peridotites. This intrusion which is considered by Hess (1960) to be a differentiate from basaltic magma contains an ultrabasic zone that is considerably thicker than the mafic zone, a reverse situation to that found in the Bushveld and Stillwater complexes. Other layered intrusions which contain comparable magnesium rich olivines are Rhum (Fo_{89}) and a small mass near Skaergaard (Fo_{92}) described by Wager (1958).

Orthopyroxenes.

Chemistry.

Four analyses of orthopyroxenes from the Mount Tawai ultrabasic rocks are given in Table 15. Calculations of the molecular per cent En (En = 100 Mg / $Mg+Fe^{2}+Fe^{3}+Mn$) shows a variation from 90.6 to 89.5. The orthopyroxenes are biaxial positive and according to the nomenclature of Deer, Howie, and Zussman (1963, vol. 2 p. 9) are enstatite although Poldervaart (1947) places the boundary between enstatite and bronzite at En_{90} Fs_{10}. In Table 14 the Mount Tawai orthopyroxenes are compared with those from other areas with respect to their En values.

In common with orthopyroxenes from the Alpine type complexes those from Mount Tawai are more magnesium-rich than those from the basal zone of the stratiform complexes. Amongst the Alpine type peridotites the orthopyroxenes from Mount Albert and Webster are distinctly more magnesium-rich than the others. Smith and Macgregor

Table 14. Comparison of Mol. per cent Fo of magnesian olivines and Mol. per cent En of orthopyroxenes from Various environments.

Type	Area	Olivine Mol%Fo	Opx. Mol%En	Source
Alpine Type peridotites	(Mount Tawai	90-93	89.5-90.6	*
	(Tinaquillo (V)	90	90-92	Mackenzie (1960)
	(Lizard (GB)	89-91	89-91	Green (1964)
	(Mount Albert (C)	90-92	92-97	Smith & Macgregor (1960)
	(Webster (USA)	92	94	Hess (1952)
	(Mount Dun (W.2)	92	91	Ross, et. al, (1954)
	(New Caledonia	92	92	Ross, et. al, (1954)
	(Zambales Range (P)	85-95	-	Rossman, et. al, (1958)
	(Dawros. (I)		86.4-91.2	Rothstein (1958)
Modules in basalt	Various	89-91	89-91.5	Ross et. al, (1954)
Garnet peridotites	Various	89-93	83-93	O'Hara (1963)
Stratiform complexes	(Stillwater	°88	89.7	Hess (1956)
	(Bushveld	°86	88.4	Hess (1952)
	(Great Dyke	°94	94	Worst (1958)
Alkaline basaltic	(Garbh Eilean	°84		Johnston (1953)
	(Black Jack	°79		Wilkinson (1957)

°Earliest formed olivine and opx only quoted.

*Ultrabasic only quoted.

(1960) describe high En orthopyroxenes from the Mount Albert complex as occurring in areas of high serpentinisation and suggest that during crystallisation increase of water vapour pressure has increased partial oxygen pressure in these areas resulting in more magnesium-rich orthopyroxenes. No evidence to support this theory has been found in the Mount Tawai ultrabasics.

The most striking result from the analyses is the wide range of alumina content. The analyses have been recalculated to six oxygen atoms and divided into two groups (Table 17). The formula for any pyroxene may be written

$$(W)_{1-p}(XY)_{1+p}Z_2O_6$$

where $W = Ca^{+2}, Na^{+1}$

$X = Mg^{+2}, Fe^{+2}, Mn^{+2}, Ni^{+2}$ p=o-1 for clinopyroxenes

$Y = Al^{+3}, Fe^{+3}, Cr^{+3}, Ti^{+4}$ p=2-1 for orthopyroxenes

$Z = Si^{+4}, Al^{+3}$.

W, X and Y are in the octahedral position and Z in the tetrahedral position. There is no evidence to suggest that other ion than Al^{+3} can enter into the Z position with Si^{+4}. The orthopyroxenes have therefore been divided into two groups, WXY, and Z and the alumina distributed between the two in the following manner.

$$Z\ Al^{+3} = X\ Al^{+3} + Z\ Ti^{+4} + Cr^{+3} + Fe^{+3} - Na+K$$

The recalculated analyses show a systematic substitution of Al^{+3} for Mg^{+2} and Si^{+4}. When calculated in this way the results, given in Table 17, show there is a cation deficiency in the Z group. Boyd and England (1960) suggest there may be solid solution along the orthopyroxene-olivine join at high pressure. There is a similar cation deficiency in the orthopyroxene analysis of peridotite nodules

Table 15. Orthopyroxene Analyses.

	T208	T383	T42	T22
SiO_2	56.0	54.1	52.9	52.6
Al_2O_3	1.3	4.5	7.1	7.4
Fe_2O_3	.4	.4	.2	.3
FeO	5.9	6.3	6.4	6.0
MnO	.2	.2	.1	.1
MgO	34.1	32.5	31.2	31.5
TiO_2	.3	.3	.3	.2
NiO	.2	.2	.1	.1
Cr_2O_3	.8	.8	.4	.4
CaO	1.3	1.4	1.8	1.7
Na_2O	.1	.1	.1	.1
K_2O	tr	tr	tr	tr
Total	100.6	100.8	100.6	100.4
*En	90.6	89.7	89.5	90.1
Ca	2.6	2.7	3.6	3.3
Mg	88.8	87.8	86.5	87.4
Fe	8.6	9.5	9.9	9.3

Specimen T208 - Orthopyroxenite 5° 29' 07" N 117° 07' 30" E.
North Tankulap river.

Specimen T383 - Harzburgite 5° 29' 45" N 117° 05' 26" E.
Melilo river.

Specimen T42 - Orthopyroxenite 5° 34' 59" N 117° 07' 55" E.
Meliau river.

Specimen T22 - Pyroxenite 5° 35' 06" N 117° 07' 53" E.
Meliau river.

Analyst, W.G. Hancock.

* Calculated from oxide mol. prop.

Table 16. Orthopyroxene Analysis Recalculated to 6 Oxygen Atoms, After Deer, Howie, and Zussman.

	T 208		T 383		T 42		T 22		
Si	1.932)	1.986	1.873)	2.000	1.830)	2.000	1.820)	2.000)	Z
Al	.054)		.127)		.170)		.180)	)	
Al	-)		.056)		.120)		.123)	)	
Fe^{III}	.012)		.008)		.004)		.008)	)	
Fe"	.170)		.181)		.185)		.172)	)	
Mn	.006)		.006)		.002)		.002)	)	
Mg	1.752)	-2.031	1.673)	-2.015	1.605)	-2.008	1.623)	-2.014)	WXY
Ti	.008)		.008)		.008)		.006)	)	
Ni	.006)		.006)		.002)		.002)	)	
Cr	.021)		.021)		.012)		.012)	)	
Ca	.052)		.052)		.066)		.062)	)	
Na	.004)		.004)		.004)		.004)	)	

Table 17. Orthopyroxene Analysis Recalculated to 6 Oxygen Atoms.

	T208		T383		T42		T22		
Si	1.932)	1.981	1.873)	1.985	1.830)	1.989	1.820)	1.985	Z
Al	.049)		.112)		.159)		.165)		
Al	.005)		.071)		.131)		.138)		
Fe^{+3}	.012)		.008)		.004)		.008)		
Fe^{+2}	.170)		.181)		.185)		.170)		
Mn	.006)		.006)		.002)		.002)		
Mg	1.752)		1.673)		1.605)		1.623)		
Ti	.008)	-2.036	.008)	-2.030	.008)	-2.019	.006)	-2.027	W,X,Y.
Ni	.006)		.006)		.002)		.002)		
Cr	.021)		.021)		.012)		.012)		
Ca	.052)		.052)		.066)		.062)		
Na	.004)		.004)		.004)		.004)		
K	-)		-)		-)		-)		

in basalt and alpine-type peridotites quoted by Ross ,Foster and Myers (1954) and in those from the Lizard enstatites given by Green (1964). In some cases this may be due to olivine contamination for complete separation is difficult.

The recalculation procedure adopted by Deer, Howie and Zussman (1963 vol. 2) where deficiencies in the Z group are made up by adding the requisite amount of Al^{+3} to complete the ideal two tetrahedral ions per unit formula is widely used in the literature and the Mount Tawai analysis have also been recalculated in this way in order that comparisons may be made. The results are given in Table 16.

The recalculated analyses show a wide substitution of aluminium for X magnesium and Z silicon.

A brief summary of alumina in orthopyroxenes from different paragenesis is given below.

Paragenesis	Wt.% Al_2O_3	Source.
Metamorphic (mainly Charnockites granulites)	.5-9.5	Howie (1963)
Volcanics	.5-3.5	Deer, Howie, Zussman (1963 vol. 2)
Stratiform complexes	.5 -2.5	" " "
Alpine type peridotites	.7 -6.5	Ross, Foster, Myers (1954) & Green (1964)
Nodules in basalt	2.1 -5.5	Ross, Foster, Myers (1954).
Garnet peridotite	1 -2	O'Hara, Mercy (1963).

It is only recently that Green (1964) has shown that orthopyroxenes from certain Alpine type peridotites contain relatively large amounts of alumina; in the Lizard orthopyroxenes it varies from 1 to 6.5% while those in the Tinaquillo peridotite may contain up to 7%. The Mount Tawai enstatites closely resemble those from the Lizard both in En ratio and alumina content. Other Alpine type peridotites however in general show enstatites with low alumina contents.

The variation of total alumina with the En ratio for various parageneses is shown in Fig. 74.

In the Skaergaard sequence of calcium poor pyroxenes alumina is fairly constant but shows a tendency to decrease at the iron-rich end. An increase in total alumina with decreasing En ratio is shown by the orthopyroxenes from the lavas of the Hakone volcano and by those from the ultrabasic rocks at Dawros.

The aluminous orthopyroxenes from the nodules in basalt, Lizard, and Mount Tawai all have very similar En ratios, but show a wide range of alumina content. Total alumina in the orthopyroxenes varies widely and is largely independent of the En ratio, although the greatest amount is found between En_{80} and En_{40}, as can be seen from the analysis quoted by Howie (1963). The majority of these are from charnockites and granulites and it has been suggested by Boyd and England (1960) that crystallisation at high pressure is the cause of the high alumina orthopyroxenes. However not all of them are aluminous. O'Hara (1963) has shown that the alumina-rich orthopyroxenes co-exist with calcium-poor garnet in granulites free from clinopyroxene whilst the reverse is true of the majority of the alumina-poor orthopyroxenes. Ramberg and de Vore (1951) suggest that orthopyroxenes between En_{80} and En_{40} more

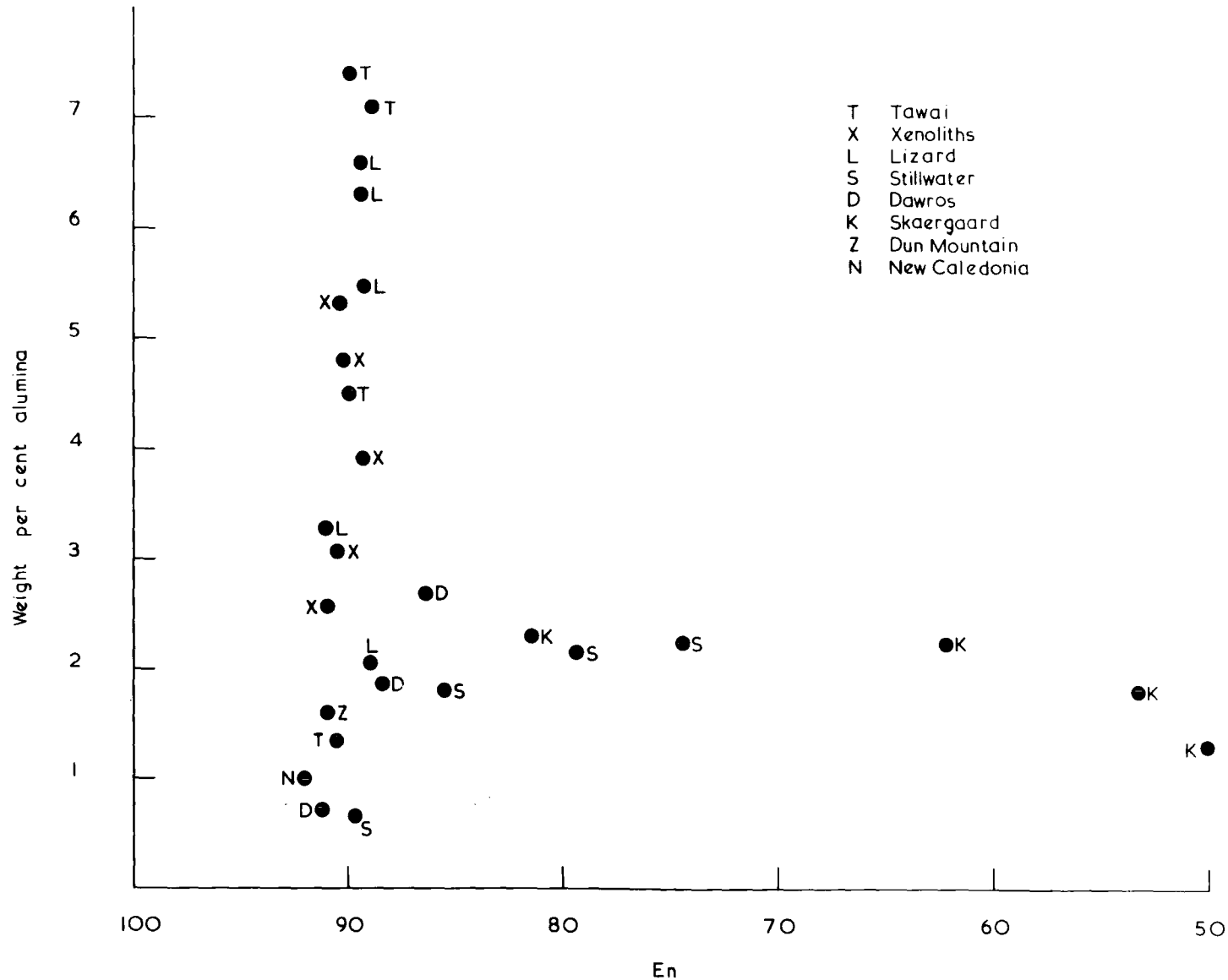

Fig.74. Relation between weight per cent alumina and molecular per cent En in calcium poor pyroxenes from plutonic igneous rocks. En $100Mg/Mg+Fe''+Fe'''+Mn$

readily accommodate alumina than either more magnesium or more iron rich types. Although this may be partially true of the metamorphic orthopyroxenes the same does not apply for other paragenesis.

Hess (1952) has suggested that pressure may favour the reaction $MgMgSiSiO_6 \rightleftharpoons MgAlAlSiO_6$ because of the resultant decrease in volume. The system $MgSiO_3 - Al_2O_3$ has been investigated by Segnit (1953) and Boyd and England (1960) who have shown that the maximum alumina substitution in enstatite at 1 bar is 5 weight per cent but at 18,000 bars and a temperature of 1400°C up to 14 weight per cent alumina, and possibly 19 weight per cent, can be accommodated in the enstatite structure. However, their experiments were made with synthetic enstatite free from Fe_2SiO_3. Howie (1963, Table 3, No. B20) has analysed a hypersthene from a hornfels containing 7.2 weight per cent alumina and it is doubtful whether this rock formed at high pressure. Hess (1952) suggested that enstatites from peridotite nodules in basalt may have been brought up from the mantle and their high alumina content is a result of pressure or high temperature of crystallisation at depth. On the other hand garnet peridotites contain low alumina orthopyroxenes and these are considered to have originated at high pressure.

Buerger (1948) from the thermodynamic considerations suggests that temperature of crystallisation controls the amount of alumina entering the pyroxene structure.

The lime content of the analysed Mount Tawai orthopyroxenes varies from 1.3 to 1.8 weight per cent and increases slightly with alumina. The orthopyroxenes contain fine exsolution lamellae of clinopyroxene which accounts for their rather high lime content. These lamellae are parallel to 100 and closely resemble orthopyroxenes

of the Bushveld type as defined by Hess (1960). Orthopyroxene of the Stillwater type have lamellae parallel to 001 and are inverted pigeonites.

The 100 lamellae are not always attributed to exsolution of clinopyroxene. Henry (1942) from single crystal photographs suggests the lamellae are due to translation on (100) accompanied by banding about (010). Brynzeel (1957) from optical studies of orthopyroxene from the Insizwa intrusion, East Griqualand, concluded that the lamellar structure is due to multiple twinning about the Z axis. However in the Mount Tawai orthopyroxenes the lamellae are frequently in optical continuity with enclosed blebs and stringers of exsolved clinopyroxene which together with their optical properties (e.g. greater birefringence than the host) leave no doubt as to their nature. Moreover in serpentinised enstatites the exsolution lamellae are frequently unaltered indicating they have a different composition to the host (Fig. 75). Hess (1960) has suggested that the orthopyroxene host and the clinopyroxene lamellae have the (100) plane in common. Buerger (1948) has shown that an interface in which the two planes have a common structure is one of minimal energy and a favourable site for unmixing to occur. Hess (1960) suggests that orthopyroxene of the Bushveld type crystallise below the inversion temperature of orthorhombic to monoclinic pyroxene (approximately 1140°C) and that the exsolution is due to slow cooling. In volcanic orthopyroxenes lamellae are poorly developed or absent probably as a result of fast cooling.

A comparison of the lime contents of calcium-poor pyroxenes from basaltic parent magmas and ultramafic 'magmas', is given by Hess (1960, p.32, Table 5). It is summarised below.

Fig. 75. Photomicrograph of serpentinised peridotite. Note the exsolution lamellae of clinopyroxene are largely unaltered whilst the host orthopyroxene is serpentinised. T24 (crossed nicols X20).

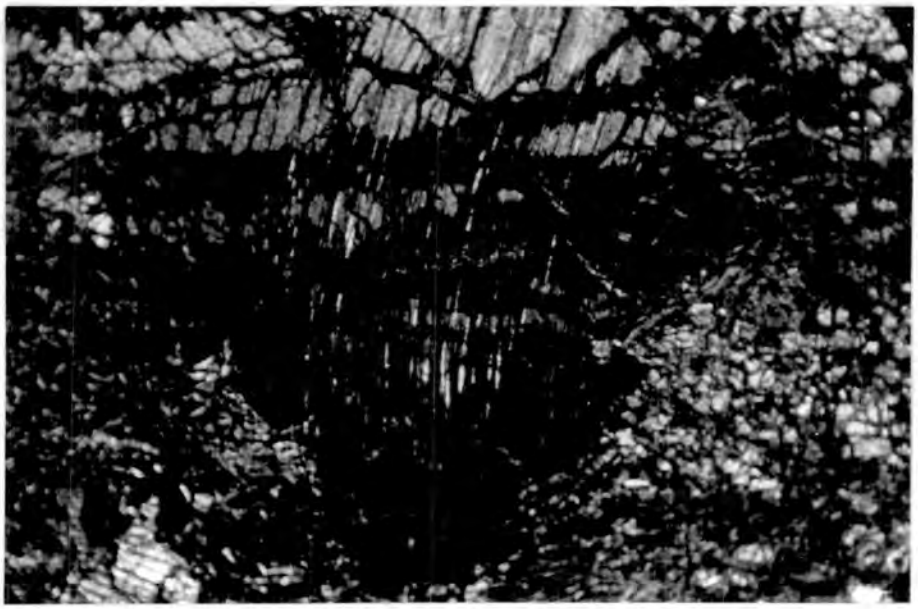

	Average Wt.% CaO	Range CaO
Orthopyroxene	- 1.6	1.3 - 1.9
Basaltic parent.		
Inverted pigeonite or pigeonite	- 4.31	3.8 - 5.1
Ultramafic parent.		
Orthopyroxene	- .9	.2 - 1.9

The Mount Tawai enstatites therefore have a slightly higher lime content than the average from an 'ultramafic parent magma', but are well below that of inverted pigeonite. There is no petrographic evidence to suggest the Mount Tawai enstatites are inverted pigeonites and it seems unlikely that two monoclinic pyroxenes could exist under the same conditions, for the Mount Tawai peridotite also contains small amounts of clinopyroxene. In the Lizard enstatites Green (1964) finds lime varying from 1.5 to 2.1 per cent. Hess (1963) points out that although, 'ultramafic', orthopyroxenes usually contain low lime contents, slightly higher values might be attained by fractional crystallisation and early separation of Ca-deficient olivine thus enriching the residual magma in lime. The orthopyroxenes from garnet peridotites, quoted by O'Hara and Mercy (1963) are noticeably lime deficient.

Atlas (1952) in a study of the synthetic system $MgSiO_3$-$CaMgSi_2O_6$ found that the amount of lime in enstatite varies with temperature as follows:-

T °C.	Number of Ca atoms per unit cell.
1100	.115
1000	.050
700	.030

In the Mount Tawai enstatites the number of Ca atoms per unit cell varies from .052 to .089 suggesting a temperature range from 1000°C to 1100°C. Both in the Lizard and the Tawai enstatites lime increases slightly with alumina and suggest that temperature may also partly control the entry of alumina into the orthopyroxene structure. The trace element content of the Mount Tawai orthopyroxenes is given in Table19 . Nickel, chromium, and manganese, are all significantly higher in the relatively low alumina orthopyroxenes than in the high alumina ones, whilst no significant variations may be seen in copper and zinc.

In Table 18 the range in weight per cent of the minor oxides of the Mount Tawai enstatites is compared with those from orthopyroxenes of approximately similar En ratios.

Table 18

	Cr_2O_3	TiO_2	MnO	NiO	
1. Tawai	0.4-0.8	0.2-0.3	0.1-0.2	0.1-0.2	
2. Lizard	0.4-0.7	0.2-0.4	0.1-0.2	n.d.	Green, 1963
3. Nodules	0.3-0.9	0.02-0.3	0.1-0.2	0.05-0.1	Ross, et al 1959
4. Alpine Type peridotites	0.6-0.8	0.02-0.2	0.1	0.1-0.2	Ross et al 1959
5. Garnet	0.02-0.2	0.05-0.1	0.1-0.2	0.003-0.005	O'Hara & Mercy 1963

2. (Green, 1963). 3. Ross et al. (1954). 4. Ross et al. (1954).
5. O'Hara and Mercy (1963).

The table shows there is a general similarity between the minor

Table 19. Pyroxene Trace Element Analysis.

No.	Mineral	Ni	Cr	Mn	Cu	Zn	
352	CPX	480	4260	1375	62	50	)
383	CPX	1200	5020	950	65	40	)
22	CPX	500	2670	930	110	50	)- Clinopyroxenes
168	CPX	300	1660	1340	175	65	)
384	CPX	290	1700	1150	215	98	)
208	OPX	1140	5180	1540	65	65	)
383	OPX	1290	5280	1610	85	65	)
42	OPX	450	2600	985	85	40	) - Orthopyroxenes
22	OPX	510	2580	990	80	50	)

Sought but not found Y, Pb, Ba, Sr, Pt.

All determinations in p.p.m.

Analyst W.G. Hancock.

oxides of the first four groups but the garnet peridotites are noticeably different in containing less Cr_2O_3 and NiO. The orthopyroxenes analysed by O'Hara and Mercy (1963) are from Norway and the kimberlite pipes of South Africa. The former contain even less Cr_2O_3 (.03- .1) than those from the latter area (.2). Other non-garnetiferous ultrabasic rocks occurring in the pipes contain slightly larger Cr_2O_3 (.2- .6).

X-ray diffraction studies.

The variation of the unit cell parameters with composition in the orthopyroxenes was first investigated by Ramberg and de Vore (1951). They plotted measurements of a_o and b_o of a series of orthopyroxenes against the molecular per cent En and from the curvature of their graphs concluded that the orthopyroxenes are not ideal mixed crystals and do not obey Vergard's law. (From now on in the text molecular per cent En will be referred to as En). Later Hess (1952) and Kuno (1954) showed that the unit cell parameters for igneous orthopyroxenes vary in a regular manner with En and conclude that the orthopyroxenes are ideal mixed crystals. Sahama and Torgeson (1949) reached similar conclusions from a study of orthopyroxene thermo-chemistry. The results of Hess and Kuno are summarised below.

(1) Substitution of Fe^{2+} for Mg results in a regular increase in a_o, b_o, c_o.

(2) Substitution of Ca increases a_o and c_o but did not affect b_o.

(3) Substitution of Al^{3+} decreased b_o, slightly increased c_o but did not affect a_o.

The determinative curves derived from these studies are given in Deer, Howie and Zussman (1963, vol. 2, p. 13). Recently Howie (1963) has investigated the cell parameters of orthopyroxenes from metamorphic rocks, which in general contain large amounts of alumina and found that the cell parameters a_o and b_o are smaller than those from igneous paragenesis. Both Hess (1952) and Howie (1963) conclude that the departure from linearity of the curves given by Ramberg and de Vore is due to their study being based on orthopyroxenes with variable amounts of alumina.

Howie presents a series of curves (Fig. 76) showing the variation of the cell parameters with En and the number of aluminium atoms in octahedral co-ordination in the unit formulae. (From now on in the text the number of aluminium atoms in octahedral co-ordination in the unit formula of orthopyroxenes will be referred to as $Al^{3+}O$). He points out that substitution of aluminium in the octahedral site giving an Al^{+3} ..... O^{2-} distance of 1.91Å compared with Mg^{2+} ..... O^{2+} of 2.06Å will lead to a decrease in the cell parameters. In enstatite the small aluminium ions would be expected to substitute for magnesium ions which are smaller than iron (Fe^{2+}) ions. Howie also shows that minor amounts of Fe^{3+}, Ti, Ca, and Mn affect the unit cell parameters. He suggests that c_o is relatively less affected by ionic substitutions involving these minor ions and $Al^{+3}O$ and may be used to obtain an approximate value of En.

The cell dimensions of the analysed orthopyroxenes from Mount Tawai together with a specimen from the Lizard were measured and the results are given in Table 20. The Lizard specimen was collected by the author on Goonhilly Downs seven hundred yards west of

Table 20. d spacings and Unit Cell dimensions of orthopyroxenes.

Specimen	En	Al^{+3}_0	Reflexion	dÅ	a_o	b_o	c_o	Average. a_o	Average. b_o	Average. c_o
			250	1.7351		8.835				
			12,0,0,	1.5215	18.258					
T 208	90.6	-	060	1.4730		8.838		18.255	8.836	5.179
			004	1.2947						
			14,5,0	1.0491	18.253		5.179			
			250	1.7290		8.805				
			1200	1.5205	18.246					
T 383	89.7	.056	060	1.4678		8.807		18.244	8.806	5.177
			004	1.2943						
			14,5,0	1.0475	18.242		5.177			
			250	1.7260		8.788				
			1200	1.5200	18.240					
T 42	89.5	.120	060	1.4648		8.789		18.243	8.788	5.174
			004	1.2934						
			1450	1.0468	18.246		5.174			
			250	1.7252		8.785				
			1200	1.5199	18.239					
T 22	90.1	.123	060	1.4644		8.786		18.239	8.785	5.178
			004	1.2946			5.178			
			14,5,0	-	-					
			250	1.7279		8.798				
			1200	1.5214	18.257			18.260	8.797	5.175
O_1 Lizard	89.5	.107	060	1.4658		8.795				
			004	1.2938						
			14.5.0	1.0477	18.264		5.175			

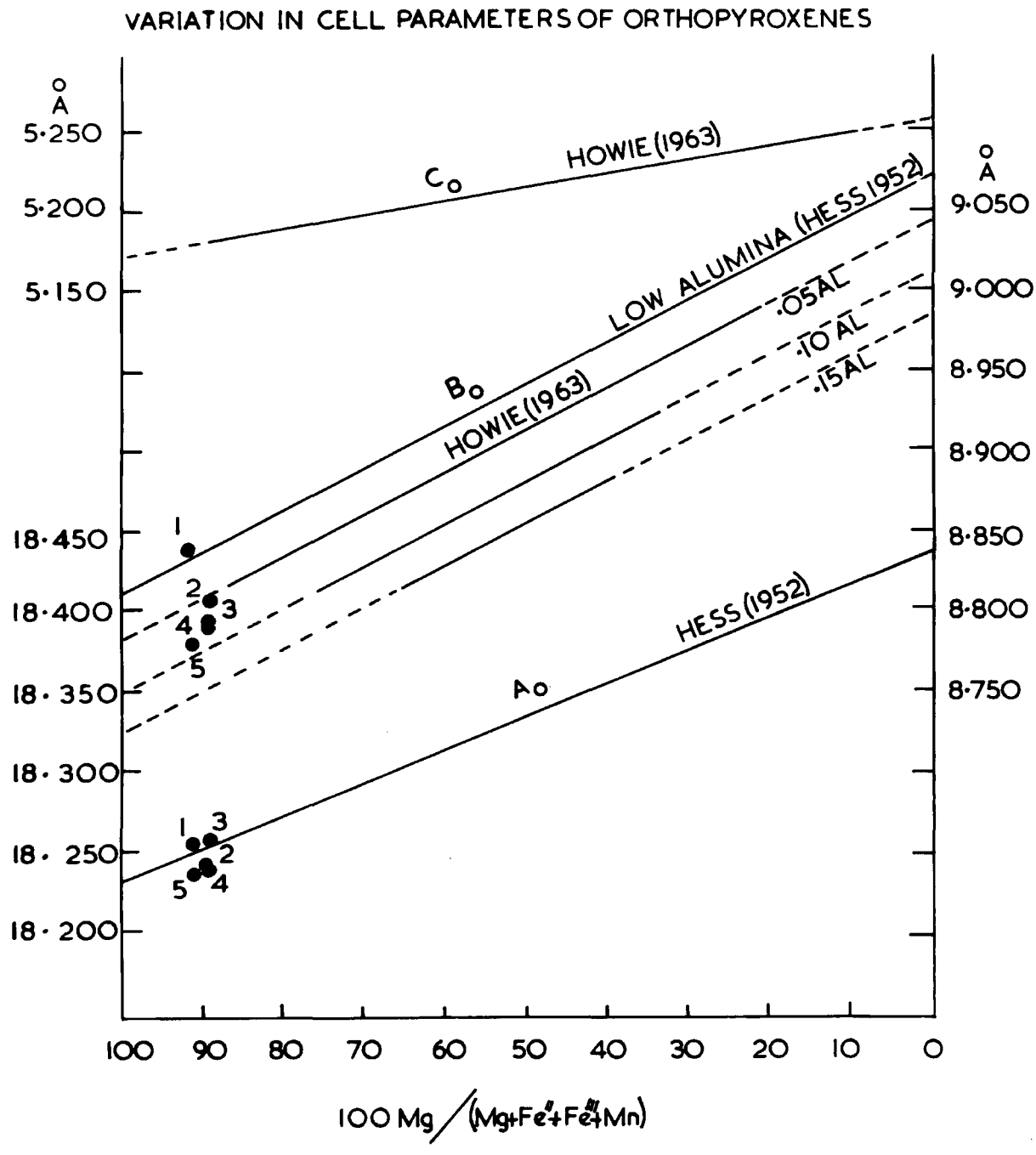

1=208, 2=383, 3=Lizard, 4=42, 5=22. Specimen numbers.

Fig.76.

Gwentor. Green has analysed an enstatite from this locality (Green 1964, No. 0,90683).

The specimens were finely ground and mixed with pure silicon powder and examined as smear mounts. Measurements were made on the Phillips High Angle X-ray diffractometer using filtered Copper radiation at 40kv and 20 ma.. Scans were made from $46^{\circ}2\theta$ to $65^{\circ}2\theta$, $72^{\circ}2\theta$ to $77^{\circ}2\theta$, and from $85^{\circ}2\theta$ to $96^{\circ}2\theta$ using a scan speed of $^{1}/_{8}$ per minute chart speed 200mm. per hour and rate meter X8. Pulse height discrimination was used to increase peak to background ratios. Following Ramberg and de Vore (1951) the a_o and b_o cell dimensions were measured initially on 12,0,0, and 0,6,0, and refined by reference to 14,5,0 and 250. The 2θ positions of these reflections is shown in Fig. 77. The c_o parameter was measured from the weak 004 reflection ($73^{\circ}2\theta$) after Howie (1963). The 2θ values were corrected by use of the silicon internal standard. The d $\mathring{A}$ spacings of the reflections are given in Table 20.

The general formula for calculating ths unit cell dimensions of orthorhombic crystals is as follows:-

$$\frac{1}{d}^2 = \frac{h}{a}^2 + \frac{k}{b}^2 + \frac{l}{c}^2$$

The calculations were made in the following manner:-

From the 12,0,0, reflections $a_o = d_{12,0,0,} \times 12.$

From the 0,6,0, reflections $b_o = d_{060} \times 6.$

Table 21. X-Ray diffraction data for Orthopyroxenes.

Source	Number	Calculated. dÅ 10,3,1,	dÅ 0,6,0,	Δ dÅ	En	Al^{+3}_{0}
	(Theoretical	1.4835	1.4677		100)	
	(2	1.4849	1.4704		94)	
	(5	1.4862	1.4724	.0138	88)	
	(8	1.4886	1.4760		79.6) Average	
Hess	(11	1.4900	1.4783		73) .010	
1952	(12	1.4913	1.4812		69)	
	(15	1.4976	1.4923		39)	
	(3a	1.4852	1.4687	.0165	89.5)	.050
El Hamad 1963	12	1.4859	1.4701	.0158	90.2	.033
		Observed.				
Green 1963	01	1.4845	1.4658	.0187	89.5	.107
	T208	1.4862	1.4730	.0132	90.6	-
	T383	1.4852	1.4678	.0174	89.7	.056
	T42	1.4842	1.4648	.0194	89.5	.120
	T22	1.4842	1.4644	.0198	90.1	.123
	T168	1.4881	1.4755	.0126	81 *	nd.
	T136	1.4893	1.4770	.0123	77 *	nd.

Al^{+3}_{0} - Number of aluminium atoms in octahedral co-ordination. * Optical determination. nd. not determined.

To check a_o on 14,5,0, using predetermined value of b_o

$$a_o = \frac{14}{\sqrt{\left(\frac{1}{d_{14,5,0}} + \frac{5}{b_0}\right)\left(\frac{1}{d_{14,5,0}} - \frac{5}{b_0}\right)}}$$

To check b_o on 250 using a predetermined value of a_o

$$b_o = \frac{5}{\sqrt{\left(\frac{1}{d_{250}} + \frac{2}{a_0}\right)\left(\frac{1}{d_{250}} - \frac{2}{a_o}\right)}}$$

From the 004 reflections $c_o = d_{004} \times 4$.

The specimens examined all have approximately the same En value (89.5 - 90.6) and all contain similar amounts of minor elements but alumina varies widely. The results show b_o decreases with increasing $Al^{+3}O$ and that a^o is also affected but to a lesser extent. The measurements of c_o show little variation.

The results for a_o and b_o are plotted in Fig. 76 on the curves of Hess (1952) and Howie (1963). Howie's determinative curves for b_o were derived from orthopyroxenes with En less than 88 and in Fig. 76 they have been projected into the field of enstatite. The calculated b_o values for the specimens examined are in general agreement with these curves.

Specimens T22, T42 and the Lizard specimens (all containing more than .100 $Al^{3+}O$) plot just above the appropriate line and Howie's graph may need slight revision in this region. Specimen T383 (.056 $Al^{3+}O$) shows close agreement with Howie's line for .050 $Al^{3+}O$ and T208 falls just above Hess's line for low alumina

orthopyroxenes.

The a_o measurements of the Mount Tawai aluminous enstatites plot slightly below the determinative line of Hess (.010 $Al^{+3}O$) indicating that aluminium substitution has a slight effect on a_o. The aluminous Lizard enstatite however plots just above this line which may be due to the slightly higher lime content of the mineral.

The c_o determinations confirm Howie's opinion that this parameter is relatively unaffected by aluminium substitutions. The measurements plot close to En 90 on Howie's determinative curve. Howie (1963) slightly modified the c_o determinative line given by Hess (1952) and the present study confirms this alteration.

The results obtained from this study are in general agreement with the determinative graphs of Hess and Howie and confirm the analysis of the orthopyroxenes.

However it is clearly necessary to find an optical or X-ray method by which the En value and $Al^{+3}O$ content of orthopyroxenes may be determined relatively quickly so that it may be applied on a regional scale. Measurement of the cell parameters followed by reference to the determinative curves of Hess and Howie is not applicable for if En is not known then it is uncertain which line to plot on. Deer, Howie and Zussman (1963, vol. 2) suggest that an estimate of En from the refractive index Nz followed by reference to the above mentioned determinative graphs is the most reliable method of obtaining $Al^{+3}O$. However this method is ambiguous for Hori (1956) has shown that $Al^{+3}O$ causes an increase in N_Z and decreases in N_x and N_y. Howie (1963) suggests that by measurement of c_o En may be determined directly. The determinative curve for c_o is extremely shallow and an accuracy of $\pm$ 7 molecular per cent

is indicated. Moreover c_o is difficult to establish accurately as suitable reflections on which to refine the determination made on 004 are not available. Single crystal photographs are the most accurate method of obtaining c_o but this method is extremely time consuming. Zwaan (1954) in an X-ray diffraction study of orthopyroxenes noticed that the reflection 10,3,1, ($62.50^{\circ}2\theta$) moved only slightly in comparison with 060 ($63.2^{\circ}2\theta$) which moved markedly with variation in alumina. Both peaks move systemmatically with variation in En but by measuring the difference between the dÅ spacings of the two peaks he was able to establish determinative curves for low aluminous (.010 $Al^{+3}O$) and aluminous (.050 $Al^{+3}O$) orthopyroxenes. However the determinative graph (Deer, Howie, Zussman 1963 vol. 2, p. 14) is again ambiguous if the En value is not known beforehand.

However it is known from Zwaan's studies, and from theoretical considerations, that the peaks 10,3,1, and 060 move systemmatically with En variation and for a series of low alumina orthopyroxene a straight line relationship should be obtained if the dÅ spacings of the two peaks are plotted against one another. The dÅ spacings have been calculated for the low alumina series (.010 $Al^{+3}O$) of orthopyroxenes given by Hess (1952) and are plotted against each other in Fig. 78. The results of the calculations are given in Table 21. A straight line relationship has been established and calibrated in molecular per cent En, and to obtain this ratio for any low alumina orthopyroxene (in range En_{100} En_{40}) it should only be necessary to measure the dÅ spacings of 10,3,1, and 060 and refer to the chart. Data for En values less than 40 are scant but when it becomes available the graph may be extended.

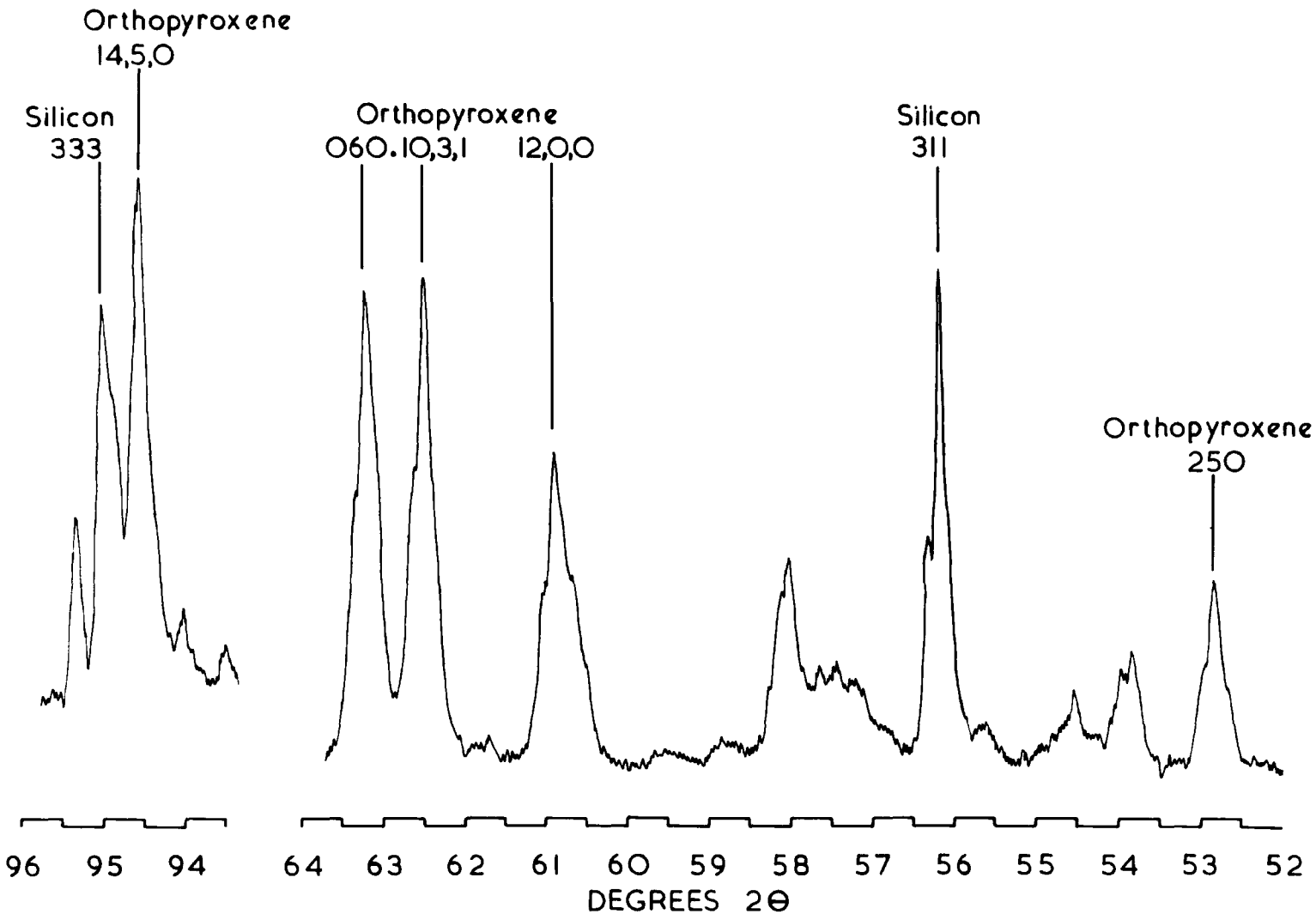

DIFFRACTOMETER RECORD OF ORTHOPYROXENE NO. T.208.

Fig.77.

The d spacings of the 10,3,1, and 060 reflections of the analysed Mount Tawai and Lizard specimens were measured together with a large number of orthopyroxenes from the Mount Tawai complex. The latter were separated by hand-picking a few large enstatitic laths from a loose crush of rock specimen. The specimens were finely ground and mixed with a silicon internal standard and examined as smear mounts of the diffractometer. Scans were made from $56^{\circ}2\theta$ to $64^{\circ}2\theta$ using a scan speed of $\frac{1}{4}^{\circ}$ per minute and chart speed 200 mm. per hour and rate meter X 8. The positions of the 10,3,1 and 060 reflections are shown in Fig. 77. The 2θ values were corrected by means of the silicon internal standard. The results for the analysed orthopyroxenes are given in Table 21, and those for Mount Tawai specimens in Table 22.

Specimens T208 plots just above the determinative line (Fig. 79) at the point indicating En 90 and two orthopyroxenes from the Mount Tawai gabbros (Table 22 Nos. T168, T136) plot almost on the line at En 81 and En 77 respectively. Determinations of the latter are in substantial agreement with those made from N_z measurements. The fact that T208 plots slightly above the line indicates the very low $Al^{+3}O$ content. The specimens of Hess on which the line was determined contain an average of .010 $Al^{+3}O$. However if the specimens are more aluminous, or contain substantial amounts of orther ions such as Ti^{+4}, Fe^{+3}, Mn^{+2}, or Ca^{+2}, then they will plot below the determinative line. The d Å spacings of 10,3,1, and 060 reflections for aluminous enstatites from other areas have been calculated and are shown in Table 21. These together with the Mount Tawai and Lizard enstatites form an aluminous series and when plotted (Figs. 78, 79) it is seen they are depressed in a line

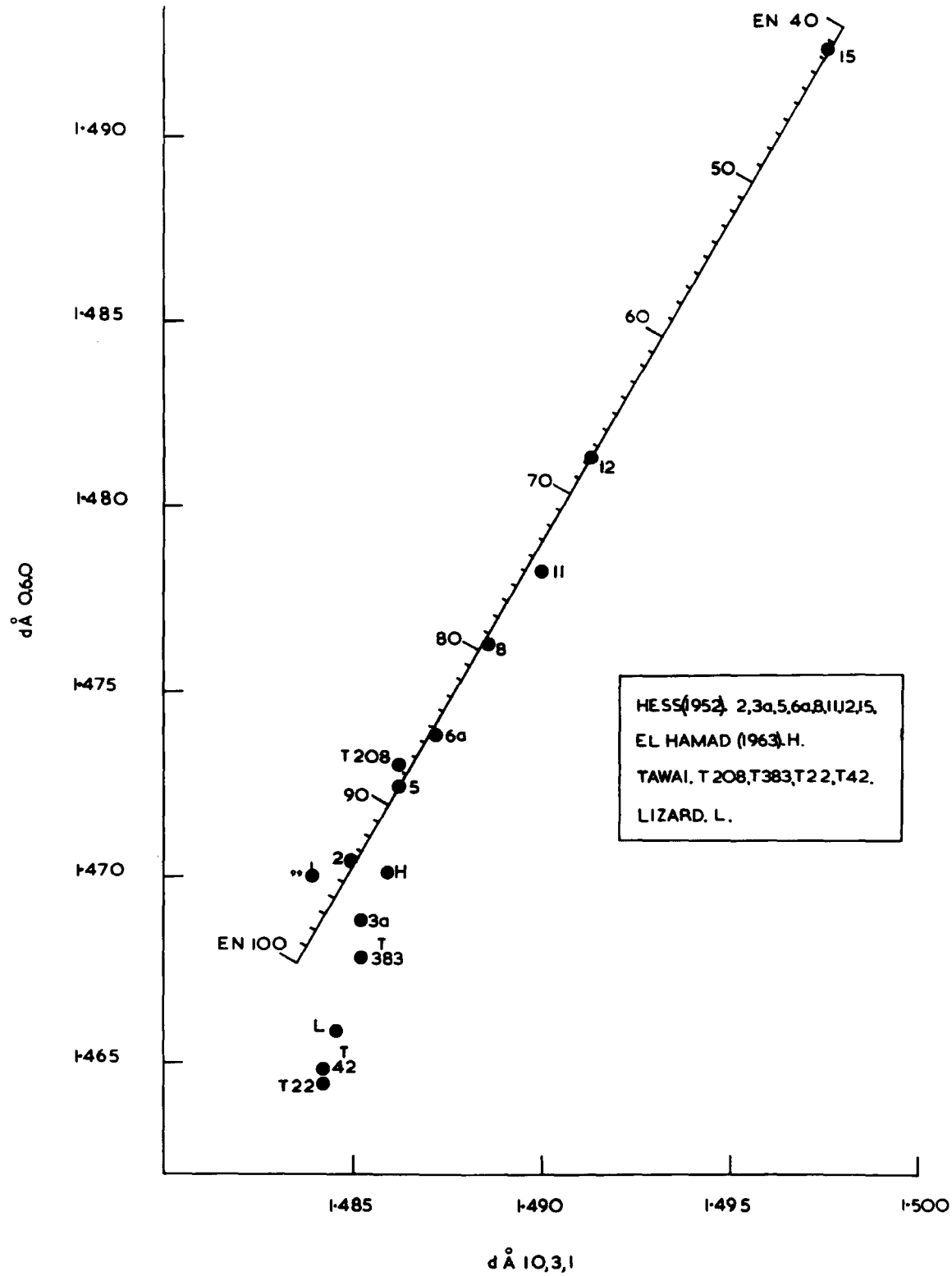

Fig.78. PLOT OF d 0,6,0 VERSUS d 10,3,1 FOR PLUTONIC IGNEOUS ORTHOPYROXENES IN THE RANGE EN 100 TO EN 40

Orthopyroxene determinative curve.

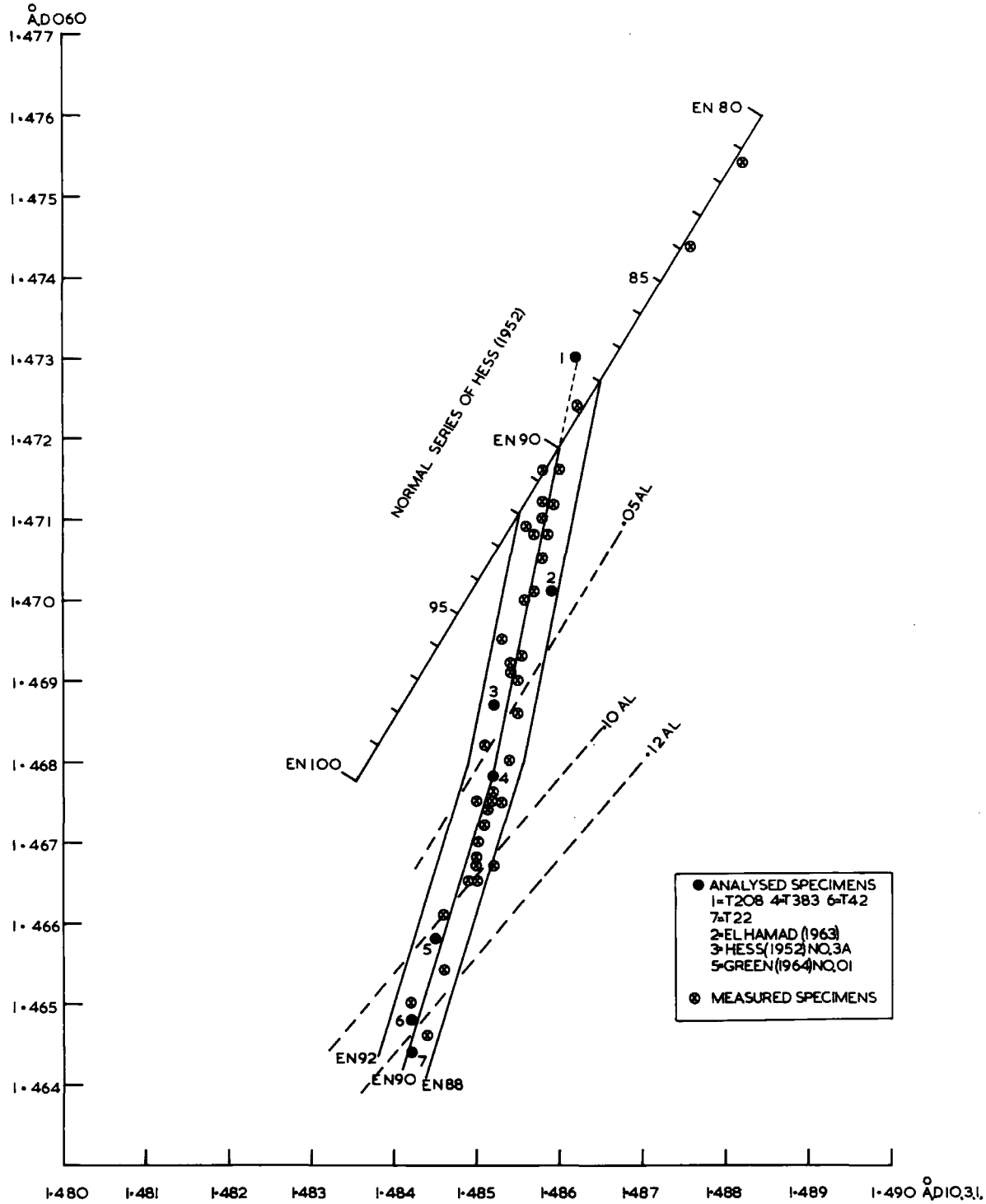

DETERMINATIVE DIAGRAM FOR ESTIMATING MOL PER CENT EN AND NUMBER OF ALUMIUMIUM ATOMS IN SIX FOLD COORDINATION OF MOUNT TAWAI ORTHOPYROXENES.

Fig.79.

from the point indicating En 90 on the low alumina curve. This line may then be calibrated in terms of known $Al^{+3}O$. By projecting lines from En 92 and En 88 parallel to the aluminous series (average En 90) it is possible to calibrate within this region for En and $Al^{+3}O$ as in Fig. 79. Further extension on either side is not advisable owing to lack of data of orthopyroxenes from igneous paragenesis.

The dÅ spacings of 10,3,1, and 060 of the non-analysed Mount Tawai specimens have been plotted on the determinative chart in Fig. 79. The results show that the majority of these from the ultrabasic rocks fall between En 91 and En 89 but there is a wide scatter along the line of the aluminous series. Estimates of En have been made using the graph but the variations are so small that they are probably within experimental error. Numerous measurements of the N_z refractive index were made but only slight variations could be detected again indicative of an almost constant En value. Estimates of $Al^{+3}O$ may be made directly from the graph.

Boyd and England (1960) also noticed the relationship between the 10,3,1, and 060 reflections and calibrated a determinative curve for synthetic aluminous enstatites by plotting the difference between the two peaks against known alumina content. Since the En ratio in the Mount Tawai enstatites appears approximately constant it is therefore possible to plot a graph of dÅ 10,3,1, 060 against known $Al^{+3}O$ and produce a working curve. This has been done in Fig. 80 using the analysed specimens. In this way a more accurate result is obtained than direct reading from the plot of 10,3,1, against 060. There is a kink in the determinative curve at .056 $Al^{+3}O$ and it is noticeable that a kink also occurs in the curve of

Determinative curve for number of aluminium atoms in six-fold coordination.

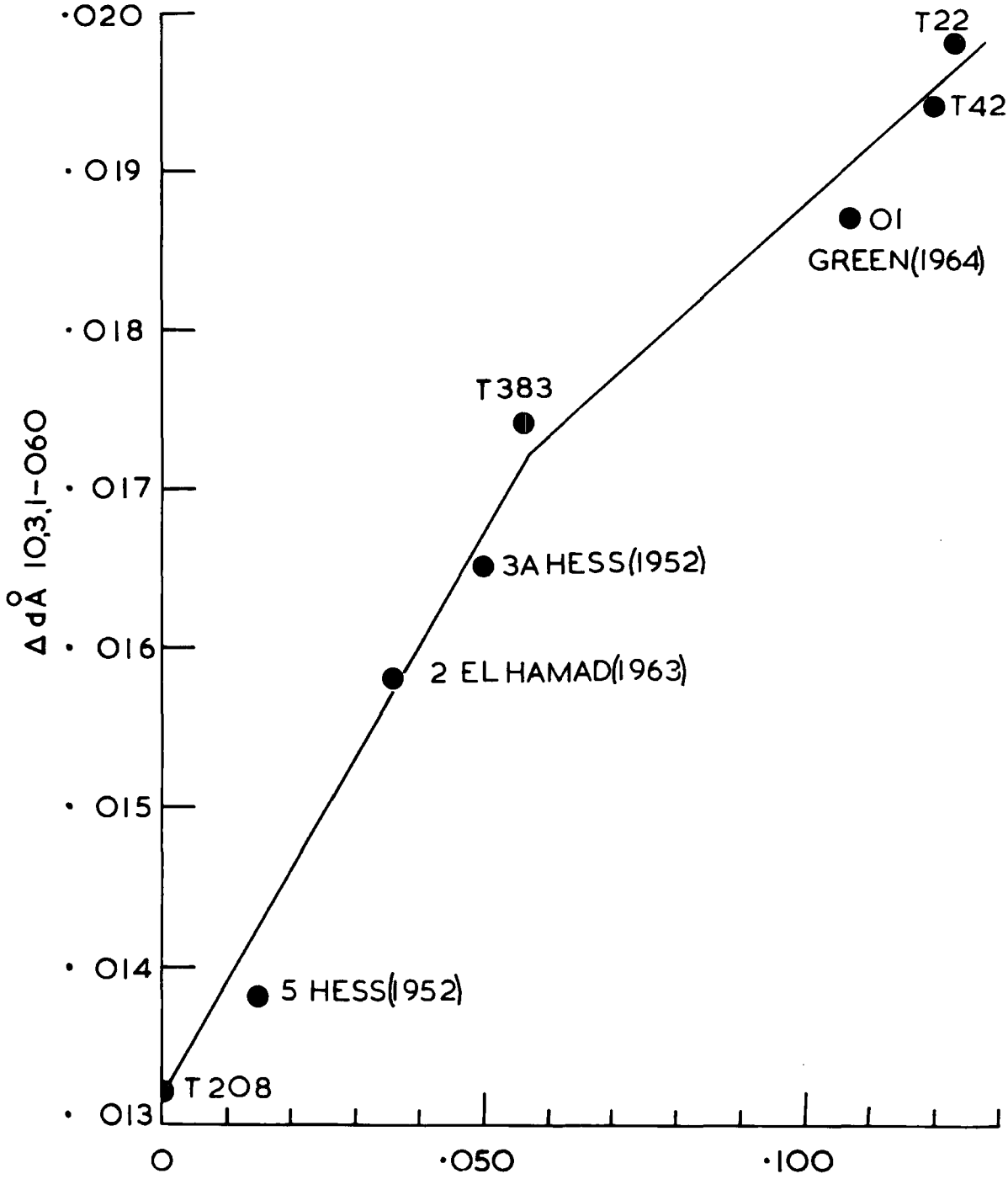

Fig.80.

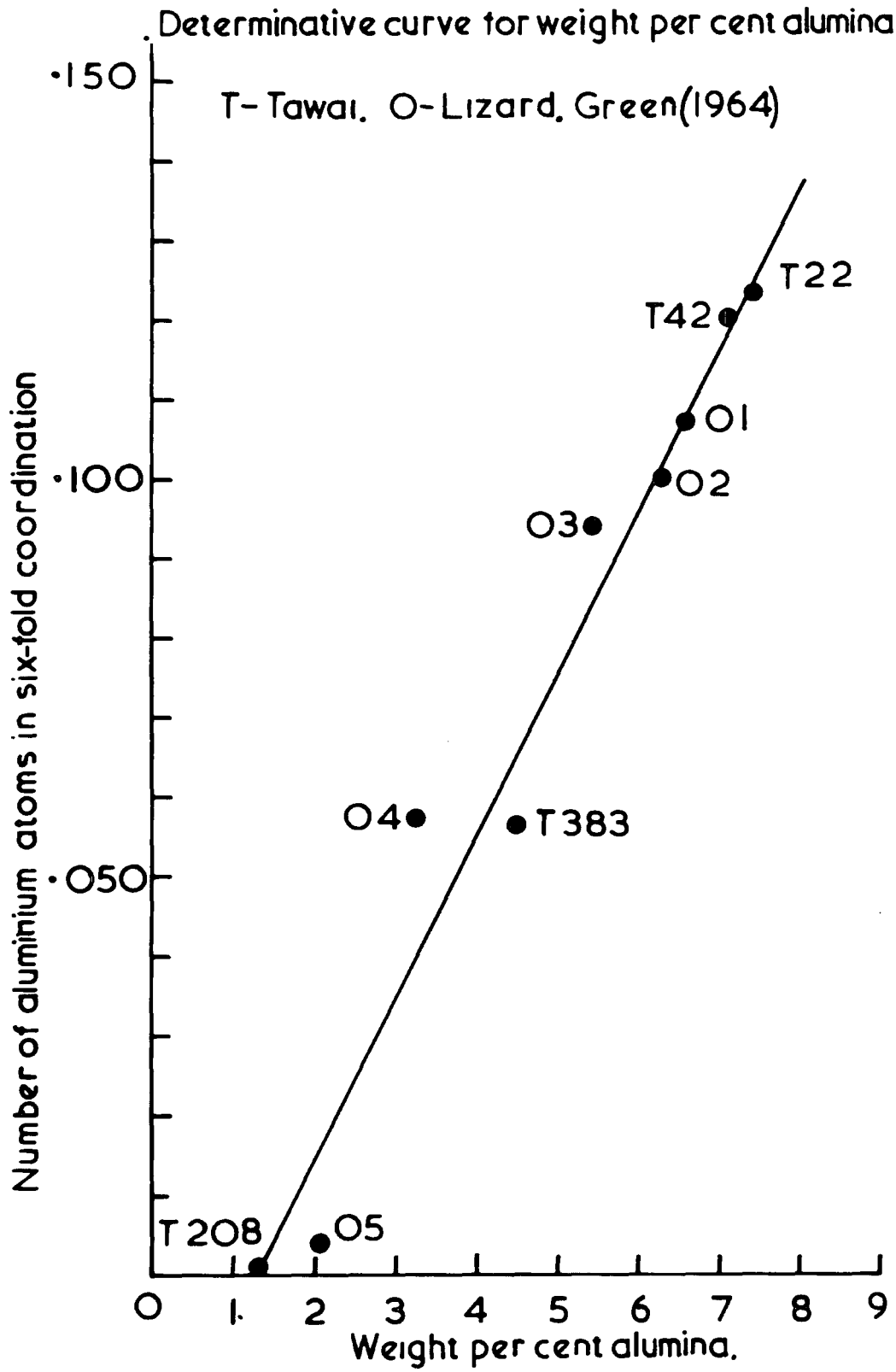
Determinative curve for weight per cent alumina.
T- Tawai. O- Lizard. Green(1964)
·150
·100
·050
Number of aluminium atoms in six-fold coordination
T22
T42
O1
O2
O3
O4
T383
T208
O5
0
1
2
3
4
5
6
7
8
9
Weight per cent alumina.

Fig.81.

Boyd and England (1960). However, the latter curve could not be used in the present study as it is based on synthetic enstatites containing no $FeSiO_3$. The working curve produced in the present study was used to interpret the non-analysed specimens and the results are given in Table 22. An estimate of total alumina has been made by reference to a graph, shown in Fig. 81, in which total alumina is plotted against $Al^{+3}O$ of analysed specimens. The graph indicates that the accuracy of the estimations is within 1% Al_2O_3. However all the results are of a comparative nature and serve to illustrate the trend of alumina variation.

Distribution of iron between co-existing olivines and orthopyroxenes.

In the ultrabasic rocks studied molecular per cent En in the orthopyroxenes is slightly less than or equal to, the molecular per cent Fo in the olivines. Bowen and Schairer (1935) in an experimental study of the system $MgO-FeO-SiO_2$ showed that at equilibrium olivine was more iron-rich than the co-existing orthopyroxene. Ramberg and de Vore (1951) have shown that in natural assemblages of these minerals olivine contains less Mg than the co-existing orthopyroxene when the average molecular fraction $X_o \pm \frac{X_p}{2}$ (X_o - molecular fraction of Mg silicate in olivine, X_p - molecular fraction of Mg silicate in orthopyroxene) is less than .65. From their diagram (1951 Fig. 1) it is seen that for co-existing orthopyroxenes and olivines with an average molecular fraction greater than .65 the reverse relationship is true.

O'Hara (1963) has recently reviewed the more magnesian assemblages and indicates in most layered intrusions, orogenic peridotites and nodules in basalt the distribution of the iron molecule

Table 22. Mineral Determinations (1) Main Tawai Block.

No.	Rock Type	Olivine		Orthopyroxene						Chrome Spinel		
		d 130 Å	Mol%Fo	d 10,3,1. Å	d 060 Å	Δ 10,3,1; 0,6,0; Å	Mol%En	Al^{+3} O	Wt.%Al_2O_3	a_o	Wt.%Cr_2O_3	Wt.%Al_2O_3
T22	P	2.7720	91.0	1.4842	1.4644	.0198	90.1 A	.123 A	7.4 A	8.184	25	44
T41	D II	2.7719	91.0							8.204	30	39
"	H	2.7724	90.2	1.4846	1.4656	.0190	89	.104	6.6			
T42	P	2.7712	92.0	1.4842	1.4648	.0194	89.5 A	.120 A	7.1 A	8.199	29	42
T48	D II	2.7714	91.8							8.217	33	36
"	H	2.7721	90.8	1.4850	1.4675	.0175	90.5	.066	4.5			
T49	D II	2.7712	92.0							8.216	31	36
"	H	2.7717	91.4	1.4853	1.4675	.0178	89.5	.074	4.9			
T55	D II	2.7715	91.6							8.217	35	36
"	H	2.7718	91.2	1.4852	1.4675	.0177	90.0	.073	4.9			
T84	H	2.7714	91.8	1.4851	1.4672	.0179	89.5	.076	5.0			
T85	D II											
"	H	2.7710	92.4	1.4849	1.4665	.0189	89.5	.089	5.6	8.201	29	39
T88	D II	2.7712	92.0							8.241	40	30
"	H	2.7712	92.0	1.4855	1.4686	.0169	89.0	.054	3.9			
T89	D II	2.7718	91.2	1.4854	1.4692	.0162	90.0	.044	3.5	8.250	42	28
T100	D II	2.7714	91.8							8.205	30	39
"	H			1.4850	1.4667	.0183	90.0	.077	5.1			
T103	D II	2.7725	90.2							8.223	35	34
"	H			1.4852	1.4676	.0176	90.0	.068	4.6			
T105	D II	2.7719	91.0							8.227	36	33
"	H			1.4854	1.4680	.0174	90.0	.062	4.4			
T109	D I	2.7716	91.6							8.279	50	22
"	H			1.4858	1.4712	.0146	89.0	.021	2.3			
T134	D II	2.7710	92.4							8.240	42 A	29 A
"	H			1.4855	1.4690	.0165	89.5	.049	3.7			
T137	D I	2.7717	91.4							8.282	51	21
"	H			1.4857	1.4710	.0147	91.0	.022	2.4			
T142	D I	2.7720	91.0							8.294	55	17
"	H			1.4858	1.4714	.0144	90.0	.018	2.2			
T194	D I	2.7713	92.0							8.282	51 F	19 F
"	H	2.7709	92.4	1.4858	1.4708	.0150	90.0	.026	2.6			
T198	D I	2.7704	93.2							8.292	54	18
"	H	2.7715	91.6	1.4857	1.4704	.0153	90.0	.031	2.8			
T207	D I	2.7705	93.0							8.288	53	19
"	H	2.7712	92.0	1.4856	1.4704	.0152	90.0	.030	2.8			
T208	P	2.7714	91.8	1.4862	1.4730	.0132	90.6 A	- A	1.3 A			
T214	D I	2.7718	91.2							8.297	56	17
T216	D I	2.7708	92.3							8.277	49 F	22 F
"	H	2.7721	91.0					.033	2.9			
T217	D I	2.7720	91.0							8.293	54	20
"	H	2.7722	92.0	1.4856	1.4700	.0156	90.0	.035	3.0			
T248	H	2.7710	92.4	1.4855	1.4693	.0162	90.0	.044	3.8			
T280	D I	2.7715	91.6							8.287	53 F	18 F
"	H			1.4860	1.4717	.0143	89.5	.016	2.1			
T294	D I									8.283	53	18
T316	D II	2.7720	90.2							8.251	43	28
"	H	2.7714	91.8	1.4852	1.4678	.0174	90.0	.063	4.6			
T346	D II	2.7712	92.0							8.216	33	36
T349	D II	2.7718	91.2							8.221	34	35
"	H			1.4850	1.4667	.0183	90.0	.077	5.1			
T355	D II	2.7712	92.0							8.240	42	29
"	H			1.4854	1.4691	.0163	90.0	.045	3.5			
T370	D II	2.7718	91.2							8.261	46	25
"	H	2.7714	91.8	1.4853	1.4695	.0158	91.0	.038	3.2			
T373	H	2.7724	90.2	1.4850	1.4668	.0182	89.5	.084	5.4			
T383	H	2.7715	91.7	1.4852	1.4678	.0174	90.1 A	.056 A	4.5 A			
T367	D II									8.261	43 F	27 F
T416	D II									8.226	36	34
"	H			1.4851	1.4674	.0177	90.0	.071	4.8			
T422	D II									8.255	41	27
T445	D II									8.274	44	22
"	H			1.4860	1.4701	.0159	88.0	.040	3.3			
T136	P.G.			1.4892	1.4770		77.0	-				
T143	P.G.			1.4896	1.4782		75.0	-				
					(2) Pantagaluang Block.							
T270	F.P.	2.7712	92.0	1.4860	1.4701	.0159	88	.040	3.3			
T271	F.P.	2.7721	91.0	1.4857	1.4701	.0156	89.5	.035	3.0	8.164	20	
					(3) Patud-Gombaran Intrusion.							
T58	H	2.7718	91.2	1.4850	1.4675	.0175	90.5	.066	4.5			
T168	O.G.	2.7765	84.0	1.4882	1.4755	.0127	81.0					
T384	O.G.	2.7750	86.1	1.4875	1.4744	.0131	84.0					
					(4) Binalik Block.							
T176	H	2.7718	91.4	1.4853	1.4675	.0178	89.0	.075	5.0			
T230	D II	2.7716	91.6							8.194	29 F	40 F
"	H	2.7712	92.0	1.4848	1.4664	.0183	90.0	.087	5.6			

P = Pyroxenite
H = Harzburgite
D1 = Type 1 Dunite
D2 = Type 2 Dunite
PG = Pyroxene Gabbro
OG = Olivine Gabbro
F.P. = Feldspathic peridotite.

A - Analytical result.
F - X-ray fluorescence result.
Specimen locations shown in Fig. 96.

between the two silicates is approximately 1:1, whereas in peridotite nodules in kimberlite, garnet peridotite slices in gneiss, and Lherzolite from the Pyrenees olivine is more iron-rich than the co-existing orthopyroxene and more closely approximates the experimental data of Bowen and Schairer (1935). O'Hara also points out that in some plutonic complexes containing zoned olivines the latter is poorer in iron than the orthopyroxene. The same is also true for assemblages from basalts.

There is therefore a considerable discrepancy between the experimental data and the relations found in the majority of the more magnesian igneous assemblages. This may be partly explained in that the experimental work involved clinohypersthenes and olivines although Schairer (1935) and Ramberg and de Vore (1951) suggest that the clino-ortho inversion does not greatly affect the Fe^{++} and Mg^{++} distribution.

The effect of temperature and pressure on the equilibrium distribution of iron between the two silicates may also be responsible for the discrepancy. Ramberg and de Vore (1951) from thermodynamic considerations indicate that with falling temperature concentration of iron in olivine increases relative to that in orthopyroxene.

O'Hara (1963) points out that the pressure and temperature of crystallisation of the layered igneous intrusions ($T = 1050^{\circ}C$, $P = 3000$ bars) is respectively higher and lower than that used in the experimental system. If the assemblages from these intrusions are considered to be in equilibrium then he argues the effect of lower temperature and higher pressure is to lower the $\frac{Fe/Mg \text{ in olivine}}{Fe/Mg \text{ in orthopyroxene}}$ ratio. He further argues that if this is the case

then in the basalt lower temperatures of crystallisation can only explain the relative iron environment of the orthopyroxene with regard to olivine.

Bowen and Schairer (1935) noted that the relations between orthopyroxenes and olivines from magnesium-rich assemblages were different from those deduced in the experimental system and suggested that this was due to the sequence of crystallisation in igneous rocks which may result in dis-equilibrium mixtures. Muir and Tilley (1957) noted that the olivine of the picrite basalts of Kilauea was more magnesium-rich than the co-existing orthopyroxene and attributed this to dis-equilibrium caused by early separation of the olivine. O'Hara (1963) suggests three ways in which dis-equilibrium mixtures may be produced.

a. Rapid crystallisation of the remaining liquid after formation of olivine phenocrysts.

b. Zoning of olivine by reaction of this mineral with the melt.

c. Sinking of crystals to form accumulates during slow cooling.

In (c) if most of the magnesian olivine is removed from the system an increase in Fe:Mg ratio of the liquid results. O'Hara argues that if now olivine crystals remaining in the liquid react with it to form orthopyroxene then this mineral will be in dis-equilibrium with the early formed olivine. If at a later date the action of convection currents or slumping brings together the olivine and the orthopyroxene, a dis-equilibrium assemblage will be produced.

O'Hara suggests that if the experimental work of Bowen and Schairer is acceptable then the mineral assemblages of the peridotite nodules in kimberlite, the garnetiferous lenses in gneisses, and the type Lherzolite of the Pyrenees, approach true equilibrium whereas those of the orogenic peridotites, the olivine nodules in basalt, and the layered igneous intrusions represent dis-equilibrium mixtures achieved by irregularities of igneous crystallisation.

The Mount Tawai assemblages fit into the dis-equilibrium category on this basis and are therefore similar to those from Mount Dun, New Caledonia and Saint Pauls' Rock. The olivines of the Mount Tawai ultrabasic rocks show no definite evidence of zoning or resorbtion and the orthopyroxene laths appear to be a primary crystallisation product. If O'Hara's evidence is valid then these dis-equilibrium mixtures could best be produced by method (c) as evidence for (b) is lacking and (a) is extremely unlikely. The evidence from the relations between the olivine and orthopyroxenes suggest the ultrabasic rock of Mount Tawai are products of igneous crystallisation.

Clinopyroxenes.

Chemistry.

Five clinopyroxene analyses areegiven in Table 23. Three are from ultrabasic rocks and two from the Telupid gabbro. T383 and T22 are clinopyroxenes co-existing with the analysed orthopyroxenes of similar number (Table 15). T352 is from a clinopyroxenite pegmatite.

Table 23. Clinopyroxene analyses.

	T352	T383	T22	T168	T384
SiO_2	52.8	51.3	51.1	52.7	53.1
Al_2O_3	2.9	5.6	7.2	3.2	2.9
Fe_2O_3	.2	.1	.5	.3	.5
FeO	4.5	3.1	3.3	6.4	4.8
MnO	.2	.1	.1	.2	.2
MgO	16.9	19.2	18.7	16.2	15.8
TiO_2	.1	.2	.4	.4	.4
NiO	.1	.1	.1	tr	tr
Cr_2O_3	.6	.7	.4	.2	.3
CaO	21.8	20.4	17.8	20.7	21.4
Na_2O	.1	.1	.1	.2	.2
K_2O	-	tr	-	tr	tr
Total	100.2	100.9	99.7	100.5	99.6
Ca	44.7	41.2	38.4	43.0	45.4
Mg	48.2	54.0	56.0	46.7	46.6
Fe	7.1	4.8	5.6	10.3	8.0
$\frac{Mg}{Mg+Fe}$	87.1	91.7	91.0	85.5	81.9

T352 - 5° 30' 41" N 117° 05' 01" E. Melio river. Pyroxenite Pegmatite.
T383 - 5° 29' 45" N 117° 05' 26" E. Melio river. Harzburgite.
T22 - 5° 34' 59" N 117° 07' 55" E. Meliau river. Pyroxenite.
T168 - 5° 35' 45" N 117° 04' 33" E. Telupid river. Olivine gabbro.
T384 - 5° 35' 32" N 117° 04' 33" E. Telupid river. Olivine gabbro.

Analyst W.G. Hancock.

Table 24. Clinopyroxene Analyses recalculated after Deer, Howie, Zussmann.

	T352		T383		T22		T168		T384	
Si	1.930)	2.000	1.843)	2.000	1.841)	2.000	1.931)	2.000	1.968)	2.000
Al	.070)		.157)		.159)		.069)		.032)	
Al	.053)		.080)		.148)		.067)		.092)	
Fe‴	.004)		.004)		.013)		.009)		.013)	
Fe	.136)		.093)		.099)		.196)		.149)	
Mn	.007)		.002)		.002)		.007)		.007)	
Mg	.919)	1.998	1.026)	2.021	1.003)	1.982	.884)	2.005	.872)	2.016
Ti	.002)		.004)		.011)		.011)		.011)	
Ni	.002)		.002)		.002)		-)		-)	
Cr	.018)		.022)		.013)		.004)		.009)	
Ca	.853)		.784)		.687)		.814)		.850)	
Na	.004)		.004)		.004)		.013)		.013)	

Table 25. Recalculated clinopyroxene analyses.

	T352		T383		T22		T168		T384	
Si	1.930)	2.003	1.843)	1.977	1.841)	2.017	1.931)	2.017	1.968)	2.046
Al	.073)		.134)		.176)		.086)		.078)	
Al	.050)		.103)		.131)		.050)		.046)	
Fe^{III}	.004)		.004)		.013)		.009)		.013)	
Fe	.136)		.093)		.099)		.196)		.149)	
Mn	.007)		.002)		.002)		.007)		.007)	
Mg	.919)	1.995	1.026)	2.044	1.003)	1.965	.884)	1.988	.872)	1.970
Ti	.002)		.004)		.011)		.011)		.011)	
Ni	.002)		.002)		.002)		-)		-)	
Cr	.018)		.022)		.013)		.004)		.009)	
Ca	.853)		.784)		.687)		.814)		.850)	
Na	.004)		.004)		.004)		.013)		.013)	

In Fig. 82 they are plotted together with the co-existing orthopyroxenes. Calculation of the Ca:Mg:Fe ratio indicates that the three clinopyroxenes from the ultrabasic rocks are endiopsides following the nomenclature of Hess (1949). In this respect they are similar to clinopyroxenes found in the earliest accumulates of layered igneous intrusions formed by differentiation of basaltic magma. The gabbro picrite of Skaergaard contains endiopside of composition $Ca_{42.4}\ Mg_{47.9}\ Fe_{9.7}$ (Brown 1957) and the average composition of that from the basal zone of the Stillwater complex is $Ca_{41}\ Mg_{52}\ Fe_{7}$ (Hess, 1960). These endiopsides are in general less magnesian-rich than those from Mount Tawai. The earliest formed clinopyroxenes from alkali basalt magmas are however more calcium-rich and are either diopside or salite as is shown by the Garbh Eilean sill described by Murray (1954). The peridotite nodules in basalt also frequently contain endiopside and the average composition of those listed by Ross et al (1954) is $Ca_{43}\ Mg_{50}\ Fe_{7}$. Alpine type peridotites in general contain endiopside, that from the Twin Sisters dunite having a composition of $Ca_{44.4}\ Mg_{52}\ Fe_{3.6}$ (Ross et al 1954). The clinopyroxenes from garnet peridotites recently analysed by O'Hara and Mercy (1963) range from $Ca_{49.7}\ Mg_{47.7}\ Fe_{2.6}$ to $Ca_{43.2}\ Mg_{53.3}\ Fe_{3.4}$.

The most striking feature of the clinopyroxene analysis is the wide variation in weight per cent alumina. The analyses have been recalculated in the same way as the orthopyroxenes and again a variable substitution of aluminium for silicon and magnesium in the tetrahedral and octahedral sites respectively is noticeable (Tables 24, 25). In this respect the clinopyroxenes are similar to those analysed from the Lizard by Green (1964). Both the Lizard and

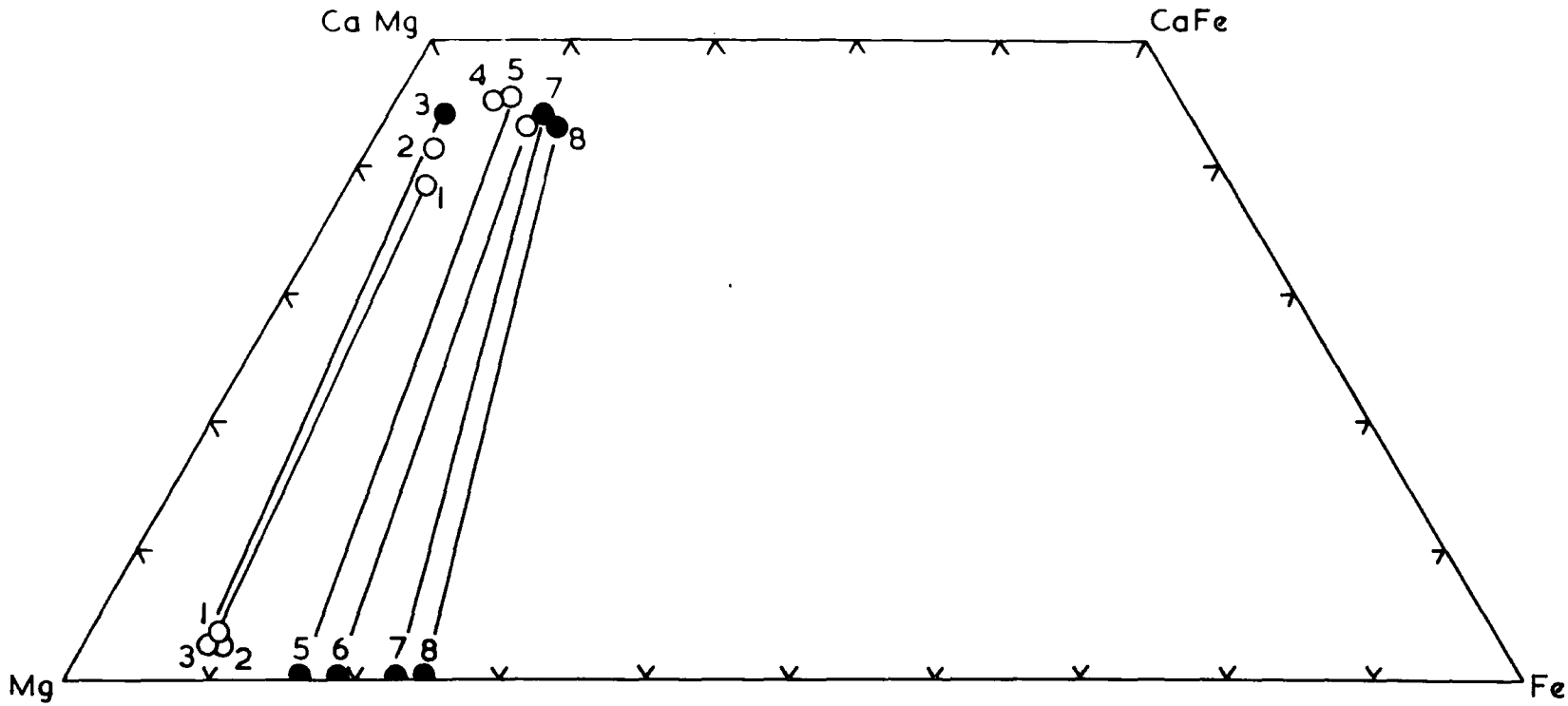

COEXISTING PYROXENES

1-T22 2-T383 3-T208 4-T 352 5-T384 6-T168 7-T136 8-T143 ANALYSED-O. X-RAY RESULT-●.

Fig.82.

Tawai clinopyroxenes (from the ultrabasic rocks) show an increase in CaO with increasing Al_2O_3. Green tentatively suggests this may be due to lower temperatures of formation of the low alumina clinopyroxenes. The majority of alpine type peridotite endiopsides contain low alumina but this may be a reflection of the small number of analysis available. Alumina in the clinopyroxenes from peridotite nodules in basalt varies from 1.7 to 5.7 weight per cent and those from garnet peridotites from 1.6 to 2.7 weight per cent, judging from the analytical data of Ross et al (1954) and O'Hara and Mercy (1963) respectively. Hess (1963, Table 9, p. 36) gives analyses of Stillwater and Bushveld clinopyroxenes ranging in the first locality from 2.3 to 3.0 weight per cent alumina, and in the second from 2.1 to 2.8.

A comparison of the Al_2O_3 contents of igneous clinopyroxenes from various paragenesis is shown in Fig. 83 where total alumina is plotted against $\frac{100Mg}{Mg + Fe''' + Fe'' + Mn}$ ratio. This ratio for Tawai ultrabasic clinopyroxenes varies from Mg_{87}-Mg_{91}, and in the Lizard specimens from Mg_{88}-Mg_{92}, and in the nodules from Mg_{88}-Mg_{91}. Despite showing only minor differences in this ratio they show a large range in Al_2O_3 content as can be seen in Fig. 83.

The Skaergaard clinopyroxenes show a decrease in alumina content with differentiation.

Zvethov (1945) prepared a series of $CaMgSi_2O_6$-$CaAl_2SiO_6$ solid solutions and placed the maximum amount of Al_2O_3 that could be dissolved in diopside between eighteen and nineteen weight per cent. Hytönen and Schairer (1960) in an investigation of aluminous diopsides in the system Enstatite-Anorthite-Diopside found that on cooling a liquid of composition Di_{75} Ca Tschermak$_{25}$ (Di=diopside

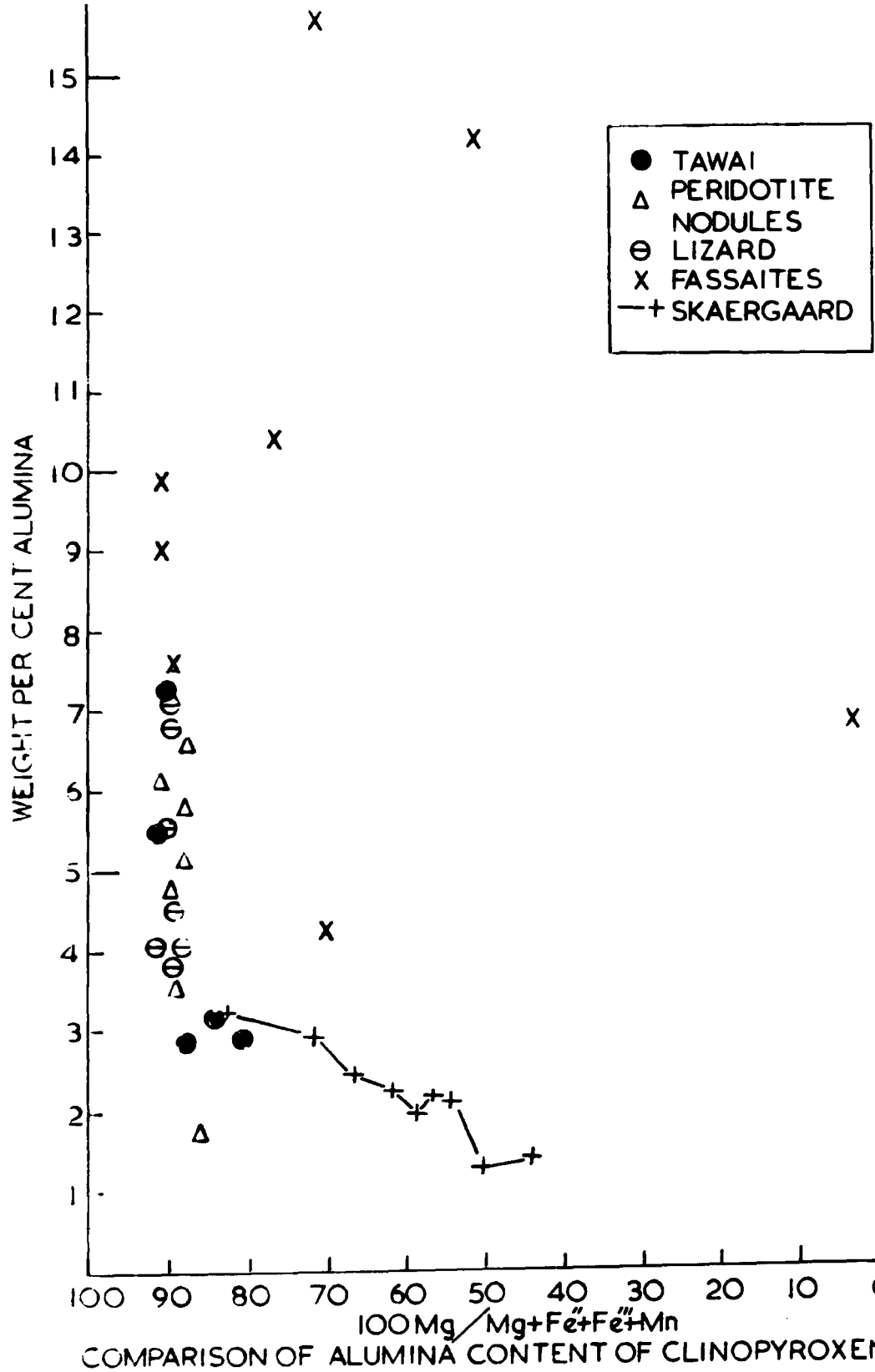

COMPARISON OF ALUMINA CONTENT OF CLINOPYROXENES

Fig.83.

$CaO:MgO.2SiO_2$ Ca Tschermak = $CaO\ Al_2O_3\ SiO_2$) diopside pyroxene crystallises at 1303°C but with further cooling the crystallising pyroxene becomes poorer in the diopside and enstatite components and richer in Ca-Tschermak's molecule. They conclude that with decreasing temperature the amount of $CaO\ Al_2O_3\ SiO_2$ in the diopside increases at least to the solidus. They also conclude that at high temperatures the diopsides are slightly richer in $MgO\ SiO_2$ than at lower temperatures. Wilkinson (1957) found that the early formed pyroxenes of the Black Jack sill were more aluminous than those which formed later, a fact which he attributed to higher temperature of formation of the former.

Hess (1960) in a comparison of the clinopyroxenes from the Stillwater and Bushveld intrusions noticed the former contain higher alumina in spite of the fact that the two magmas seem to be identical. He suggested that a temperature of crystallisation indicated by the pyroxene inversions are also similar, pressure might be the controlling factor, and perhaps the Stillwater complex had a thicker cover than the Bushveld. Sakata (1957) showed that in synthetic aluminous diopsides the cell parameters a_o and b_o decrease with increasing alumina substitution.

Hess also recorded that substitution of Al^{+3} in the octahedral site resulted in marked contraction of the unit cell and concluded that high pressure would presumably favour increased Al_2O_3 in the clinopyroxene.

Kushiro (1960) suggests that silica deficiency is a controlling factor in deciding the amount of Z Al that will substitute for silicon. He considers that in clinopyroxenes formed from relatively silica deficient alkaline basalt magmas there is wider substitution

of Z Al for Si than in those derived from tholeiitic magmas. In the former electric neutrality is maintained by substitution of Ti^{+4} and Fe^{+3} atoms in the octahedral site. Support for Kushiro's hypothesis is found in the aluminous clinopyroxenes of metamorphosed limestones described by Tilley (1938) which show marked substitution of Z Al for Si. In the recalculated analysis of one of these clinopyroxenes given in Deer, Howie and Zussman (1963, vol.2, p.164, Table 25, No.1) the electric neutrality is maintained by substitution of Al^{+3} in the Y position together with minor amounts of Ti^{+4} and Fe^{+3}. The same situation may be seen in the recalculated analysis of the Mount Tawai orthopyroxene and clinopyroxene except that minor amounts of Cr^{+3} also help balance the charges.

Trace element data for the analysed clinopyroxenes are given in Table 19. Nickel and chromium are higher in the peridotite clinopyroxene than those from the gabbro, whilst the reverse is true for manganese, copper and zinc. In the peridotite clinopyroxenes nickel, chromium and manganese are higher in the relatively low alumina specimen than in the high alumina one. A marked increase in copper is noted in the aluminous clinopyroxene T22. The pegmatitic clinopyroxene, T352, shows relatively low nickel and high manganese characteristic of the gabbroic clinopyroxenes but contains more chromium.

A comparison between the weight per cent of minor oxides in the clinopyroxenes from the Mount Tawai ultrabasic rocks and those from other environments is given in Table 26.

Soda is extremely low in the Mount Tawai and Stillwater clinopyroxenes and contrasts strongly with the amount found in those from the garnet peridotites and peridotite nodules in basalt. Few

Table 26

Comparison of minor oxides in clinopyroxenes.

	Na_2O	Cr_2O_3	TiO_2	MnO	NiO
Mount Tawai	0.1 - 0.2	0.4 - 0.7	0.1 - 0.4	0.1 - 0.2	0.1
Alpine Type peridotites	0.5 - 0.8	0.7 - 0.9	0.1	0.1	.03- .04
Garnet peridotites	1 - 1.8	0.2 - 1.6	0.1 - 0.2	0.04- 0.1	.04-0.1
Nodules in basalt	0.3 - 2.1	0.8 - 2.1	0.2 - 0.8	0.1 - 0.16	.04
Stillwater	0.2 - 0.4	1.09- 1.18	0.2 - 0.3	0.1	.05

analyses of clinopyroxene from Alpine type peridotites are available but those quoted by Ross et al (1954) appear to contain higher alkalies than the Mount Tawai ones. Cr_2O_3 in the Mount Tawai endiopsides is slightly lower than the average for clinopyroxenes from Alpine type peridotites. The large amounts of Cr_2O_3 found in the Stillwater and some of the peridotite nodules in basalt endiopsides have not been found in those from Mount Tawai.

TiO_2 is slightly higher than the average for the Alpine type peridotites and nodules endiopsides but compare with that from the Stillwater complex.

MnO is fairly constant in all the groups but lowest in the garnet peridotites.

NiO is slightly greater in the Mount Tawai and garnet peridotite clinopyroxenes than in the other groups.

X-ray diffraction studies.

The method by which the Ca:Mg:Fe ratio of the common clinopyroxenes may be estimated from the unit cell dimensions b and a sin β has been outlined by Brown (1960), who showed that in the common clinopyroxenes the three major substitutions affected the cell dimensions in the following way:-

(1) Fe^{2+} for Mg^{2+} - results in a regular increase in b and a sin β

(2) Fe^{2+} for Ca^{2+} - results in a regular increase in b and decrease in a sin β

(3) Mg^{2+} for Ca^{2+} - results in a regular decrease in b and a sin β

The variations in the cell dimensions b and a sin β were plotted on the pyroxene part of the Ca SiO_3 - Mg SiO_3 - Fe SiO_3 triangular diagram. (Brown 1963, Fig. 5, p.28); this chart then provides a means for estimating the Ca:Mg:Fe ratio of the common clinopyroxenes from X-ray diffraction data.

In order to provide the diagnostic data the methods used by Brown required lengthy calculations based on the use of a large number of reflections in order that cross checks could be obtained for each cell parameter. If it can be accepted that a knowledge of b and a sin β is all that is now required then the 2θ values for good 060 and 600 reflections (~~then the 2θ values for good 060 and 600 reflections~~) provide the necessary information for a relatively simple and rapid calculation of these parameters. The general formula for calculating the cell dimensions of monoclinic crystals is

$$d_{hkl} = \frac{1}{\sqrt{\dfrac{h^2}{a^2 \sin^2\beta} + \dfrac{l^2}{c^2 \sin^2\beta} + \dfrac{2hl \cos\beta}{ac \sin^2\beta} + \dfrac{k^2}{b^2}}}$$

This may be rewritten

$$\frac{1}{d^2_{hkl}} = \frac{h^2}{a^2 \sin^2\beta} + \frac{l^2}{c^2 \sin^2\beta} + \frac{2hl \cos\beta}{ac \sin^2\beta} + \frac{k^2}{b^2}$$

for the 060 reflection

$$\frac{1}{d^2} = \frac{k^2}{b^2} \qquad b_o = 6 \times d_{060}$$

Fig.84.

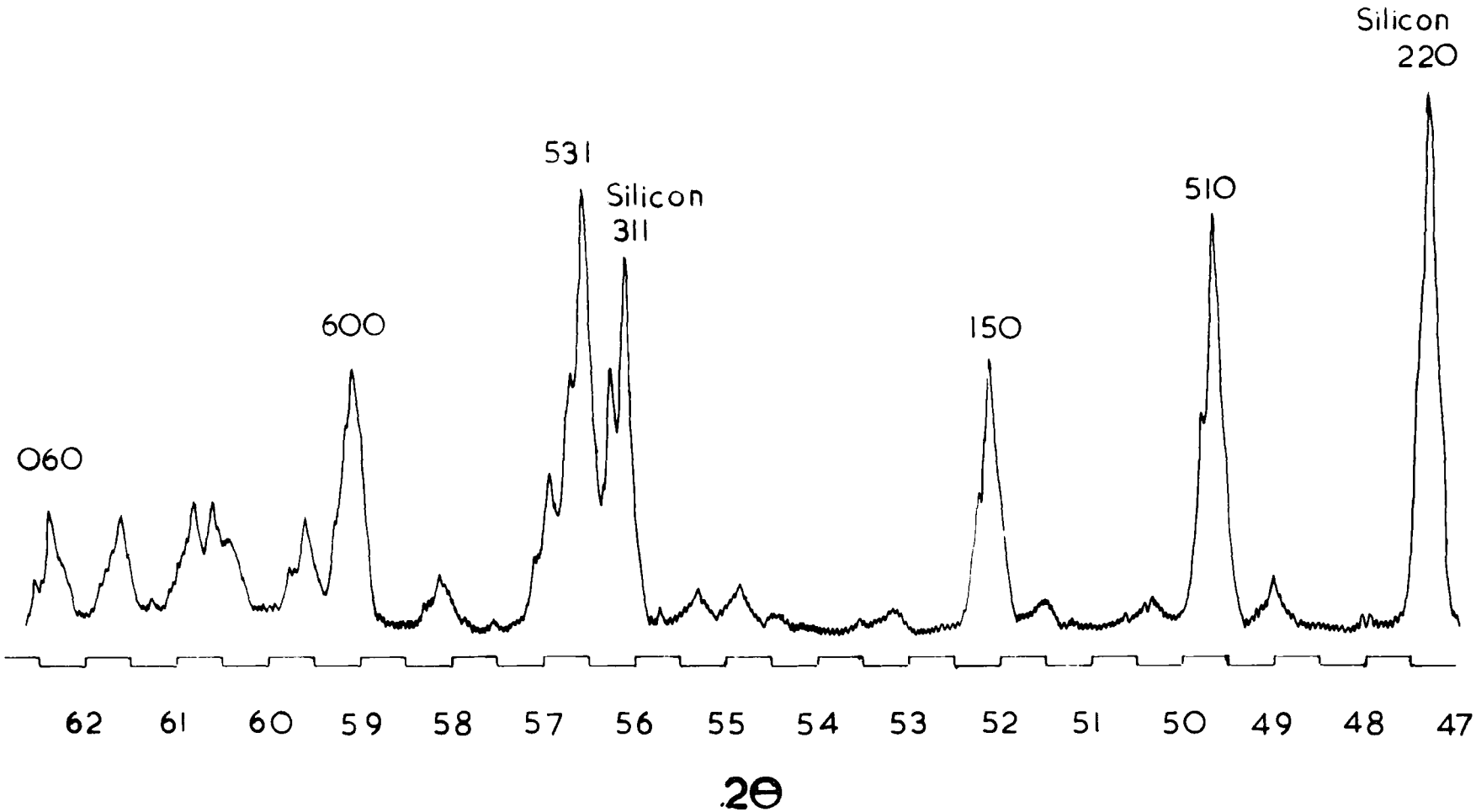

. Diffractometer record of clinopyroxene T136.

and for the 600 reflection

$$\frac{1}{d^2} = \frac{h^2}{a^2 \sin^2\beta}, \qquad a \sin\beta = 6 \times d_{600}$$

To test whether good 600 and 060 reflections could be obtained from a wide range of clinopyroxenes, several analysed specimens from the Skaergaard intrusion (kindly provided by Dr. G. M. Brown) and from the Mount Tawai complex were examined. The specimens range in composition from endiopside to ferro-hedenbergite and contain only small amounts of the cations Ti^{4+}, Na^{+}, Fe^{3+}. Brown (1960, p. 32) showed that in clinopyroxenes containing more than .05 aluminium atoms to six oxygen atoms in six-fold co-ordination, a reduction in b occurred, and in order to substantiate this two aluminous clinopyroxenes from Mount Tawai (Nos. T22, T383) were examined.

The samples were finely gound with 1-2 m.g. of pure silicon powder and examined as smear mounts. Measurements were made with a Phillips High Angle X-ray diffractometer using filtered copper radiation at 40kv and 20 m.a.. A reconnaissance traverse was run on each of the specimens at $\frac{1}{4}^{\circ}2\theta$ per minute, chart speed 200 mm. per hour 1°, 1°, 1°, slits and the 600 and 060 reflections indexed with the aid of charts provided by Dr. G. M. Brown. These reflections occur in a traverse between $58^{\circ}2\theta$ and $64^{\circ}2\theta$. This range was then examined in detail using a scan speed of $^{1}/_{8}$ per minute chart speed 200 mm. per hour, rate meter 8, time constant 8 and 4°, 2°, 4°, slits. Pulse height discrimination was used to increase the peak to background ratio. In all samples 060 and 600 were found to be usable but 060 was occasionally ragged especially in the ferrohedenbergite

E. G. 4489. To check the b dimension obtained from 060 the 150 reflection may be measured and b obtained by substitution d_{150} and a sin β from 600 into the following equation derived from the general formula.

$$b_o = \frac{5}{\sqrt{\left(\frac{1}{d_{150}} + \frac{1}{a\sin\beta}\right)\left(\frac{1}{d_{150}} - \frac{1}{a\sin\beta}\right)}}$$

In a similar way a sin β can be checked from the 510 reflection by substituting d_{510} and b into the following equation:-

$$a\sin\beta = \frac{5}{\sqrt{\left(\frac{1}{d_{510}} + \frac{1}{b_o}\right)\left(\frac{1}{d_{510}} - \frac{1}{b_o}\right)}}$$

In all of the specimens examined the 150 reflection gave good resolution. The 510 reflection gave good resolution except on the iron-rich specimens E.G. 4316 and E.G. 4489.

To obtain the 510, 150, 600 and 060 reflections a traverse from $47^{\circ}2\theta$ to $63^{\circ}2\theta$ was made using the above conditions. The peak positions were accur ately measured by reference to known silicon reflections at 2θ $47.302^{\circ}2\theta$ and $56.122^{\circ}2\theta$. A typical traverse over this range is shown in Fig. 84. Each specimen was run twice and the peak positions established within $\pm 01^{\circ}2\theta$. The results from eight clinopyroxenes are summarised in Table 27, which also compares the Ca:Mg:Fe ratios obtained by X-ray calculation and those obtained from chemical analysis. In all cases except T22 and T383 a close correlation is found. In these specimens b is depressed and a sin β and b meet outside the clino-enstatite-

Table 28. Clinopyroxene Determinations.

Rock Type	Specimen	aSinβ	b_o	Ca	Mg	Fe
Pyroxenite pegmatite	T148	9.378	8.922	45	44	11
" "	T266	9.372	8.918	44.5	45.5	10
" "	T310	9.378	8.920	45.5	44.5	10
" "	T352	9.368	8.916	45	46	9
Harzburgite	T119	9.352	8.901	44.5	52	3.5
	T195	9.354	8.904	44.5	50.5	5
	T137	9.342	8.905	42.5	52	5.5
	T383	9.349	8.892			
Pyroxenite band	T22	9.307	8.865			
	T81	9.324	8.880			
	T208	9.348	8.903	44	52	4
Pyroxene dunite	T89	9.318	8.868			
Olivine gabbro	T166	9.366	8.910	45.5	48	6.5
" "	T167	9.348	8.904	43.5	51.5	5
" "	T168	9.376	8.921	45	44.5	10.5
" "	T218	9.354	8.904	44.5	50.5	5
" "	T384	9.666	8.915	44.5	46.5	9
Pyroxene gabbro	T136	9.372	8.922	44	45	11
" "	T143	9.374	8.928	43	42.5	14.5
" "	T331	9.378	8.928	43.5	42	14.5

$^{o}b_o$ depressed outside of Mg-Ca Mg join.

diopside join on the determinative chart of Brown (1960).

In all of the Mount Tawai specimens good resolution of 060 and 600 was obtained and sixteen further specimens were examined in which these two reflections only were measured, and the cell dimensions calculated directly from them. Results are given in Table 28 together with the estimations of the Ca:Mg:Fe ratio obtained from the determinative chart of Brown. In Fig. 85, some of the results are plotted on the determinative chart of Brown (1960).

Composition.

The results from the analytical and X-ray work are plotted in Fig. 86. The clinopyroxenes have not been studied on a regional scale owing to the sparse occurrence of this mineral in the harzburgite.

The chemical analysis of the clinopyroxene from a harzburgite (T383) and a pyroxenite band (T22) are endiopside and the X-ray data for other similar specimens also appear to lie in this field. The latter measurements however are not conclusive for it is not known if the cell parameters are affected by alumina substitution. The only means of knowing is if the cell parameters b_o and $a \sin\beta$ plot outside of the determinative chart. This is clearly the case with T81 and T89. The analyses show that alumina increases together in co-existing pyroxenes. The clinopyroxene specimens that plot inside the chart in the field of endiopside were selected from harzburgite in which the orthopyroxene contains relatively low alumina and it seems reasonable to assume that they are not unduly displaced from their true positions.

The clinopyroxenite pegmatites plot on the boundary between

Fig. 85.

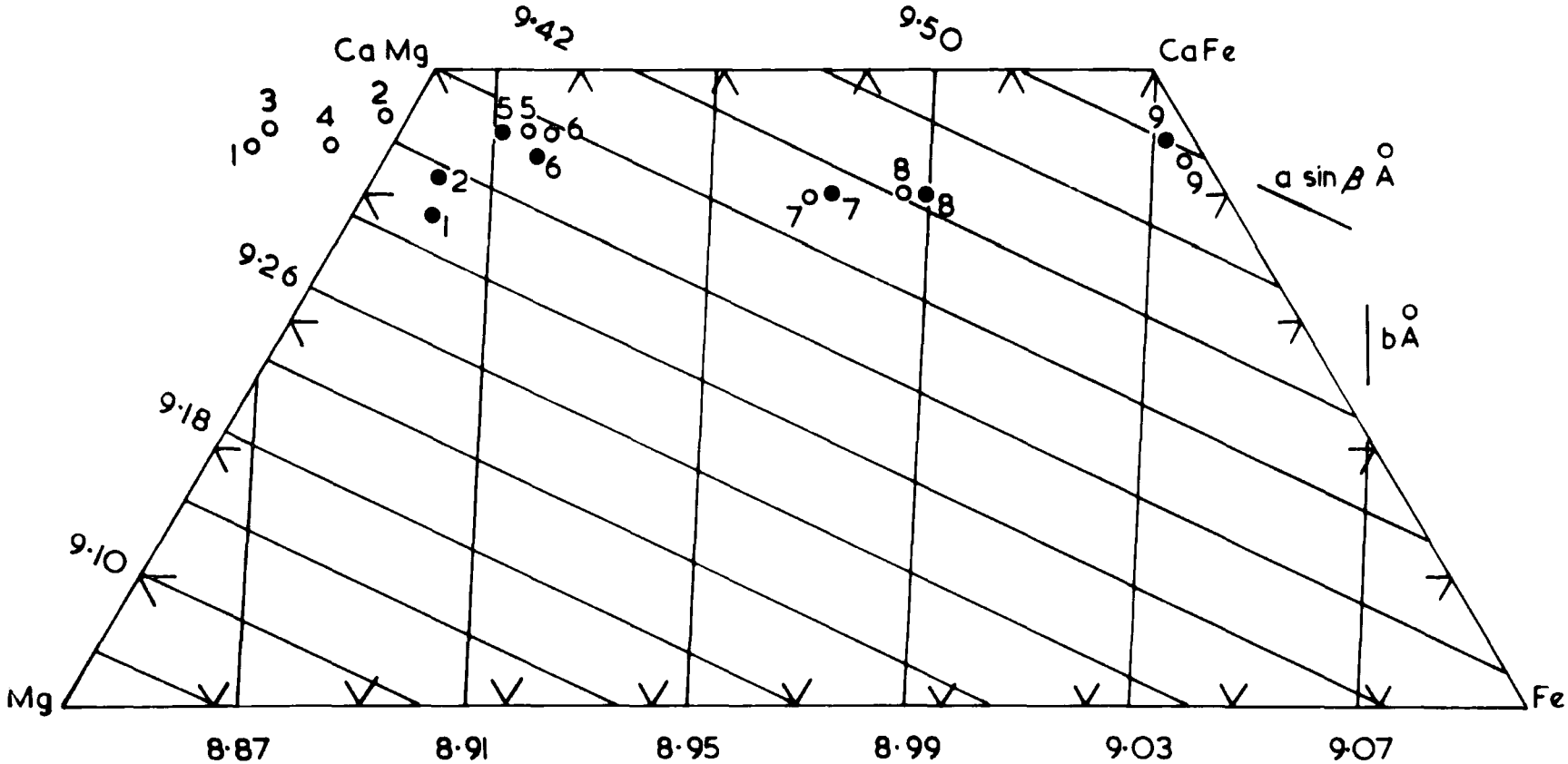

THE UNIT CELL DIMENSIONS OF SELECTED TAWAI AND SKAERGAARD CLINOPYROXENES PLOTTED ON THE DETERMINATIVE CHART OF BROWN 1960. ANALYSED PLOT-● . X-RAY PLOT-o
1-T22 2-T383 3-T89 4-T81 5-T352 6-T168 7-EG 4314 8-EG 4316 9-EG 4489

diopside, endiopside, salite and augite. The chemical analysis of T352 shows a low alumina content and the X-ray data is therefore more reliable. They vary from $Ca_{45}\ Mg_{46}\ Fe_{9}$ to $Ca_{45}\ Mg_{44}\ Fe_{11}$ and are more iron-rich than the clinopyroxenes from the peridotite.

The two chemical analyses of clinopyroxenes from olivine gabbro vary from $Ca_{43}\ Mg_{46.7}\ Fe_{10.3}$ to $Ca_{45.4}\ Mg_{46.6}\ Fe_{8}$. Large pegmatitic crystals sometimes found in the olivine gabbro appear from the X-ray data to be endiopside appraoching diopside and range from $Ca_{43.5}\ Mg_{51.5}\ Fe_{5}$ to $Ca_{45.5}\ Mg_{48}\ Fe_{6.5}$. The possibility of alumina substitutions affecting the X-ray data for these clinopyroxenes however cannot be ruled out.

The clinopyroxenes from the pyroxene gabbro are more iron-rich than those from the olivine gabbro and range from $Ca_{44}\ Mg_{45}\ Fe_{11}$ to $Ca_{43}\ Mg_{42.5}\ Fe_{14.5}$.

The general trend of the Mount Tawai clinopyroxenes is shown in the Ca-Mg-Fe diagram, Fig. 87, which also compares the trends of clinopyroxenes from the Lizard, Stillwater, Skaergaard and Garbh Eilean complexes. The field of clinopyroxenes from the peridotite nodules in basalt is also shown.

Relations between co-existing ortho- and clino-pyroxenes.

Hess (1941) suggested that when the compositions of co-existing calcium-rich and calcium-poor pyroxenes from igneous rocks are plotted on the triangular diagram $Ca_{\beta}^{SiO_3}$-Mg SiO_3-Fe SiO_3 a projection of the line joining the two compositions would intersect the Mg SiO_3-Ca SiO_3-line at about $Wo_{75}\ En_{25}$.

Wilson (1960) accepted this suggestion and inferred that in metamorphic pyroxenes departures from this ideal intersection were

Fig.86.

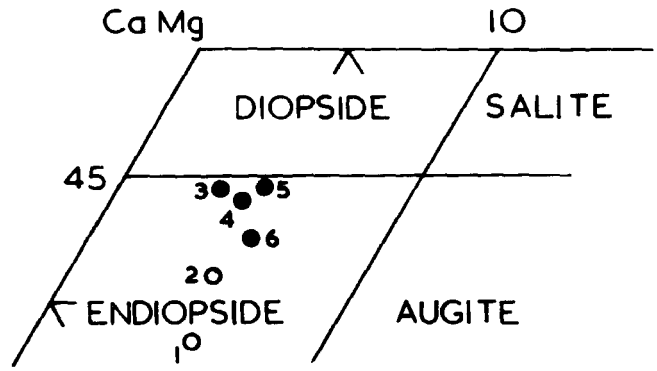

PERIDOTITE CPX.
1 T22
2 T383
3 T119
4 T208
5 T195
6 T137

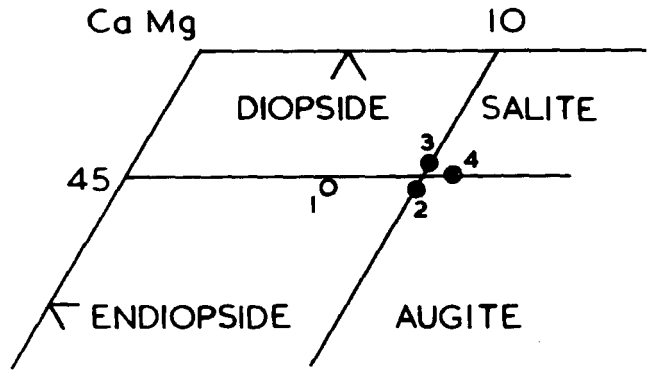

MAFIC PEGMATITE.
CPX.
1 T352
2 T266
3 T310
4 T148

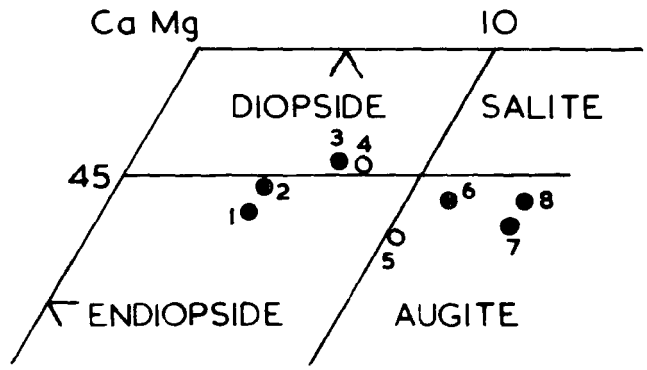

GABBRO CPX.
1 T167
2 T218
3 T166
4 T384
5 T168
6 T136
7 T143
8 T331

Ca:Mg:Fe PLOT OF THE TAWAI CLINOPYROXENES.
Analysed o . X-RAY determination ●

Fig.87.

Ca:Mg:Fe PLOT OF TAWAI AND VARIOUS OTHER CLINOPYROXENES

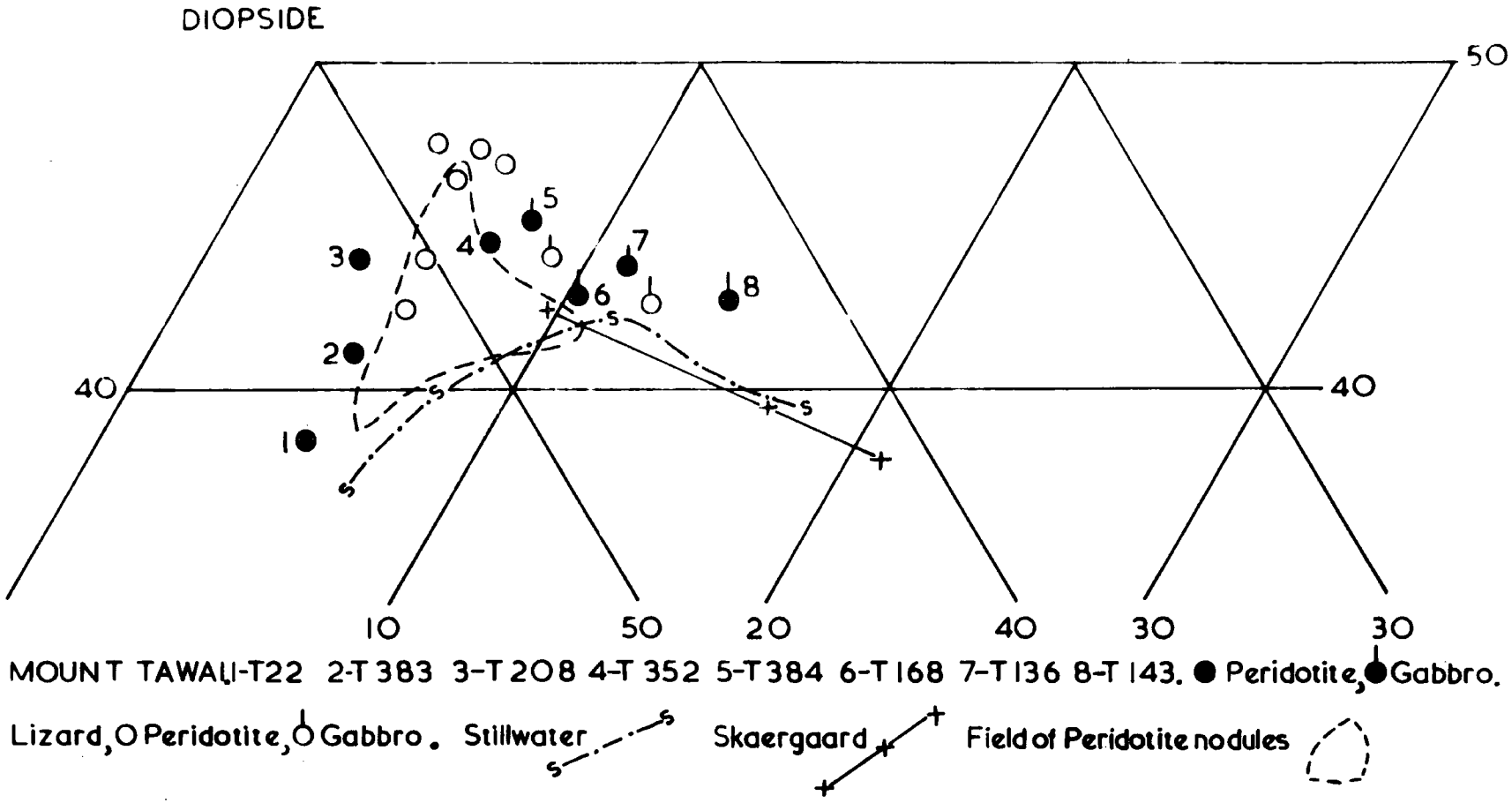

MOUNT TAWALI-T22 2-T383 3-T208 4-T352 5-T384 6-T168 7-T136 8-T143. ● Peridotite, ● Gabbro.

Lizard, O Peridotite, O Gabbro. Stillwater S S Skaergaard + + + Field of Peridotite nodules

indicative of dis-equilibrium conditions.

Brown (1961) however has shown from a large number of analyses that there is little evidence for a standard value for the tie-line intersections. He calculated the average value as Wo_{82} En_{18} but because of the wide scatter on both sides of the Wo apex concluded that little petrological significance could be attached to tie-line intersections. Brown, however, made the interesting point that the tie-lines for the co-existing pyroxenes from peridotite nodules in basalt (Ross et al 1954) intersect the $CaSiO_3$-$FeSiO_3$ side of the triangle. El Hamad (1963) however found that the reverse relationship was true for the pyroxenes from the nodules at Carlton Hill, the intersection occurring at Wo_{70}. Brown, however, pointed out that if the intersection occurs on the $CaSiO_3$-$MgSiO_3$ join then the orthopyroxene is enriched in iron relative to the clinopyroxene but if it takes place on the $CaSiO_3$-$FeSiO_3$ join then the reverse is true. The clinopyroxenes from the peridotite nodules mentioned above are unusual in having a higher iron to magnesia ratio than the co-existing orthopyroxene. Muir and Tilley (1958) indicated that the clinopyroxenes from volcanic rocks also have their clinopyroxenes relatively enriched in iron.

The tie-line intersections for the analysed pairs of pyroxenes have been extrapolated and T383 cuts the $CaSiO_3$-$MgSiO_3$ join at Wo_{82} En_{18} and T22 at Wo_{98} En_2. The tie-line intersection for the co-existing pyroxene of specimen T208 have also been extrapolated using the analysed orthopyroxene and the X-ray determination of the clinopyroxene. This tie-line intersects the $CaSiO_3$-$MgSiO_3$ line at Wo_{79} En_{21}. All of the tie-line intersections thus indicate that the orthopyroxenes are richer in Fe^{++} relative to Mg^{++} than the

clinopyroxenes.

A theoretical approach to the distribution of Fe^{++} and Mg^{++} between co-existing calcium-poor and calcium-rich pyroxenes has been investigated by Kretz (1961) and Bartholomé (1961). The latter author shows the conditions of equilibrium to be

$$\left(\frac{Fe^{++}}{Mg}\right)_{\text{Ca poor pyroxene}} = \left(\frac{Fe^{++}}{Mg}\right)_{\text{Ca rich pyroxene}} \times K(T)$$

K(T) is the distribution co-efficient and Bartholomé indicates for the co-existing pyroxene from metamorphic rocks the value is 1.8, for those from igneous rocks of the Bushveld, Stillwater type 1.4, and for those from olivine nodules in basalt 1.2. He suggests that K(T) is rather an insensitive geological thermometer. Kretz (1961) considers that the effect of variations of minor elements Al^{+3}, Ti^{+4}, Fe^{+3} and of different pressures of crystallisation are negligible in comparison with temperature effects. The distribution co-efficient for the pyroxene pairs T208, T383, and T22 have been extrapolated and are 1.2, 1.2 and 1.1 respectively. These values agree reasonably well with K(T) distribution co-efficients calculated for co-existing pyroxene from peridotite nodules in basalt but are lower than those for basic igneous rocks and metamorphic rocks. If it is accepted that the distribution co-efficient is temperature controlled then the Mount Tawai assemblages, which show no signficcant variation in K(T) amongst themselves, crystallised at a higher temperature than basic igneous rocks. Green (1964) found that the co-existing pyroxenes from the Lizard peridotite have K(T) values between 1.3 and 1.4 these being slightly higher than those of basic igneous rocks.

The distribution of alumina between co-existing pyroxenes has also been considered by Green who examined the variation of Al^{+3} in the Z position with Si in a number of assemblages and by analogy with K(T) he derived the following co-efficient.

$$K\ Al = \frac{(Z\ Al/Si)\ Cpx}{(Z\ Al/Si)\ Opx}$$

He derived the following K Al values for co-existing calcium-rich and calcium-poor pyroxenes.

Lizard - Primary peridotite	- 1.2 - 1.3
Lizard - Recrystallised peridotite	- 1.6
Nodules in basalt	- 1.14 - 1.35
Metamorphic ultrabasics	- 1.50 - 1.53
Accumulates from basaltic magmas	- 1.35, 1.14, 0.82

Values of K Al less than one indicate the orthopyroxene to contain more alumina than the clinopyroxene. The alumina silicon distribution co-efficient has been extrapolated for the co-existing pyroxenes T383 and T22 and are 1.26 and 0.87 respectively, and these fall in the range of values calculated by Green for co-existing pyroxenes from igneous plutonic rocks. They are however significantly lower than the K Al values for ultrabasic granulites and the Lizard recrystallised peridotite. Green has tentatively suggested that the distribution co-efficient of silicon and aluminium maybe pressure sensitive and that the recrystallised Lizard assemblages formed at a lower pressure than the primary one. Obviously a great deal more experimental work is needed to elucidate the value of the

silicon aluminium distribution co-efficient but on the present standing of Green's work the Mount Tawai assemblages appear to be primary and not recrystallised.

Chrome Spinel.

Chemistry.

The general formula for the spinel group of minerals is RO R_2O_3. In the chrome spinels RO consists mainly of bivalent magnesia and iron and R_2O_3 mainly of oxides of trivalent chromium, iron and aluminium. A general formula is therefore (Mg Fe)O(Cr,Al,Fe)$_2O_3$. The majority of chromite analyses show that the ratio of R_2O_3 to RO is approximately 1:1 although significant departures from this ideal situation have been recorded by Stevens (1944). A prism, Fig. , devised by W. D. Johnston Jr. and described by Stevens (1944) illustrates the variations in spinel composition. The end members of this prism are ferrochromite FeO Cr_2O_3, hercynite FeO Al_2O_3, magnetite FeO Fe_2O_3, magnesiochromite MgO Cr_2O_3, spinel MgO Al_2O_3 and magnesioferrite MgO Fe_2O_3.

Thayer (1944) has shown how it is convenient to state the composition of chromite in terms of molecular ratios of the R_2O_3 and RO constituents. Such an example is Cr_{65} Al_{33} Fe_3 (Mg_{68} Fe_{32}) and as the Fe_2O_3 and FeO can be calculated by difference a shortened version may be stated as Cr_{65} Al_{33} (Mg_{68}). This method is the best for expressing chromite compositions for the entire range of chromite is covered by a single set of standard constituents and ratios and the normative composition of a given chromite is quickly deduced. The norm of the above example would be

Chromite	(Mg Fe) Cr_2O_4	65
Spinel	(Mg Fe) Al_2O_4	33
Magnetite	Fe Fe_2O_4	3
MgO/FeO		68/32

Chromite samples from various parts of North Borneo have been analysed by Naylor Benzon and Co. Ltd. and are given in Table 29. These are commercial analyses of lump ore in which the chromite together with the gangue minerals is analysed in order that the weight per cent of silica may be determined which is a limiting factor in assessing the value of refractory ores. There is no reason to believe that silica enters into the chromite molecule and in Table 29 the analyses have been recalculated by removing silica together with the appropriate amount of magnesium serpentine. Serpentine is the most common gangue mineral although small amounts of chlorite are always present. In No. T134 small amounts of diopside are present and CaO, MgO and SiO_2 have been removed in the recalculation. Titania is noticeably absent in all the analyses except T134. Titanium could not be detected in a thoroughly cleaned up specimen of the ore and is assumed to be present in the gangue. Ilmenite exsolution lamellae are absent from all the specimens examined.

The molecular ratios of the Borneo chromites are given in Table 29 and a fair approach to balance between molecular R_2O_3 and RO is shown. In four of the six specimens R_2O_3 slightly exceeds RO and suggests that alumina is present in the gangue minerals probably in the chlorite. However the differences are so small they can be ignored. In the two specimens where RO exceeds R_2O_3 it is possible

Table 29. North Borneo Chromite Analyses provided by Naylor, Benzon & Company, Limited.

	Bangii	Bidu-Bidu Hills			Tawai	Segama
	BB 120	NB1	NB2	NB3	T134	L549
SiO_2	1.30	1.75	3.40	4.92	5.88	7.85
Al_2O_3	15.29	16.09	16.69	16.57	24.46	24.05
TiO_2	-	-	-	-	.50	-
Fe_2O_3 *	14.65	12.45	11.98	11.15	13.54	13.80
MgO	14.49	15.39	16.65	17.60	17.37	18.80
CaO	.47	.30	.32	.20	.86	.35
Cr_2O_3	55.76	50.42	48.30	45.93	35.59	32.90
Na_2O	-	.04	.03	.03	.02	-
K_2O	-	.02	.02	.02	-	-
Ignition Loss	-	2.60	2.71	2.80	1.04	3.0

*Total iron as Fe_2O_3.

Chrome Spinel recalculated to 100%

Cr_2O_3	27.23	55.19	54.92	53.91	42.05	40.99
Al_2O_3	15.69	17.61	18.97	19.44	28.90	29.96
FeO	13.55	12.28	12.27	11.80	14.20	15.49
MgO	13.53	14.92	13.84	14.85	14.85	13.56

Mol Ratios X 1000

Cr_2O_3	376	363	361	355	277	270
Al_2O_3	154	173	186	191	283	294
	530	536	547	546	560	564
MgO	336	370	343	368	368	336
FeO	188	171	170	164	197	215
	524	541	513	532	565	551
Chromite	71	67.5	66	65	49.3	47.9
Spinel	29	32.2	34	35	50.4	52.1
Magnetite	?	.3	?	?	.3	?
MgO	64.1	69.0	66.9	69.2	65.6	61.0
FeO	35.9	31.0	33.1	30.8	34.4	39.0

Table 27. Clinopyroxene Unit Cell Dimensions.

Specimen	hkL	dÅ	$a\sin\beta$	b_o	Average $a\sin\beta$	Average b_o	Ca. Mg. Fe. X-Ray	Ca. Mg. Fe. Chemical
	510	1.834	9.370					
T352	150	1.752		8.917	9.368	8.916	45:46:9	44.7:48.2:7.1
	600	1.561	9.366					
	060	1.486		8.916				
	510	1.830	9.351					
T383	150	1.747		8.893	9.349	8.892		41.2:54:4.8
	600	1.558	9.348					
	060	1.482		8.892				
	510	1.821	9.302					
T22	150	1.742		8.868	9.307	8.865		38.4:56:5.6
	600	1.552	9.312					
	060	1.477		8.862				
	510	1.835	9.374					
T168	150	1.753		8.921	9.376	8.921	45:44.5:10.5	43:46.7:10.3
	600	1.563	9.378					
	060	1.487		8.922				
	510	1.832	9.361					
T384	150	1.752		8.915	9.366	8.915	44.5:46.5:9	45.4:46.6:8
	600	1.562	9.372					
	060	1.486		8.916				
	510	1.840	9.399					
E.G.4314	150	1.762		8.969	9.403	8.969	40:29:31	40.2:27.6:32.2
	600	1.568	9.408					
	510	1.844	9.421					
E.G. 4316	150	1.765		8.985	9.423	8.986	40.5:22:37.5	40:21:39
	600	1.571	9.426					
	060	1.498		8.988				
	510	-						
E.G.4489	150	1.775		9.033	9.498	9.038	43.5:1.5:55.5	44.5:2:53.5
	600	1.583	9.498					
	060	1.507		9.042				

to calculate the excess FeO as Fe_2O_3. Ferrous iron determinations in chromite are particularly difficult and in the analyses total iron has been determined as Fe_2O_3.

Seven partial analyses of the Mount Tawai chromite have been made using X-ray fluorescence techniques. The specimens were separated from the gangue minerals using the magnetic separator and heavy liquids. The last trace of serpentine were removed by working in dilute hydrochloric acid. Alumina could not be determined accurately enough by X-ray fluorescence and has been calculated by subtraction. The molecular ratios have been determined and are given in Table 30 , and in all the specimens molecular RO exceeds molecular R_2O_3. The excess FeO has been converted to Fe_2O_3 and the analyses recalculated to 100 per cent as shown in Table 30. The normative calculations proposed by Thayer have been computed for both sets of analyses and is given in Tables 29 and 30.

From the results it is seen that there is a wide variation in normative chromite and spinel whilst the MgO/FeO variation is small. Normative magnetite is extremely low. The wide range in normative chromite and spinel shown in chromites from various parts of Borneo is also found in the Mount Tawai specimens.

A comparison of the Mount Tawai chromites with those from other areas is given in Table 31. The Mount Tawai ores range from $Cr_{66-33}\ Al_{32-67}\ (Mg_{71-64})$ which closely resembles the range found in the Cuban chromites of $Cr_{60-30}\ Al_{40-67}\ (Mg_{65-75})$ reported by Thayer (1944). The latter are higher slightly lower in normative chromite and a little high in normative spinel. The very high normative chromites found in the Guatamalan deposits however is not seen in the Tawai ores. The Tawai ores with the highest normative

Table 30. Tawai Chromite Analyses and Calculations.

		T268	T268a	T194	T216	T367	T230	
	Cr_2O_3	53.7	52.7	51.6	49.5	43.7	29.1	
	FeO	13.4	13.0	13.9	13.6	13.1	15.8	Locality.
	MgO	14.7	14.9	14.8	15.0	16.1	15.0	
	Al_2O_3	18.2	19.4	19.7	21.9	27.1	40.1	T268-5° 29' 32" N 117° 09' 03" E
Molecular ratios X 100								
	Cr_2O_3	353	347	339	326	287	191	T194-5° 28' 00" N
	Al_2O_3	178	190	193	215	266	393	117° 08' 5" E
		531	537	532	541	553	589	
	MgO	367	372	368	375	402	375	T216-5° 29' 46" N
	FeO	186	180	193	189	182	219	117° 07' 41" N
		553	552	561	564	584	594	5° 29' 45" N
Excess R.O.		.022	.015	.029	.023	.031	.010	T367-117° 05' 26" E
Wt. % Fe_2O_3		1.1	0.8	1.60	1.3	1.6	0.5	
Recalculated to 100%	Cr_2O_3	53.6	52.6	51.5	49.4	43.6	29.1	T230-5° 27' 23" N
	Al_2O_3	18.2	19.4	19.6	21.9	27.0	40.0	117° 10' 24" N
	Fe_2O_3	1.1	.8	1.6	1.3	1.6	0.5	
	MgO	14.7	14.9	14.8	15.0	16.1	15.0	
	FeO	12.4	12.3	12.5	12.4	11.7	15.4	
Thayer Norm	Chromite	65.5	64.0	62.7	59.3	51.0	32.6	
	Spinel	32.2	35.1	35.5	39.2	47.2	66.9	
	Magnetite	1.3	.9	1.8	1.5	1.8	.5	
	MgO	68.1	68.5	67.9	68.6	71.3	63.8	
	FeO	31.9	31.5	32.1	31.4	28.7	36.2	

Analyst W.G. Hancock.

chromite are not unlike those found from Hangha, Sierra Leone, in which the chromite also occurs in non-feldspathic dunite.

Thayer (1944) in reviewing the Caribbean chromites quotes an overall range of $Cr_{25-80}\ Al_{15-75}\ (Mg_{65-75})$ and suggests that ores rich in normative chromite occur in feldspar free dunites and those high in normative spinel in feldspathic peridotite and often closely associated with troctolite. He points out that in the East Oregon field of America, with a range of $Cr_{38-71}\ Al_{56-27}\ Mg_{69-58}$, there is an increase in ferrous iron from the high alumina to high chromite groups and here the ores are associated with peridotite, pyroxenite and gabbro. In the Pacific coast ores of the U.S.A., which occur in dunite associated with saxonite the chromite range from $Cr_{60-75}\ Al_{35-15}\ (Mg_{56-70})$ the chief variation being in the MgO/FeO ratio.

The Stillwater and Bushveld type ores are relatively rich in iron and normative magnetite and contrast markedly with the Tawai chromites. The early formed chrome spinel of the Great dyke, $Cr_{71}\ Al_{21}\ (Mg_{75})$ are however not unlike those from the Alpine type peridotites although with differentiation this is changed to $Cr_{65}\ Al_{23}\ (Mg_{60})$. These chromites however differ from those of the Stillwater and Bushveld in lower normative spinel and Mg/Fe ratio.

The chrome-spinel from peridotite nodules in basalt contain very high normative spinel and are close to $Cr_{20}\ Al_{75}\ (Mg_{80})$. They are also very rich in MgO.

Trace element data for the chromium spinels is given in Table 32. Small amounts of zinc and copper have been detected but do not show any significant variation with Cr_2O_3. Minor amounts of zinc have been found in several Yugoslavian ores by Deleon (1955) and a chromite containing 2.62 weight per cent ZnO has been described

Table 31. Comparison of Compositions of Chrome Spinels. (In Mol. per cent)

District.	Paragenesis.	(R_2O_3) 100 Cr	(R_2O_3) 100 Al	(RO) 100 Mg	Source.
Mount Tawai. N. B.	Dunite-harzburgite	66-33	36-67	64-71	
Hangha. B.M.A.	Dunite	62	37	65	Dunham et.al. (1958)
Pacific Coast U.S.A.	Dunite-Saxonite	75-60	15-35	45-75	Thayer (1946)
East Oregon U.S.A.	Peridotite-gabbro	71-38	27-56	58-69	Thayer (1946)
Cuba	Peridotite-troctolite	60-30	40-67	65-75	Thayer (1946)
Guatamala	Dunite	80	15	70	Thayer (1946)
Mount Dun N.Z.	Dunite	62	26	66	Ross et.al. (1954)
Nodule in basalt	Peridotite	20	75	80	O'Hara (1963)
Bushveld S.A.	Bronzitite	62-55	30-39	35-48	Thayer (1946)
Stillwater S.A.	Feldspathic peridotite	69-52	26-39	45-61	Thayer (1946)
Great Dyke S.A.	Feldspathic peridotite.	71-65	21-23	60-75	Worst (1958)

by Donath (1931) from Norway.

Nickel is present in amounts up to 1670 ppm (approx. 0.2 weight per cent NiO) and shows a tendency to increase with alumina, a reverse situation to that found in the pyroxenes.

X-ray diffraction studies.

Stevens (1944) in a study of a large number of chromite specimens showed that with increasing chromium content the unit cell parameter a_o incfeases. He found that interchange of ferrous iron and magnesia had only a minor effect on the unit cell but that substitution of ferric iron or chromium causes a marked increase. Stevens (1944 p.26, Fig.2) plotted cell edge against chromium content and found that the majority of specimens plotted approximately on a straight line. Points lying well off the line contain high Fe_2O_3. Smith and Macgregor (1960) reported a similar relationship and suggest that cryptic variation in the spinels of Alpine type peridotites may be best studied by determination of the cell parameters since in general they contain low weight per cent Fe_2O_3.

The unit cell parameters have been determined for the analysed Borneo chromites and the results given in Table 33. They were extrapolated from the dÅ spacing of the 333 reflection (57°-$59^\circ 2\theta$). The general formula for calculation of the cell parameter a_o of cubic crystals is

$$a_o = d\sqrt{h^2+k^2+l^2}$$

and therefore for the 333 reflection

$$a_o = \frac{d_{333} \times 9}{\sqrt{2}}$$

Table 32. Chromite Trace element data.

No	Wt.%Cr_2O_3	Zn	Cu	Ni
BB120	57.2	330	75	740
NB1	55.2	445	75	705
T268	53.7	450	215	610
T194	51.6	415	110	745
T216	49.5	475	100	775
T367	43.7	705	290	660
T134	42.1	610	35	1240
LS49	40.1	555	90	1195
T230	29.1	535	90	1670

Determinations in ppm.

Analyst W.G. Hancock.

This method was devised by Mr. A. R. Ramsden for the calculation of the unit cell parameters of spinels. Checks were made using other reflections and the method found to be reliable.

The samples were finely ground with pure silicon powder and examined as smear mounts. Measurements were made with a Phillips High Angle X-ray diffractometer using filtered copper radiation at 40kv and 20 m.a.. Scans were made from $56^{\circ}2\theta$ to $59^{\circ}2\theta$ using $1^{\circ},1^{\circ},1^{\circ}$, slits rate meter 16, chart speed 200mm. per hour and scan speed $\frac{1}{4}^{\circ}$ per minute. The angle of 2θ of the 333 reflections was corrected using a silicon internal standard at $56.122^{\circ}2\theta$.

In Fig. 88 weight per cent chromium is plotted against the unit cell dimension and a straight line relationship, similar to that obtained by Stevens (1944), established. In the same diagram weight per cent alumina is plotted against the unit cell and a straight line, with a reverse slope to that of the chromium line, obtained. These two determinative curves have been used to estimate the weight per cent chromium and alumina in a large number of specimens whose cell parameters have been determined by the above described method. Results are given in Table 22. The graphs indicate an accuracy of slightly less than two per cent Cr_2O_3 but all results are comparative and illustrate the overall trend.

The results of the cell edge determinations show that the type two dunites contain a chrome spinel richer in normative spinel and poorer in normative chromite than the type one dunites.

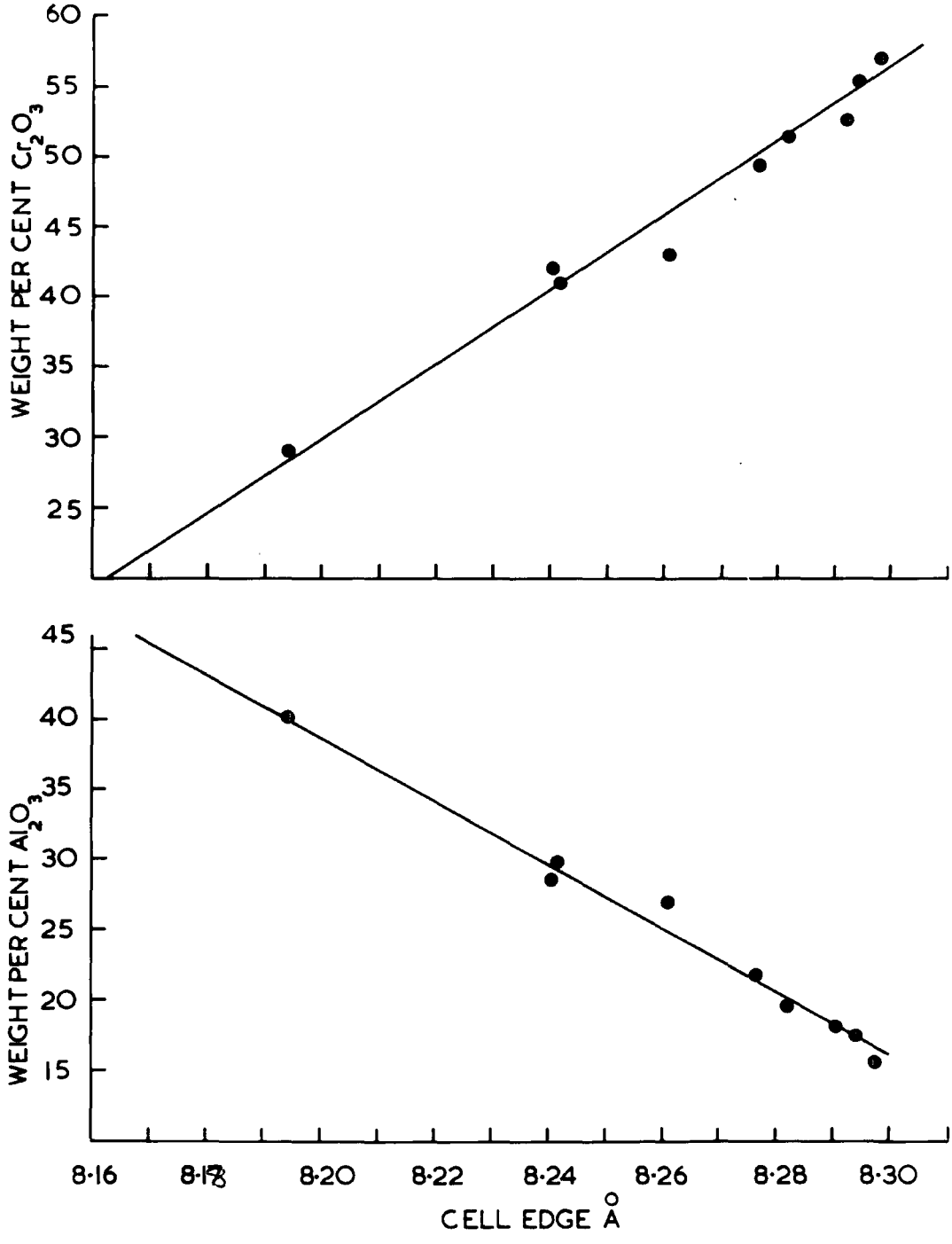

VARIATION OF CELL EDGE WITH Cr_2O_3 AND Al_2O_3 IN BORNEO CHROMITES

Fig.88.

Table 33. Unit Cell Dimensions of Analysed Chromites.

Specimen	dÅ 333	A_o	Cr_2O_3	Al_2O_3
T230	1.5770	8.1941	29.1	40.0
LS49	1.5862	8.2419	41.0	29.9
T134	1.5859	8.2403	42.1	28.9
T367	1.5899	8.2610	43.6	27.0
T216	1.5929	8.2767	49.4	21.9
T194	1.5939	8.2819	51.5	19.6
T268	1.5959	8.2923	53.6	18.2
NB1	1.5962	8.2938	55.2	17.6
BB120	1.5969	8.2975	75.2	15.7

THE VARIATION OF THE PRIMARY MINERALS.

The mineralogy of the main Tawai block has been studied in detail in order to determine the type and degree of cryptic variation of the primary minerals. Specimens were collected from the dunite lenses and the immediate wall rock wherever possible and the spinel and olivine examined from the former and the olivine and orthopyroxene from the latter. Few clinopyroxene determinations have been made owing to the sparsity of this mineral in the peridotite.

Olivine.

Forty five X-ray diffraction determinations of olivine over the main Tawai block (Table 22) were made but no systematic variation could be detected with height above sea level or distance from centre. The overall variation is from $Fo_{90.2}$ to Fo_{93} with the majority between Fo_{91} and Fo_{92}. In the majority of the peridotite-dunite pairs examined the olivine of the latter is slightly more magnesium rich than that of the former. A similar variation has recently been reported by Lipman (1964) for the Wolf Greek ultrabasic batholith in California. The highest Fo values have been recorded from type one dunites (specimens 198, 207, Table 22) but the majority of the determinations show that the two types of dunite cannot be distinguished by Fo content of the olivine.

Orthopyroxene.

The chemical analyses of the orthopyroxenes from the main Tawai block indicate only slight variations in the En ratio. This is confirmed by the X-ray data from a large number of orthopyroxenes

(Table 22). The X-ray diffraction method of estimating the En ratio is not particularly suitable for detecting minor changes in the En ratio but the results obtained are comparative and no systematic variation of the Fo content of the olivine and the En ratio of the orthopyroxene could be detected. The chemical analyses and the X-ray diffraction data however do show a considerable variation in the Al_2O_3 content of the orthopyroxenes; these results (Table 22) are plotted on the outline map of the Tawai block, Fig. 89, and they show that the alumina content of the orthopyroxenes increases as the block is traversed in a westerly direction. Approximate contours have been drawn on the map and they are slightly oblique to the general elongation of the block.

Clinopyroxene.

The clinopyroxenes from the main Tawai block have not been studied systematically. That alumina increases together in co-existing pyroxenes is shown by the analyses of the pyroxene pairs T22 and T383. Specimens (T119, T195, T137, T208, Table 29) co-existing with low alumina orthopyroxenes and have been determined by X-ray diffraction. The cell dimensions b_o of these specimens is not depressed outside the determinative chart of Brown (1960) indicating a low alumina content. On the other hand specimens T81 and T89 co-exist with relatively high alumina orthopyroxenes and the determinations of b_o fall outside of the determinative chart indicating relatively high alumina.

The available evidence therefore suggests that alumina in the clinopyroxene also increases westward with that in the orthopyroxene.

Fig.89.

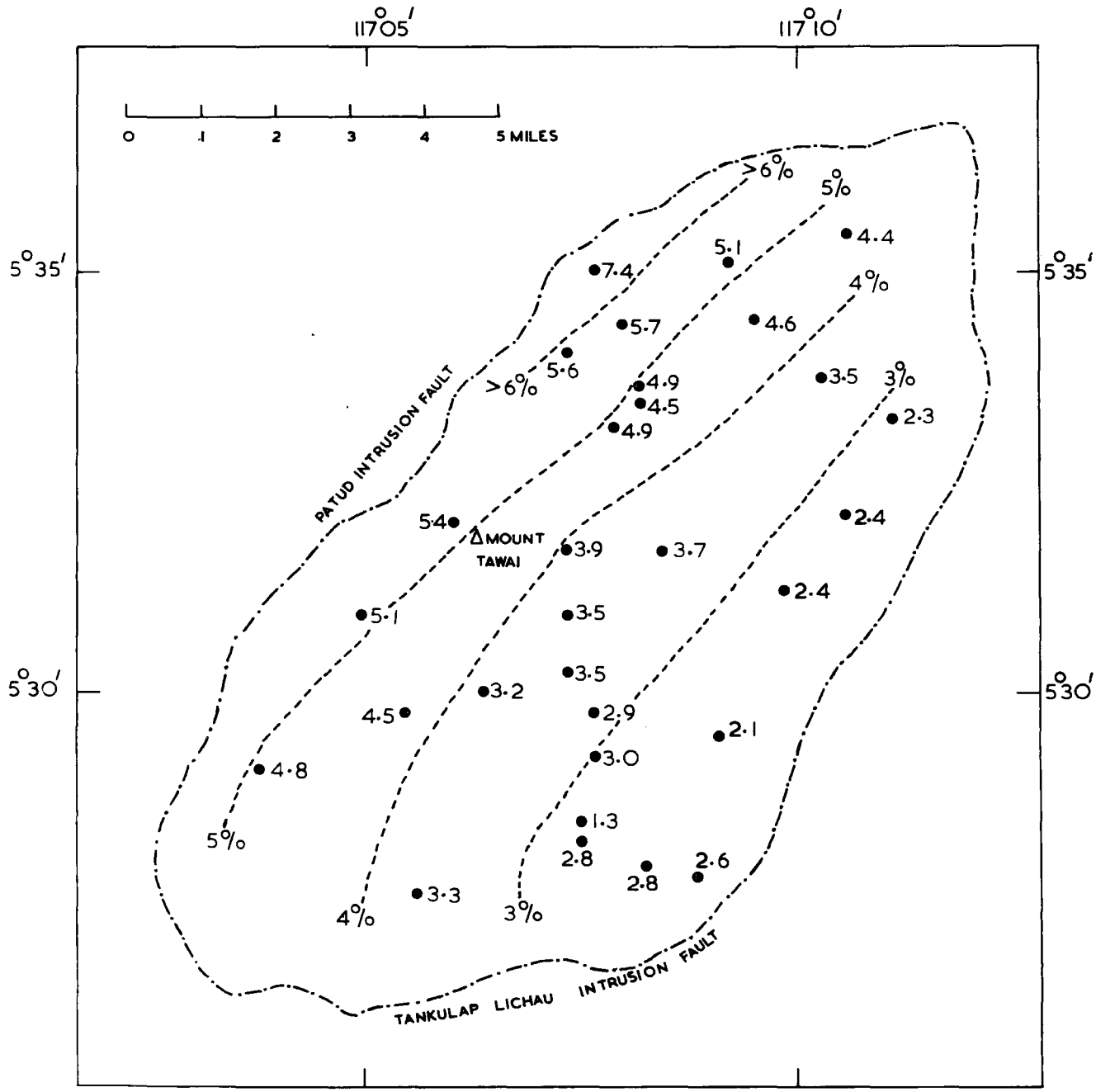

AL_2O_3 VARIATION IN THE ORTHOPYROXENES OF THE MAIN TAWAI BLOCK.

Fig.90.

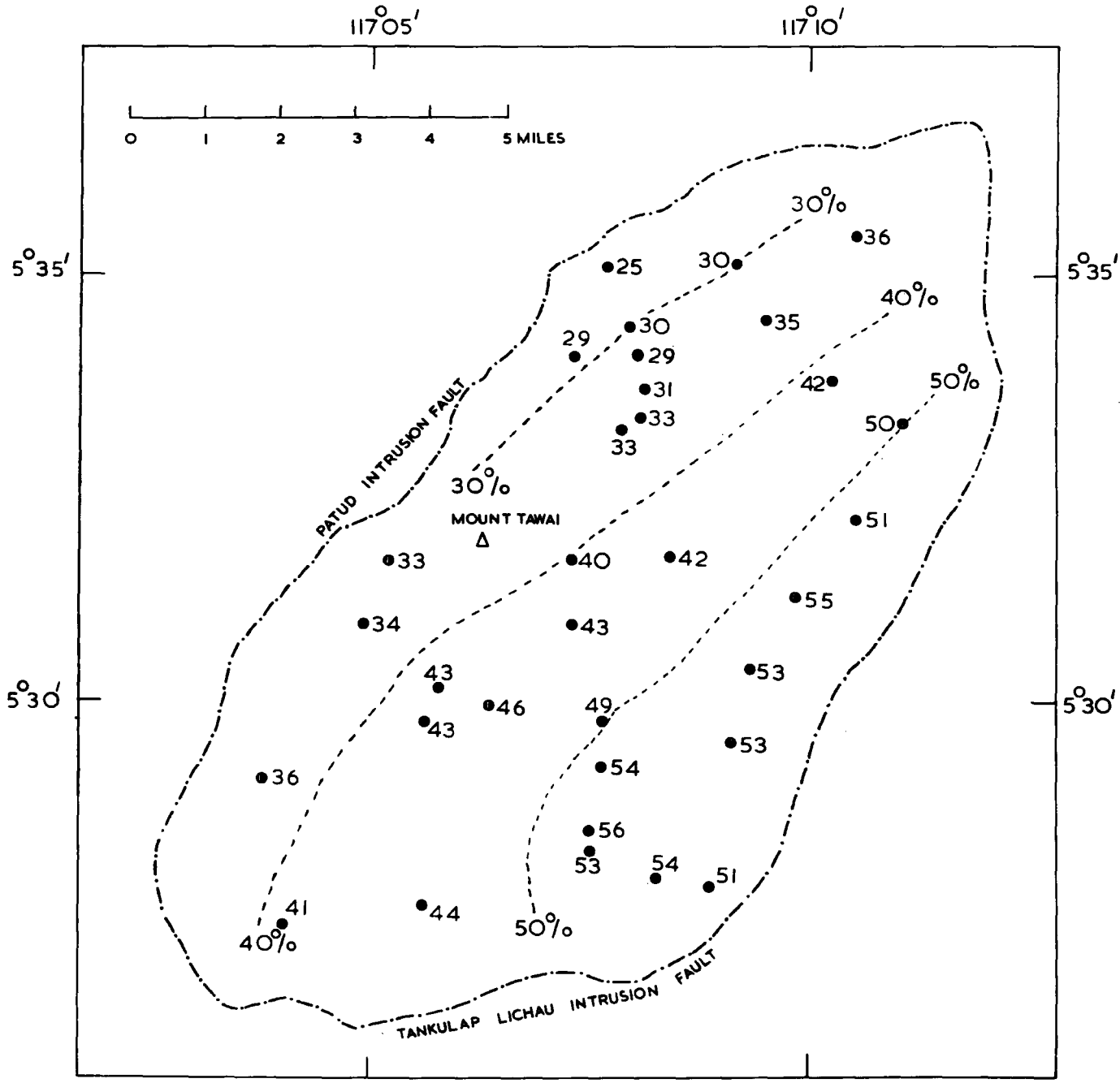

Cr_2O_3 VARIATION IN THE CHROMITES OF THE MAIN TAWAI BLOCK.

DURHAM UNIVERSITY SCIENCE LIBRARY 13 AUG 1964

Chromium spinel.

The analyses and X-ray diffraction data of the chrome spinels indicate a wide variation in Cr_2O_3 and Al_2O_3 content. The results of these studies have been plotted on the outline map of the main Tawai block, Fig. 90, and a decrease in Cr_2O_3 content in a westerly direction is noted. Approximate contours have been drawn and they are slightly oblique to the main trend of the Tawai block and sub-parallel to the contours of the alumina in orthopyroxene curves.

In Fig. 91 the alumina content of the orthopyroxenes is plotted against the chromium content of the spinel for the dunite-peridotite pairs examined. The graph shows that orthopyroxenes poor in Al_2O_3 co-exist with chrome spinels relatively rich in Cr_2O_3 and therefore relatively low in Al_2O_3, whilst the reverse is true for aluminous orthopyroxenes which co-exist with alumina-rich and chromium-poor spinels. O'Hara (1963) has pointed out that the data given by Ross et al (1954) for co-existing orthopyroxenes and chrome spinels from intrusive peridotites and olivine nodules in basalt also show a similar relationship. He also points out that the Norwegian peridotites contain low alumina orthopyroxene and low alumina spinel and agree with the above correlation. The variation from high chrome low alumina spinels to low chrome high alumina spinels has also been reported from the Holguin and Sagua de Tanamo district of Cuba by Thayer (1946) and from the Zambates range in the Phillipines by Fernandez et al (1957) but unfortunately no determinative work on the pyroxenes has been carried out. It is of importance though that the Cuban deposits mentioned above occur in dunite (Thayer 1946 p.213) regardless of the spinel composition. Both in the Phillipines and Cuba the high alumina spinel occurs near gabbro whilst the high

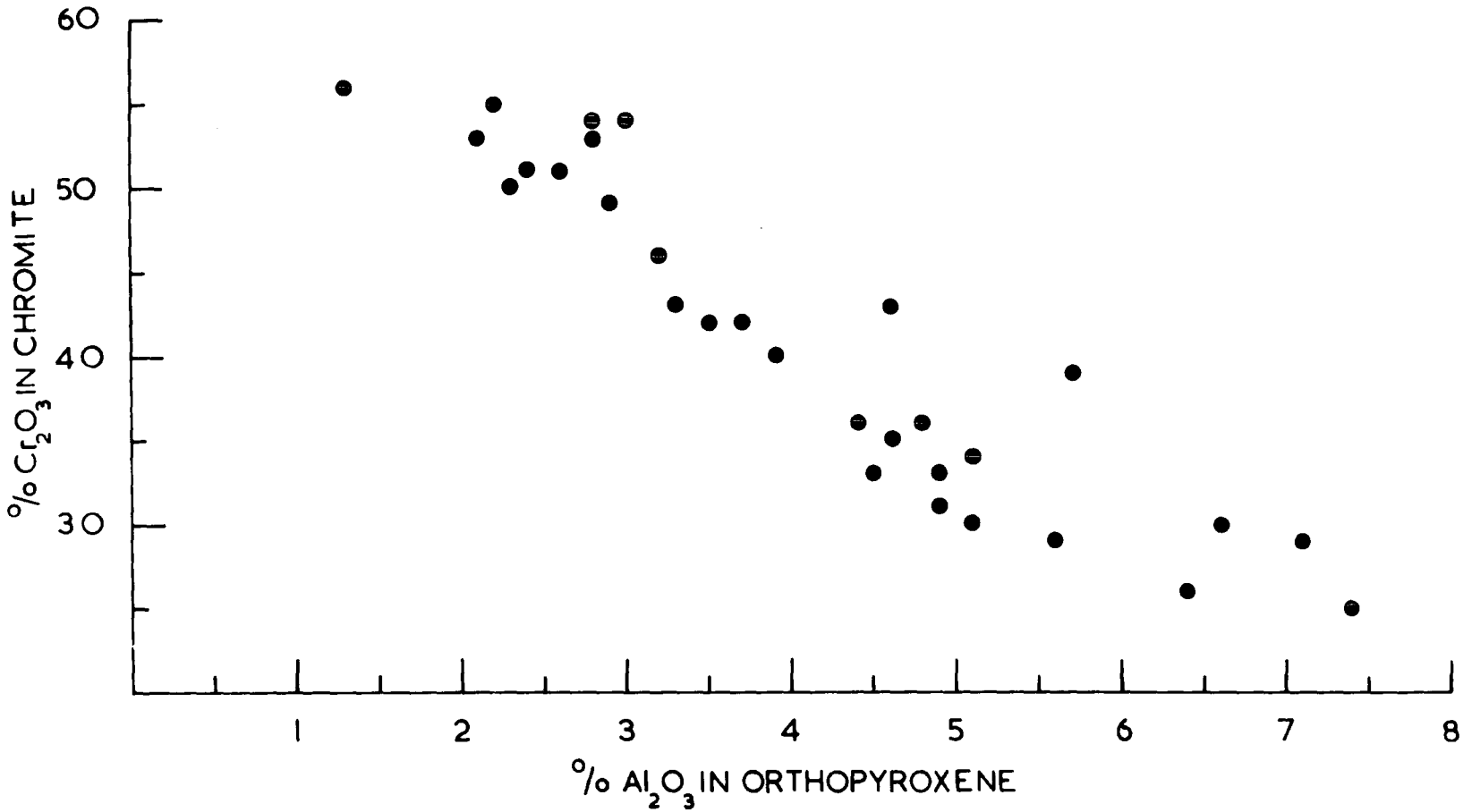

VARIATION OF Cr_2O_3 CONTENT OF CHROMITE WITH Al_2O_3 CONTENT OF ASSOCIATED ORTHOPYROXENE.

Fig. 91.

Cr_2O_3 ores are located in the centre of ultrabasic bodies.

The overall mineral variation in the main Tawai block may therefore be summarised as

Eas
Western flank. Low alumina orthopyroxene and clinopyroxene - high Cr_2O_3 chrome spinel.

Wes
Eastern flank. High alumina orthopyroxene and clinopyroxene - low Cr_2O_3 chrome spinel.

The mineralogy of the Patud, Binalik and Pantagaluang tectonic units has not been studied in sufficient detail to establish a spinel pyroxene trend. Preliminary results indicate the Patud and Binalik units contain aluminous pyroxenes comparable with the upper (high alumina pyroxene, low Cr_2O_3 spinel) and intermediate range found in the main Tawai block whilst those from the Pantagaluang fall in the lower part of this range.

Olivine gabbro - Pyroxene gabbro.

Two types of gabbro have been located in the Mount Tawai igneous complex and their mineralogy is compared in the following table.

	Olivine Fo%	Opx En%	Cpx Ca - Mg - Fe	Plagioclase An%
Olivine gabbro -	84	81	43.5-51.5-5	70
	86	84	45-44.5-10.5	80
Pyroxene gabbro -	ab.	75	44 - 45 - 11	68
		1	1	
		77	43.5-42 - 14.5	57

The ultrabasic rocks, olivine gabbros, and pyroxene gabbros form a series in which the olivines and pyroxenes show a decrease of the $\frac{Mg}{Mg+Fe}$ ratio. In the gabbros there is also a decrease in the anorthite content of the plagioclase when passing from olivine gabbro to pyroxene gabbro. The thin feldspathic bands found in the peridotite (specimens 271, 270, Table 22) form an intermediate phase between the ultrabasic rocks and the gabbros. Although the Fo content of the olivine and the En content of the enstatite is similar to that of the peridotite the feldspar present is anorthite. The X-ray diffraction data indicate that the orthopyroxene of the feldspathic bands contains relatively low alumina whilst the pyroxenes of the gabbro are also low in alumina.

It must be stressed that although peridotite, feldspathic peridotite, olivine gabbro, and pyroxene gabbro form a natural series nowhere in the field can they be found in that order. Moreover, when the gabbros and peridotite are seen in juxtaposition a sharp contact separates them and only occasionally can a gradational phase be seen. These features plus the dominance of the ultrabasic rocks over the basic gabbros is a characteristic of the Alpine type peridotites.

THE PETROGENESIS OF THE BASIC AND ULTRABASIC ROCKS.

The field evidence.

The interpretation of the pre-intrusive, pre-serpentinisation history of the Mount Tawai complex depends largely upon the significance of the dunite lenses and bands formed within the peridotite. These structures may be interpreted as follows:-

(1) Primary igneous banding.

(2) Bands and pods streaked out during crystalline flow.

(3) Metasomatic bands.

The rudimentary gravity stratified chromite bands in the type one dunites are indicative of an accumulative origin. Similar chromite bands have been described from Alpine type ultrabasic intrusives by Dunham et al (1958) and Rothstein (1957). Both at Hangha and Mount Tawai the chromite bands are not as sharply defined as those seen in the classical stratiform complexes. The type two dunites of Mount Tawai show little evidence of gravity accumulation, the spinels occurring as blotches or in thin bands. Similar evidence has been recorded from the Zambates range in the Phillipines by Peoples et al (1958) who noted that layering in dunite is better developed near metallurgical ore (high Cr_2O_3) than near refractory ore (high Al_2O_3). In the Tawai area this is partly a reflection of the higher specific gravity of the Cr_2O_3 rich ores than the Cr_2O_3 poor spinels and also of the fact that a great deal of the latter type is interstitial to olivine and pyroxene.

The lens shaped nature of the dunite outcrops could be attributed to streaking and during emplacement of a crystalline or near-

crystalline intrusion. The gneissose foliation in the peridotite was almost certainly developed during emplacement in the near-crystalline state yet this structure is often discordant to the dunite lenses. Moreover dunite lenses are present when the gneissose foliation is absent. Non-deformed textures in the dunite and associated wall rock from many localities are also indicative of a non-tectonic origin for the lenses. It is difficult to imagine the delicate orthopyroxene coronas seen around the spinel, shown in Fig. 66, being preserved in a dunite lens formed by streaking out. Bowen and Tuttle (1949) suggest that if water vapour undersaturated with SiO_2 were passed through a crack in pyroxenite the rock adjacent to the crack would be converted to dunite. This theory when applied to the Mount Tawai dunites does not explain the concentration of chrome spinel in the dunite nor does it explain the chemical changes found in the spinel.

The chromite bands in the type one dunites largely favour the first hypothesis. If this is accepted then the bands must have formed in a near horizontal position and their present attitude attributed to tilting during emplacement of the complex. The lenticular and irregular shape of the dunite may be explained by olivine and spinel accumulating in hollows and channels on the floor of a pile of already precipitated minerals. The minor swirls and folds in the chromite bands are explained by slumping since no intense brecciation of the olivine or chromite is found. Structures resembling wedge bedding may be cited as evidence for current action.

The evidence from the gabbro is less clear. Ophitic texture and orthopyroxene rims around olivine indicate the gabbro has crystallised from a magma. Recently Mackenzie (1961) has interpreted

the gabbroic rocks of the Tunaquillo complex as metamorphosed country rock but his hypothesis has been seriously challenged by Thayer (1961). In the Mount Tawai complex gneissose textures predominate in the pyroxene gabbro but occasionally non-cataclastic banded textures are seen in the olivine gabbro. On the available evidence it is difficult to tell whether this banding is due to flowage of the magma or accumulative processes. However the gabbro outcrops are small in the Tawai area but further north in the Zambates range of the Phillipines, where larger amounts of gabbro occur, Rossman et al (1957) has described layering in gabbro containing structures that resemble unconformities and channels in sedimentary rocks.

The dunite dykes and irregular shaped intrusive bodies are a major problem. Similar occurrences in Cyprus have been interpreted by Wilson (1958) as being formed from peridotite by a metasomatic process involving progressive extraction of SiO_2 during the passage of undersaturated water vapour. Such an hypothesis invokes introduction of chromium spinel, for both in Cyprus and Mount Tawai chromite segregations are found in the intrusive dunites. It seems more likely that the dunite intrusives are merely dunite pods that after accumulation have been mobilised, probably during the first stages of emplacement, and intruded as a mush of olivine and chromite. The latter mineral is usually brecciated but the former only shows slight signs of deformation. This can only be explained if the olivine was surrounded by a thin film of intergranular fluid that has since been expelled.

The large irregular bunches of clinopyroxenite have Mg/Fe ratios lower than the clinopyroxenes found in the enclosing peridotite but

similar to those found in the gabbros. Trace element data also suggests a connection between the pyroxene of the gabbros and the diopsidic pegmatites. The clinopyroxenite bunches seldom enclose chrome spinel and it is suggested they represent clusters of pyroxene crystals that sank through the mush of accumulated crystals during crystallisation of an overlying gabbroic fraction.

The field evidence in general supports the idea that the ultrabasic rocks are accumulates, and this is supported by the mineralogical changes found in the spinels and pyroxenes. The nature and origin of the parent magma is discussed in the next section.

The nature and differentiation of the parent magma.

The two chief hypothesis on the nature of the parent magma from which Alpine type peridotites are derived are those of Hess (1938) who postulates a primary ultrabasic magma and those of Bowen (1949) who considers they are differentiates of basaltic magma. The arguments for and against these hypothesis are well known and need not be repeated in detail here. They are ably summarised in Turner and Verhoogen (1961, Chapter 11).

The main objections to the hypothesis of Hess is that ultrabasic lavas are not found at the surface and that ultrabasic magmas can only exist at very high temperatures. The view of Bowen is opposed by the evidence that large scale differentiates of gabbroic composition are not found in association with the Alpine type peridotites. Differences in mineralogy between Alpine type peridotite and the basal zone of complexes derived from basaltic magma have been shown in the previous sections and may be cited as further evidence

against the hypothesis of Bowen.

In the Mount Tawai complex the area of gabbroic rocks present is less than one per cent of that of the peridotite. However mistakes in petrogenetic interpretations are easily made through consideration of too small an area and the regional picture should be taken into consideration. In the Labuk area as a whole the gabbroic fraction is about ten per cent, in the Segama area to the south (Fitch, 1955) and the island region to the north (Fitch, 1960) it is around thirty per cent, and in the Phillipines about forty per cent. In no part of this long peridotite belt does the gabbroic fraction amount to ten times that of the ultrabasic's present; which is the amount of differentiate required if the peridotites are to be considered derived from a basaltic parent. The gabbro peridotite contacts are always sharply defined and only rarely can a gradational zone of feldspathic peridotite be found separating them. Moreover the gabbro and peridotite are usually interbanded in a haphazard manner and cannot be divided into a series of units as in the classical stratified complexes.

The presence of the gabbroic portion of these Alpine type peridotites should not then be overlooked in theories involving petrogenesis. Very few examples may be cited where gabbro is entirely absent from a belt of ultrabasic rocks. The dunite lenses found in the Kambui schists of the Kenema district, Sierra Leone, (Dunham et al 1958) could be cited as such an example.

The only known basic rock capable of differentiation into gabbroic peridotite fractions comparable with those found in the Labuk area, and Alpine peridotites in general, would be one of picritic composition.

Drever (1956) from his studies on Ubekendt Ejland suggested that widespread picritic magmas may exist, However picritic rocks are notably absent in large quantities from most orogenic zones. Hess (1960, p.239) suggests that the peridotites of Venezuela are derived from upper mantle material. The exact nature of this upper mantle material is not known and hypotheses vary from chrondritic rocks (Vinogradov, 1961), eclogite, (Birch, 1952) and garnet peridotite (O'Hara, 1964). Besides a different magma type from that which gave rise to the layered stratiform complexes, a different mechanism of differentiation is also required to explain the sharpness between the gabbroic and ultrabasic fractions of the Alpine type peridotites.

An interesting experiment involving the zone melting of chrondritic material has recently been reported by Vinogradov (1961). A cylinder 12 cm. long and 1 cm. in diameter containing a fine powder of the silicate fraction of a chrondritec was baked to 1200°C and subjected to zone melting at 1600±50°C. Zone melting involved heating a narrow zone at one end of the cylinder to fusion and then moving the heater on slowly so that the meniscus of the liquid phase passed over the solid phase. After repeating the process many times a refractory phase and a fusible phase were produced. On cooling the material was examined and the fusible phase proved to be basaltic glass with pyroxene crystals and the refractory phase mainly rod-like olivine crystals. The refractory phase produced was much larger than the fusible one. Vinogradov postulates the mantle is made of chrondritic material and is differentiated into basaltic magma and dunite by melting out and de-gassing, a process he considers analogous to zone melting. Zone melting of chrondritic material

may therefore be an important process in the petrogenesis of Alpine type peridotites for it provides a mechanism by which two contrasting phases may be produced and one in which the basaltic fraction is less than the ultrabasic one. However the field and petrographic evidence indicate that the Mount Tawai complex, and many other Alpine type peridotites have passed through an accumulative stage and it is difficult to interpret them using Vinogradov's hypothsis without considerable modification.

Recent advances relating to the system $CaO-MgO-Al_2O_3-SiO_2$, which contains the system diopside-forsterite-anorthite and anorthite-forsterite-silica also throws some light on a mechanism by which the gabbroic and ultrabasic fractions of a magma may be separated. The major difficulty in interpreting the Mount Tawai assemblages in terms of this system is the absence of plagioclase from the bulk of the ultrabasic rocks. As the system stands at the moment it is impossible to arrive at an enstatite, diopside, forsterite, spinel assemblage without involving anorthite. Rothstein (1961) suggested that high pressure causes depression of the liquidus temperatures to the point where the spinel and diopside fields become contiguous. Yoder and Chinner (1960, p.80) have shown that in the system grossular-pyrope at high water pressure (PH_2O = 10,000 bars) that anorthite and forsterite are incompatible and pyroxene solid solutions and spinel may exist at the liquidus. Yoder and Tilley (1961, p.108) conclude that the assemblage anorthite-forsterite is unstable at very high load pressure. There is, then, reasonable experimental evidence to support Rothstein's hypothesis. He points out however that the effect of high pressure on the system $CaO-MgO-Al_2O_3-SiO_2$ will not totally exclude anorthite and he further

envisages that if the temperature interval between the crystallisation of olivine and pyroxene on the one hand and plagioclase on the other is made sufficiently large then it is possible for the ultrabasic fraction to crystallise completely before anorthite. In applying these principles to the Dawros peridotite he concludes that the magma from which it precipitated was a water-rich basaltic type. The existence of a feldspathic phase at Dawros has been recognised by Leake (1964). However, it cannot be agreed that the original magma was basaltic for there is not enough differentiate to account for the peridotite. However the principle of differentiation outlined by Rothstein could well apply to a more basic magma.

The overall variation in the mineralogy of the main Tawai block may be represented in the tetrahedron CaO (MgFe)O-Al_2O_3-SiO_2 and the adjoining plane (MgFe)O-Al_2O_3-Cr_2O_3. A perspective diagram, after O'Hara and Mercy (1963) is given in Fig. 92. The latter authors used this diagram to illustrate the difference in the pyroxene spinel assemblages of Alpine type peridotites (low Al_2O_3 pyroxenes - high Cr_2O_3 spinels) and nodules in basalt (high Al_2O_3 pyroxenes, low Cr_2O_3 spinels). (At the time of O'Hara and Mercy's publication the information regarding the Lizard and Turaquillo assemblages was not in print.) These variations are almost exactly those seen in the main Tawai block as it is traversed in a westerly direction. Assemblages A,A,A, in Fig. 92 represents the compositions of the low Al_2O_3 pyroxenes and high Cr_2O_3 spinels and assemblage B,B,B, represents the high Al_2O_3 pyroxenes, low Cr_2O_3 spinels. The movement of the two pyroxene-spinel composition plane may be ascribed to temperature, pressure, or a crystallisation sequence.

A great deal of experimental and theoretical work has been

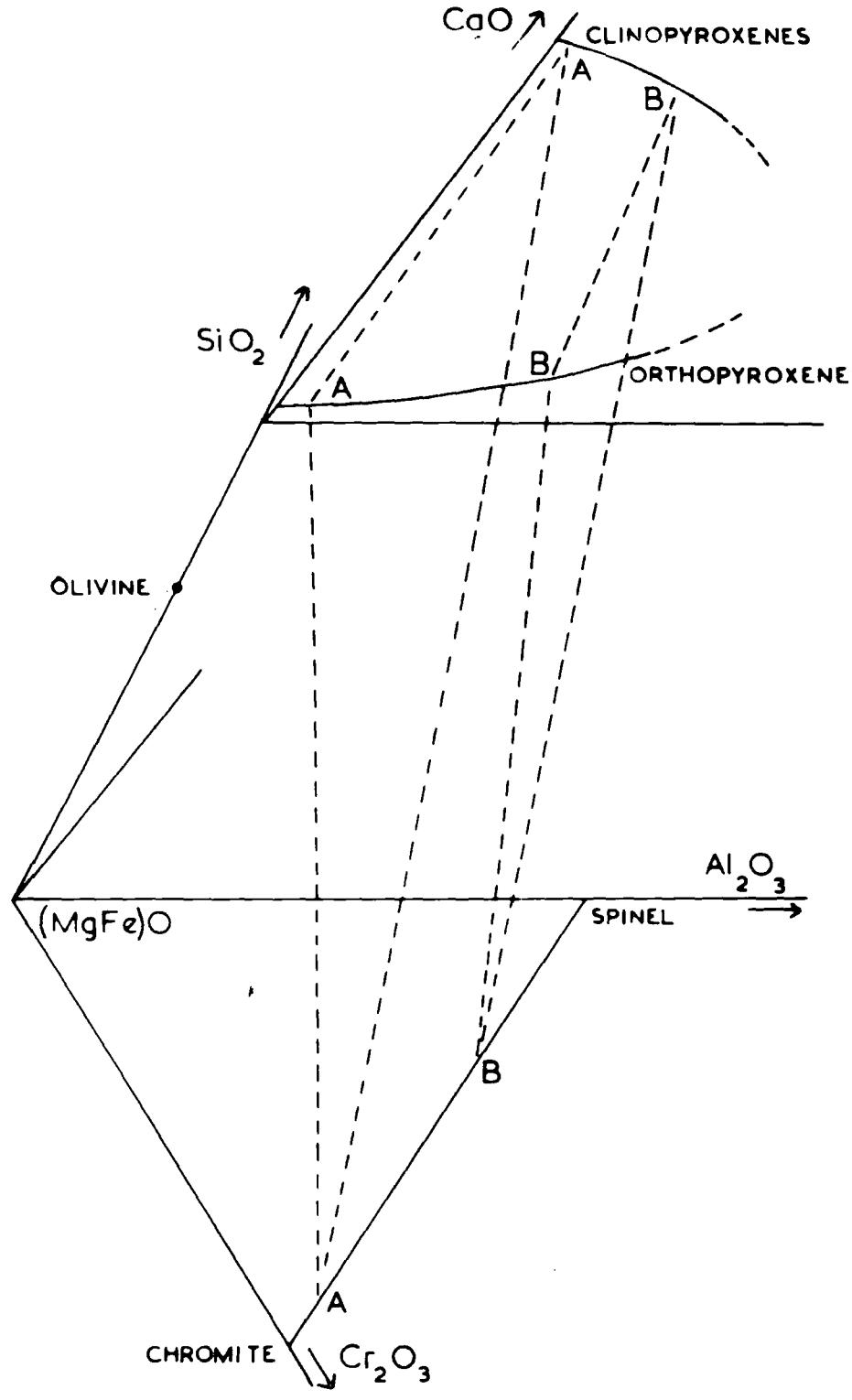

Fig.92. Perspective diagram of part of the tetrahedron $(MgFe)O-Al_2O_3-CaO-SiO_2$ and the adjacent system $(MgFe)O-Al_2O_3-Cr_2O_3$.

carried out on pyroxene systems. Following Bartholomé (1961) and Kretz (1961) the small differences in the distribution co-efficient K(T) between the co-existing pyroxenes suggests temperature was constant during the crystallisation of the aluminous and non-aluminous assemblages. It therefore appears that temperature variations does not control the movement of the plane AAA to BBB (Fig. 92).

That pressure is the controlling factor is suggested by the work of Boyd and England (1961) and would therefore imply an increasing pressure gradient extending across the main Tawai block from east to west. As the eastern edge is interpreted as being towards the base of the original magma chamber this would imply a pressure gradient increasing upwards from the floor. Green (1964) has postulated that the primary assemblage of aluminous orthopyroxene, aluminous clinopyroxene, spinel and olivine of the Lizard peridotite is a direct consequence of the high load pressure of the initial crystallisation and that the recrystallised assemblage of low alumina pyroxene, olivine and spinel is due to recrystallisation at low load pressure of the original primary assemblage. The presence of plagioclase in the recrystallised rocks is attributed to the reaction in which the aluminous pyroxenes recrystallise to normal pyroxenes and anorthite. Little evidence for recrystallisation of the pyroxenes of the Mount Tawai ultrabasic rocks can be found and plagioclase is nearly always absent. Green's interpretation of the Lizard assemblage cannot be applied to the Tawai area.

Very little is known about the pressure temperature conditions influencing the introduction of alumina into the spinel structure. Vinogradov (1961) states that the substitution of Al^{+3} by Cr^{+3} has little effect on the melting point of various chrome spinels. The

system Cr_2O_3-MgO-SiO_2 has been investigated by Keith (1954) who shows that from a liquid of suitable composition pichrochromite, proto-enstatite and cristobalite crystallise at a ternary eutectic at 1546°C. The adjoining plane Al_2O_3-MgO-SiO_2 investigated by Rankin and Merwin (1918) shows forsterite, spinel and cordierite crystallising at 1370°C. Neither system is adequate to explain th six component system CaO-MgO-FeO-Al_2O_3-Cr_2O_3-SiO_2 found in the Mount Tawai ultrabasic rocks.

Chromites rich in normative spinel have been reported by Thayer (1946), Smith (1958), Stoll (1958) and Rossman (1959) as occurring in ultrabasic rocks near gabbro boundaries and have been interpreted as due to reaction between anorthite and olivine. Osborn and Tait (1952) show that at temperatures above 1320°C liquids of suitable composition intermediate between anorthite and forsterite, will on cooling, form a transient spinel phase. In this system if equilibrium conditions are maintained spinel disappears with further cooling and it can accumulate only if removed by crystal settling. This spinel however willcontain little chromium. Bowen (1928, p.280) has suggested that if spinel is not removed and reacts with the liquid plagioclase and olivine are formed but any Cr_2O_3 present will be thrown out. Bowen also points out that reaction of basaltic liquid with spinel will give only plagioclase and olivine and Cr_2O_3 is thrown out and is seen as picotite grains. Both Stoll (1958) and Thayer (1946) cite evidence of plagioclase rims between olivine and chromite as evidence of this reaction. In the Masinloc deposit described by Stoll (1958) plagioclase rims around chromite are not always found and it must be doubted that the reaction postulated by Bowen could account for the magnitude of the Masinloc

deposits, individual ore bodies of which measure 1800 feet long, 950 feet wide and 175 feet thick. Small ore bodies of high alumina chromite also occur in the Beeston range described by Bailey (1963) at a gabbro peridotite contact.

The absence of plagioclase from the Beeston deposits and from the small chrome patches seen in the Mount Tawai type two dunites argues against an origin involving Bowen's hypothesis. The petrographic evidence from the type two dunites show that the aluminous chromite nearly always occurs in anhedral patches between olivine grains. Euhedral chromite grains are absent from the Masinloc and Beeston ores. The thin bands of chromite pyroxenite found in some of the type two dunites show anhedral chromite has crystallised between tabular pyroxenes and in places appears to replace them. These bands together with the interstitial patches confirm the opinion that most of the aluminous chromite has crystallised in situ after precipitation of olivine, orthopyroxene and clinopyroxene. These interstitial chromites may be explained by:-

(a) Precipitation from a residual liquid rich in Al_2O_3 and Cr_2O_3.

(b) Immiscible liquid segregation.

(c) Resolution of earlier precipitated chromite.

(d) Growth of settled chromite involving diffusion.

(e) Exsolution processes.

Residual liquids rich in Cr_2O_3 have not been reported in the experimentally investigated systems involving Cr_2O_3. Schairer and Yagi (1952) in an investigation of the system $FeO-Al_2O_3-SiO_2$ report a near terminal point of crystallisation involving fayalite, iron

cordierite, and hercynite, and indicate that iron-rich spinels are soluble in silica bearing liquids. Fockema and Mendelssohn (1954) postulate a residual Cr-rich liquid to explain the cross-cutting veinlets of chromite in the Bushveld. There is no direct experimental evidence to suggest that crystallisation of a melt of suitable composition will lead to residual concentration of Cr and Al, but nevertheless the large deposits of the Masinloc type might be best explained by such a process.

It may also be suggested that the interstitial chromite represents a Cr enriched liquid that has separated by immiscible liquid segregation from the original melt and has later crystallised in situ between then olivine grain boundaries. Such an hypothesis is not easy to prove and it would be difficult to understand why the early formed chromite accumulated as sunken crystals. In the phase diagram of the system $MgO-SiO_2-Cr_2O_3$ investigated by Keith (1954) a two-liquid region occurs at high values of the ratio $Cr_2O_3-+SiO_2:SiO_2$. Fisher (1950) describes an experiment in which melts made from gabbro and chromite separated into a Cr-rich liquid and a Cr-poor liquid at 1400°C and the former on crystallisation yielded chromite and olivine.

Not all of the alumina rich chromite is anhedral for occasionally small euhedral and sub-euhedral grains are found and it may be suggested that the large anhedral patches have grown from these by adcumulus growth. Adcumulus growth would involve diffusion from the overlying melt or from within the already crystallised part of the magma. Hess (1952) has suggested that diffusion controlled by temperature gradients, set up by cooling from the top and bottom of the original magma chamber, may result in growth of minerals after

crystallisation. Rothstein (1961) has suggested that adcumulus growth involving diffusion from an overlying melt has played an important part in the petrogenesis of the Dawros peridotite. The role of diffusion is difficult to estimate but if it has occurred then no evidence of growth has been found, indicating constant temperature conditions.

An alternative process would be resolution of already deposited chromite. If chrome spinels reacted with trapped interstitial liquid after settling to produce a Cr-rich liquid then on cooling chromite would be precipitated.

Yet another hypothesis is that the high alumina chromite has been exsolved from one of the silicate minerals. Examples of possible exsolution of spinel from olivine and clinopyroxene have been quoted earlier. The euhedral spinel enclosed in orthopyroxene could also be cited as evidence. There is however, no mineralogical data that indicates that large amounts of Cr can be dissolved in olivine, orthopyroxene, or clinopyroxene. Clinopyroxenes containing up to 1.2 weight per cent have been described by Hess (1949, p.647, No.5) but a great deal more is obviously necessary.

Of these (a) and (b) are the most plausible but none can be entirely ruled out.

The most rational conclusion from the variations in the mineral assemblages would be that they represent a crystallisation sequence in which the alumina content of the two pyroxenes and the spinel gradually increases. However as the K(T) distribution co-efficient of the co-existing pyroxenes and the Mg/Fe ratio in the olivine and pyroxenes is constant it cannot be proposed that falling temperature accompanied the changes. It also seems unlikely that a pressure

gradient increasing from the top to the bottom of the original magma chamber could exist thus accounting for the more aluminous pyroxenes on the western side of the main Tawai block. The crystallisation was probably accomplished under isobaric and isothermal conditions. Most petrologists agree that the most likely source of a magma of predominantly ultrabasic composition would be in the mantle below the Mohorovicic discontinuity. It seems most probable that the Mount Tawai complex, and Alpine type peridotites is general, have been formed from a melt of upper mantle material at very high temperature and pressure. The temperature and pressure were probably so high that anorthite could not form but enabled alumina to be dissolved in the pyroxenes when it became available. The first spinels formed were the chromium-rich varieties followed by the more aluminous varieties with advancing crystallisation. The abrupt change from gabbro to peridotite may be explained by a fall in temperature and possibly pressure which enabled plagioclase to form and was accompanied by a fall in the Mg/Fe ratios of the olivines and pyroxenes. Ringwood and Green (1963, p.941) suggest that plagioclase assemblages are not stable at depths below 50km. and temperatures in excess of 600°-700°C.

The ultrabasic and basic rocks of the Mount Tawai complex are therefore considered to have formed originally in a magma chamber in the upper mantle and to have been precipitated from a melt derived by fusion of upper mantle material. A major problem with the hypothesis however, is the relative absence of inter-precipitated minerals in the ultrabasic assemblages. Occasionally both pyroxenes and spinel are seen as inter-precipitate minerals but usually in the non-deformed specimens an interlocking texture is found between the

main minerals. Olivine and both pyroxenes both appear to be of primary precipitate origin. Wager (1958) indicates that any crystal accumulate at the time of formation would be accompanied by between 40% and 60% of interprecipitate liquid. The composition of the pore liquid material will have the composition of the liquid existing at that time. Both Hess (1960) and Wager (1958) suggest that diffusion from the overlying melt will cause adcumulus growth of the precipitated minerals and therefore a reduction in pore space must occur. The weight of the overlying accumulate would also cause interprecipitate liquid to migrate upwards. If such an hypothesis can be used to explain the absence of interprecipitate minerals then the present interlocking texture may be attributed to recrystallisation or sintering together of the accumulated crystals under the influence of interfacial tension. The latter process is suggested by Voll (1960).

The exact nature of the parent magma of the Mount Tawai and similar complexes is mere speculation on the nature of the upper mantle. The requirement is that this material should be capable of differentiating into a minor gabbroic phase and a major peridotite phase. The fact that the gabbroic phase associated with these complexes is variable in amount suggests the source has a variable composition; although it may be partly explained by tectonic processes during intrusion after differentiation. It may be argued that the peridotite represents the basal zone of a layered basic complex derived from basaltic magma but this would require that large intrusions of this type are present under most orogenic zones.

Geological thought in general favours the idea that the Mohorovicic discontinuity represents a gradation from the basic rocks of the

crust to peridotite and dunite of the mantle. Ringwood (1962) suggests these pass down into a more primitive material he calls 'pyrolite', which is thought to consist of three parts of dunite to one of basalt. The pyrolite in turn grades downwards into garnet peridotite through a transitional phase. He suggests feldspathic pyrolite may exist directly below the Mohorovicic discontinuity in the upper mantle of oceanic areas. Ringwood (1959) has calculated an average mantle composition from chrondritic evidence and finds there is close agreement between the chemical composition of this and a pyrolite (Ringwood and Green, 1963, p.939). The pyrolite composition was calculated from average dunite and basalt, analysis 10a. Green (1964) has recently advocated that a melt having the composition of the Lizard peridotite did primarily exist at depth and has given rise to the ultrabasic rocks of that area. The fact that a large body of gabbro almost a third of the size of the peridotite is found in the locality, however, leaves Green's interpretation open to doubt. The nodules in basalt contain assemblage varying from gabbroic to peridotite in composition and may be interpreted other than xenoliths of the mantle. O'Hara and Mercy (1963) argue on theoretical considerations involving the geothermal gradient that Alpine type peridotites, and some or all of the peridotite nodules in basalt, cannot be unaltered representatives of the composition and mineral assemblages of the upper mantle. O'Hara and Mercy suggest that the most likely material forming the upper mantle would be garnet peridotite. Garnet peridotite xenoliths in kimberlite pipes favour this idea.

The available field data from the Borneo ultrabasic belt indicates the ratio of peridotite, dunite, and gabbro to be 15.1.4.

An average gabbro composition has been calculated from specimens R38, R24, J202, NB 10,337, an average peridotite composition from T58 and T364 and T48 taken as an average dunite. (All on a water free basis). A composite analysis of the three averages has been computed using peridotite, dunite and gabbro in the ratio 15.1.4. and is shown in Table 34; and compared with Ringwood's (1959) mantle composition from chrondrites. There is general agreement between the two, the main differences being in the higher magnesia and soda of the chrondrite composition. The pyrolite composition of Ringwood and Green (1963) is also compared and has higher magnesia and lower alumina. If Ringwood's estimates of the average mantle composition are acceptable then the above calculation suggests that the Borneo ultrabasics could be derived from material below the Mohorovicic discontinuity.

Yoder and Tilley (1962) have rejected the idea that the upper mantle is formed of eclogite on the grounds that they consider this rock to be a derivative of some other rock type.

Further speculation on the nature of the upper mantle is beyond the scope of this thesis. It is concluded that the Mount Tawai complex has been formed by fusion of the upper mantle and differentiated initially at high temperatures and pressure into a minor gabbroic phase and major peridotitic phase.

Table 34. Comparison of composite analysis with possible mantle material.

	1. Average gabbro.	2. Average peridotite.	3. Dunite.	4. Composite.	5. Mantle Comp. from Ringwood (1959)	6. Pyrolite (Ringwood & Green 1963)
SiO_2	47.5	43.8	40.7	44.4	44.69	43.06
Al_2O_3	19.2	2.6	.4	5.7	4.09	3.99
FeO	8.1	8.6	7.6	8.5	7.81	8.15
MgO	10.6	42.0	50.6	36.2	39.08	39.32
CaO	11.1	1.8	-	3.6	3.19	2.65
Na_2O	2.1	-	-	.4	1.14	.61
K_2O	.3	-	-	.1		.22
TiO_2	1.0	.1	-	.3		.58
NiO	-	.4	.2	.3		.39
MnO	.1	.1	.1	.1		.13
Cr_2O_3	-	.6	.4	.4		.42
Total	100	100	100	100	100	100*

1. Average of gabbro analyses. Table 6.
2. Average of T58,T364.
3. T48.
4. Computed from 1,2,3, in ratio 15.1.4.
5. Mantle composition from Chordritic Model. Ringwood (1959)
6. Pyrolite 1:3 ratio of basalt to dunite. Ringwood and Green (1963).

*Includes.
P_2O_5.08.
H_2O.21.
CO.02.

THE HYDROTHERMAL ROCKS.

Rodingites.

The term rodingite was introduced by Marshall (1911) to describe dyke-like rocks intrusive into peridotite, consisting of grossular, clinopyroxene and prehnite, from the Roding river near Mount Dun, New Zealand. Miles (1950) and Bloxam (1954) have described rodingite, of similar mineralogy and occurring in similar environments to the New Zealand specimens and consider them to be garnetised gabbros.

Field Occurrence.

Numerous small dykes, veins, and irregular shaped bodies of gabbroic appearance occur throughout the Mount Tawai complex. Thin section examination shows the dyke rock is altered gabbro whose mineralogy is similar to the rodingites described by the above mentioned workers. The veins vary from a few inches wide to dykes 6' thick which pinch and swell along the strike. They cannot be traced for any great distance along the strike. The majority of these rodingites occur in the contact fault zones, intrusive into serpentinised peridotite. In hand specimen the rock varies from a normal gabbroic appearance with the feldspar a pinkish grey colour to a chalky white rock studded with green crystals. The latter specimens break with a flinty fracture and darken on exposure to sunlight.

The rodingites are best seen just within the main ultrabasic contact on the Telupid river. For half a mile upstream from the contact irregular veins, dykes, and tabular bodies are found in

sheared serpentinite. The contact sheared serpentinite is bleached white. The intrusive bodies have no common strike and frequently cross cut each other. They do not extend out into the country rock. Other notable rodingite localities are found below the main fall on the Melio river and at the main ultrabasic contact exposed by the numerous tributaries of the Lichau river. The large gabbro bodies described in a previous section also show alteration to rodingite around their margins.

Petrography.

Thin section examination of the dyke rocks has revealed all gradations from partially altered gabbro to a rock which is made up almost completely of calc-silicate minerals and which shows only a trace of subophitic texture. The following descriptions are representative of the numerous thin sections studied.

Specimen T343 was collected from the northern contact of the Telupid gabbro. The handspecimen has the texture of a normal gabbro but the leucocratic crystals are a chalky white colour. The thin sections show that the feldspar is almost completely replaced by a turbid brown amorphous material in which minute rounded colourless garnet are set. Serpentinised and partially altered olivine is present together with relatively fresh pyroxenes. The latter are slightly altered to uralitic amphibole.

Specimen T159 collected from the Telupid river section is a rock dead white in colour studded with green phenocrysts of clinopyroxene up to 15mm. long. The thin section shows the groundmass is made up almost completely of closely packed colourless garnet crystals, individual crystals measuring between .01 and .05mm. in

size (Fig. 93). The garnet has n = 1.680 and A_o=11.98 indicative of a member of the hydrogrossular series of Hutton (1943). The clinopyroxenes, individual crystals of which measure 15mm. long by 7mm. wide are colourless, ragged around the edges being replaced by tremolite, and are twinned. The clinopyroxene has a sinβ 9.340 and b_o 8.928 indicating a composition of Ca_{48} Mg_{40} Fe_{12} which is richer in the wollatonite molecule than the normal gabbro clinopyroxene. Sheaves of chlorite, irregular aggregates of epidote and veins of calcite are abundant. A brown turbid amorphous substance clouds many of the crystals.

Specimen T134, collected from a vein at the base of the main falls on the Melio river, is a fine grained dirty white rock flecked with pink and violet. In thin section it is seen to be composed of a matte of granular and columnar aggregates of epidote showing anomalous blue interference colours. Pseudomorphs of tremolite after clinopyroxene can also be distinguished. A little relict plagioclase can be made out amidst the groundmass and a faint ophitic texture is still recognisable. Green pleochroic chlorite and small nests of hydragarnet occur in the groundmass.

Specimen T288 was collected from a sheared dyke just within the main ultrabasic contact on the southernmost tributary of the Lichau river. The hand specimen is a hard light brown mottled rock containing thin white veins. The thin section shows a groundmass consisting of a felt of epidote and tremolite with occasional prehnite fans. The veins are filled with delicate fans (Fig.94) of prehnite, up to 3mm. across, showing arcuate extinction.

Fig. 93. Photomicrograph of rodingite. This rock consists of a matte of hydrogarnet crystals and plates of clinopyroxene. T159 (crossed nicols X150).

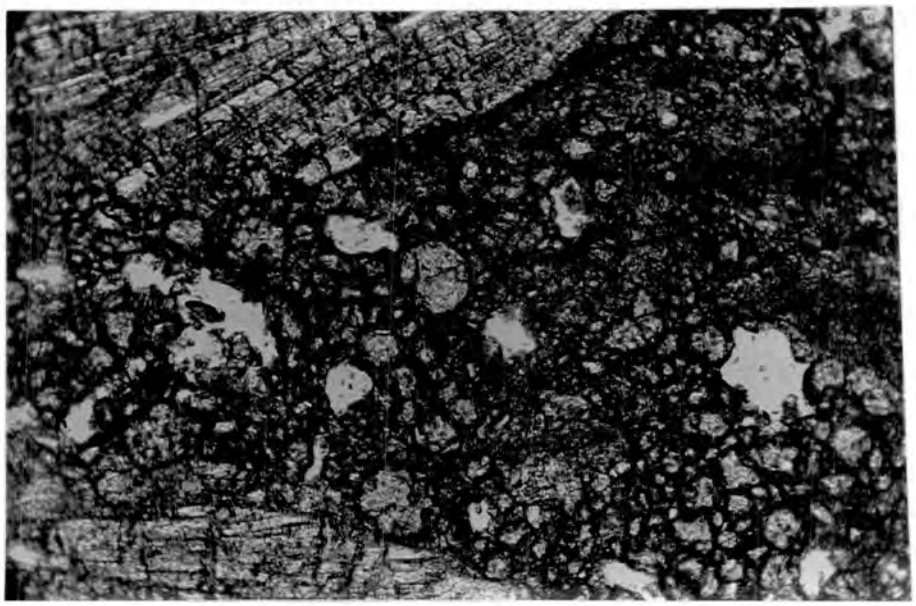

Hydrogarnet rocks.

Field Occurrence.

Irregular networks of anastomosing veins and blocks of hydrogarnet bearing rocks that cannot readily be associated with altered gabbro also occur within the peridotite. They are most commonly found in the internal breccia zones. The veins sometimes cut the breccias and at other times filled up the cracks in between the sheared peridotite. The veins seldom exceed six inches in width. Isolated blocks, up to six feet long, and four feet wide, are scarce and unevenly distributed within the batholith. A prominent block occurs in sheared peridotite two hundred feet west of the summit of Mount Tawai. The irregular networks are best seen three hundred yards upstream from the main ultrabasic contact on the northernmost tributary of the Pantagaluang river, where a stockwork six feet wide is located. The veins do not contain fragments of serpentine and are filling cracks within sheared serpentinite.

Petrography.

In hand specimen the hydrogrossular rocks have a fine grained dead white appearance and occasionally contain prominent grey brittle phenocrysts.

Specimen T331 is a typical dead white coloured vein collected from the Pantagaluang exposure. In the hand specimen individual garnet crystals up to 2mm. in diameter can be seen. In thin section the garnets are seen as rather ragged subeuhedral and euhedral dodecahedra set in a matrix of a felt of chlorite. The garnets are extensively intergrown with chlorite. The garnets are aniso-

tropic showing abnormal bluish grey interference colours, and show sector twinning (Fig. 95). They also appear to be zoned. Lozenge shaped sphene crystals are found in the groundmass and intricately intergrown with the garnet. The garnet has n = 1.725 and a unit cell dimension 11.88 Å.

Specimen T444 is part of the loose block occurring near the summit of Mount Tawai. In hand specimen it is a dead white chalky rock containing prominent greyish brittle phenocrysts. The thin section shows the groundmass to consist of small (.01 - .02mm. in diameter) closely packed colourless garnet crystals set in a turbid brown matrix. The phenocrysts, up to 4mm. in length, are a length fast chlorite having nZ=1.590 and a very low 2V. X-ray diffraction shows the mineral to be a 14 Å chlorite with a diffraction pattern similar to that of clinochlore.

Specimen T386 was collected from a chalky white vein intrusive into a breccia in the Talibu river. It consists of small (.01 - .02mm. in diameter) tightly packed garnet crystals with extremely high relief, n = 1.880, set in a dirty brown amorphous matrix. The X-ray diffraction pattern indicates the garnet is andradite. Sheaves of wollastonite and needles of tremolite occur in the groundmass. Sphene showing brown cores and buff margins is seen intergrown with the andradite.

Hydrogarnet-mineralogy.

Both the above described rocks and the rodingites are characterised by a relatively unusual garnet showing a much lower refractive index and larger a_o cell dimension than grossularite. An X-ray diffraction pattern of specimen T444 (Table 35) is similar to that

Fig. 94. Photomicrograph of prehnite fans in rodingite. T288 (crossed nicols X20).

of hibschite. This mineral is a member of the hydrogarnet series. Flint and Wells (1941) have shown from experiments with synthetic materials that there is complete solid solution between $3CaO-Al_2O_3-3SiO_2$ (grossularite) and $3CaO\ Al_2O_3\ 6H_2O$ (hydrogarnet). Only minerals in the range grossularite to $3CaO-Al_2O_3-3SiO_2-2H_2O$ are known to occur naturally and this series has been termed the hydrogrossular series by Hutton (1943). The most hydrated member is hibschite and intermediate garnet have been variously called plazolite, hydrogarnet, grossularoid and garnetoid. Yoder (1950) has shown that the cell edge increases with hydration. The cell edge of specimens were measured and are given below.

	a_o Å
Specimen T332	11.88
Specimen T444	11.92
Specimen T159	11.98
Specimen T134	11.99

Determinations were made on the diffractometer by measuring the 2θ position of the 400 reflections (2θ 30°) using silicon K, reflections at 2θ 28.44 as an internal standard. The measurements indicate a variation from close to grossularite (grossularite a_o = 11.65 Å) to hibschite (a_o = 12.0 Å).

X-ray powder photographs were taken initially but even after long exposure (24 hours) the back reflections were still weak. A diffuse halo on the photographs at d = 4Å suggests the brown amorphous material invariably associated with the hydrogarnets is opal.

Tremolite Rocks.

Field Occurrence.

Tremolitic rocks are abundant in the Mount Tawai batholith. Three modes of occurrence have been noted.

1. Small nodular masses situated around or just within the main contact.
2. Asbestiform tremolite associated with the intrusion faults and internal breccias.
3. Flanking quartz-pegmatite intrusions.

The first type is uncommon in the Tawai area. A small body of nodular tremolite is found in the "V" between the Binalik and main Tawai intrusion and is exposed in the Lichau river. It is about six feet long and four feet wideand completely surrounded by brecciated sandstone and shale. The mass is composed of felted needles of light green tremolite that grade from coarse to fine phases in a matter of inches. These nodular masses are best seen around the Bidu-Bidu intrusion in thennorthern Labuk where they form small hills around the mouth of the Bidu-Bidu river.

The second mode of occurrence is the commonest. Asbestiform actinolite-tremolite needles are found in all the fault zones. Sometimes the needles are wrapped around boulders of peridotite in the fault breccia or at other times they form zones in which the needles are aligned parallel to the strike of the disturbance. Brittle needles up to six inches in length are common and they vary from blue-green to bright emerald green in colour. They are strikingly displayed at the Melio Falls where bright emerald green needles are

found sticking to the fault face.

Tremolite flanking quartz pegmatite intrusions is also of common occurrence. In some exposures the tremolite needles are arranged parallel to sides of the intrusions, whilst in others they are unorientated. The zone of alteration seldom exceeds three feet. At the main ultrabasic contact on the Ruku-Ruku river a quartz pegmatite is found intrusive into the contact fault breccia. Plates of dark green tremolite up to 1 inch long are developed throughout the breccia.

Petrography.

Specimen T183 was collected from the nodular mass described in the upper headwater of the Lichau river. The thin section shows a fibrous matte of tremolite needles showing no preferred orientation intimately intergrown with pale green chlorite. The tremolite is a faint brown and shows $Z \wedge c$ 16° and a large 2V. Pseudomorphs of tremolite after pyroxene are distinguishable and a few scattered altered chromite crystals are present.

Specimen T363 was collected from the fault face of the Melio Falls. The thin section shows a mass of pale green tremolite plates (4mm. long, 2m. wide) and needles tightly packed together. The specimen is extremely pure and has been analysed (Table 36). The tremolite shows $Z \wedge c$ 17°, nZ=1.645 and a large 2V.

Specimen T358 is a typical asbestiform tremolite rock collected from a shear zone in the Upper Tankulap. In thin section the tremolite needles are seen to be closely packed in subparallel alignment. Tremolite needles replacing both olivine and pyroxene are seen. It is a faint brown, has a high 2V, $Z \wedge c$ 15°, and nZ=1.650. The

Table 35. Mineral Identification.

Hydrogarnet.

Sp. T444.		Hibschite Pabst 1942.		
dÅ	I	dÅ	I/I_1	hkL
4.74	40	4.89	5	211
2.98	30	3.00	80	406
2.658	100	2.68	100	420
2.536	10	2.57	20	332
2.429	15	2.46	50	422
2.332	10	2.36	40	431
2.171	9	2.19	50	521
		2.12	5	440
2.001	5	1.95	60	611,532
1.929	15	1.89	5	620
1.716	5	1.73	50	444
1.647	15	1.66	60	640
1.5900	40	1.61	80	642
1.4900	9	1.50	50	800
1.3300	9	1.35	50	840

Diffractometer. Trace.

A.S.T.M. - Hibschite.
4.6723.

tremolite is extensive, replaced by aggregates of chlorite showing anomolous blue interference colours. Minor puckers are present in the tremolite needles, and chromite granules occur along the fibre edges.

Specimen T348 was collected from the breccia on the Ruku-Ruku contact close to the pegmatite intrusive. In thin section plates, up to 3mm. long and 1mm. wide, needles and irregular aggregates of tremolite are seen set in a matrix of finely disseminated calcite, chlorite and talc. The latter two minerals are clearly replacing the tremolite. The tremolite is pale green in colour, shows excellent basal sections, has a large 2V and has nZ=1.655.

Chemistry.

The bright emerald green tremolite , specimen T363, has been analysed, the result is shown in Table 36. A little chlorite was present in the sample. In the same table the result is compared with an analysis of a chrome-tremolite quoted by Dunham et al (1950) from Dilma, Sierra Leone. The Tawai specimen is seen to have a lower MgO content than the Sierra Leone specimen and high Al_2O_3 and Cr_2O_3. The bright emerald green colour of the Tawai specimen may be correlated with its high Cr_2O_3 content. When polished it is not unlike jade in appearance.

Silico-carbonate rocks.

Field Occurrence.

The sheared serpentinite found in the internal breccia zones and the fault zones is often replaced by a hard dirty white, reddish

Table 36. Tremolite Analyses.

	Sp. T363.	Chrome Tremolite Dilma.*
SiO_2	54.2	54.9
Al_2O_3	4.5	1.2
Fe_2O_3	1.0	.5
FeO	2.1	2.8
MnO	.2	.08
MgO	22.1	25.3
TiO_2	tr	.21
Cr_2O_3	1.2	.5
NiO	.1	
CaO	12.3	12.7
NaO	.7	.6
K_2O	tr	nil
H_2O^+	)2.2	.93
H_2O^-	)	.27
Total	100.6	100.00

Sp. T363	Nos. of atoms - 24 (O,Oh,F)	
Si	7.44)	8
Al	.56)	
Al	.16)	
Ti	-)	
Fe^{+3}	.10)	
Cr	.13)	
Mg	4.51)	5.17
Fe^{+2}	.24)	
Mn	.02)	
Ni	.01)	
Na	.13)	
Ca	1.81)	1.99
K	-)	
OH	2.01)	
F	-)	2.01

* Analyst R.A. Chalmers. Dunham et. al. (1958).

T363 Melio Falls - 5° 29' 45" N.
117° 05' 26" E.

T363 Analyst W.G. Hancock.

weathering, rock. Thin sections show this rock to consist of various admixtures of calcite and amorphous or cryptocrystalline silica. All gradations between partially replaced and totally altered serpentinite are found. Many of the smaller serpentinite breccias are almost completely replaced and only a few remnants of serpentinite can be found in a hard white matrix. All other rock types have been affected by the thin type of alteration, but always in tectonically disturbed areas. Silicified and calcified gabbros, peridotites, basalts, tuffs and sediments have been recorded. The silicified rocks usually contain disseminations of sulphides, mainly chalcopyrite and pyrite. These minerals together with chalcophenite and pyrrhotite occur in small ore bodies in a silico-carbonate zone in the Bidu-Bidu Hills.

Petrography.

Specimen T139 is a typical serpentinite that has been almost completely altered to calcite and dirty brown silica. In thin section a serpentinite texture can still be distinguished by the rock consist of finely disseminated calcite and turbid amorphous silica. Black magnetite streaks outline the original serpentinite texture.

Specimen T340 is a white and pink mottled rock that in thin section is seen to consist of a groundmass of turbid opaline material and finely divided calcite. Pseudomorphs of pyroxene, completely replaced by calcite but still showing pyroxene cleavage are present. Chromite crystals, completely unaltered, are seen in the groundmass. The rock is an altered harzburgite.

Specimen T149 in hand specimen is dirty white fine grain and

Fig. 95. Photomicrographs of hydrogarnet veins. T332. Above, euhedral hydrogarnet in chlorite groundmass (crossed nicols X20) Below, euhedral hydrogarnet showing sector twinning. (Crossed nicols X60).

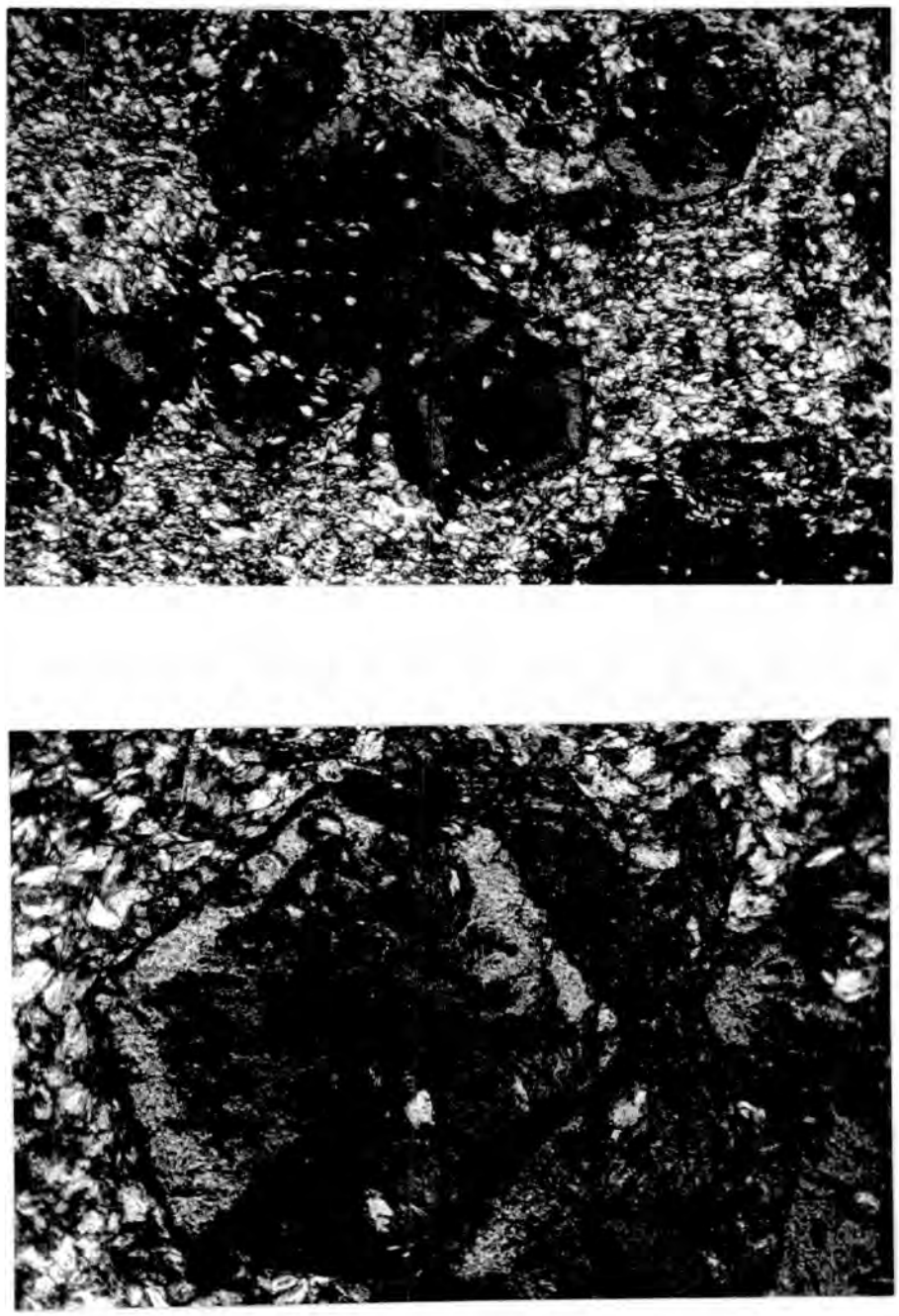

polishes with a marble-like lustre. The thin sections show it to consist almost totally of a dark dirty turbid amorphous opal cut by a network of irregular calcite veins. A few partially altered pyroxene and plagioclase laths are present indicating the rock is an altered gabbro.

Petrogenesis

The tremolitic rocks, the rodingites, the hydrogrossular rocks and the silicified and calcified rocks are all clearly post-serpentinisation in age. Their common occurrence in tectonically disturbed zones and their characteristic lime silicate mineralogy indicate a common genetic origin. The rodingites have clearly been formed by alteration of gabbro and the tremolite rocks by alteration of peridotite. The origin of the hydrogarnet veins and blocks is more problematical.

Rodingites have been described by various authors from many parts of the world and in all the descriptions (Turner 1930, Arshinov et al 1930, Watson 1942, Miles 1951, Bloxam 1954) they are clearly derived from gabbroic dyke rocks either intrusive into, or occurring close to, peridotite or serpentinite. The original gabbro has in each case been altered to calc-silicate minerals. Watson (1954) and Bilgrami (1960) have presented analytical data of normal gabbro and its associated rodingite and it is clear that lime has been introduced. Theories on the origin of the lime are as follows:-

(a) Introduced from outside by hydrothermal solutions

(Bloxam 1954)

(Turner 1934)

(b) Introduced from the peridotite; the lime being derived during serpentinisation and breakdown of the pyroxene. (Bilgrami 1960)

The ultrabasic rocks in the Tawai area are mainly harzburgites and poor in clinopyroxene. Moreover during serpentinisation clinopyroxene is the last mineral to be affected. It is usually altered to tremolitic amphibole and the lime is therefore retained. It would seem more likely that lime bearing solutions operating in the shatter zones have altered the gabbro to rodingite. The same solutions would also account for the silico-carbonate alteration and the formation of tremolite from peridotite. Tremolite flanking quartz pegmatites may possibly have derived the necessary lime from these intrusions. The absence of anthophyllite from the shear zones and the quartz pegmatite selvedges is very noticeable. Anthophyllite is strongly developed at Hangha in Sierra Leone at dunite/quartz pegmatite contacts. Almost certainly the presence of lime in the contact zones of the Tawai area has controlled the formation of tremolite in preference to anthophyllite.

Hydrogarnet besides being recorded from rodingites has also been described from metamorphic aureoles, Belyankin and Petrov (1939) describe this mineral from a teschenite/chalk marl contact in Georgia, Pabst (1941) from a metamorphosed marl in Bohemia and Mason (1957) from an andesite/limestone contact in New Zealand. At the last mentioned occurrence cristobalite and opal occur in the hydrogarnet zones of the aureole. Opaline material is associated with all the hydrogarnet bearing rocks of the Tawai area. The isolated blocks of hydrogarnet-bearing rock could therefore represent metamorphosed siliceous limestone. The irregular veins may represent remobilised

metamorphic material of this nature. Andradite recorded in one vein is also a typical mineral produced in the metamorphism of limestone. The formation of hydrogarnet in the rodingites in preference to other calc-silicate minerals suggest that lime was introduced under unusual conditions; possibly the very wet environment in which the reactions took place accounts for the formation of this unusual mineral. Yoder (1950) suggests that the lowest temperature of formation of hydrogarnet is about 300°C at atmospheric pressure.

It is therefore concluded that lime-bearing solutions, originally derived by metamorphism of siliceous limestone at depth, have affected the alteration of gabbro and peridotite and were responsible for the deposition of the hydrogarnet-bearing veins. Blocks of hydrogarnet rock may be remnants of metamorphosed siliceous limestone.

THE WEATHERING DEPOSITS.

Field Occurrence.

Unlike many other equatorial countries North Borneo is not covered by a thick layer of laterite. This is a consequence of the hilly relief and the young sedimentary formations of the country. In most of the areas underlain by ultrabasic rocks the soil sover is particularly thin and on the mountain flanks is almost non-existent. Along the ridge tops however a red soil usually containing numerous pellets of iron ore is found. Pits show the soil to extend from between 5' to 25' before bed rock is encountered. The soil profile is very immature and contains numerous boulders of partially weathered peridotite. It is only on the flat surface of the Tawai plateau that a considerable thickness and area of weathered material is found. The surface of the plateau is extremely swampy and a hard layer of compact iron ore is found beneath the surface of the water. Dry patches just above the swamp level are littered with boulders and pellets of iron ore. Many of the boulders are only partially decomposed. They increase in number and size as the plateau is traversed northwards. Diamond drilling indicates the average thickness of the iron ore is about thirty feet. The ore is of three main types.

(1) Cellular iron ore.

(2) Compact iron ore.

(3) Clay iron ore with pellets.

The profile from surface to bed rock is illustrated by the following pit sections:

4' Loose lumps of cellular ore in clay.

3' Compact layer of iron ore.

15' Clay with pellets and cellular boulders.

3' Porous bed rock.

Unaltered ultrabasic.

The compact layer is the only regular feature of the soil profile. The ore is often poorly banded consisting of alternate dark brown hard layers and soft yellow with brown light ones. The hard layers contain a hard shiny opaline material. This layer undoubtedly marks the upper limit of the water table. In other places the hard pan consists of a vesicular laterite. The soil immediately above and below the hard pan contains numerous pellets of pea iron ore. They are often cemented together into nodular masses. Nodular masses of vesicular ore also occur throughout the profile. The vesicular ore contains numerous tortuous channels which are sometimes filled with clay material. Boulders of partially decomposed peridotite occur throughout the profile.

Mineralogy.

The iron ores have been examined by X-ray diffraction. Both the vesicular ore and the hard pan consists of the iron hydroxide goethite -FeO-OH. The X-ray diffraction pattern is given in Table 37. The diffraction pattern of the clay is very similar to that of the ore and consists mainly of finely divided goethite but a peak at d = 10Å indicates the presence of a mica, and a weak peak at d = 7Å the presence of a clay mineral probably kaolinite.

Polished specimens of the ore shows numerous inclusions of

Table 37. Mineral Identification - Goethite.

Specimen 665.

dÅ	I/I_2	dÅ	I/I_2	hkL
4.94	6	5.0	20	020
4.15	100	4.21	100	110
3.35	20	3.37	20	120
2.675	24	2.69	80	130
2.571	18	2.57	20	021
		2.51	100 R	
2.500	13	2.48	20	040
2.430	78	2.44	70	111
2.232	9	2.25	20	121
2.176	12	2.18	40	140
		2.09	5	220
		2.00	10	131
		1.920	10	041
		1.803	20	211
		1.774	5	141
1.710	36	1.719	50	221
		1.689	20	240
1.559	12	1.660	10	060

A.S.T.M. 8-97.

chromite embedded in the goethite.

Chemistry.

Two analyses of the iron ore provided by Naylor Benson and Co. Ltd. are given in Table 38 where they are compared with the peridotite analysis T364. The marked leaching of silica and magnesia and the relative concentration of iron, alumina, nickel, cobalt, and titanium, is apparent from the comparison. Unfortunately the data for the whole of the plateau is not available at the moment.

Origin.

There can be little doubt that the goethite covering represents a residual deposit derived from weathering of ultrabasic rock. Lindgren (1913) states that, "in 100 pounds of typical serpentine there are 1.5 pound of alumina and 10 pounds of ferrous oxide. When the magnesia and silicia are removed in solution and the iron oxidised there remains approximately 11.75 pounds of limonite, 3.8 pounds of bauxite and kaolin and at the most 2 pounds of minor constituents. This residual of 17.55 pounds contains 7.8 pounds or 44.4% of metallic iron as an iron ore".

From the large number of decomposed and partially decomposed boulders of peridotite scattered throughout the soil profile and on the surface it is doubtful whether the goethite has been totally derived from the underlying peridotite. These boulders increase in number and size northwards and are interpreted as a large talus deposit formed at the base of the Melio-Tankulap fault scarp. The swamp conditions on the plateau have probably existed since the initial formation of the feature. These conditions are partly a

Table 38. Comparison of Tawai Iron Ore with Peridotite.

	Iron Ore 1	Iron Ore 2	Peridotite 364
SiO_2	2.50	4.90	39.8
TiO_2	.67	.67	.1
Al_2O_3	7.03	3.79	1.9
Fe_2O_3	72.26	78.60	4.4
FeO	-	.97	4.3
CaO	-	-	1.5
MgO	.72	.49	39.6
Na_2O	.09	.09	.1
K_2O	.08	.08	tr
Cr_2O_3	1.33	.44	.5
MnO	-	-	.2
NiO	2.16	.63	.3
So_3	.09	.07	
CoO	.46	.24	tr
Loss	13.42	9.75	
P_2O_5	.06	.06	
H_2O			7.9
Total	100.87	100.78	100.6

Iron Ore 1 - Cellular ore from surface.

Iron Ore 2 - Compact ore from hard pan.

Iron Ore Analysis provided by Naylor, Benson, and Company, Limited.

result of ground water not being able to percolate down through the hard pan and partly a result of the fast mountain streams slowing up and spreading out at the base of the fault scarp. The pH of the swamp water must have been such that oxidising conditions only prevailed for magnetite, siderite and pyrite are absent. The many bulbous ores found in the swamp areas also suggest that some of the ore has been formed as a direct precipitate from iron rich water.

The goethite deposit is therefore interpreted as a direct weathering product of ultrabasic rock in situ and of an overlying talus deposit. Direct precipitation from iron-rich groundwater has certainly added to the deposit.

This deposit is very similar to those found on elevated plateaux in the Mayari district of Cuba where Weld (1909) has described 'limonite', overlying peridotite.

The Tawai goethite deposit is best described as an ore body in embryo. The mantle of rock waste is not yet sufficiently weathered to be of importance as an iron ore deposit, but the relatively high concentration of Ni and Co could be of value in the future.

THE HISTORY OF THE MOUNT TAWAI PERIDOTITE.

The detailed field, petrological, and mineralogical studies of the rocks of Mount Tawai indicate that the peridotite has a complex history involving at least four distinct phases. These are as follows:-

(1) Pre-Intrusive phase.

(2) Intrusive phase.

(3) Fault emplacement phase.

(4) Post fault emplacement phase.

Pre-Intrusive phase.

It is considered that the ultrabasic and basic rocks of Mount Tawai have differentiated from a magma produced by fusion of the upper mantle at very high temperature and pressure. The differentiation resulted in a major peridotite zone overlain by a gabbroic phase. During the precipitation of the ultrabasic phase only olivine, orthopyroxene, chromium spinel and minor clinopyroxene were precipitated. Periods in which only olivine and chromium spinel were precipitated were frequent but short-lived. The rudimentary stratified chromite bands indicate the spinel accumulated under the effects of gravity. The olivine and chrome spinel probably accumulated in hollows and channels on the floor of a pile of already precipitated crystals. Minor swirls and disturbances in the chromite bands may be cited as evidence for the presence of magmatic currents during differentiation. The composition changes observed in the pyroxene and chrome spinels are considered to be due to magmatic differentiation under high temperature-high pressure conditions. When the temperature of the overlying

magma dropped sufficiently a gabbroic phase was precipitated.

Intrusive phase.

The overlying gabbro phase is then considered to have been intruded probably while still in a semi-solid condition. No indication of gravity banding has been found in the gabbros and the banding found is best attributed to flowage of a new crystalline magma. The intrusion of the gabbroic phase would create a pre-heated path up which hot semi-crystalline blocks of the ultrabasic differentiate are considered to have risen. During the intrusion the blocks were tilted and flow banding developed roughly parallel to the sides of the blocks. Metamorphism of the country rock into which the blocks were intruded took place. In the innermost part of the aureole metamorphic rocks of garnet amphibolite facies were produced indicating a temperature of between 550°C and 750°C.

During the initial intrusion some of the olivine chrome-spinel accumulates were intruded as dykes and irregular shaped bodies. The petrographic evidence shows that the chromite of these dykes is considerably brecciated and would suggest the dykes were intruded as crystalline mushes. A similar origin is envisaged for the anorthosite dykes and intrusions. The numerous gabbro dykes were intruded during this stage and may represent squeezed out interstitial liquid.

When the intrusions cooled at depth they then underwent serpentinisation. The available evidence is slightly in favour of an autometasomatic origin for the water.

Fault emplacement.

After serpentinisation renewed upward movement of the peridotite blocks occurred. This final emplacement was affected solely by fault intrusion greatly accelerated by movement up the marginal serpentinite zones. Differential movement between different parts of the large blocks resulted in large normal faults. The thin strongly serpentinised tectonic wedges were probably extremely plastic at this stage, and during intrusion tended to conform to the local structure. The Patrud Gombaran arcuate intrusion is interpreted in this way for part is concordant with the regional strike of the folded sediments. During the final emplacement the metamorphic aureole was broken up and isolated blocks were carried up in the fault intrusion zones. Numerous gabbro inclusions were also caught up in the peridotite during this phase. Sliding and slumping of the wet serpentinite during this phase produced the internal breccia zones. The final stages of emplacement were accompanied by injection of calc-silicate veins and local hydrothermal alteration of the gabbro and peridotite, the lime probably being obtained from remobilised limestone. Quartz pegmatites were intruded into the fault zones during the final stage of emplacement.

The final stages of emplacement are envisaged as taking place in late or post-Pleistocene times and having profound effects on the river system initiated in the late Miocene.

The Tawai peridotite is only one of a belt and already evidence is emerging as to the different ages of emplacement of the individual bodies. Bailey (1963) suggests the Beeston ultrabasics in the Segama area are Miocene in age, Fitch (1958) suggests that some of

the Labuk and Segama peridotites are Upper Cretaceous and Eocene, and in the Phillipines Van Bemmelen (1949) shows the ultrabasics were emplaced in the Oligocene. The evidence therefore shows that the peridotites of the North Borneo-Phillipines ultrabasic belt were not all intruded at the same time and therefore cannot be correlated with one particular orogeny in the manner envisaged by Hess (1948). It seems more likely that the peridotite belt marks a major zoned of weakness up which large ultrabasic bodies are likely to be intruded at any time.

COMPARISON OF THE MOUNT TAWAI PERIDOTITE WITH OTHER AREAS.

Thayer (1960) summarised the various kinds of ultrabasic complex and concluded that two main types could be distinguished, the stratiform complex and the Alpine type complex and that a gradational series between the two could be traced. He emphasises that the gabbroic rock must be included as an integral and important part of the Alpine type problem. Thayer points out that the Alpine type complex differs from the stratiform in their irregular shape, irregular distribution of rock types, and the absence of chilled margins or contact metamorphic effects. He further points out that layering in the Alpine type peridotites is irregular and extreme compositional contrasts are common and that cryptic layering is absent. In composition the Alpine type peridotites are also different in that the peridotites are olivine-rich and that feldspar is rare, and that Mg/Fe ratios in olivine and pyroxene are greater than in the stratiform complexes. Thayer also emphasises the allotriomorphic and cataclastic texture of true Alpine type peridotites in contrast with the euhedral settled crystals of the stratiform complexes. He concluded that true Alpine type peridotites have been emplaced as mushes of already differentiated crystals.

The Mount Tawai peridotite is clearly a gradational type. It contains features associated with an accumulative origin and those associated with semi-solid intrusion. In this connection it is similar to ultrabasic complexes described from Papua by Green (1961) and Phillipines by Peoples (1957). These types are clearly not stratiform complexes, but nevertheless show accumulative features.

Unlike most Alpine type peridotites the Mount Tawai complex is

considered to have been intruded as a hot semi-crystalline series of tectonic units. Recently three other hot peridotites have been distinguished. Mackenzie (1961) has described a high temperature peridotite from Tinaquillo, Venezuela, which shows many similar features to the Mount Tawai complex. The peridotite is composed mainly of harzburgite and contains irregular inclusions of gabbroic rocks which Mackenzie considers to be metamorphosed country rock. Thayer (1961) however has questioned this latter interpretation and regards them as normal Alpine type gabbro. Green (1964) has recently shown the pyroxenes of the Tinaquillo harzburgite to be aluminous.

Smith and Macgregor (1960) describe a metamorphic aureole 1000' wide around the Mount Albert ultrabasic complex and show the highest grade of metamorphism reached to be granulite facies.

Green (1964) concludes that the Lizard peridotite has been intruded as a hot crystalline diapir during a period when the country rocks were undergoing metamorphism.

Thayer (1960) p.256) believes "the ratio of gabbroic to peridotitic rocks in the Alpine type complex is essentially accidental and not very significant genetically". However in no described case of an Alpine type peridotite does the gabbro fraction exceed the peridotite in the ratio of 10:1. Indeed in most cases the latter is greatly dominant and the writer believes this is of genetic importance and argues against derivation of most Alpine type peridotites from differentiation of basaltic type magma. Nevertheless the existence of the gabbro fraction must not be ignored and the writer does not believe that Alpine type peridotites have been precipitated from a peridotite magma. It seems more likely they are differentiates of partial fusion of upper mantle material and the difference

between individual Alpine type peridotites are best explained by imhomogeneites in the region of fusion.

No account of an igneous body within the Indonesia Archipelago can be complete without a reference to Van Bemmelen's (1949) ideas outlined in his monumental treatise "The geology of Indonesia". He believes that the ultrabasic rocks are a result of metasomatism of the country rocks by a basic front moving ahead of an acid front in an orogenic area. Van Bemmelen's ideas like those of Termier and Termier (1956) are aptly summed up by a phrase from Buddington (1956) who writes "that wherever the authors (Termier and Termier) consider the plutonic rocks they wear the fashionable, 'frosted', spectacles through whose diffused light the deeper portions of the crust or a geosynclinal prism of sediments are seen as a place of actively diffusing ions or other units effecting whatever kind of transformation or metasomatism is needed to form whatever kind of rock it is desired to explain".

A vast amount of work on the Indonesian peridotites is still required to be done before the regional picture unfolds. In the Celebes an area of ultrabasic rocks equal to that found in North Borneo occurs and are as yet relatively untouched. One intrusion alone measures fifty miles by sixty five miles. However North Borneo, the Phillipines and the Celebes are recommended for intensive research for these are extremely young geological provinces. They are not covered by a blanket or laterite nor extensively metamorphosed and they contain almost every known major igneous rock type; surely they must contain many answers to the major petrogenetic problems.

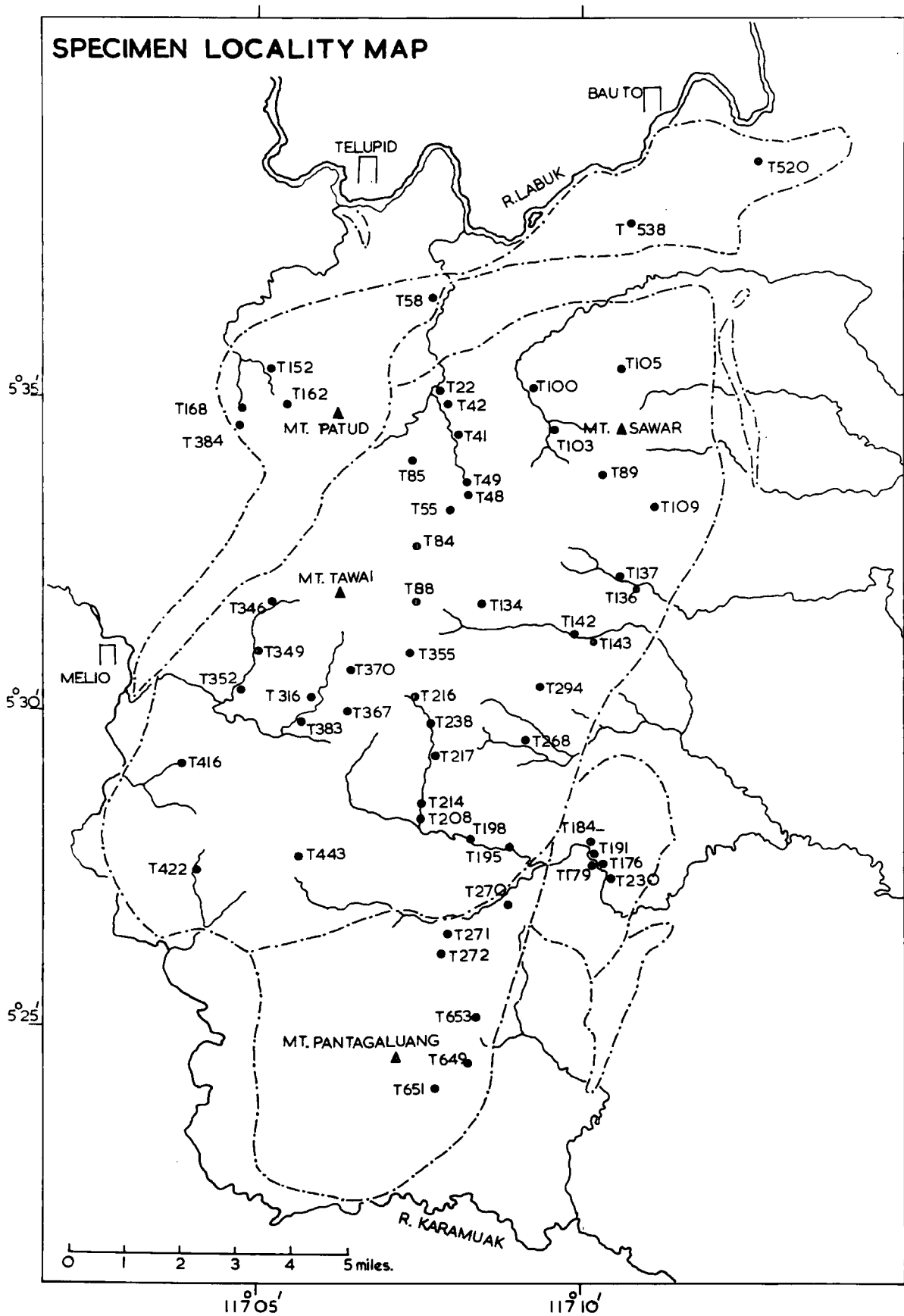
SPECIMEN LOCALITY MAP
BAU TO
TELUPID
R. LABUK
T520
T538
T58
T152
T162
T168
T384
MT. PATUD
T22
T42
T41
T85
T49
T48
T55
T84
T105
T100
MT. SAWAR
T103
T89
T109
T137
T136
MT. TAWAI
T88
T134
T346
T142
T143
T349
T355
T370
MELIO
T352
T316
T216
T294
T367
T238
T383
T368
T217
T416
T214
T208
T198
T184
T191
T195
T176
T179
T230
T422
T443
T270
T271
T272
T653
MT. PANTAGALUANG
T649
T651
R. KARAMUAK
0 1 2 3 4 5 miles.
5°35'
5°30'
5°25'
117°05'
117°10'

Fig. 96.

APPENDIX

Analytical methods.

Rapid Analysis.

The rocks and minerals, apart from the chrome spinels, were analysed by the methods devised by Shapiro and Brannock (1952) and modified by Riley (1958). The procedure used in this laboratory was followed. All the specimens except clinopyroxene T383 and amphibole T363 were examined in duplicate.

Solution B was prepared in the normal way using 0.5 gram of sample. The following oxides were determined using the appropriate aliquots of solution B.

TiO_2 - determined photometrically by means of a yellow compound formed by the addition of hydrogen peroxide to the acid solution.

Al_2O_3 - determined photometrically. Iron was first removed as ferrous-dipryidyl complex and alumina extracted with a solution of 8 - hydroxy - quinoline in chloroform after adjusting the pH to 5. Interference by titanium requires a small correction in the calculation.

CaO-MgO - determined by titration of suitable aliquots of Solution B with standard Versine. CaO was determined by using Murexide as indicator. The total CaO and MgO was determined by titration using Eriochrome Black T as indicator. The CaO equivalent is subtracted from this titration and the amount of MgO thus obtained.

Iron and alumina interference are removed by precipitating their hydroxides with NH_4OH at the correct pH.

Na_2O-K_2O - determined on the flame photometer using aliquots of solution B as recommended by Shapiro and Brannock.

Solution A was prepared in the normal way using 0.1 grams of sample. Silica is then determined in the acidified solution by the molybdenum blue method.

Ferrous oxide - determined by the classical method. 0.5 grams of sample is attacked with a mixture of sulphuric and hydrofluoric acids, care being taken to avoid oxidation of the ferrous iron. Ferrous iron is then titrated with standard potassium permanganate.

H_2O^+ and H_2O^- - the method given by Washington (1930), employing the Penfield tube, has been used for the determination of water.

X-ray fluorescence.

Trace chemical analyses for Cu, Zn, Ni, Mn, Cr, have been performed by the addition method described by Hirst and Dunham (1963). A Phillips vacuum X-ray spectrograph was used with topaz and Lithium fluoride analysing crystal. The scintillation counter and the standard electronic and recording panels were used.

Specimen T352 was used as a matrix for the rock and mineral, except the chromites, determinations. For the chromites specimen BB120 was used. Precision was checked by running a series of replicates. The minor oxides NiO, MnO, and Cr_2O_3 were calculated from the results by using oxide conversion factors. Checks were made on the analysed chrome chlorite and tremolite from Hangha (Dunham et al 1958) and the method found to be satisfactory. Specimens were examined as finely ground powders.

The major constituents Cr_2O_3, total iron oxide, and MgO of the chromites were determined by X-ray fluorescence. A series of analysed samples was obtained by Mr. R. Phillips from the Associated Chemical Laboratories and were used as standards. The chromites were

examined as pellets made from finely ground powder. Each specimen was run with a similar standard and working curves produced by plotting counts per second specimen divided by counts per second standard against known composition. The following conditions were used.

	Crystal	Counter	Peak	2θ	Discriminator
Cr_2O_3	- Topaz	Scintillation	CrKBl	100.40	-
Total Iron	- Topaz	Scintillation	FeKBl	80.62	-
MgO	- A.D.P.	Flow counter	MgKAl	107.04	Used

A satisfactory working curve for alumina could not be determined. The method of dissolving the sample in borax glass was tried but was not successful.

Mineral Separations.

Mineral separations were carried out by using the magnetic separator, heavy liquids, and handpicking. The samples were ground to pass 110 mesh, washed and dried, and the pyroxenes separated from olivine and spinel on the magnetic separator. Clino and orthopyroxene were then separated on the magnetic separator and further purified by handpicking and heavy liquid methods. Point counting showed a 99.8% purity for the clinopyroxene and 98% purity for the orthopyroxene. The latter is particularly difficult to separate completely from olivine.

REFERENCES

ARSHINOV, V.V. and MERENKOV, B.J., 1930. Petrology of the chrysolite asbestos deposits of the Krasnouralky Mine in the Ural Mountains. Trans. Inst. Econ. Min., No. 45, Moscow.

A.S.T.M. index, 1960. Index to the X-ray powder data file. American Society for Testing Materials.

ATLAS, L. 1952. The polymorphism of $MgSiO_3$ and solid state equilibrium in the system $MgSiO_3$-$CaMgSi_2O_6$. Jour. Geol., Vol.60, p.125.

BAILEY, P.S., 1963. The chromiferous ultrabasic rocks of Mount Beeston, North Borneo. Unpub. M.Sc. thesis, Durham University.

BARTHOLOMÉ, P., 1961. Co-existing pyroxenes in igneous and metamorphic rocks. Geol. Mag., Vol.98, pp.346-348.

BASTIN, E.S., 1950. Interpretation of ore textures. Geol. Soc. Amer. Memoir, No.45.

BATTEY, M.H., 1960. The relationship between the preferred orientation of olivine in dunite and the tectonic environment. Amer. J. Sci., Vol.258, pp.574-584.

BENSON, W.N., 1918. The origin of serpentine. Amer. J. Sci., Vol. 46, pp.693-731.

---------- , 1926. The tectonic conditions accompanying the intrusion of basic and ultrabasic igneous rocks. Mem. Nat. Acad. Sci., Washington, 19, No.1.

BELYANKIN, D.S., and PETROV, V.P., 1939. Hibschite in Georgia. Doklady Acad. Sci. U.S.S.R., Vol.24, p.349-354.

BILGRAMI, S.A., 1960. Serpentinite-limestone contact at Zhob Valley. Amer. Min., Vol.45, pp.1008-1009.

---------- , and HOWIE, R.A., 1960a. Mineralogy and petrology of a rodingite dike, Hindubagh, Pakistan. Amer. Min., Vol.45, pp.791-801.

BIRCH, F. 1952. Elasticity and Constitution of the Earth's interior. J. Geophys. Res., Vol.57, pp.227-286.

BLOXAM, T.W., 1954. Rodingite from the Girvan-Ballantrae Complex, Ayrshire. Miner. Mag., Vol.30, pp.525-528.

BOWEN, N.L., 1928. The evolution of the igneous rocks. (Reprinted 1956, Dover publication).

---------- , and SCHAIRER, J.F., 1935. The system MgO-FeO-SiO_2. Amer. J. Sci., Vol.29, pp.151-217.

---------- , and TUTTLE, O.F., 1949. The system MgO-SiO_2-H_2O. Bull. Geol. Soc. Amer., Vol.60, pp.439-460.

BOYD, F.R., and ENGLAND, J.L., 1960. Minerals of the mantle. Yearb. Carnegie Instn., Vol.59, pp.47-52.

BROTHERS, R.N., 1960. Olivine nodules from New Zealand. Intl. Geol. Cong. Reports, 21st. Sess. Pt. 13, pp.68-81.

BROWN, G.M., 1957. Pyroxenes from the early and middle stages of fractionation of the Skaergaard intrusion - East Greenland. Miner. Mag., Vol.31, pp.511-543.

BROWN, G.M., 1960. The effect of ion substitution on the unit cell dimensions of the common clinopyroxenes. Amer. Min., Vol.45, pp.15-38.

---------- , 1961. Co-existing pyroxenes in igneous assemblages: a re-evaluation of the existing data on Tie-line Orientations. Geol. Mag., Vol.98, pp.333-345.

BRYNZEEL, D., 1957. A petrographic study of the Waterfall Gorge profile at Insizwa. Annal. Univ. Stellenbosch, Shand Mem., Vol.p.484.

BUERGER, M.J., 1948. The role of temperature in mineralogy. Amer. Min., Vol.33, pp.101-127.

BUDDINGTON, A.F., 1956. Review of "L'Evolution de la lithosphere" by H. Termier and G. Termier. Amer. J. Sci., Vol.254, pp.646-648.

CAMERON, E.N., and EMERSON, M.E., 1959. The origin of certain chromite deposits of the eastern part of the Bushveld Complex. Econ. Geol., Vol.54, pp.1151-1211.

COOKE, H.C., 1937. Thetford, Disraeli and Eastern Half of Warwick map areas, Quebec. Geol. Survey, Canada. Mem.211 pp.86-140.

DAVIS, E.F., 1918. The Radiolarian Cherts of the Franciscan group. Univ. Calif. Pub., Bull. Dept. Geol., Vol.11, pp.270-274.

DEER, W.A., HOWIE, R.A., and ZUSSMAN, J. 1963. Rock-forming Minerals. Five volumes (Longmans Press).

DELEON, G. 1955. Geochemical investigations of Yugoslav chromites. Zbornik rador Geol. Inst. Jovan Zhujovic, Vol.8, p.333.

DONATH, M. 1931. Zinc bearing chromite. Amer. Min., Vol. 16, pp. 484-487.

DUNHAM, K.C., PHILLIPS, R., CHALMERS, R.A., and JONES, D.A., 1958. The chromiferous ultrabasic rocks of eastern Sierra Leone. Col. Geol. Min. Resources. Bull. Suppl. No.3.

DU RIETZ, T. 1935. Peridotites, serpentines and soapstones of northern Sweden. Geol. För. Förh. Stockholm, Vol.57, pp.250-252.

ESKOLA, P., VUORISTO, U., and RANKAMA, K, 1937. An experimental, illustration of the spilite reaction, Comme. Geol. Finlande Bull., Vol.119, pp.61-68.

ENGEL, A.E.J., and ENGEL, C.G., 1951. Origin and evolution of hornblende-andesine amphibolites and kindred facies. (Abstract). Bull. Geol. Soc. Amer., Vol.62, p.1435.

FAIRBAIRN, H.W., 1949. Structural petrology of Reformed Rocks. (Addison-Wesley Press Inc.)

FAWLEY, A.P., 1959. Mwahanza Hill nickel deposit, Central Province. Rec. Geol. Surv. Tanganyika, Vol.7, (for 1957) pp.49-55.

FENNER, C.N., 1931. The residual liquids of crystallising magmas. Miner. Mag. Vol.22, pp.539-560.

FERNANDEZ, N.S., PEOPLES, J.W., SAMANIEGO,S., and CRUZ, M., 1957. Chromite in the Zambales Range. Bull. Geol. Soc. Amer., Vol.68, p.1778.

FISHER, R., 1950. Entmischungen in Schmelzen aus Schwermetallogen, Silikaten und Phosphaten. Neus. Jahrb. f. Min., Abh., Vol.81, pp.315-364.

FITCH, F.H., 1956. The geology and mineral resources of part of the Segama valley and Darvel Bay area. Brit. Borneo Geol Surv. Mem. 4.

---------- , 1958. The Geology and Mineral Resources of the Sandakan area. Brit. Borneo Surv. Mem.9.

---------- , 1960. British Borneo. Brit. Borneo Geol. Survey Ann. Report., pp.6-7.

FLINT, D.E., DE ALBEAR, J.F., and GUILD, P.W., 1948. Geology and chromite deposits of the Camagüey Province, Cuba. U.S. Geol. Survey Bull. Vol.954-B. pp.39-63.

FLINT, E.F., and WELLS, L.S., 1941. Relationship of the garnet-hydrogarnet series to the sulphate resistance of Portland cements. Nat. Bur. Standars, Jour. Research, Vol.27, pp.171-180.

FOCKEMA, R.A.P., and MENDELSSOHN, E., 1954. Note on an unusual occurrence of chromite in the eastern Transvaal. Geol. Soc. S. Africa. Trans., Vol.57, pp.77-82.

FRANCIS, G.H., 1956. The serpentine mass at Glen Urquhart, Invernessshire, Scotland. Amer. J. Sci. 254, pp.201-226.

GRAHAM, R.P.D., 1917. Origin of massive serpentine and chrysolite asbestos, Black Lake-Thetford Area, Quebec. Econ. Geol., Vol.12, pp.154-202.

GREEN, D.H., 1961. Ultramafic breccias from the Musa valley, eastern Papua. Geol. Mag.y Vol.98, pp.1-26.

---------- , 1963. Alumina content of enstatite in a Venezuelan high Temperature peridotite. Bull. Geol. Soc. Amer., Vol. 74, pp.1397-1402.

GREEN, D.H., and RINGWOOD, A.E., 1963. Mineral assemblages in a model mantle composition. J. Geophys. Res., Vol.68, pp.937-45.

---------- , 1964. The petrogenesis of the high-temperature peridotite intrusion in the Lizard area, Cornwall. J. Petrol., Vol.5, No.1., pp.134-188.

GRIGGS, D.T., PATERSON, M.S., HEARD, H.C., and TURNER, F.J., 1960. Annealing recrystallisation in calcite crystals and aggregates. Geol. Soc. Amer., Memoir 79, pp.21-37.

GRIGGS, D.T., TURNER, F.J., HEARD, H.C., 1960. Deformation of rocks at 500° and 800°C. Geol. Soc. Amer. Memoir 79, pp.39-104.

HALL, A.L., 1930. Asbestos in the Union of South Africa. Union of S. Africa Geol. Surv. Mem.12,.

HAMAD, S. EL., 1963. The chemistry and mineralogy of the olivine nodules of Carlton Hill, Derbyshire. Miner. Mag., Vol.33, pp.483-497.

HARKER, A., 1956. Metamorphism. (London: Methuen and Co. Ltd.)

HATCH, F.H., WELLS, A.K., and WELLS, M.K., 1952. The petrology of the igneous rocks. 11th. edition. (London)

HENRY, N.F.M., 1942. Lamellar structure in orthopyroxenes. Miner. Mag., Vol.26., pp.179-188.

HESS, H.H., 1933. The problem of serpentinisation. Econ. Geol., Vol.28, pp.634-657.

--------- , 1938. A primary peridotite magma. Amer. J. Sci., Vol.35, pp.321-344.

--------- , 1941. Pyroxenes of common mafic magmas, part 2. Amer. Min., Vol.26, pp.573-594.

--------- , 1948. Major structural features of the Western North Pacific, an interpretation of H.O.5485, Bathymetric chart, Korea to New Guinea. Bull. Geol. Soc. Amer. Vol.59, pp.416-445.

--------- , 1949. Chemical composition and optical properties of common clinopyroxenes. Amer. Min., Vol.34, pt.1, pp.621-666.

--------- , SMITH, R.J., and DENGO, G., 1952. Antigorite from the vicinity of Caracas, Venezuela. Amer. Min., Vol.27, pp.68-75.

--------- , 1952. Orthopyroxenes of the Bushveld type, ion substitutions and changes in unit cell dimensions. Amer. J. Sci. Bowen vol. pp.173-187.

--------- , 1955. Serpentines, orogeny, and epeirogeny. Amer. Special Paper No.62, pp.391-408.

HESS, H.H., 1960. Stillwater Igneous complex - Montana. Geol. Soc. Amer. Memoir 80.

--------- , 1960a. Caribbean research project progress report. Bull. Geol. Soc. Amer., Vol.71, 235-40.

HIRST, D.M., and DUNHAM, K.C., 1963. Chemistry and petrography of the Marl slate of S.E. Durham, England. Econ. Geol., Vol. 58, pp.912-940.

HORI, F., 1956. Effects of constituent cations on the refractive indices of orthopyroxenes. Min. Journn. (Japan), Vol.1, pp.356-362.

HOWIE, R.A., 1963. Cell parameters of orthopyroxenes. Min. Soc. of Amer. Special Paper 1, pp.213-222.

HUTTON, C.O., 1943. Hydrogrossular, a new mineral of the garnet-hydrogarnet series. Trans. Roy. Soc. N.Z., Vol. 73, pp.174-180.

HYTÖNEN, K., and SCHAIRER, J.F., 1961. The plane enstatite-anorthite-diopside and its relations to basalts. Yearb. Carneg. Instn. Vol.60, pp.125-141.

JACKSON, E.D., 1960. X-ray determinative curve for natural olivine of composition Fo_{80-90}. U.S. Geol. Surv. Proff. Paper. No.400-B. p.B432.

---------- , 1961. Primary textures and mineral associations in the Ultramafic Zone of the Stillwater complex. Prof. Paper U.S. Geol. Surv., No.358,.

JOHANNSON, A., 1938. A descriptive petrology of the igneous rocks. Vol.4. (Chicago.)

JOHNSTON, R., 1953. The olivines of the Garbh Eilean sill, Shiant Islands. Geol. Mag. Vol.90, pp.161-171.

KEEP, F.E., 1929. Geology of the Shabani mineral belt, Belingwe district. Geol. Survey, Southern Rhodesia, Bull. 12, pp.101-2.

KEITH, M.L., 1954. The system $MgO-Cr_2O_3-SiO_2$. Jour. Amer. Ceram. Soc., Vol. 37, pp.490-496.

KRETZ, R., 1961. Some applications of thermodynamics to co-existing minerals of variable composition. Examples - Orthopyroxene-clinopyroxene and orthopyroxene-garnet. Journ. Geol. Vol.69, pp.361-387.

KUNO, H., 1954. Study of orthopyroxenes from volcanic rocks. Amer. Min., Vol.39, pp.30-46.

KUSHIRO, I., 1960. Si-Al relation in clinopyroxenes from igneous rocks. Amer. J. Sci., Vol. 258, pp.155-203.

LEAKE, B.L., 1964. New light on the Dawros Peridotite, Connemara, Ireland. Geol Mag., Vol.101, pp.63-74.

LIECHTI, P., 1960. The geology of Sarawak, Brunei, and the western part of North Borneo. Brit. Borneo Geol. Survey Bull. 3.

LINDGREN, W., 1913. Mineral deposits. 1st. Edition. MaGraw - Hill Book Comp. Ltd.

LIPMAN, P.W., 1964. Structure and origin of an ultramafic pluton in the Klamath Mountains, California. Amer. J. Sci., Vol.262, pp.199-221.

MACKENZIE, D.B., 1960. High temperature Alpine type peridotite from Venezuela. Bull. Geol. Soc. Amer., Vol.71, pp. 303-318.

MARSHALL, P., 1911. The geology of the Dun Mountain subdivision, Nelson. N.Z. Geol. Surv., Bull. 12, pp.31-51.

MASON, B., 1957. Larnite, Scawtite, and hydrogrossular from Tokatoka, New Zealand. Amer. Min., Vol.42, pp.379-392.

MILES, K.R., 1951. Garnetised gabbros from the Eulamina district. Geol. Surv. W. Aust., Bull. 103 part 2.

MUGGE, O., 1898. Über Translationen und verwandte Erscheinungen in Krystallen. Neues Jahrb. Mineral. Geol. Pal., Vol. 1, pp.71-158.

MUIR, I.D., and TILLEY, C.E., 1957. Contributions to the petrology of Hawaiian basalts, 1. The picrite basalts of Kilauea. Amer. J. Sci., Vol.255, p.241.

MURRAY, R.J., 1954. The clinopyroxenes of the Garbh Eilean sill, Shiant Isles. Geol. Mag., Vol.91, pp.17-31.

NOCKOLDS, S.R., 1954. Average chemical compositions of some igneous rocks, Bull. Geol. Soc. Amer., Vol. 65, pp.1007-1032.

O'HARA, M.J., 1963. Distribution of iron between co-existing olivines and calcium-poor pyroxenes in peridotites, gabbros, and other magnesian environments. Amer. J. Sci., Vol.261, pp.32-46.

O'HARA, M.A., and MERCY, E.L.P., 1963. Petrology and Petrogenesis of some garnetiferous peridotites. Trans. of Royal Soc. Edin. Vol.LXV No.12. pp.251-314.

OSBORN, E.F., and TAIT, D.B., 1952. The system diopside-forsterite-anorthite. Amer. J. Sci., Bowen vol., pp.413-434.

PABST, A., 1942. Re-examination of hibschite. Amer. Min. Vol.27, pp.783-792.

POLDERVAART, A., 1947. The relationship of orthopyroxene to pigeonite. Miner. Mag. Vol.28, p.164.

------ ------- , 1950. Correlation of physical properties and chemical composition in the plagioclase, olivine, and orthopyroxene series. Amer. Min. Vol.35, pp.1067-1079.

PEOPLES, J.W., GONZALES, M.L., FERNANDEZ, N.S., and VICTORIO, V., 1957. The ultramafic and mafic rocks of the Zambales Range, Luzon, Phillipines. Bull. Geol. Soc. Amer. Vol.68, p.1736.

RANKIN, G.A., and MERWIN, H. E., 1918. The system $MgO-Al_2O_3-SiO_2$. Amer. J. Sci. 4th. Serv. Vol. 45, p.332.

RAGEN, D.M., 1963. Emplacement of the Twin Sisters Dunite. Amer. J, Sci., Vol.261, pp.549-565.

RAMBERG, H., and DE VORE, G., 1951. The distribution of Fe^{++} and Mg^{++} in co-existing olivines and pyroxenes. Jour. Geol., Vol.59, pp.193-210.

RHEINHARD, M., and WENK, E., 1951. The geology of the Colony of North Borneo. Brit. Borneo Survey Bull. 1.

RILEY, J.P., 1958. The rapid analysis of silicate rocks and minerals. Anal. Chem. Acta. pp.413-428.

RINGWOOD, A.E., 1959. On the chemical evolution and densities of the planets. Geochim. et Cosmochim. Acta, 15, pp.257-283.

---------- , 1962. A model for the upper mantle, 2. Journ. Geophys. Res. Vol.67, pp.4473-4477.

RIODON, P.H., 1955. The genesis of asbestos in ultrabasic rocks. Econ. Geol. Vol.50, pp.67-82,.

ROSS, C.S., FOSTER, M.D., and MYERS, A.T., 1954. Origin of dunites and of olivine rich inclusions in basaltic rocks. Amer. Min., Vol.39, pp.693-737.

ROSSMAN, D.L., FERNANDEZ, N.S., FONTANOS, C.A., and ZEPEDA, Z.C., 1959. Chromite deposits on Insular chromite Reservation No.1. Zambales, Phillipines. Phillipine Bur. Mines. Sp. project series. Pub. No. 19.

ROTHSTEIN, A.V.T., 1957. The Dawros peridotite, Connemara, Eire. Quart. J. Geol. Soc., Vol. 113, pp.1-25.

---------- , 1961. A synorogenic peridotite at Dawros, Connemara. Acta Geologica (Budapest). Tomus 6, pp. 221-232.

RUICKMICK, J.C., and NOBLE, J.A., 1959. Origin of the ultramafic complex at Union Bay, South East Alaska. Bull. Geol. Soc. Amer. Vol.70, pp.981-1018.

SAHAMA, Th. G., and TORGESON, D.R., 1949. Some examples of the application of thermo-chemistry to petrology. Jour. Geol., Vol.57, pp.255-262.

SAKATA, Y., 1957. Unit cell dimensions of synthetic aluminium diopsides. Jap. Jour. Geol. Geog., Vol.28, p.161.

SANDEL, E.B., and GOLDICH, S.S., 1943. The rare metallic constituents of American igneous rocks. Jour. Geol. Vol.51, pp.99-115.

SEGNIT, E.R., 1953. Some data on synthetic aluminous and other pyroxenes. Miner. Mag. Vol.30, pp.218-226.

SELFRIDGE, G.C., Jr., 1936. An X-ray and optical investigation of the serpentine minerals. Amer. Min. Vol.21, pp.463-503.

SCHAIRER, J.F., and YAGI, Kenzo, 1952. The system FeO-Al_2O_3-SiO_2. Amer. J. Sci. Bowen Vol., pp.471-515.

SHAPIRO, L., and BRANNOCK, W.W., 1952. Rapid Analysis of Silicate Rocks. Geol. Surv. Amer. Circ. 165.

SMITH, C.H., 1958. Bay of Islands Complex, Western Newfoundland, Canada. Geol. Surv. Mem. 290.

---------- , and MACGREGOR, I.D., 1960. Ultrabasic intrusive conditions illustrated by the Mount Albert Ultrabasic pluton, Gaspe, Quebec. Abst. in Bull. Geol. Soc. Amer., Vol.71, p.1978.

STEINMANN, G., 1905. Geologische Beobachtungen inden Alpen. Vol.2. Berichte naturf. Ges. Freiburg i/B.Bd 14.

STEVENS, R.E., 1944. Composition of some chromites of the western hemisphere. Amer. Min., Vol.29, pp.1-34.

STOLL, W.C., 1958. Geology and Petrology of the Masinloc Chromite deposit, Zambales, Luzon, Phillipine Islands. Bull. Geol. Soc. Amer., Vol.69, pp.419-448.

SRIRAMADAS, A., 1957. Diagrams for the correlation of Unit Cell edges and refractive indices with the chemical composition of Garnets. Amer. Min., Vol.42, pp.294-298.

SUNDIUS, N., 1930. On the spilitic rocks. Geol. Mag. Vol.67, pp.1-17.

TABER, S., 1917. The origin of chrysotile veins. Econ. Geol. Vol.12, pp.476-9.

TALIAFERRO, N.L., 1943. Franciscan-Knoxville problem. Bull. Amer. Ass. Petr. Geol. Vol.27, pp.109-219.

TERTSCH, H., 1922. Studien am Westrande des Dunkelsteiner Granulit massives: Min. pet. Mitt., Band 35, pp.177-214.

THAYER, T.P., 1946. Preliminary chemical correlation of chromite with the containing rocks. Econ. Geol., Vol.41, pp.202-217.

---------- , 1960. Some critical differences between Alpine type and stratiform peridotite-gabbro complexes. 21st. Int. Geol. Cong. Report, Copenhagen, Section 13, pp.247-259.

--------- -, 1961. Is the Tinaquillo, Venezuela, "Pseudogabbro", metamorhpic or magmatic? Bull. Geol. Soc. Amer. Vol.72, pp.1565-1569.

TILLEY, C.E., 1938. Aluminous pyroxenes in metamorphosed limestones. Geol. Mag., Vol.75, pp.81-85.

---------- , 1947. The dunite mylonites of Saint Paul's rocks (Atlantic). Amer. J. Sci., Vol.245, pp.488-491.

TUREKIAN, K.K., and WEDEPOHL, K.M., 1961. Distribution of the elements in some major units of the earth's crust. Bull. Geol. Soc. Amer. Vol.72, pp.175-191.

TURNER, F.J., 1930. The metamorphic and intrusive rocks of southern Westland. Trans. N.Z. Inst. Vol.63, pp.178-284.

TURNER, F.J., 1942. Preferred orientation of olivine crystals in peridotites with special references to New Zealand examples. Trans. Roy. Soc. N.Z., Vol.72, pp.280-300.

---------- , HEARD, H., and GRIGGS, D.T., 1960. Experimental Deformation of Enstatite and accompanying inversion to clino-enstatite. 21st. Int. Geol. Cong. Report, Copenhagen, Section 15, pp.399-408.

---------- , and VERHOOGEN, J. 1960. Igneous and Metamorphic Petrology. Second edition. (McGraw-Hill Book).

UMBGROVE, J.H.F., 1938. Geological history of the East Indies. Bull. Amer. Ass. Petr. Geol., Vol.22, pp.1-70.

VAN BEMMELEN, R.W., 1949. The geology of Indonesia, Vol.IA. Printing Office, The Hague.

VENING MEINESZ, F.A., 1940. The earth's crust deformation in the East Indies. Proc. Kon. Ak. v. Wetensch., Amsterdam, Vol. 43, pp.278-293.

VINOGRADOV, A.P., 1961. The origin of the material of the earth's crust - Communication. Geochemistry No.1, pp.1-32.

VOLL, G., 1960. New work on petrofabrics. Liverpool and Manchester Geol. Jour., Vol.2, Pt. 3, pp.503-567.

WAGER, L.R., and DEER, W.A., 1939. Geological investigations in East Greenland. Part III - The petrology of the Skaergaard intrusion, Kangerlugssuaq. Medd. Grønland, Bd 105, Nr. 4.

---------- , 1958. Beneath the earth's crust. Adv. Sci., 15, pp. 31-45.

WARREN, B.E., and HERING, K.W., 1941. The random structure of chrysotile asbestos. Phys. Rev. Vol.59, p.925 (Abst.)

WASHINGTON, H.S., 1930. The chemical analysis of rocks.

WATSON, K.P., 1942. Zoisite-prehnite alteration of gabbro. Amer. Min. Vol.27, pp.638-645.

WATSON, K.D., 1953. Prehnitization of Albitite. Amer. Min., Vol,88, pp.197-206.

WELD, C.M., 1909. The residual ores of Cuba. Trans. Amer. Inst. Min. Eng., Vol. 40, pp.299-312.

WHITTAKER, E.J.W., and ZUSSMAN, J. 1956. The characterisation of serpentine minerals by X-ray diffraction. Miner. Mag., Vol.31, pp. 107-126.

WILKINSON, J.F.G., 1953. Some aspects of the Alpine-type serpentinites of Queensland. Geol. Mag., Vol.90, pp. 305-321.

---------- , 1957. The clinopyroxenes of a differentiated teschenitic sill near Gunnedah, New South Wales. Geol. Mag., Vol. 94, pp.123-134.

WILSHIRE, H.G., TALBOT, J.R., HOBBS, B.E., and SWEATMAN, T.R., 1963. Xenoliths and Xenocrysts from lavas of the Kerguelen Archipelago. Amer. Min., Vol.48, pp.159-180.

WILSON, A.F., 1960. Co-existing pyroxenes. Geol. Mag., Vol. 97, pp.1-17.

WILSON, R.A., 1959. The Geology of the Xeros-Troodos Area. Geol. Surv. Dept. Cyprus. Mem.1.

WORST, B:G., 1958. The differentiation and structure of the Great Dyke of Southern Rhodesia. Trans. Geol. Soc. S. Afr. Vol. 61, pp. 283-354.

YODER, H.S., 1950. Stability relations of grossularite. Jour. Geol., Vol. 58, pp.221-253.

YODER, H.S., and SAHAMA, Th. G., 1957. Olivine X-ray determinative curve. Amer.Min. Vol.42, pp.475-491.

YODER, H.S. Jnr., and CHINNER, G.A., 1960. Almandite-pyrope-water system at 10,000 bars. Yearb. Carneg. Instn. 59, pp. 81-84.

YODER, H.S., and TILLEY, C.E., 1961. Derivation of Magma Types from a Primary magma. Yearb. Carneg. Instn. Vol. 60, pp. 106-113.

ZVETHOV, A.I., 1945. Synthesis of alumina pyroxenes and dependence of their optics on composition. Mem. Soc. Russe. Min. Ser.2, Vol. 74, p.215.

ZWAAN, P.C., 1954. On the determination of pyroxenes by X-ray powder diagrams. Leidse Geol. Mededelingen, Vol. 19, p.167.

DURHAM UNIVERSITY SCIENCE 13 AUG 1964 LIBRARY